

UC Riverside

UC Riverside Electronic Theses and Dissertations

Title

The Systematics of Oraseminae (Hymenoptera: Eucharitidae): Phylogenetics, Taxonomic Revision, and Larval Evolution

Permalink

<https://escholarship.org/uc/item/5r73h9kf>

Author

Baker, Austin James

Publication Date

2020

Supplemental Material

<https://escholarship.org/uc/item/5r73h9kf#supplemental>

License

<https://creativecommons.org/licenses/by/4.0/> 4.0

Peer reviewed|Thesis/dissertation

UNIVERSITY OF CALIFORNIA
RIVERSIDE

The Systematics of Oraseminae (Hymenoptera: Eucharitidae): Phylogenetics, Taxonomic
Revision, and Larval Evolution

A Dissertation submitted in partial satisfaction
of the requirements for the degree of

Doctor of Philosophy

in

Entomology

by

Austin James Baker

June 2020

Dissertation Committee:

Dr. John M. Heraty, Chairperson

Dr. Christiane Weirauch

Dr. Richard Stouthamer

Dr. Mark Springer

Copyright by
Austin James Baker
2020

The Dissertation of Austin James Baker is approved:

Committee Chairperson

University of California, Riverside

Acknowledgements

The text of the dissertation, in part, is a reprint of the material as it appears in Inverse dispersal patterns in a group of ant parasitoids (Hymenoptera: Eucharitidae: Oraseminae) and their ant hosts (Austin J. Baker, John M. Heraty, Jason Mottern, Junxia Zhang, Heather M. Hines, Alan R. Lemmon, and Emily Moriarty Lemmon, 2020) and Larval morphology and life history of *Eutrichosoma mirabile* Ashmead and description of a new species of *Eutrichosoma* (Hymenoptera, Chalcidoidea) (Austin J. Baker and John M. Heraty, 2020). The co-author John M. Heraty listed in these publications directed and supervised the research which forms the basis for this dissertation. The co-authors Heather M. Hines, Alan R. Lemmon, and Emily Moriarty Lemmon listed in the first publication provided technical expertise in probe design and molecular sequencing. The co-authors Jason Mottern and Junxia Zhang listed in the first publication provided expertise in database management and phylogenetic reconstruction. Additionally, I would like to acknowledge the following sources of funding: National Science Foundation grants (DEB 1257733 and 1555808), USDA National Institute of Food and Agriculture Hatch project (1015803), Harry Scott Smith Biological Control Award, Robert and Peggy van den Bosch Memorial Scholarship, and Lauren and Mildred Anderson Immature Insects Award.

ABSTRACT OF THE DISSERTATION

The Systematics of Oraseminae (Hymenoptera: Eucharitidae): Phylogenetics, Taxonomic Revision, and Larval Evolution

by

Austin James Baker

Doctor of Philosophy, Graduate Program in Entomology
University of California, Riverside, June 2020
Dr. John M. Heraty, Chairperson

The subfamily Oraseminae (Hymenoptera: Chalcidoidea: Eucharitidae) is a circumtropical group of parasitoid wasps that specialize on ants in the subfamily Myrmicinae (Hymenoptera: Formicidae). Multiple phylogenetic inference methods, including parsimony, maximum likelihood, Bayesian, and coalescence, with the largest to date sampling of taxa for this subfamily allow us to elucidate their dated biogeography, ancestral host ant genus, diversification rates, and provide valuable data for revising the constituent genera and species. Using molecular datasets comprised of Illumina sequences from Anchored Hybrid Enrichment probe capture, Sanger sequences from paired primers, and a combination of the previous two datasets, we show that Oraseminae has likely dispersed from the Old World into the New World across a tropical Beringian Land Bridge approximately 24–33 Ma. This dispersal, which seemed to have occurred around the same time but in the opposite direction of their ancestral host ants in the genus *Pheidole*, led to an increased diversification rate in the exclusively New World genus, *Orasema*. Including the species described herein, *Orasema* comprises 94 described

species organized into 16 species groups with several unplaced taxa. There are 22 new species described and 7 redescriptions with comprehensive distribution maps, plant and ant host association data, and digitally imaged photo plates, which represents the largest revision of this genus to date. Within the superfamily Chalcidoidea, eucharitid wasps, along with their sister family, Perilampidae, have a unique morphology for their first-instar larvae called planidia, which are hypermetamorphic, highly mobile, and strongly sclerotized. Relationships to this planidial clade have historically been difficult to establish. A morphological phylogenetic analysis of the planidial larvae that includes the newly discovered, less-derived larva in the species *Eutrichosoma mirabile* Ashmead (Pteromalidae) has provided evidence of a close relationship to the Eucharitidae and Perilampidae, allowing us to make more informed predictions on the origin and natural history of planidial larvae in Chalcidoidea.

Table of Contents

Introduction	1
---------------------------	---

Chapter 1: Inverse Dispersal Patterns in a Group of Ant Parasitoids (Hymenoptera:

Eucharitidae: Oraseminae) and Their Ant Hosts

Abstract	10
Introduction	11
Methods and Materials	18
Results	32
Discussion	40
Conclusions	48
References	50
Figures and Tables	60

Chapter 2: A Revision of the New World Ant Parasitoid Genus *Orasema*

(Hymenoptera: Eucharitidae)

Abstract	85
Introduction	86
Methods and Materials	90
Results	94
References	212

Figures	215
Chapter 3: Larval Morphology and Life History of <i>Eutrichosoma mirabile</i> Ashmead and Description of a New Species of <i>Eutrichosoma</i> (Hymenoptera: Chalcidoidea)	
Abstract	259
Introduction	259
Methods and Materials	261
Results	273
Discussion	280
References	283
Figures	287
Conclusions	290
Appendix A: List of Supplemental Files	292

List of Figures

Figure 1.1: The lifecycle of a typical orasemine wasp	60
Figure 1.2: The distribution of genera in Oraseminae	61
Figure 1.3: BEAST chronogram of the Top 25 AHE loci	62
Figure 1.4: BEAST analysis of the Combined dataset	63
Figure 1.5: Additional phylogenetic comparative methods	64
Figure 1.6: Parsimony tree of Sanger dataset	65
Figure 1.7: Parsimony tree of AHE dataset	66
Figure 1.8: Parsimony tree of Combined dataset	67
Figure 1.9: Maximum likelihood tree of Sanger dataset	68
Figure 1.10: Maximum likelihood tree of AHE dataset	69
Figure 1.11: Maximum likelihood tree of Combined dataset	70
Figure 1.12: BEAST tree of Sanger dataset	71
Figure 1.13: BEAST tree of AHE 26–50 dataset	72
Figure 1.14: BEAST tree of AHE 51–75 dataset	73
Figure 1.15: BEAST tree of Combined dataset	74
Figure 1.16: DEC biogeography tree of Combined dataset	75
Figure 1.17: DEC+J biogeography tree of Combined dataset	76
Figure 1.18: ASTRAL tree of AHE dataset	77
Figure 2.1: Time tree summarizing phylogenetic relationships of <i>Orasema</i>	215
Figure 2.2: <i>Orasema</i> immature stages	216

Figure 2.3: Comparison of surface sculpture in <i>Orasema</i>	217
Figure 2.4: Diagnostic features for <i>Orasema</i>	218
Figure 2.5: Distribution of species in <i>Orasema coloradensis</i> species group	219
Figure 2.6: <i>Orasema coloradensis</i>	220
Figure 2.7: Comparison of dorsal mesosoma of female <i>Orasema coloradensis</i>	221
Figure 2.8: <i>Orasema iridescens</i>	222
Figure 2.9: <i>Orasema scaura</i>	223
Figure 2.10: <i>Orasema violacea</i>	224
Figure 2.11: Distribution of species in <i>Orasema bakeri</i> species group	225
Figure 2.12: <i>Orasema bablyi</i>	226
Figure 2.13: <i>Orasema bakeri</i>	227
Figure 2.14: <i>Orasema dubitata</i>	228
Figure 2.15: <i>Orasema polymyrmex</i>	229
Figure 2.16: <i>Orasema texana</i>	230
Figure 2.17: Distribution of species in <i>Orasema tolteca</i> species group	231
Figure 2.18: <i>Orasema castilloae</i>	232
Figure 2.19: Immature stages of <i>Orasema tolteca</i>	233
Figure 2.20: <i>Orasema tolteca</i>	234
Figure 2.21: Distribution of species in <i>Orasema sixaolae</i> species group	235
Figure 2.22: <i>Orasema brachycephala</i>	236
Figure 2.23: <i>Orasema nebula</i>	237
Figure 2.24: <i>Orasema sixaolae</i>	238

Figure 2.25: <i>Orasema tinalandia</i>	239
Figure 2.26: Distribution of species in <i>Orasema acuminata</i> species group	240
Figure 2.27: <i>Orasema acuminata</i>	241
Figure 2.28: <i>Orasema cerulea</i>	242
Figure 2.29: Distribution of species in <i>Orasema hippocephala</i> species group	243
Figure 2.30: <i>Orasema chrysozona</i>	244
Figure 2.31: <i>Orasema hippocephala</i>	245
Figure 2.32: Distribution of species in <i>Orasema johnsoni</i> species group	246
Figure 2.33: <i>Orasema johnsoni</i>	247
Figure 2.34: <i>Orasema spyrogaster</i>	248
Figure 2.35: Distribution of species in <i>Orasema heacoxi</i> species group	249
Figure 2.36: <i>Orasema heacoxi</i>	250
Figure 2.37: <i>Orasema masonicki</i>	251
Figure 2.38: Distribution of unplaced <i>Orasema</i> species	252
Figure 2.39: <i>Orasema brasiliensis</i>	253
Figure 2.40: <i>Orasema cirrhocnemis</i>	254
Figure 2.41: <i>Orasema monstrosa</i>	255
Figure 2.42: <i>Orasema mutata</i>	256
Figure 2.43: <i>Orasema psarops</i>	257
Figure 2.44: <i>Orasema roppai</i>	258
Figure 3.1: <i>Eutrichosoma mirabile</i> immature stages	287
Figure 3.2: Parsimony tree from larval morphology	288

Figure 3.3: *Eutrichsoma burksi* 289

List of Tables

Table 1.1: Oraseminae ant and plant host records	78
--------------------------------------------------------	----

Introduction

The superfamily Chalcidoidea (Hymenoptera) is a highly diverse clade of minute wasps that are primarily parasitoids of other insects. This diversity is illustrated not only by their ability to speciate (over 22,000 described species and 100,000–500,000 estimated total species (Heraty *et al.*, 2013; Noyes, 2015)) but also by their diverse life histories (parasitoids, gall-makers, fig pollinators), diverse range of size (0.13 mm *Dicopomorpha* adults to 20 mm *Leptofoenus* adults (Heraty *et al.*, 2013)), and diverse larval morphologies (hymenopteriform, planidiaform, mymariform, vesiculate, caudate (Clausen, 1940)). Within Chalcidoidea, the Planidial Larva Clade (PLC; Baker & Heraty, 2020) consists of the families Eucharitidae, Perilampidae, and the subfamily Eutrichosomatinae (Pteromalidae) (Heraty *et al.*, 2013). Members of the PLC are hypermetamorphic, a developmental phenomenon where the larvae undergo a distinct metamorphosis between the first and second instars (Pinto, 2009) in addition to the normal pupal metamorphosis undergone by all holometabolous insects. The research in this dissertation has led to a better understanding of their phylogenetic relationships, which provides a foundation for understanding the evolution of the interesting phenomena occurring in this group, such as ant host specialization and biogeography in Oraseminae (Eucharitidae) as well as morphological and behavioral development of the larvae within the PLC. Additionally, the taxonomic revisions of the genera *Orasema* (Eucharitidae) and *Eutrichosoma* (Pteromalidae) provided herein are essential to any

further research into these groups by providing names, descriptions, and diagnostic images for their constituent species, which are necessary for proper identification.

Oraeminae are specialist parasitoids of ants in the subfamily Myrmicinae (Formicidae). They are found throughout the tropics worldwide and into subtropical and temperate environments in North America. There is a single New World genus, *Oraema* Cameron, and twelve Old World genera (Burks *et al.*, 2017). To better understand the relationships among these genera, their biogeography (how they came to be distributed worldwide), and their patterns of diversification, we employ a variety of phylogenetic inference methods (parsimony, maximum likelihood, Bayesian, coalescence) using two distinct datasets (Sanger sequencing and Anchored Hybrid Enrichment) independently and combined with a broad sampling of taxa in this subfamily.

Sanger sequencing, which is a single-gene sequencing technology using paired primers, has long been used for obtaining genetic sequences for phylogenetic studies, and many large datasets have been built using this technology. While labor-intensive, this type of sequencing remains a relatively cheap way to sequence a few genes for many taxa. Using Sanger sequencing, we have built a dataset consisting of five gene loci and 203 taxa across Oraeminae and their outgroups (Baker *et al.*, 2020). Next-generation sequencing (NGS) technologies using the Illumina sequencing platform are more efficient and cheaper alternatives to Sanger sequencing that allow for hundreds to thousands of genes to be sequenced simultaneously for taxa. Using Anchored Hybrid Enrichment (AHE) (Lemmon *et al.*, 2012) targeted probe capture, an Illumina-based NGS method, we were able to obtain 348 gene loci for 92 taxa across Oraeminae and

their outgroups (Baker *et al.*, 2020). Combining the Sanger and AHE datasets resulted in a matrix with a large and sometimes prohibitive amount of missing data. We were able to compensate for this and run parameter-rich dating analyses by subsampling the AHE dataset with sets of 25 phylogenetically informative loci selected by the program PhyDesign (López-Giráldez & Townsend, 2011) or by constraining the tree topology to match the maximum likelihood analyses of the combined data while using the Sanger data for node age calibration.

The biogeographic history of Oraseminae can be hypothesized using dated trees (chronograms) and compared to the biogeographic history of their inferred ancestral host ant genus, *Pheidole* Westwood. Recent studies suggest that *Pheidole* dispersed from the New World into the Old World (Economo *et al.*, 2015a; Economo *et al.*, 2015b; Ward *et al.*, 2015; Economo *et al.*, 2019) in a timeframe that closely coincides with estimates for Oraseminae dispersing from the Old World to the New World (Murray *et al.*, 2013; Baker *et al.*, 2020). The Bering Land Bridge (BLB) is a connection between western North America and eastern Russia that has existed on and off from approximately 65 Ma to 5.5 Ma (Sanmartín *et al.*, 2001; Milne, 2006) and likely supported tropical to subtropical flora and fauna before approximately 15 Ma (Wolfe, 1993; Milne, 2006). This timing and climate support the dispersal patterns of both Oraseminae and their ancestral host ant, *Pheidole* (Formicidae: Myrmicinae).

The New World genus *Orasema* is more diverse (in terms of species numbers) and more abundant (in terms of collection records) than all of the Old World genera of Oraseminae combined. This may represent a distinct increase in diversification rates

correlated to dispersing into the New World. This genus currently contains 72 described species organized into 11 species groups, but it includes far more diversity at both the species and species group levels. *Orasema* has a large distribution, with collection records as far north as southern Canada and as far south as central Argentina, and they are known to parasitize ants from at least four genera of Myrmicinae, *Pheidole*, *Solenopsis* Westwood, *Temnothorax* Mayr, and *Wasmannia* Forel.

The phylogenetic hypotheses of Chapter 1 (Baker *et al.*, 2020) provide strong support for relationships in the genus *Orasema* and allow for a robust, data-driven revision of this genus. Several groups have recently been revised, including the Old World genera of Oraseminae (Burks *et al.*, 2017), the *Orasema simulatrix* and *wayqecha* species groups (Herreid & Heraty, 2017), the *Orasema festiva* species group (Burks *et al.*, 2015), the *Orasema stramineipes* species group (Burks *et al.*, 2018), the *Orasema lasallei* species group (Heraty & Baker, In Press), and the *Orasema xanthopus* species group (Heraty *et al.*, 1993). This still leaves many groups to describe in this diverse genus, including several that have no currently described species. The work herein includes descriptions of 8 species groups with 29 described species, completing the revision of all major groups in this genus with the exceptions of the *susanae* group, *vianai* group, and *cockerelli* group. Taxonomic keys to species groups and species are provided, and photographic plates for all described species are included to improve identifications for *Orasema*.

Within the PLC, the eucharitid subfamilies Oraseminae, Eucharitinae, and Gollumiellinae and the perilampid subfamilies Perilampinae and Philomidinae all have

highly-derived planidial morphology for their first-instar larvae. This is indicated by their strongly-sclerotized terga, darkened (tanned) cuticle, high degree of mobility, and distinctly different morphology of the second instar (hypermetamorphosis). The perilampid subfamily Chrysolampinae has less distinctly planidiaform larvae (Darling & Miller, 1991), however, it still fits within the behavioral characteristics associated with the other PLC subfamilies. Specifically, the majority of these larvae are ectoparasitic koinobionts, which means they feed externally on their host and parasitize their host without arresting its development.

Several studies have looked at the relationships within the PLC based on larval morphological characters (Heraty & Darling, 1984; Darling, 1992). Another study based on adult morphology and Sanger sequence data places the subfamily Eutrichosomatinae (Pteromalidae) within the PLC (Heraty *et al.*, 2013). Prior to the study herein (Baker & Heraty, 2020), nothing was known of the larval morphology of Eutrichosomatinae, but based on their phylogenetic position, we predicted that the first instars would be planidiaform, or if not objectively planidiaform, they would have behavioral characteristics, like Chrysolampinae, that place them within this group. With their larval morphology, we could update the previous larval morphological datasets with more characters and taxa to see what relationship was supported by the first instars.

Eutrichosoma mirabile Ashmead (Eutrichosomatinae) is the most widespread and easily collected species of its subfamily. It is distributed across North America and is generally not rare in collections. Little is known about its natural history except that it has been reared from seed-feeding weevils, *Auleutes* sp. and *Smicronyx* sp. (Curculionidae)

found on the plants *Helianthus* and *Parthenium* (Asteraceae) (Crawford 1908; Bouček 1974; Charlet and Seiler 1994). By collecting larvae of *E. mirabile* and examining its behavior, we gain a better understanding of its life history and are able to learn about the evolutionary history of planidial larvae by placing this group phylogenetically.

References

- Baker, A.J. & Heraty, J.M. (2020) Larval morphology and life history of *Eutrichosoma mirabile* Ashmead and description of a new species of *Eutrichosoma* (Hymenoptera, Chalcidoidea). *Journal of Hymenoptera Research*, **75**, 67–85.
- Baker, A.J., Heraty, J.M., Mottern, J., Zhang, J., Hines, H.M., Lemmon, A.R. & Lemmon, E.M. (2020) Inverse dispersal patterns in a group of ant parasitoids (Hymenoptera: Eucharitidae: Oraseminae) and their ant hosts. *Systematic Entomology*, **45**, 1–19.
- Bouček, Z. (1974) The pteromalid subfamily Eutrichosomatinae (Hymenoptera: Chalcidoidea). *Journal of Entomology*, **43**, 129-138.
- Burks, R.A., Heraty, J.M., Dominguez, C. & Mottern, J.L. (2018) Complex diversity in a mainly tropical group of ant parasitoids: revision of the *Orasema stramineipes* species group (Hymenoptera: Chalcidoidea: Eucharitidae). *Zootaxa*, **4401**, 1–107.
- Burks, R.A., Heraty, J.M., Mottern, J., Dominguez, C. & Heacox, S. (2017) Biting the bullet: revisionary notes on the Oraseminae of the Old World (Hymenoptera, Chalcidoidea, Eucharitidae). *Journal of Hymenoptera Research*, **55**, 139–188.
- Burks, R.A., Mottern, J. & Heraty, J.M. (2015) Revision of the *Orasema festiva* species group (Hymenoptera: Chalcidoidea: Eucharitidae). *Zootaxa*, **3972**, 521–534.
- Charlet, L.D. & Seiler, G.J. (1994) Sunflower seed weevils (Coleoptera: Curculionidae) and their parasitoids from native sunflowers (*Helianthus*) in the Northern Great Plains. *Annals of the Entomological Society of America*, **87**, 831-835.
- Clausen, C.P. (1940) *Entomophagous Insects*. McGraw-Hill Book Company, Inc., New York and London.
- Crawford, J.C. (1908) Some new Chalcidoidea. *Proceedings of the Entomological Society of Washington*, **9**, 157-160.
- Darling, D.C. (1992) The life history and larval morphology of *Aperilampus* (Hymenoptera: Chalcidoidea: Philomidinae), with a discussion of the phylogenetic affinities of the Philomidinae. *Systematic Entomology*, **17**, 331-339.
- Darling, D.C. & Miller, T.D. (1991) Life history and larval morphology of *Chrysolampus* (Hymenoptera: Chalcidoidea: Chrysolampinae) in western North America. *Canadian Journal of Zoology*, **69**, 2168-2177.

- Economo, E.P., Huang, J.P., Fischer, G., *et al.* (2019) Evolution of the latitudinal diversity gradient in the hyperdiverse ant genus *Pheidole*. *Global Ecology and Biogeography*, **28**, 456–470.
- Economo, E.P., Klimov, P., Sarnat, E.M., Guenard, B., Weiser, M.D., Lecroq, B. & Knowles, L.L. (2015a) Global phylogenetic structure of the hyperdiverse ant genus *Pheidole* reveals the repeated evolution of macroecological patterns. *Proc Biol Sci*, **282**, 20141416.
- Economo, E.P., Sarnat, E.M., Janda, M., *et al.* (2015b) Breaking out of biogeographical modules: range expansion and taxon cycles in the hyperdiverse ant genus *Pheidole*. *J Biogeogr*, **42**, 2289–2301.
- Heraty, J.M. & Baker, A.J. (In Press) New species of *Orasema* (Hymenoptera: Eucharitidae) from Central and South America. *Journal of Natural History*.
- Heraty, J.M., Burks, R.A., Cruaud, A., *et al.* (2013) A phylogenetic analysis of the megadiverse Chalcidoidea (Hymenoptera). *Cladistics*, **29**, 466-542.
- Heraty, J.M. & Darling, D.C. (1984) Comparative morphology of the planidial larvae of Eucharitidae and Perilampidae (Hymenoptera: Chalcidoidea). *Systematic Entomology*, **9**, 309-328.
- Heraty, J.M., Wojcik, D.P. & Jouvenaz, D.P. (1993) Species of *Orasema* parasitic on the *Solenopsis saevissima*-complex in South America (Hymenoptera: Eucharitidae, Formicidae). *Journal of Hymenoptera Research*, **2**, 169–182.
- Herreid, J.S. & Heraty, J.M. (2017) Hitchhikers at the dinner table: a revisionary study of a group of ant parasitoids (Hymenoptera: Eucharitidae) specializing in the use of extrafloral nectaries for host access. *Systematic Entomology*, **42**, 204–229.
- Lemmon, A.R., Emme, S.A. & Lemmon, E.M. (2012) Anchored hybrid enrichment for massively high-throughput phylogenomics. *Syst Biol*, **61**, 727–744.
- López-Giráldez, F. & Townsend, J.P. (2011) PhyDesign: an online application for profiling phylogenetic informativeness. *BMC Evol Biol*, **11**, 1–4.
- Milne, R.I. (2006) Northern Hemisphere plant disjunctions: a window on tertiary land bridges and climate change? *Ann Bot*, **98**, 465–472.
- Murray, E.A., Carmichael, A.E. & Heraty, J.M. (2013) Ancient host shifts followed by host conservatism in a group of ant parasitoids. *Proceedings of the Royal Society Biological Sciences Series B*, **280**, 20130495.

- Noyes, J.S. (2015) *Universal Chalcidoidea Database*.
www.nhm.ac.uk/entomology/chalcidoids/index.html [accessed on Sep 30].
- Pinto, J.D. (2009) Hypermetamorphosis. *Encyclopedia of Insects* (ed. by V.H. Resh & R.T. Carde), pp. 484-486. Academic Press.
- Sanmartín, I., Enghoff, H. & Ronquist, F. (2001) Patterns of animal dispersal, vicariance and diversification in the Holarctic. *Biological Journal of the Linnean Society*, **73**, 345-390.
- Ward, P.S., Brady, S.G., Fisher, B.L. & Schultz, T.R. (2015) The evolution of myrmicine ants: phylogeny and biogeography of a hyperdiverse ant clade (Hymenoptera: Formicidae). *Systematic Entomology*, **40**, 61–81.
- Wolfe, J.A. (1993) An analysis of Neogene climates in Beringia. *Palaeogeography Palaeoclimatology Palaeoecology*, **108**, 207–216.

Chapter 1: Inverse Dispersal Patterns in a Group of Ant Parasitoids (Hymenoptera: Eucharitidae: Oraseminae) and their Ant Hosts

Abstract

When postulating evolutionary hypotheses for diverse groups of taxa using molecular data, there is a tradeoff between sampling large numbers of taxa with a few Sanger sequenced genes or sampling fewer taxa with hundreds to thousands of next-generation sequenced genes. High taxon sampling enables the testing of evolutionary hypotheses that are sensitive to sampling bias (i.e. dating, biogeography, and diversification analyses), whereas high character sampling improves resolution of critical nodes. In a group of ant parasitoids (Hymenoptera: Eucharitidae: Oraseminae), we analyze both of these types of datasets independently (203 taxa with five Sanger loci; 92 taxa with 348 anchored hybrid enrichment loci) and in combination (229 taxa, 353 loci) to explore divergence dating, biogeography, host relationships, and differential rates of diversification. Oraseminae specialise as parasitoids of the immature stages of ants in the subfamily Myrmicinae (Hymenoptera: Formicidae), with ants in the genus *Pheidole* being their most common and presumed ancestral host. A general assumption is that the distribution of the parasite must be limited by any range contraction or expansion of its host. Recent studies support a single New World to Old World dispersal pattern for *Pheidole* approximately 11–22 Ma. Using multiple phylogenetic inference methods (parsimony, maximum likelihood, dated Bayesian, and coalescent analyses), we provide a robust phylogeny showing that Oraseminae dispersed in the opposite direction, from Old

World to New World, approximately 24–33 Ma, which implies that they existed in the Old World prior to their presumed ancestral hosts. Their dispersal into the New World appears to have promoted an increased diversification rate. Both the host and parasitoid show single unidirectional dispersals in accordance with the presence of the Beringian Land Bridge during the Oligocene, a time when the changing northern climate likely limited the dispersal ability of such tropically adapted groups.

Introduction

Next generation sequencing (NGS) methods in phylogenetics are becoming increasingly popular for resolving contentious relationships among taxa (Maddison, 2016). Anchored hybrid enrichment (AHE) has been developed as an efficient and low cost means to sequence hundreds of orthologs that provide phylogenetic signal at both deep and shallow scale analyses (Lemmon *et al.*, 2012; Lemmon & Lemmon, 2013). In comparison, traditional Sanger sequencing is an affordable, though less efficient, means to sequence a few loci for many individuals. Having both types of datasets provides the opportunity to combine taxon-rich and character-rich datasets to create a phylogeny that is well sampled with high backbone support; however, this combination results in large amounts of missing data. To test the efficacy of combining these two types of datasets, we compare the results from analyses using separate (Sanger-only and AHE-only) and combined (Sanger+AHE) datasets analyzed under multiple phylogenetic frameworks (parsimony, maximum likelihood, Bayesian inference, coalescence) to thoroughly explore the

phylogenetics, dating, ancestral host associations, and biogeography of a group of ant parasitoids.

In the Northern Hemisphere, biogeographic hypotheses are complicated by the on and off connections between continents and high variability in climatic conditions (Sanmartín *et al.*, 2001; Milne, 2006). The North Atlantic Land Bridges (NALB's) were important for faunal exchange prior to about 50 Ma (Thulean) and 39 Ma (De Geer) (McKenna, 1983; Tiffney, 1985), while the Bering Land Bridge (BLB), which connected Western North America to Eastern Eurasia from approximately 65 Ma to 5.5 Ma (Sanmartín *et al.*, 2001; Milne, 2006), is considered to be a more likely route for more recently dispersed groups. The change in climate and associated flora and fauna in the Northern Hemisphere during the Tertiary allows the BLB hypothesis to explain distributions of both tropical and temperate biota. Groups with disjunct tropical or subtropical distributions likely crossed the BLB before ~15 Ma, when the northern climate was warm with high equability (i.e. low variation between summer and winter temperatures) (Wolfe, 1993; Milne, 2006), a pattern commonly seen in dated phylogenies (e.g. lizards: Brandley *et al.* (2011); Gamble *et al.* (2011); Townsend *et al.* (2011); snakes: Burbrink & Lawson (2007); Wüster *et al.* (2008); Guo *et al.* (2012); Chen *et al.* (2013); butterflies: Condamine *et al.* (2013); ambush bugs: Masonick *et al.* (2017); and ants: Blaimer *et al.* (2016)). We investigate the timing and patterns of dispersal relative to these events in a parasitoid lineage and its ant hosts.

Parasitoids are a specialised subset of holometabolous insect parasites whose larvae feed on and kill a single arthropod host (Askew, 1971; Eggleton & Belshaw,

1992). The wasp family Eucharitidae is composed of obligate ant parasitoids and is the only insect family known to specialise on attacking ant brood (Clausen, 1941; Heraty, 1994b; Heraty, 2000; Heraty, 2002). They exhibit both host specificity and a high degree of endemism, which makes them an excellent candidate for studies of ancient host associations and modelling of biogeographic events (Heraty, 1994b; Heraty, 2000).

Oraeseminae (Hymenoptera: Eucharitidae) parasitoid wasps are common throughout tropical and subtropical environments worldwide, with only a few widespread species found in temperate environments in the Nearctic. Oraeseminae are specialised parasitoids of the ant subfamily Myrmicinae (Clausen, 1941; Heraty, 1994b; Heraty, 2000; Heraty, 2002; Lachaud & Pérez-Lachaud, 2012), which includes some of the world's most invasive ant genera: *Pheidole* Westwood, *Solenopsis* Westwood, *Wasmannia* Forel, and *Monomorium* Mayr (GISD, 2015). The most common host based on the vast majority of host records (Table 1.1) is *Pheidole*, a genus with a worldwide distribution and a well-documented single dispersal event from the New World to the Old World (Moreau, 2008), estimated to have occurred in the Middle Miocene (11–13 Ma) (Ward *et al.*, 2015; Economo *et al.*, 2019) or Late Oligocene (22–27 Ma) (Economo *et al.*, 2015a; Economo *et al.*, 2015b). If the ancestral host of Oraeseminae is *Pheidole*, it would be expected that they would have dispersed intercontinentally together or at least Oraeseminae would have been absent from the Old World prior to the arrival of *Pheidole*. However, a prior phylogenetic analysis of Eucharitidae (with limited sampling within Oraeseminae) using five gene regions suggested the New World clade within Oraeseminae was derived from the Old World taxa approximately 20–23 Ma (Murray *et al.*, 2013).

This intercontinental inverse dispersal between a parasitoid and its host seems counterintuitive and thus needs to be rigorously tested with increased taxon and gene sampling.

Oraeinae have a dynamic and unconventional life history whose evolution can be better understood within a phylogenetic framework (Fig. 1.1). These wasps use a specialised (expanded) ovipositor to hollow a cavity in plant tissue in which one or more eggs are deposited (Clausen, 1940b; Heraty, 2000). The first instar larvae (planidia; <0.15 mm in size) emerge on the plant and are responsible for gaining access to the ant brood. The larvae are hypermetamorphic (Pinto, 2009), meaning that the active sclerotised planidia do not closely resemble the later larval instars, which are sessile and hymenopteriform (Wheeler, 1907; Clausen, 1940a; Heraty, 2000). The exact means by which the planidia infiltrate the ant colony have never been directly observed; however, it is presumed that planidia gain access by targeting one of the ants' food sources. Proposed mechanisms include random attachment to foraging ants, phoretic attachment to an intermediate host (prey item) such as immature leafhoppers or thrips, or aggregating near or in extrafloral nectaries (EFNs) of plants and being picked up by feeding ant workers (Clausen, 1941; Das, 1963; Wilson & Cooley, 1972; Johnson *et al.*, 1986; Carey *et al.*, 2012; Herreid & Heraty, 2017). In the latter case (and perhaps all cases), the planidia are proposed to be transported by the adult ants within the infrabuccal pocket in their mouthparts and passed to the ant larvae via trophallaxis (Herreid & Heraty, 2017). With any of these nest infiltration methods, a tight tritrophic association is required, in which the plant has to be available and a suitable host for both the wasp and foraging ants.

Oraseminae species tend to specialise on certain plant structures for oviposition. The preferences can be partitioned into those that deposit eggs into leaves or green stems (or banana skins), into involucre bracts of unopened flower buds, and near EFNs (Heraty, 1994a; Heraty, 1994b; Heraty, 2000; Carey *et al.*, 2012; Herreid & Heraty, 2017). Some species have very specific plant hosts, for example, *Orasema simulatrix* Gahan oviposits only near leaf EFNs of *Chilopsis linearis* (Cav.) Sweet (desert willow), while for others plant hosts can be very broad, for example, *Orasema simplex* Heraty oviposits onto the leaves of at least eight plant families (Varone & Briano, 2009). Generalist species likely focus more on a particular plant structure rather than plant species. None of the Old World species have been associated with oviposition into the involucre bracts of flower buds, which is likely derived behaviour within the New World *Orasema* Cameron, instead choosing either leaves or green stems (Das, 1963; Kerrich, 1963; Heraty, 2000). Because of a general focus on plant structure over plant species, we expect that plant host is not likely to be a limiting factor for establishment and spread of many of the species.

Once the planidium is carried back to the nest and attaches to an ant larva, it will feed in a state of semi-arrested development until the host ant pupates (Wheeler, 1907; Clausen, 1940a; Clausen, 1941). In all known Oraseminae, the planidium burrows just under the larval cuticle, usually on the dorsal thoracic region, and the larva then feeds and expands (sometimes over 100× its original size) without changing instars (Wheeler, 1907; Heraty, 2000). After the ant pupates, the wasp migrates to the ventral region of the thorax and develops through its second and third instars, which results in a desiccated living ant

pupa that cannot continue its development (Wheeler, 1907; Clausen, 1940a; Heraty & Murray, 2013). All myrmicine ants have naked pupae (lacking cocoons), and thus, parasitoid larvae are exposed throughout their development. *Formica* L. (Formicinae) (Johnson *et al.*, 1986) and *Eciton* Latreille (Dorylinae) (Heraty, 1990; Heraty, 1994b) have been proposed as potential Oraseminae hosts based on indirect associations in the field (they were not observed developing in nests). However, the complete pupal cocoons of these genera make them unlikely associations for an orasemine parasitoid. We are confident that neither *Eciton* nor *Formica* are valid host associations, leaving only Myrmicinae as a host for the entire subfamily.

Pheidole comprises the majority of host records, both numerically and in all biogeographic regions where Oraseminae is found (Table 1.1). Among the other credible host records, *Solenopsis* is a known host for species in five New World species groups of *Orasema* (Wheeler, 1907; Wheeler & Wheeler, 1937; Heraty *et al.*, 1993; Varone *et al.*, 2010). In a few cases, *Pheidole* is one of several hosts, for example, *O. minutissima* Howard attacks both *Wasmannia* and *Pheidole* in the Caribbean (Mann, 1918; Heraty, 1994a; Burks *et al.*, 2018), *Orasema minuta* Ashmead attacks both *Temnothorax* Mayr and *Pheidole* in Florida (Heraty, 1990), and an undescribed species of *Orasema* in Mexico (sp. 2 near *bakeri*) attacks both *Tetramorium* Mayr and *Pheidole* (Heraty, 1990). *Monomorium* is the host of *Zuparka monomoria* (Heraty) from Madagascar (Heraty, 2000), and it is the only known host in the Old World other than *Pheidole*. Thus, use of a host other than *Pheidole* is both rare and geographically differentiated.

Oraseminae is one of four subfamilies within Eucharitidae (Burks, 1979; Bouček, 1988; Heraty, 2002; Heraty *et al.*, 2004). It is the second most diverse subfamily (after Eucharitinae), including 13 genera and 89 described species (Heraty, 2017). Until recently, Oraseminae included four genera: *Orasema sensu lato* (worldwide), *Indosema* (Afrotropical/Indian), *Timioderus* (Afrotropical), and *Orasemorpha* (Australasian) (Heraty, 1994b; Heraty, 2000; Heraty, 2002). In all previous phylogenetic analyses of this subfamily using molecular data, *Orasema s.l.* was polyphyletic (Heraty *et al.*, 2004; Heraty & Darling, 2009; Murray *et al.*, 2013). Based largely on preliminary analyses with the data presented herein, the Old World Oraseminae were revised and are now represented by 12 genera (Burks *et al.*, 2017). *Orasema sensu stricto* is now recognised as an exclusively monophyletic New World genus and is by far the most diverse in terms of morphology, life history, and geographic distribution, ranging as far north as southern Canada (50.2°N) and as far south as central Argentina (40.5°S), and containing nine *Orasema s.s.* species groups (Heraty, 2000). Our analyses herein constitute the most comprehensive attempt at determining the relationships among the genera and species groups of Oraseminae, both in terms of taxon and gene sampling. Taken together, a taxon- and sequence-rich phylogeny of Oraseminae obtained from combining Sanger and AHE datasets enables examination of their complex life histories, host associations, biogeography and timing relative to their hosts, and serves as a framework for future classification.

Methods and Materials

Georeferencing

We documented the worldwide distribution and abundance of Oraseminae using a total of 12,673 specimens of Oraseminae that were databased and georeferenced in FileMaker Pro 11.0v.3 ® using material borrowed from over 70 museum collections. Unless exact coordinates were provided on the label, coordinates were estimated using Google Earth (earth.google.com). Collection localities were plotted using Google Maps (maps.google.com).

Taxon Sampling

Analyses were performed on the following three datasets:

1. The “Sanger sequencing dataset” (Sanger) contains 203 taxa in the family Eucharitidae with 164 specimens of Oraseminae and 39 outgroup taxa from three subfamilies: Akapalinae (1 specimen), Gollumiellinae (6), and Eucharitinae (32). All genera in Oraseminae except *Matantas* Burks & Heraty from New Caledonia are represented. All described species groups, as well as some newly proposed species groups and unplaced taxa within *Orasema* are represented (Heraty, 1994b; Heraty, 2000) (Table S1.2). The previously proposed *smithi*- and *costaricensis* species groups have been redefined as the *stramineipes* species group (Burks *et al.*, 2018), and the *tolteca* group has been sunk into the *cockerelli* group. We also recognise two new morphologically distinct species groups, the *sixaolae*- (previously in *smithi* species group) and *susanae* species groups. Several species cannot as yet be placed confidently

into defined species groups and may require recognition of additional species groups; however, these do not include any described species, which precludes their definition at this time.

2. The “Anchored Hybrid Enrichment dataset” (AHE) contains 92 eucharitid taxa, with 85 specimens of Oraseminae and 7 outgroup taxa representing all three previously mentioned subfamilies. All of the AHE taxa were included in the Sanger dataset with the exception of *Akapala* (explained below). Eight of the 12 Old World genera (12 specimens) and 9/10 species groups (described and new) of *Orasema* (73 specimens) are represented. *Orasema* was intensively sampled for future species delimitation in particularly difficult species groups: the *coloradensis* species group (14 specimens), *cockerelli* species group (18 specimens), and *stramineipes* species group (19 specimens) (Table S1.2).

3. The “Sanger+AHE dataset” (Combined) contains 229 taxa. In this combined taxon set over half of the samples are represented by Sanger data only, thus allowing us to provide a combined phylogeny but potentially being complicated by missing data. The taxa are the same as those in the Sanger set with the following exceptions. *Akapala astriaticeps* (Girault) is a chimera of two specimens from the same collection event (D4286, AHE data; and D0360a, Sanger data), *Orasema yaax* Burks *et al.* is a chimera of two species from the same collection event (D4079, AHE; and D3733, Sanger), and *Orasema coloradensis* (D4891) used the Sanger data of another specimen from the same collection locality (D3756) for the BEAST analysis. The following taxa were included in the Combined dataset but excluded from the Sanger dataset to reduce redundancy

because they matched other specimens with more complete Sanger data: *Colocharis napoana* Heraty (D4288), *Orasema coloradensis* (D3148, D3227, D4213, D4219, D4221, D4520, D4653, D4891), *O. near coloradensis* (D3937), *O. costaricensis* Wheeler & Wheeler (D4628), *O. evansi* Burks *et al.* (D3799, D3765, D4648), *O. minutissima* (D4207, 3810, 2766, 2808), *O. rapo* (Walker) (D3808), *O. simulatrix* (transcriptome), *O. sixaolae* Wheeler & Wheeler (D2683, D4694), *O. stramineipes* Cameron (D4705), *Orasema* sp. (D4230), and *Zuparka fisheri* Heacox & Dominguez (D0638b).

Specimens were collected from malaise traps, yellow pan traps, ant nests, or sweep netting vegetation and stored in 95% ethanol at -80° C for tissue preservation. Voucher specimens were imaged, databased, point mounted, and specimens were deposited with identification numbers in the museums listed in Table S1.2. The majority of extracted specimens are primary DNA vouchers (used for sequencing), but in the few cases where the primary voucher was destroyed, we created secondary DNA vouchers from specimens included in the same collecting event.

Gene Sampling

Extraction. Most specimens were extracted using DNeasy[®] blood and tissue kit manufactured by Qiagen (Valencia, CA, USA) with 1 µL RNase A added after incubation, but some older extractions were performed with phenol-chloroform or Chelex[®] following the methods of Heraty *et al.* (2004). PCR products were purified with DNA Clean & Concentrator[™] -5 kits by Zymo Research (Irvine, CA, USA). PCR

product concentrations were determined using Nanodrop 2000c (Thermo Scientific™) or Qubit® 2.0 Fluorometer (Invitrogen).

Sanger sequencing. The Sanger sequencing dataset includes 5 gene regions: 18S ribosomal DNA, 28S D2 rDNA, 28S D3–5 rDNA, COI barcoding mitochondrial DNA, and COI NJ mtDNA. Each gene was PCR amplified individually and Sanger sequenced from both primers. Samples for Sanger sequencing were sent to Retrogen Inc. (San Diego, CA, USA) for sequencing on an Applied Biosystems 3730xl DNA Analyzer. Chromatograms were inspected for base calling errors and edited in Mesquite v.3.31 (Maddison & Maddison, 2017b) using Chromaseq v.1.2 (Maddison & Maddison, 2017a). In four cases where Sanger sequencing failed for specimens with AHE data, partial sequences of the genes were recovered from unmapped AHE reads using aTRAM (Allen *et al.*, 2015) and closely related reference sequences from the Sanger dataset. Sequences were uploaded to GenBank with the accession numbers listed in Table S1.2. The concatenated alignment is 3,046 characters. The primers, alignment lengths, and thermocycler protocols are listed in Table S1.3.

AHE locus selection and probe design. The AHE probe set that we initially used was developed for Ichneumonoidea (Hymenoptera) (Sharanowski *et al.*, in prep). We refer to this probe set as *Hym_Ich*. As a starting point, this probe set leveraged the 941-locus Coleoptera alignments developed by Haddad *et al.* (2017). These 941 loci were derived by identifying homologous coding regions across 13 insect species, including representatives of Hymenoptera, Diptera, Lepidoptera, Strepsiptera, Coleoptera, Anoplura, and Hemiptera, which were aligned and used to target conserved, single-copy

exons compared to Coleoptera reference genomes for a Coleoptera-specific probe set. Using the same approach, a Hymenoptera-specific enrichment kit was developed using references from Hymenoptera. Methods for AHE locus selection and probe design followed Hamilton *et al.* (2016). For the 941 loci, the assembled reference genome of the red flour beetle (*Tribolium castaneum*) was used to identify and extract the best matching region in each of the two Hymenoptera genomes, the bumblebee (*Bombus impatiens*) and a parasitoid wasp (*Nasonia vitripennis*). The extracted regions were then aligned using MAFFT (v7.023b, with `-genafpair` and `-maxiterate 1000` flags, Katoh & Standley (2013)). To increase representation of diverse lineages across Hymenoptera in the *Hym_Ich* probe set, 12 assembled hymenopteran genomes (*Apis mellifera* (The Honeybee Genome Sequencing Weinstock *et al.*, 2006); *Bombus impatiens* (Sadd *et al.*, 2015); *Nasonia vitripennis* (The Nasonia Genome Working Werren *et al.*, 2010); seven ant species (Gadau *et al.*, 2012); and two braconid genomes including *Microplitis demolitor* (Burke *et al.*, 2018) and *Diachasma alleoleum*, (NCBI GCA_001412515.1 unpublished i5K genome, Hugh Robertson)) and 11 Illumina sequenced unassembled ichneumonoid genomes covering both Braconidae and Ichneumonidae (Sharanowski *et al.*, in prep) were scanned for anchor regions using the *Nasonia vitripennis* sequences as a reference from the pairwise alignments generated above. For the 12 assembled genomes, 4,000 bp surrounding the region that best matched the reference were isolated, and each sequence was used for probe design. For the unassembled genomes, reads were merged and trimmed following Rokyta *et al.* (2012) and then mapped to the reads of the *Nasonia vitripennis* sequences. The consensus sequences from the resulting assemblies were then

extended into the flanks, producing up to a 4,000 bp sequence for each species at each locus. Alignments were generated for each locus from each of the 24 target species using MAFFT. After visual inspection in Geneious (Kearse *et al.*, 2012), the alignments were trimmed and masked such that flanking regions not containing all of the reference sequences were trimmed out and sequences obviously misaligned in internal regions were masked to produce well-aligned regions containing no poorly aligned sequences. To ensure sufficient enrichment efficiency, we removed loci that contained fewer than 50% of the taxa. Kmer profiles were analyzed to identify and mask repetitive alignment regions in each locus, following Hamilton *et al.* (2016). This process resulted in 528 anchor loci and 13 loci targeted for their function (total target size is 212,392 bp). These loci are represented with 120 bp probes tiled at 2X density across each of the 24 sequences to produce 57,066 probes.

For Chalcidoidea, we aimed to improve the enrichment efficiency of the *Hym_Ich* target loci through comprehensive representation of the superfamily and related outgroups in Proctotrupomorpha using chalcid sequences from 47 assembled 1KITE transcriptomes and two published genomes (see Table S1.6 for details) (Peters *et al.*, 2018). We refer to this new probe set as *Hym_Cha*. The same general procedure was followed for probe design as with *Hym_Ich*. More specifically, following Hamilton *et al.* (2016), we scanned each genome and transcriptome for the target anchor regions using single exon *Nasonia vitripennis* probe region sequences as references. For each locus, we then isolated up to 4,000 bp containing the best matching region for each species, which in many cases now spanned multiple exon regions, and then aligned the resulting

sequences across species using MAFFT. Following visual inspection in Geneious, we trimmed the alignments down to well-aligned regions and masked poorly aligned regions. After removing overlapping regions of adjacent loci, we identified and masked repetitive regions in the alignments (see Hamilton *et al.* (2016) for methodological details). The final alignments resulting from this procedure contained 421,012 sites distributed across 441 loci. We tiled 120 bp probes at 1.8X density across all sequences in each alignment. After removing redundant probes, the final probe set contained 171,070 probes.

Our AHE dataset includes specimens sequenced from the *Hym_Ich* (42 taxa) and *Hym_Cha* (49 taxa) probe sets (Table S1.2) and the *Orasema simulatrix* transcriptome. The *Hym_Cha* probe set includes the same but fewer loci than *Hym_Ich*, but with extended probe regions for included loci. Using the additional reference taxa, we reassembled, aligned, and masked the read data for our final taxon set using the same methods above and trimmed the alignments to exclude data not present in taxa sequenced from the *Hym_Ich* probe set.

AHE data collection. AHE data were collected at the Center for Anchored Phylogenomics (www.anchoredphylogeny.com). Extracted DNA was used for 8-bp single-indexed library preparation following Lemmon *et al.* (2012) and Prum *et al.* (2015). The indexes were chosen so that at least two differences existed between all combinations. During demultiplexing, reads with indexes that did not match exactly to one of the expected indexes were removed (no tolerance for mismatched indexes). Libraries were combined equally into ~16-sample pools prior to enrichment using the *Hym_Ich* or *Hym_Cha* probe sets contained within an Agilent XT SureSelect kit.

Enriched library pools were further pooled and sequenced on 2 PE150 Illumina 2500 lanes (~46 samples per lane, 96Gb of total sequencing effort). After removing poor quality reads using the Casava high chastity filter, paired reads were demultiplexed (with no mismatches tolerated) then merged following Rokyta *et al.* (2012). Merged and unmerged reads were assembled with a quasi-de-novo assembler (Hamilton *et al.*, 2016) using *Orasema simulatrix*, *Eucharis adscendens*, *Sycophila biguttata*, and *Eurytoma brunniventris* as references. To reduce the effects of possible low levels of misindexing and sample contamination, the resulting assembly clusters containing fewer than 25 reads were removed from downstream analyses. Consensus sequences from clusters passing the filter were then compared to generate a pairwise sequence similarity matrix that was used to determine orthology (see Hamilton *et al.* (2016) for details). After aligning orthologous sequence sets in MAFFT (v.7.023b, with `genafpair` and `-maxiterate 1000` flags, Katoh & Standley (2013)), alignments were auto-trimmed as follows: 60% identity was required to designate a site as conserved, sequence regions containing less than 10 of 20 common bases in conserved sites were masked, and sites containing fewer than 38 unmasked, unambiguous characters were removed (details of the auto-trimmer given in Hamilton *et al.* (2016)). Finally, alignments were inspected in Geneious v.9 (Kearse *et al.*, 2012), and all remaining misaligned regions were removed. The final AHE alignments contained 92 taxa, 348 loci, and 279,468 characters with 16.6% missing data. There is very little variation in AT/GC content among taxa in these datasets (Table S1.7).

Combining datasets. The Combined dataset contains the AHE dataset concatenated with the Sanger dataset for a total of 353 loci and 282,514 characters with

approximately 66% missing data (~51% of the missing data is from Sanger specimens with no AHE data).

Deposition

Aligned matrices, partition files, probe sequences, and program files are deposited in Dryad (doi:10.5061/dryad.df66th2). Sanger sequences and AHE read data are available in GenBank.

Phylogenetic Analyses

Alignments for Sanger sequencing data were performed in MAFFT v.7 with the E-INS-i option selected (Katoh & Standley, 2013). Individual gene alignments were concatenated with SequenceMatrix (Vaidya *et al.*, 2011). All final alignments were spot checked in Geneious v.10.2.3 (Kearse *et al.*, 2012).

The Sanger matrix was partitioned with the following scheme: 18S, 28S D2, 28S D3–5, COI BC/NJ (1st and 2nd codon positions), and COI BC/NJ (3rd codon positions). Two different partitioning schemes were tested for the AHE data matrix: 1) partitioning by gene region (348 partitions), and 2) partitions resulting from PartitionFinder 2 (Lanfear *et al.*, 2017) using the rcluster search (Lanfear *et al.*, 2014) with the --raxml option (Stamatakis, 2006) (151 partitions). Both schemes resulted in identical RAxML phylogenies with negligible differences in bootstrap support values, and further analyses were partitioned only by gene region. The Combined dataset was a combination of the 5 Sanger partitions plus the 348 AHE partitions, resulting in 353 partitions. The Sanger, AHE, and Combined datasets were analyzed with parsimony and maximum likelihood to

check for consistency and the influence of a model-based approach on inferences from the dataset. Parsimony analyses were performed with TNT v.1.1 (Goloboff *et al.*, 2008) and PAUP* v.4.0a (Swofford, 2002) using equal weights. TNT analyses were run using the New Technology Search and default settings for Sectorial Search, Ratchet, Drift, and Tree Fusing, and finding the minimum length 10 times. PAUP* analyses were performed using Stepwise Addition Search and 100 replicates, and in cases where TNT found a shorter tree, PAUP* was used to verify the TNT trees and to assess tree statistics. Maximum likelihood analyses were performed in RAxML-HPC2 v.8.2.10 on XSEDE (Stamatakis, 2014) via the CIPRES Science Gateway (Miller *et al.*, 2010) using default parameters (GTRCAT for rapid bootstraps and GAMMA for ML optimization) from two different starting seeds (12345 and 98765) to check that the trees converged on the same topology.

Dating Analyses

All dating analyses were performed in BEAST v.2.4.4 (Drummond & Rambaut, 2007) on XSEDE via the CIPRES Science Gateway (Miller *et al.*, 2010) or through the University of California, Riverside computing cluster. For the Sanger dataset, we included all five gene regions with no *a priori* constraints on the topology. In the Combined dataset, there is a large amount of missing data for taxa without AHE. Because of this, our BEAST analysis of the combined data used only the five Sanger genes to calibrate dates on a fixed tree topology from the Combined RAxML analysis, which was made ultrametric using non-parametric rate smoothing in Mesquite.

Dates were calibrated for these analyses using a relaxed lognormal molecular clock using the Baltic amber (44.1 ± 1.1 Ma; Ritzkowski, 1997) fossil taxon *Palaeocharis rex* (Eucharitidae: Eucharitinae) (Heraty & Darling, 2009) to constrain the stem of *Psilocharis* following the methods of Murray *et al.* (2013). While there is contention about the exact date of Baltic amber (37.7 ± 3 Ma; Kaplan *et al.*, 1977; Perkovsky *et al.*, 2007), we chose to use the dates from Ritzkowski (1997) to keep results comparable to Murray *et al.* (2013). The prior for this node was set to lognormal with the mean (in real space) at 8.08, standard deviation at 1.0, and offset at 39.2, with dates estimated from two independent runs with 500 million generations each, sampling every 50,000 for the Sanger analysis and one run with 50 million generations, sampling every 50,000 for the Combined analysis. Tracer v.1.6.0 (Rambaut *et al.*, 2014) was used to verify that the chains reached an appropriate effective sample size (ESS) and converged. LogCombiner v.2.4.4 and TreeAnnotator v2.4.4 were used to remove 10% of the trees as burnin and compute the maximum clade credibility tree (MCC).

The AHE dataset was too large to effectively sample in BEAST, so subsets of 25 loci were selected for branch length calibration on a fixed tree topology (AHE RAxML tree) that was made ultrametric with non-parametric rate smoothing in Mesquite. Three independent subsets were selected based on their phylogenetic informativeness profiles resulting from PhyDesign (Lopez-Giraldez & Townsend, 2011) with a JC model: the first subset contained the 25 highest ranked loci (1st–25th) for phylogenetic informativeness over the time period encompassing the diversification of the ingroup (from the crown to terminal bifurcations of Oraseminae), the second subset contained the next 25 most

informative loci for that time period (26th–50th), and the third subset followed the same pattern (51st–75th) (Table S1.4). Alternative evolutionary models were tested in PhyDesign, but had no effect on the ranking of loci. Only one specimen of *Psilocharis* was sampled for AHE; since the *Palaeocharis* fossil calibration could no longer be used at the stem of *Psilocharis* (lack of a *Psilocharis* node), we chose instead to use a secondary calibration date for the crown of Eucharitinae from Murray *et al.* (2013). The crown node age of Eucharitinae was set to a normal distribution with the mean at 52.0, sigma at 7.8, and offset at 0.95, which gives a 95% probability range of 40.1–65.8 Ma. A uniform root age prior of 45–100 Ma was used to constrain the maximum age, and 100 Ma was conservatively chosen for the maximum based on oldest fossil Chalcidoidea known: Mymaridae in Cretaceous amber from upper Albian deposits (Poinar & Huber, 2011). The three data subsets were each analyzed from a single run using the fixed tree AHE topology for 150 million generations sampled every 20,000 to test for congruence amongst dates. Maximum clade credibility trees were computed using the same methods as the other datasets.

Host Associations

Ancestral host mapping was performed on the RAxML tree from the Combined dataset using unordered parsimony reconstruction in Mesquite. This tree was chosen because it is the most taxon inclusive dataset and also is in accordance with the topology of the AHE results. Outgroups were coded for host ant subfamily (Ectatomminae, Formicinae, Myrmeciinae, and Ponerinae), whereas all Oraseminae only parasitise

species in the subfamily Myrmicinae. Because the host ant subfamilies do not overlap between our outgroups and ingroup, we coded Oraseminae for host ant genus (*Monomorium*, *Pheidole*, *Solenopsis*, *Temnothorax*, and *Wasmannia*). Taxa with unknown hosts were left ambiguous if no closely related taxa (same genus or species group of *Orasema*) had known hosts, but if closely related taxa had a host record, then it was carried over to other species in the same clade. See Table 1.1 for complete host information.

Biogeography

Biogeographic analyses were run on the Combined BEAST chronogram as it was the most taxon inclusive. Dispersal-Extinction-Cladogenesis (DEC) with and without jump dispersal (DEC+J) models (Matzke, 2014) were tested using BioGeoBEARS (Matzke, 2013). Biogeographic regions included: Nearctic, Neotropical, Australasian, Oriental, Afrotropical, Madagascan, Indian, and Palearctic. Dispersal probability multipliers between regions were established for each historical epoch (Walker *et al.*, 2012) in the dated phylogeny (Table S1.5). These values were chosen subjectively using the methods of Condamine *et al.* (2013) (based on the principles of Ree & Smith (2008)) and based on palaeogeographic reconstructions of the continents through time (Blakey, 2008). The dispersal probability for travelling from any biogeographic region to itself was set to 1; regions that were connected without a significant barrier were given a rate of 0.5; regions that were separated by a narrow barrier, such as an ocean strait splitting two relatively close landmasses, were given a rate of 0.25; any combination of the above

scenarios had a probability that was the product of multiplying the other probabilities (e.g. region 1 is connected to region 2, which is narrowly separated from region 3; the probability of going from 1 to 3 is $0.5 \times 0.25 = 0.125$); and any dispersal separated by more than two unconnected regions was given a probability multiplier of 0.01.

Diversification Analysis

Diversification rates were assessed in the program BAMM (Bayesian Analysis of Macroevolutionary Mixtures) (Rabosky *et al.*, 2014) using the BEAST tree for the Combined dataset to maximise taxon inclusion. Taxon sampling percentages were calculated for Old World genera and species groups in *Oreasema* (or estimated for groups currently under revision) and used in the analysis to account for missing taxa. *Matantias*, the only unsampled genus, was accounted for in the global sampling fraction. The MCMC chain was run for 1 million generations, reaching stationarity, and sampled every 1,000. Ten percent of the chain was discarded as burn-in. Statistics for the analysis were examined in the R package BAMMtools (Rabosky *et al.*, 2014).

Coalescence

To assess the impact of coalescence on the tree topology, we ran a coalescent analysis in ASTRAL-II v.4.10.12 (Mirarab & Warnow, 2015). We generated 348 gene trees in RAxML for the AHE dataset with 100 rapid bootstraps per tree. Gene trees were visually inspected for anomalous relationships as a measure of quality control. Distantly-related taxa appearing identical (contamination) and ingroup taxa on excessively long

branches (sequencing error) were removed. Branches in gene trees with bootstrap scores of 10 or less were contracted into polytomies with the software Newick Utilities (Junier & Zdobnov, 2010).

Likelihood Mapping

To rigorously assess the support of Old World Oraseminae paraphyly, support for the sister relationship between *Leiosema* and the remaining orasemine taxa in the AHE dataset (RAxML AHE tree) was further tested using quartet likelihood mapping in the software TREE-PUZZLE v.5.3 (Schmidt *et al.*, 2002). Taxa were binned into four groups: a) outgroups (7 taxa), b) *Leiosema* (2 taxa), c) *Timioderus* (2 taxa), and d) remaining Oraseminae (81 taxa). These four groups represent the four connection points to the internal branch separating *Leiosema* from the remaining Oraseminae on an unrooted tree. Each sampled quartet selects one random taxon from each of the four groups. Support is established by comparing how many times each of the three possible topologies (four taxon unrooted trees) is sampled. We sampled 10,000 random quartets.

Results

Georeferencing

The map of Oraseminae collection localities (Fig. 1.2) is a comprehensive summary of the distributions of each genus, as well as an indication of the relative abundances of those genera. *Orasema* are noticeably more common and diverse in the

New World, when compared to Oraseminae in the Old World. While this is likely impacted by collecting bias, extensive collecting by JMH in both hemispheres supports the conclusion that the Old World genera of Oraseminae (700 specimens) are far less plentiful than *Orasema* in the New World (11,845 specimens).

Sanger Sequencing

For the 203 specimens included in the Sanger dataset: 18S was successfully sampled for 173 specimens (complete or partial sequences), 28S D2 for 203 specimens, 28S D3–5 for 193 specimens, COI BC for 74 specimens, and COI NJ for 144 specimens, with a total of 28.1% missing data (specimen data and GenBank numbers in Table S1.2, alignment lengths in Table S1.3). COI sequences were manually checked for stop codons to identify and remove NUMTs, which were only found in COI BC of a single species, *Orasema minutissima*.

Anchored Hybrid Enrichment

The anchored hybrid enrichment dataset contains 348 gene regions with a total alignment length of 279,468 nucleotides for 92 taxa. An average of 83 taxa were successfully captured per locus (standard deviation is 8.1), with 16.5% missing data overall, and the average locus length was 803 bp (standard deviation is 325.8).

Combining Data Matrices

Having a large proportion of missing data is a necessary consequence of concatenating a taxon-rich Sanger dataset with a character-rich AHE dataset. Taxa that only have Sanger sequence data (missing AHE) comprise 52% (119/229) of the sampled taxa, which accounts for at most ~1% of the total data (3,046/282,514 characters). Thus, 51% of the data in the Combined matrix is missing because of concatenating the Sanger and AHE matrices, resulting in a total of 66.1% missing data.

Phylogenetic Analyses

Sanger dataset. Parsimony (Fig. 1.6) and maximum likelihood (ML) (Fig. 1.9) analyses of the Sanger sequencing dataset produced slightly different tree topologies; both support the monophyly of Oraseminae and the reciprocal monophyly of the Old World Oraseminae and New World *Orasema*. A strict consensus of the 20 most parsimonious trees (4,161 steps, Retention Index=0.73) was poorly resolved, although Eucharitinae and Eucharitini (excluding *Neolosbanus* and *Psilocharis*) were monophyletic, and Oraseminae (Bootstrap Score=94), Old World Oraseminae (BS<50), and *Orasema s.s.* (BS=65) were each monophyletic. The best scoring ML analysis (Fig. 1.9) had outgroup relationships that were in accord with Murray *et al.* (2013), including monophyly of Gollumiellinae and a sister group relationship between *Psilocharis* (the fossil reference taxon) and the remaining Eucharitinae. Oraseminae (BS<50), Old World Oraseminae (BS=72), and *Orasema s.s.* (BS=95) were each monophyletic. The ML tree supports the monophyly of all of the Old World genera, with exception of the genus

Hayatosema from Africa and Southeast Asia, which was polyphyletic. The species groups of *Orasema* in the ML analysis are mostly monophyletic, with the exception of the *cockerelli*- and *xanthopus* species groups.

AHE dataset. Parsimony analysis of the anchored hybrid enrichment dataset (Fig. 1.7) produced a single tree with 412,925 steps (RI=0.77), which was nearly identical to the ML tree (Fig. 1.10). All ML analyses for this dataset produced identical trees regardless of starting seed or partitioning scheme. The two differences between the parsimony and ML trees include a paraphyletic Gollumiellinae (outgroup) in parsimony versus being monophyletic in ML and slightly different positions of *Cymosema waterworthae* Burks & Mottern and *Ivieosema confluens* Burks within the Old World Oraseminae; neither hypothesis is highly supported by bootstrap scores in either analysis. Otherwise, phylogenies resulting from both analyses are highly supported at both deep and shallow nodes. Oraseminae (BS 100 MP/100 ML) and *Orasema s.s.* (BS 100/100) were each monophyletic, but in contrast to the Sanger results, the Old World Oraseminae were always paraphyletic with *Leiosema* monophyletic and sister to the remaining Oraseminae (BS 100/100). All of the species groups of *Orasema s.s.* were monophyletic and strongly supported (BS 100/100) in both analyses. Relationships between species groups and the *incertae sedis* species were identical in both analyses with high support (BS 100/100) for all but the single *bakeri* group species. The coalescent analysis in ASTRAL produced a species tree that was highly congruent with the tree topologies of concatenated analyses with the position of *Timioderus* and *Ibitya* shifted slightly within the Old World group (Fig. 1.18).

To further assess support for the *Leiosema* sister group relationship, which is important to our biogeographic hypotheses, all gene trees were scored based on the position of *Leiosema*: 42.5% unequivocally support *Leiosema* as sister to the remaining Oraseminae, 36.5% do not support this relationship, and 21% are ambiguous (often because of missing outgroups). Additionally, likelihood mapping resulted in 64.1% of sampled quartets supporting the relationship: (outgroup, *Leiosema*), (*Timioderus*, other Oraseminae); 35.5% of quartets support: (outgroup, other Oraseminae), (*Leiosema*, *Timioderus*); and support for other hypotheses is negligible (Fig. 1.5).

Combined dataset. Parsimony and ML analyses of the Combined dataset produced trees with similar topologies but with much lower support on the parsimony tree (Figs 1.8 and 1.11, respectively). In accordance with other analyses, Oraseminae (BS <50 MP, 99 ML) and *Orasema s.s.* (BS 95/100) were each monophyletic, and in accordance with the AHE results, the Old World Oraseminae were paraphyletic with *Leiosema* monophyletic (BS 55/100) and sister to the remaining Oraseminae (BS <50/86). Within *Orasema s.s.*, species groups were monophyletic, with only the *xanthopus* species group not monophyletic in both analyses (Figs 1.8, 1.11), and the *cockerelli* species group not monophyletic in the parsimony analysis (Fig. 1.8). The relationships between species groups in the Combined ML tree were the same as in the AHE trees, whereas the parsimony tree had low support and slightly different relationships. The *susanae* species group was not sequenced for AHE and was placed between the *festiva*- and *stramineipes* groups in both results.

Dating Analyses

The BEAST analysis of the Sanger dataset (Fig. 1.12) was the only dating analysis not constrained by a fixed tree topology because the size of the dataset was within the limits of the computational power of BEAST. Even so, this dataset was run on a computing cluster for increasingly long generation times (up to 500 million), and with two runs combined, only reached a moderate effective sample size (ESS posterior=135). Because this is the only BEAST analysis generated without a fixed tree topology, it is the only tree where we report posterior probability values. The topology of the BEAST tree is nearly identical to the ML tree with all of the genera and species groups recovered and only a few changes in species group relationships within *Orasema* (*bakeri*-, *simulatrix*-, *wayqecha* groups, and some *incertae sedis*). Oraseminae and *Orasema s.s.* are fully supported (posterior=100). The mean crown age of Oraseminae is 34 Ma (95% HPD=23–45) and the mean crown age of *Orasema* is 25 Ma (95% HPD=17–34).

Three BEAST analyses run on different subsets of the AHE dataset were performed on the fixed AHE ML tree topology (Fig. 1.10). The ‘Top25’ (Fig. 1.3) and ‘26–50’ (Fig. 1.13) subsets reached reasonable posterior ESS values at 150 million generations (posterior ESS=284 and 158, respectively); however, the analysis for ‘51–75’ subset (Fig. 1.14) ended prematurely around 6.1 million generations but still achieved high ESS values (posterior ESS=319). Because of the fixed tree topology, other ESS values across the three analyses were very high, typically ranging from 1000–6000, with the exception of the UCLD mean and standard deviation, which were less than 200. The variation in dates among the analyses is reasonably small (e.g. the mean crown age for

Oraseminae is 43 (26–58), 48 (31–67), and 45 (28–60) Ma, and the mean crown age of *Orasema* is 28 (17–39), 33 (20–46), and 29 (18–39) Ma for ‘Top25’, ‘26–50’, and ‘51–75’ respectively) (Figs 1.3, 1.13, 1.14).

Our dated analysis of the Combined dataset (Fig. 1.15) used the fixed Combined ML tree topology (Fig. 1.11) and only Sanger data, which is available for all taxa (30% missing data), to calibrate branch lengths. The mean crown age of Oraseminae is 35 (26–47) Ma, and the mean crown age of *Orasema* is 24 (17–33) Ma.

Taken together, these dates place the mean crown age of *Orasema* between 20–33 Ma, which spans the early Miocene to the early Oligocene, and the mean crown age of Oraseminae is between 30–48 Ma, which spans the early Oligocene to the early Eocene (Fig. 1.3).

Biogeography

Using the dated Combined tree topology and estimated dispersal rates (Table S1.5), both DEC (Fig. 1.16) and DEC+J (Figs 1.4, 1.17) analyses support an African origin for Oraseminae and a North American origin for *Orasema* in the New World. DEC+J shows higher support for these same conclusions and is a better fitting model with a lower AIC score. This is expected because the *j* parameter allows for founder-event speciation, in which dispersal can occur at cladogenesis (chance dispersal) rather than being restricted to anagenesis (range expansion) (Matzke, 2014). This may have happened with *Orasema*, where there was a single dispersal event into the New World

followed by a relatively rapid isolation event with the loss of favorable conditions for dispersal back across the BLB.

In the Old World, both DEC and DEC+J analyses support transitions from Africa through Oriental/Australasian regions leading up to a single New World dispersal event. While the support values along the Old World backbone are not strong across all phylogenetic analyses (Figs 1.6–1.12), there is strong support in every analyses for a single New World clade. Two independent dispersals to Australia are proposed, one in *Cymosema* and one in the *Orasemorphia/Australosema* clade. There are also two independent dispersals to Madagascar, once in the *Ibitya/Zuparka* clade and once in *Ivieosema*. All of these proposed dispersals occurred more recently than 30 Ma, long after Madagascar and Australia were separated from Africa (Sanmartín & Ronquist, 2004).

Ancestral Host Mapping

Parsimony reconstruction on the dated Combined ML tree topology (Fig. 1.5) inferred *Pheidole* to be the ancestral host along the backbone of the tree. As many as four separate shifts onto *Solenopsis* are inferred in the New World. Shifts onto other host genera, including *Monomorium*, *Wasmannia*, and *Temnothorax*, each happened once in *Zuparka monomoria*, *Orasema minutissima*, and *O. minuta*, respectively. The other host shift to *Tetramorium* is not shown because the taxon is missing from the phylogeny (*bakeri* group: *O. sp. 2 nr. bakeri* from Mexico) (Heraty, 1990).

Diversification Analysis

The diversification rate analysis from BAMM (Fig. 1.5) supported a single rate shift between the Old World and New World taxa with the highest probability (posterior probability = 0.3, the highest out of 42 credible shift sets). In other words, an increase in diversification rate in Oraseminae was most likely correlated to dispersing to the New World. The posterior probabilities of alternative credible shift sets drop off precipitously (e.g. 2nd most supported = 0.12, 3rd = 0.11, 4th = 0.034).

Discussion

Dating and Biogeography

The biogeographic history of Oraseminae and their primary host ants, *Pheidole*, is unique to the best of our knowledge because of their intercontinental dispersals in opposite directions around the same time period (Fig. 1.2). Sanger data support monophyly of both Old World and New World lineages, thus, no direction of dispersal can be inferred (Figs 1.6, 1.9, 1.12). All of the analyses that incorporate AHE sequence data (AHE and Combined datasets), however, unequivocally support an Old World to New World dispersal event indicated by a grade of Old World taxa leading to a single New World clade (Figs 1.7–1.8, 1.10–1.11). Given the magnitude of difference in the quantity of sampled loci and characters between Sanger (5 loci: 3,046 characters) and AHE (348: 279,468) datasets, the stability of the AHE data set (similar results in parsimony and ML; concatenation and coalescence), and additional support measures

(the majority of gene trees and sampled quartets favouring paraphyly in the AHE dataset), we conclude Old World paraphyly to be more likely. The opposite hypothesis (New World to Old World) is never supported in any analysis of Oraseminae, including analyses of independent loci. The dated analyses of Oraseminae (Figs 1.3, 1.12–1.15) place the mean crown age of *Orasema* between 24–33 Ma (Oligocene), which can be used as an estimate of the minimum age of dispersal to the New World. This is slightly older than the estimate of Murray *et al.* (2013), which is around 20 Ma. This range of dates is too recent for Gondwanan vicariance or dispersal across North Atlantic Land Bridges (NALB's), leaving dispersal across a Beringian Land Bridge (BLB) or chance oceanic dispersal as more likely hypotheses. By examining their host ant biogeography, we can further refine our biogeographic hypotheses.

Pheidole is the most parsimonious ancestral host for Oraseminae (Fig. 1.5); however, the host of *Leiosema*, which is sister to the rest of Oraseminae in all analyses incorporating AHE data, is unknown. The *Pheidole* dispersal from the New World to the Old World is highly supported by all molecular phylogenetic analyses of this genus (Moreau, 2008; Economo *et al.*, 2015a; Economo *et al.*, 2015b; Ward *et al.*, 2015; Economo *et al.*, 2019), but the age of the Old World crown group varies between analyses. The phylogeny of Ward *et al.* (2015) places the Old World crown age at approximately 12 Ma (Middle Miocene). This analysis used 27 fossil calibration points (20 within Myrmicinae; 7 outgroups), but their sampling of *Pheidole* was sparse (4 New World taxa; 3 Old World taxa). By comparison, the phylogeny of Economo *et al.* (2015b) placed the Old World crown age at approximately 22 Ma (Early Miocene) using an

extensive sampling of *Pheidole* (2 New World; 177 Old World) selected from an earlier undated analysis of 285 species (107 New World; 173 Old World; 5 widespread) (Economo *et al.*, 2015a), but this analysis lacks any calibration points except for a minimum age constraint on the root node (crown *Pheidole*) at 59.8 Ma (Economo *et al.*, 2015a) based on the phylogeny of Ward *et al.* (2015). The lack of calibration points in their analysis was due to the difficulty of assigning presumed *Pheidole* fossils to clades within the genus (Economo *et al.*, 2015a). The most recent analysis (Economo *et al.*, 2019) places the Old World crown age at 11–13 Ma based on 449 ingroup taxa and eight nuclear loci using the same calibration as Economo *et al.* (2015b). A *Pheidole* specimen assumed to be in Baltic amber (44.1 Ma; Dubovikoff, 2011) would have complicated the biogeographic scenario by preceding the earliest possible date for Old World *Pheidole*, however, this specimen is now considered to be from copal (‘immature amber’ from a much more recent time; Perkovsky, 2016). Regardless of the difference between dates, both phylogenies suggest that the dispersal and distribution of extant *Pheidole* is too recent to be explained by Gondwanan vicariance or dispersal across the NALB’s.

The monophyly of *Pheidole* in the Old World and Oraseminae in the New World both suggest the dispersal and establishment of a single ancestor, which could have been accomplished over a land-based filter bridge (*sensu* Simpson, 1940) or by chance dispersal through over-water rafting (*sensu* de Queiroz, 2005). We argue against chance over-water dispersal for Oraseminae because it would require a parasitised nest of *Pheidole* to have dispersed back into the New World after establishment in the Old World, and there is no phylogenetic evidence to suggest that either group dispersed back

into their native range. The probability of Oraseminae surviving outside of a host nest on a transoceanic voyage combined with the probability of successfully developing on a novel host upon arriving in the New World would make dispersing without their host highly unlikely. Instead, the dispersal of these wasps would likely require a land bridge tightly correlated with the presence and establishment of *Pheidole*, which would allow each group to cross in opposite unidirectional patterns. Thus, dispersing across the BLB during a period of high temperature and equability (>15 mya; Wolfe, 1993; Milne, 2006) is the best-supported and most logical biogeographic hypothesis for both Oraseminae and *Pheidole*, which are predominantly tropical groups. The northern climate would have experienced some cooling between 50–35 Ma, followed by a period of fluctuation in the Oligocene to Early Miocene with decreased cold-month temperatures and increased aridity and then a period of progressive cooling after 15 Ma (Milne, 2006; Eldrett *et al.*, 2009). The climatic conditions of the Oligocene may have facilitated a filter across Beringia, such that a limited number of species of *Pheidole* and Oraseminae were able to occupy and cross the land bridge but with changing climatic conditions limiting any further backcrossing as seen in more temperate groups (e.g. ants (Branstetter, 2009; Jansen *et al.*, 2010); bumble bees (Hines, 2008); and blue butterflies (Vila *et al.*, 2011)). An open, more climatically favourable corridor would have allowed many crossings in both directions, creating a mixture of Old World and New World clades, which is not seen in either group. The mean crown age for Oraseminae is between 34–48 Ma (Figs 1.3, 1.12–1.15), which represents a minimum age for shifting to Myrmicinae as hosts (assuming *Leiosema* parasitises *Pheidole*) and is significantly earlier than the proposed

invasion and spread of *Pheidole* in the Old World (Economato *et al.*, 2015ab; Ward *et al.*, 2015; Economato *et al.*, 2019). This could be explained by at least two hypotheses: 1) Oraseminae was present in the Old World on some unknown ancestral host and underwent multiple host shifts to *Pheidole* after its arrival, or 2) the invasion of New World *Pheidole* predates the diversification of Oraseminae in the Old World despite the results from the dating analyses. Either way, the Old World Oraseminae underwent a host shift to *Pheidole* of New World origin that allowed for a favourable crossing into the New World.

Dispersal into the New World by Oraseminae is accompanied by a tremendous increase in diversification and abundance within *Orasema*. This diversification is complemented by a wider array of oviposition strategies, morphologies, and host preferences than are found in the Old World genera. This pattern may indicate that shifting onto *Pheidole* or dispersing into a new area with a diversity of potential *Pheidole* host species increased the diversification rate for Oraseminae. This is supported by our diversification rates analysis from BAMM (Fig. 1.5), which shows that the single most likely rate shift configuration is a single shift between Old World and New World taxa.

Combining Datasets

Missing data have long been a contentious issue in phylogenetics, and it has resurfaced in the era of phylogenomics (Wiens, 2003; Lemmon *et al.*, 2009; Wiens & Morrill, 2011; Streicher *et al.*, 2016). Our combined dataset, with ~51% missing data (artifact of concatenation; not including missing data from independent datasets), is just

over the threshold found to maximise branch support at 50% (Streicher *et al.*, 2016). However, it should be noted that the highly uneven distribution of missing data makes our combined matrix substantially different than that of Streicher *et al.* (2016). While we did not assess the impact of missing data with simulated datasets, our empirical analyses show no signs of taxa with AHE data (or without) clustering together (Figs 1.8, 1.11), which might be expected if missing data are affecting tree topologies. Additionally, the AHE ML tree (Fig. 1.10) and the Combined ML tree (Fig. 1.11) have identical topologies for the 92 AHE taxa, indicating that the addition of Sanger data and taxa did not change the relationships inferred from AHE data. Missing data can have an impact on branch length estimates as well (Lemmon *et al.*, 2009), but we avoided this problem in our dating analysis of the combined dataset by using only the Sanger data, which was available for every taxon. Using similar concatenation methods, Peloso *et al.* (2015) found that increased character sampling for a subset of taxa (i.e. adding AHE data to some but not all taxa with Sanger data) generally lead to increased tree resolution (parsimony consensus) and increased support values (ML), while increasing taxon sampling (i.e. adding taxa with Sanger data to a matrix with Sanger+AHE data) increased support in shallow nodes but not in deeper nodes.

In our study, the Sanger dataset alone, using either parsimony or likelihood, resulted in monophyly of the Old World Oraseminae, albeit with little or no support. The AHE data alone strongly supported Old World paraphyly; however, the AHE dataset alone would not have thoroughly sampled across Oraseminae for either our host association or biogeographic studies. By combining datasets, we were able to produce

comprehensive phylogenies with strong backbone support driven by the wealth of character information from AHE and the numerous taxa available through the Sanger dataset. For dated trees, having a large dataset with a high percentage of missing data presented a hurdle for some analyses, but subsampling data by prioritizing the genes with the highest phylogenetic informativeness (AHE) and using a fixed tree topology based on the complete datasets (AHE and Combined) were effective methods for efficiently analyzing next-generation sequence data in programs like BEAST. The consistency of the dates produced by the three independent subsets of the AHE dataset (no overlapping gene regions among them) showed that this sampling method did not misrepresent the signal in the total AHE dataset; however, these three analyses did produce older dates than either the Sanger or Combined analyses, which relied entirely on Sanger data (Fig. 1.3).

Phylogenetics of Oraseminae

This study has the most comprehensive sampling of orasemine taxa and genetic data compared to any previous phylogenetic analyses of this group (Heraty, 1990; Heraty, 1994b; Heraty, 2000; Heraty *et al.*, 2004; Murray *et al.*, 2013). All genera except *Matantas* are represented, and all species groups in *Orasema* are represented, although there are still many species that we were unable to include either because they were rare or specimens were too old to obtain quality DNA.

Results from all analyses support the monophyly of Oraseminae and its sister group relationship to Eucharitinae. Gollumiellinae is most often sister to Eucharitinae + Oraseminae, except in the parsimony analyses of the AHE and Combined datasets (Figs

1.7–1.8), in which it is paraphyletic. This paraphyly is likely an artifact of the outgroup sampling and did not impact any of our results.

The generic-, species group-, and species-level classifications in Oraseminae are broadly supported across analyses with one major exception in the genus *Hayatosema*, where the African species never grouped with the species from SE Asia. The proposed reorganization of genera resulting from our analyses was addressed in the recent revision of the Old World genera (Burks *et al.*, 2017). The supplementary material provides a detailed description of relationships across analyses for Oraseminae.

Georeferencing

Oraseminae are more diverse in the number of species and morphological variability in the New World (Fig. 1.2). While the southern limits of their distribution are similar between the Old World and New World, the New World taxa range much farther north. Oraseminae are far more diverse in the tropics but with a number of Nearctic species in the *Orasema bakeri*-, *cockerelli*-, *coloradensis*-, and *simulatrix*-species groups found predominately in desert environments. Most of the northerly records are from a single widespread species, *Orasema coloradensis*, which is known to oviposit on a wide variety of plants, occurs in a wide variety of habitats (mostly open scrub) from Florida to British Columbia and is a confirmed parasitoid of both *Pheidole* and *Solenopsis*. While not a candidate to be the sister group of the New World *Orasema*, these behaviors are what we might envision in a generalist species able to move easily into a new host/habitat niche (i.e. capable of crossing a temperate Beringian Land Bridge).

Life History Evolution

Life history traits beyond ant host association (e.g. oviposition strategy, plant hosts, etc.) are difficult to analyze within a phylogenetic context in Oraseminae because of the scarcity of information for Old World taxa, especially *Leiosema*, and some New World taxa. Ant host associations, more than any other life history character, are far better understood and seem to be more of a limiting factor for dispersal and diversification in Oraseminae. This phylogeny provides a framework for future analyses of these traits.

Conclusions

By analyzing taxon-rich and character-rich datasets independently and combined, we have shown a most likely scenario whereby Oraseminae originated in the Old World and dispersed once into the New World during the Oligocene. Based on climatic conditions and biogeographic analyses, the most likely route of dispersal was across the Beringian Land Bridge. Their primary host ant, *Pheidole*, originated in the New World and dispersed into the Old World around the same time and likely across the same land bridge. Our results suggest that Oraseminae were well established in the Old World prior to the invasion of New World *Pheidole*, and multiple lineages may have shifted to this novel host. The difference in diversity and abundance of Oraseminae in the Old World and New World indicates that shifting onto *Pheidole* as a new host or dispersing into a new geographic area allowed the parasitoids to diversify more rapidly.

Our study shows how both phylogenetic and biogeographic information of a group of relatively specialised parasitoids can potentially inform us about both themselves and their hosts. No formal biogeographic hypothesis has ever been proposed to explain how *Pheidole* dispersed into the Old World, but using the context of Oraseminae biogeography and dating analyses, we strongly believe that the only way the parasitoids could enter the New World would have been across a host-occupied land bridge during suitable climatic conditions, and therefore, propose that *Pheidole* likely dispersed across the Beringian Land Bridge.

References

- Allen, J.M., Huang, D.I., Cronk, Q.C. & Johnson, K.P. (2015) aTRAM - automated target restricted assembly method: a fast method for assembling loci across divergent taxa from next-generation sequencing data. *BMC Bioinformatics*, **16**. DOI: 10.1186/s12859-015-0515-2.
- Askew, R.R. (1971) *Parasitic Insects*. American Elsevier, New York.
- Blaimer, B.B., LaPolla, J.S., Branstetter, M.G., Lloyd, M.W. & Brady, S.G. (2016) Phylogenomics, biogeography and diversification of obligate mealybug-tending ants in the genus *Acropyga*. *Molecular Phylogenetics and Evolution*, **102**, 20–29.
- Blakey, R.C. (2008) Gondwana paleogeography from assembly to breakup - a 500 million year odyssey. *Resolving the Late Paleozoic ice age in time and space* (ed. by R.C. Fielding, T.D. Frank & J.L. Isbell), pp. 1–28. Geological Society of America Special Paper, Boulder, Co.
- Bouček, Z. (1988) *Australasian Chalcidoidea (Hymenoptera): a biosystematic revision of genera of fourteen families, with a reclassification of species*. CAB International, Wallingford, UK.
- Brandley, M.C., Wang, Y., Guo, X., de Oca, A.N., Fera-Ortiz, M., Hikida, T. & Ota, H. (2011) Accommodating heterogeneous rates of evolution in molecular divergence dating methods: an example using intercontinental dispersal of *Plestiodon* (*Eumeces*) lizards. *Systematic Biology*, **60**, 3–15.
- Branstetter, M.G. (2009) The ant genus *Stenammina* Westwood (Hymenoptera: Formicidae) redefined, with a description of a new genus *Propodilobus*. *Zootaxa*, **2221**, 41–57.
- Burbrink, F.T. & Lawson, R. (2007) How and when did Old World ratsnakes disperse into the New World? *Molecular Phylogenetics and Evolution*, **43**, 173–189.
- Burke, G.R., Walden, K.K.O., Whitfield, J.B., Robertson, H.M. & Strand, M.R. (2018) Whole genome sequence of the parasitoid wasp *Microplitis demolitor* that harbors an endogenous virus mutualist. *G3: Genes, Genomics, Genetics*, **8**, 2875–2880.
- Burks, B.D. (1979) Family Eucharitidae. *Catalog of Hymenoptera in America north of Mexico* (ed. by K.V. Krombein, P.D. Hurd, Jr., D.R. Smith & B.D. Burks), pp. 875–878. Smithsonian Institution Press, Washington, D.C.

- Burks, R.A., Heraty, J.M., Dominguez, C. & Mottern, J.L. (2018) Complex diversity in a mainly tropical group of ant parasitoids: revision of the *Orasema stramineipes* species group (Hymenoptera: Chalcidoidea: Eucharitidae). *Zootaxa*, **4401**, 1–107.
- Burks, R.A., Heraty, J.M., Mottern, J., Dominguez, C. & Heacox, S. (2017) Biting the bullet: revisionary notes on the Oraseminae of the Old World (Hymenoptera, Chalcidoidea, Eucharitidae). *Journal of Hymenoptera Research*, **55**, 139–188.
- Carey, B., Visscher, K. & Heraty, J.M. (2012) Nectary use for gaining access to an ant host by the parasitoid *Orasema simulatrix* (Hymenoptera, Eucharitidae). *Journal of Hymenoptera Research*, **27**, 47–65.
- Chen, X., Huang, S., Guo, P., *et al.* (2013) Understanding the formation of ancient intertropical disjunct distributions using Asian and Neotropical hinged-teeth snakes (*Sibynophis* and *Scaphiodontophis*: Serpentes: Colubridae). *Molecular Phylogenetics and Evolution*, **66**, 254–261.
- Clausen, C.P. (1940a) The immature stages of the Eucharidae. *Proceedings of the Entomological Society of Washington*, **42**, 161–170.
- Clausen, C.P. (1940b) The oviposition habits of the Eucharidae (Hymenoptera). *Journal of the Washington Academy of Sciences*, **30**, 504–516.
- Clausen, C.P. (1941) The habits of the Eucharidae. *Psyche (Cambridge)*, **48**, 57–69.
- Condamine, F.L., Sperling, F.A.H. & Kergoat, G.J. (2013) Global biogeographical pattern of swallowtail diversification demonstrates alternative colonization routes in the Northern and Southern hemispheres. *Journal of Biogeography*, **40**, 9–23.
- Das, G.M. (1963) Preliminary studies on the biology of *Orasema assectator* Kerrich (Hym., Eucharitidae), parasitic on *Pheidole* and causing damage to leaves of tea in Assam. *Bulletin of Entomological Research*, **54**, 373–378.
- de Queiroz, A. (2005) The resurrection of oceanic dispersal in historical biogeography. *Trends in Ecology & Evolution*, **20**, 68–73.
- Drummond, A.J. & Rambaut, A. (2007) BEAST: Bayesian evolutionary analysis by sampling trees. *BMC Evolutionary Biology*, **7**, 214.
- Dubovikoff, D. (2011) The first record of the genus *Pheidole* Westwood, 1839 (Hymenoptera: Formicidae) from the Baltic amber. *Russian Entomological Journal*, **20**, 255–257.

- Economo, E.P., Huang, J.P., Fischer, G., *et al.* (2019) Evolution of the latitudinal diversity gradient in the hyperdiverse ant genus *Pheidole*. *Global Ecology and Biogeography*, **00**, 1–15.
- Economo, E.P., Klimov, P., Sarnat, E.M., Guenard, B., Weiser, M.D., Lecroq, B. & Knowles, L.L. (2015a) Global phylogenetic structure of the hyperdiverse ant genus *Pheidole* reveals the repeated evolution of macroecological patterns. *Proceedings of the Royal Society Biological Sciences Series B*, **282**, 20141416.
- Economo, E.P., Sarnat, E.M., Janda, M., *et al.* (2015b) Breaking out of biogeographical modules: range expansion and taxon cycles in the hyperdiverse ant genus *Pheidole*. *Journal of Biogeography*, **42**, 2289–2301.
- Eggleton, P. & Belshaw, R. (1992) Insect parasitoids: an evolutionary overview. *Philosophical Transactions: Biological Sciences*, **337**, 1–20.
- Eldrett, J.S., Greenwood, D.R., Harding, I.C. & Huber, M. (2009) Increased seasonality through the Eocene to Oligocene transition in northern high latitudes. *Nature*, **459**, 969–973.
- Gadau, J., Helmkampf, M., Nygaard, S., *et al.* (2012) The genomic impact of 100 million years of social evolution in seven ant species. *Trends in Genetics*, **28**, 14–21.
- Gamble, T., Bauer, A.M., Colli, G.R., Greenbaum, E., Jackman, T.R., Vitt, L.J. & Simons, A.M. (2011) Coming to America: multiple origins of New World geckos. *Journal of Evolutionary Biology*, **24**, 231–244.
- GISD (2015) *Global Invasive Species Database*. <http://www.iucngisd.org/gisd/> [accessed on 1/10/2017].
- Goloboff, P.A., Farris, J.S. & Nixon, K.C. (2008) TNT, a free program for phylogenetic analysis. *Cladistics*, **24**, 1–13.
- Guo, P., Liu, Q., Xu, Y., *et al.* (2012) Out of Asia: natricine snakes support the Cenozoic Beringian dispersal hypothesis. *Molecular Phylogenetics and Evolution*, **63**, 825–833.
- Haddad, S., Shin, S., Lemmon, A.R., *et al.* (2017) Anchored hybrid enrichment provides new insights into the phylogeny and evolution of longhorned beetles (Cerambycidae). *Systematic Entomology*, **43**, 68–89.
- Hamilton, C.A., Lemmon, A.R., Lemmon, E.M. & Bond, J.E. (2016) Expanding anchored hybrid enrichment to resolve both deep and shallow relationships within the spider tree of life. *BMC Evolutionary Biology*, **16**. DOI: 10.1186/s12862-016-0769-y.

- Heraty, J.M. (1990) Classification and evolution of the Oraseminae (Hymenoptera: Eucharitidae). Texas A&M University, Entomology, Ph.D. thesis.
- Heraty, J.M. (1994a) Biology and importance of two eucharitid parasites of *Wasmannia* and *Solenopsis*. *Exotic ants: biology, impact and control of introduced species* (ed. by D.F. Williams), pp. 104–120. Westview Press, Oxford.
- Heraty, J.M. (1994b) Classification and evolution of the Oraseminae in the Old World, including revisions of two closely related genera of Eucharitinae (Hymenoptera: Eucharitidae). *Life Sciences Contributions*, **157**, 1–174.
- Heraty, J.M. (2000) Phylogenetic relationships of Oraseminae (Hymenoptera: Eucharitidae). *Annals of the Entomological Society of America*, **93**, 374–390.
- Heraty, J.M. (2002) A revision of the genera of Eucharitidae (Hymenoptera: Chalcidoidea) of the world. *Memoirs of the American Entomological Institute*, **68**, 1–359.
- Heraty, J.M. (2017) Catalog of World Eucharitidae, 2017. UC Riverside. <https://hymenoptera.ucr.edu/EucharitidaeCatalog2017.pdf>.
- Heraty, J.M. & Darling, D.C. (2009) Fossil Eucharitidae and Perilampidae (Hymenoptera: Chalcidoidea) from Baltic amber. *Zootaxa*, **2306**, 1–16.
- Heraty, J.M., Hawks, D., Kostecki, J.S. & Carmichael, A. (2004) Phylogeny and behaviour of the Gollumiellinae, a new subfamily of the ant-parasitic Eucharitidae (Hymenoptera: Chalcidoidea). *Systematic Entomology*, **29**, 544–559.
- Heraty, J.M. & Murray, E. (2013) The life history of *Pseudometagea schwarzii*, with a discussion of the evolution of endoparasitism and koinobiosis in Eucharitidae and Perilampidae (Chalcidoidea). *Journal of Hymenoptera Research*, **35**, 1–15.
- Heraty, J.M., Wojcik, D.P. & Jouvenaz, D.P. (1993) Species of *Orasema* parasitic on the *Solenopsis saevissima*-complex in South America (Hymenoptera: Eucharitidae, Formicidae). *Journal of Hymenoptera Research*, **2**, 169–182.
- Herreid, J.S. & Heraty, J.M. (2017) Hitchhikers at the dinner table: a revisionary study of a group of ant parasitoids (Hymenoptera: Eucharitidae) specializing in the use of extrafloral nectaries for host access. *Systematic Entomology*, **42**, 204–229.
- Hines, H.M. (2008) Historical biogeography, divergence times, and diversification patterns of bumble bees (Hymenoptera: Apidae: *Bombus*). *Systematic Biology*, **57**, 58–75.

- Jansen, G., Savolainen, R. & Vepsäläinen, K. (2010) Phylogeny, divergence-time estimation, biogeography and social parasite-host relationships of the Holarctic ant genus *Myrmica* (Hymenoptera: Formicidae). *Molecular Phylogenetics and Evolution*, **56**, 294–304.
- Johnson, J.B., Miller, T.D., Heraty, J.M. & Merickel, F.W. (1986) Observations on the biology of two species of *Orasema* (Hymenoptera: Eucharitidae). *Proceedings of the Entomological Society of Washington*, **88**, 542–549.
- Junier, T. & Zdobnov, E.M. (2010) The Newick utilities: high-throughput phylogenetic tree processing in the UNIX shell. *Bioinformatics*, **26**, 1669–1670.
- Kaplan, A.A., Grigelis, A.A., Strelnikova, N.I. & Glikman, L.S. (1977) Stratigraphy and correlation of Palaeogene deposits of south-western cis-Baltic region. *Soviet Geology*, **4**, 30–43.
- Katoh, K. & Standley, D.M. (2013) MAFFT multiple sequence alignment software version 7: improvements in performance and usability. *Molecular Biology and Evolution*, **30**, 772–780.
- Kearse, M., Moir, R., Wilson, A., *et al.* (2012) Geneious Basic: an integrated and extendable desktop software platform for the organization and analysis of sequence data. *Bioinformatics*, **28**, 1647–1649.
- Kerrich, G.J. (1963) Descriptions of two species of Eucharitidae damaging tea, with comparative notes on other species (Hym., Chalcidoidea). *Bulletin of Entomological Research*, **54**, 365–371.
- Lachaud, J.-P. & Pérez-Lachaud, G. (2012) Diversity of species and behavior of hymenopteran parasitoids of ants: a review. *Psyche*, **2012**. DOI: 10.1155/2012/134746.
- Lanfear, R., Calcott, B., Kainer, D., Mayer, C. & Stamatakis, A. (2014) Selecting optimal partitioning schemes for phylogenomic datasets. *BMC Evolutionary Biology*, **14**. DOI: 10.1186/1471-2148-14-82.
- Lanfear, R., Frandsen, P.B., Wright, A.M., Senfeld, T. & Calcott, B. (2017) PartitionFinder 2: new methods for selecting partitioned models of evolution for molecular and morphological phylogenetic analyses. *Molecular Biology and Evolution*, **34**, 772–773.

- Lemmon, A.R., Brown, J.M., Stanger-Hall, K. & Lemmon, E.M. (2009) The effect of ambiguous data on phylogenetic estimates obtained by maximum likelihood and Bayesian inference. *Systematic Biology*, **58**, 130–145.
- Lemmon, A.R., Emme, S.A. & Lemmon, E.M. (2012) Anchored hybrid enrichment for massively high-throughput phylogenomics. *Systematic Biology*, **61**, 727–744.
- Lemmon, E.M. & Lemmon, A.R. (2013) High-throughput genomic data in systematics and phylogenetics. *Annual Review of Ecology, Evolution, and Systematics*, **44**, 99–121.
- Lopez-Giraldez, F. & Townsend, J.P. (2011) PhyDesign: an online application for profiling phylogenetic informativeness. *BMC Evolutionary Biology*, **11**, 1–4.
- Maddison, D.R. (2016) The rapidly changing landscape of insect phylogenetics. *Current Opinion in Insect Science*, **18**, 77–82.
- Maddison, D.R. & Maddison, W.P. (2017a) *Chromaseq: a Mesquite package for analyzing sequence chromatograms. Version 1.3.* <http://mesquiteproject.org/packages/chromaseq>.
- Maddison, W.P. & Maddison, D.R. (2017b) *Mesquite: a modular system for evolutionary analysis. Version 3.31.* <http://mesquiteproject.org>.
- Mann, W.M. (1918) Myrmecophilous insects from Mexico. *Psyche*, **25**, 104–106.
- Masonick, P., Michael, A., Frankenberg, S., Rabitsch, W. & Weirauch, C. (2017) Molecular phylogenetics and biogeography of the ambush bugs (Hemiptera: Reduviidae: Phymatinae). *Molecular Phylogenetics and Evolution*, **114**, 225–233.
- Matzke, N.J. (2013) *BioGeoBEARS: biogeography with Bayesian (and likelihood) evolutionary analysis in R scripts. R package, version 0.2.1, published July 27, 2013 at:* <http://CRAN.R-project.org/packages=BioGeoBEARS>.
- Matzke, N.J. (2014) Model selection in historical biogeography reveals that founder-event speciation is a crucial process in island clades. *Systematic Biology*, **63**, 951–970.
- McKenna, M.C. (1983) Holarctic landmass rearrangement, cosmic events, and Cenozoic terrestrial organisms. *Annals of the Missouri Botanical Garden*, **70**, 459–489.
- Miller, M.A., Pfeiffer, W. & Schwartz, T. (2010) Creating the CIPRES Science Gateway for inference of large phylogenetic trees. *Proceedings of the Gateway Computing Environments Workshop (GCE)*, New Orleans, LA, 1–8.

- Milne, R.I. (2006) Northern Hemisphere plant disjunctions: a window on tertiary land bridges and climate change? *Annals of Botany*, **98**, 465–472.
- Mirarab, S. & Warnow, T. (2015) ASTRAL-II: coalescent-based species tree estimation with many hundreds of taxa and thousands of genes. *Bioinformatics*, **31**, i44–52.
- Moreau, C.S. (2008) Unraveling the evolutionary history of the hyperdiverse ant genus *Pheidole* (Hymenoptera: Formicidae). *Molecular Phylogenetics and Evolution*, **48**, 224–239.
- Murray, E.A., Carmichael, A.E. & Heraty, J.M. (2013) Ancient host shifts followed by host conservatism in a group of ant parasitoids. *Proceedings of the Royal Society Biological Sciences Series B*, **280**, 20130495.
- Peloso, P.L.V., Frost, D.R., Richards, S.J., *et al.* (2015) The impact of anchored phylogenomics and taxon sampling on phylogenetic inference in narrow-mouthed frogs (Anura, Microhylidae). *Cladistics*, **32**, 1–28.
- Perkovsky, E.E. (2016) Tropical and holarctic ants in Late Eocene ambers. *Vestnik Zoologii*, **50**, 111–122.
- Perkovsky, E.E., Rasnitsyn, A.P., Vlaskin, A.P. & Taraschuk, M.V. (2007) A comparative analysis of the Baltic and Rovno amber arthropod faunas: representative samples. *African Invertebrates*, **48**, 229–245.
- Peters, R.S., Niehuis, O., Gunkel, S., *et al.* (2018) Transcriptome sequence-based phylogeny of chalcidoid wasps (Hymenoptera: Chalcidoidea) reveals a history of rapid radiations, convergence, and evolutionary success. *Molecular Phylogenetics and Evolution*, **120**, 286–296.
- Pinto, J.D. (2009) Hypermetamorphosis. *Encyclopedia of Insects* (ed. by V.H. Resh & R.T. Carde), pp. 484–486. Academic Press.
- Poinar, G., Jr. & Huber, J.T. (2011) A new genus of fossil Mymaridae (Hymenoptera) from Cretaceous amber and key to Cretaceous mymarid genera. *Zookeys*, **130**, 461–472.
- Prum, R.O., Berv, J.S., Dornburg, A., Field, D.J., Townsend, J.P., Lemmon, E.M. & Lemmon, A.R. (2015) A comprehensive phylogeny of birds (Aves) using targeted next-generation DNA sequencing. *Nature*, **526**, 569–573.

- Rabosky, D.L., Grudler, M., Anderson, C., *et al.* (2014) BAMMtools: an R package for the analysis of evolutionary dynamics on phylogenetic trees. *Methods in Ecology and Evolution*, **5**, 701–707.
- Rambaut, A., Suchard, M.A., Xie, D. & Drummond, A.J. (2014) *Tracer v1.6*, Available from <http://beast.bio.ed.ac.uk/Tracer>.
- Ree, R.H. & Smith, S.A. (2008) Maximum likelihood inference of geographic range evolution by dispersal, local extinction, and cladogenesis. *Systematic Biology*, **57**, 4–14.
- Ritzkowski, S. (1997) K-Ar-Altersbestimmungen der bernsteinführenden sedimente des Samlandes (Paläogen, Bezirk Kaliningrad). *Metalla, Sonderheft*, **66**, 19–23.
- Rokyta, D.R., Lemmon, A.R., Margres, M.J. & Aronow, K. (2012) The venom-gland transcriptome of the eastern diamondback rattlesnake (*Crotalus adamanteus*). *BMC Genomics*, **13**. DOI: 10.1186/1471-2164-13-312.
- Sadd, B.M., Barribeau, S.M., Bloch, G., *et al.* (2015) The genomes of two key bumblebee species with primitive eusocial organization. *Genome Biology*, **16**. DOI: 10.1186/s13059-015-0623-3.
- Sanmartín, I., Enghoff, H. & Ronquist, F. (2001) Patterns of animal dispersal, vicariance and diversification in the Holarctic. *Biological Journal of the Linnean Society*, **73**, 345–390.
- Sanmartín, I. & Ronquist, F. (2004) Southern hemisphere biogeography inferred by event-based models: plant versus animal patterns. *Systematic Biology*, **53**, 216–243.
- Schmidt, H.A., Strimmer, K., Vingron, M. & von Haeseler, A. (2002) TREE-PUZZLE: maximum likelihood phylogenetic analysis using quartets and parallel computing. *Bioinformatics*, **18**, 502–504.
- Simpson, G.G. (1940) Paleontology: mammals and land bridges. *Journal of the Washington Academy of Sciences*, **30**, 137–163.
- Stamatakis, A. (2006) RAxML-VI-HPC: maximum likelihood-based phylogenetic analyses with thousands of taxa and mixed models. *Bioinformatics*, **22**, 2688–2690.
- Stamatakis, A. (2014) RAxML version 8: a tool for phylogenetic analysis and post-analysis of large phylogenies. *Bioinformatics*, **30**, 1312–1313.

- Streicher, J.W., Schulte, J.A., II & Wiens, J.J. (2016) How should genes and taxa be sampled for phylogenomic analyses with missing data? An empirical study in iguanian lizards. *Systematic Biology*, **65**, 128–145.
- Swofford, D.L. (2002) *PAUP* v.4.0: phylogenetic analysis using parsimony (* and other methods)*. Sinauer, Sunderland, Massachusetts, USA.
- Tiffney, B.H. (1985) The Eocene north Atlantic land bridge: its importance in Tertiary and modern phytogeography of the northern hemisphere. *Journal of the Arnold Arboretum*, **66**, 243–273.
- Townsend, T.M., Leavitt, D.H. & Reeder, T.W. (2011) Intercontinental dispersal by a microendemic burrowing reptile (Dibamidae). *Proceedings of the Royal Society Biological Sciences Series B*, **278**, 2568–2574.
- Vaidya, G., Lohman, D.J. & Meier, R. (2011) SequenceMatrix: concatenation software for the fast assembly of multi-gene datasets with character set and codon information. *Cladistics*, **27**, 171–180.
- Varone, L. & Briano, J. (2009) Bionomics of *Orasema simplex* (Hymenoptera: Eucharitidae), a parasitoid of *Solenopsis* fire ants (Hymenoptera: Formicidae) in Argentina. *Biological Control*, **48**, 204–209.
- Varone, L., Heraty, J.M. & Calcaterra, L.A. (2010) Distribution, abundance and persistence of species of *Orasema* (Hym: Eucharitidae) parasitic on fire ants in South America. *Biological Control*, **55**, 72–78.
- Vila, R., Bell, C.D., Macniven, R., *et al.* (2011) Phylogeny and palaeoecology of *Polyommatus* blue butterflies show Beringia was a climate-regulated gateway to the New World. *Proceedings of the Royal Society Biological Sciences Series B*, **278**, 2737–2744.
- Walker, J.D., Geissman, J.W., Bowring, S.A. & Babcock, L.E. (2012) Geologic Time Scale v.4.0: Geological Society of America.
- Ward, P.S., Brady, S.G., Fisher, B.L. & Schultz, T.R. (2015) The evolution of myrmicine ants: phylogeny and biogeography of a hyperdiverse ant clade (Hymenoptera: Formicidae). *Systematic Entomology*, **40**, 61–81.
- Weinstock, G.M., Robinson, G.E., Gibbs, R.A., *et al.* (2006) Insights into social insects from the genome of the honeybee *Apis mellifera*. *Nature*, **443**, 931–949.
- Werren, J.H., Richards, S., Desjardins, C.A., *et al.* (2010) Functional and evolutionary insights from the genome of three parasitoid *Nasonia* species. *Science*, **327**, 343–348.

- Wheeler, G.C. & Wheeler, E.W. (1937) New hymenopterous parasites of ants (Chalcidoidea: Eucharidae). *Annals of the Entomological Society of America*, **30**, 163–175.
- Wheeler, W.M. (1907) The polymorphism of ants, with an account of some singular abnormalities due to parasitism. *Bulletin of the American Museum of Natural History*, **23**, 1–93.
- Wiens, J.J. (2003) Missing data, incomplete taxa, and phylogenetic accuracy. *Systematic Biology*, **52**, 528–538.
- Wiens, J.J. & Morrill, M.C. (2011) Missing data in phylogenetic analysis: reconciling results from simulations and empirical data. *Systematic Biology*, **60**, 719–731.
- Wilson, T.H. & Cooley, T.A. (1972) A chalcidoid planidium and an entomophilic nematode associated with the western flower thrips. *Annals of the Entomological Society of America*, **65**, 414–418.
- Wolfe, J.A. (1993) An analysis of Neogene climates in Beringia. *Palaeogeography Palaeoclimatology Palaeoecology*, **108**, 207–216.
- Wüster, W., Peppin, L., Pook, C.E. & Walker, D.E. (2008) A nesting of vipers: phylogeny and historical biogeography of the Viperidae (Squamata: Serpentes). *Molecular Phylogenetics and Evolution*, **49**, 445–459.

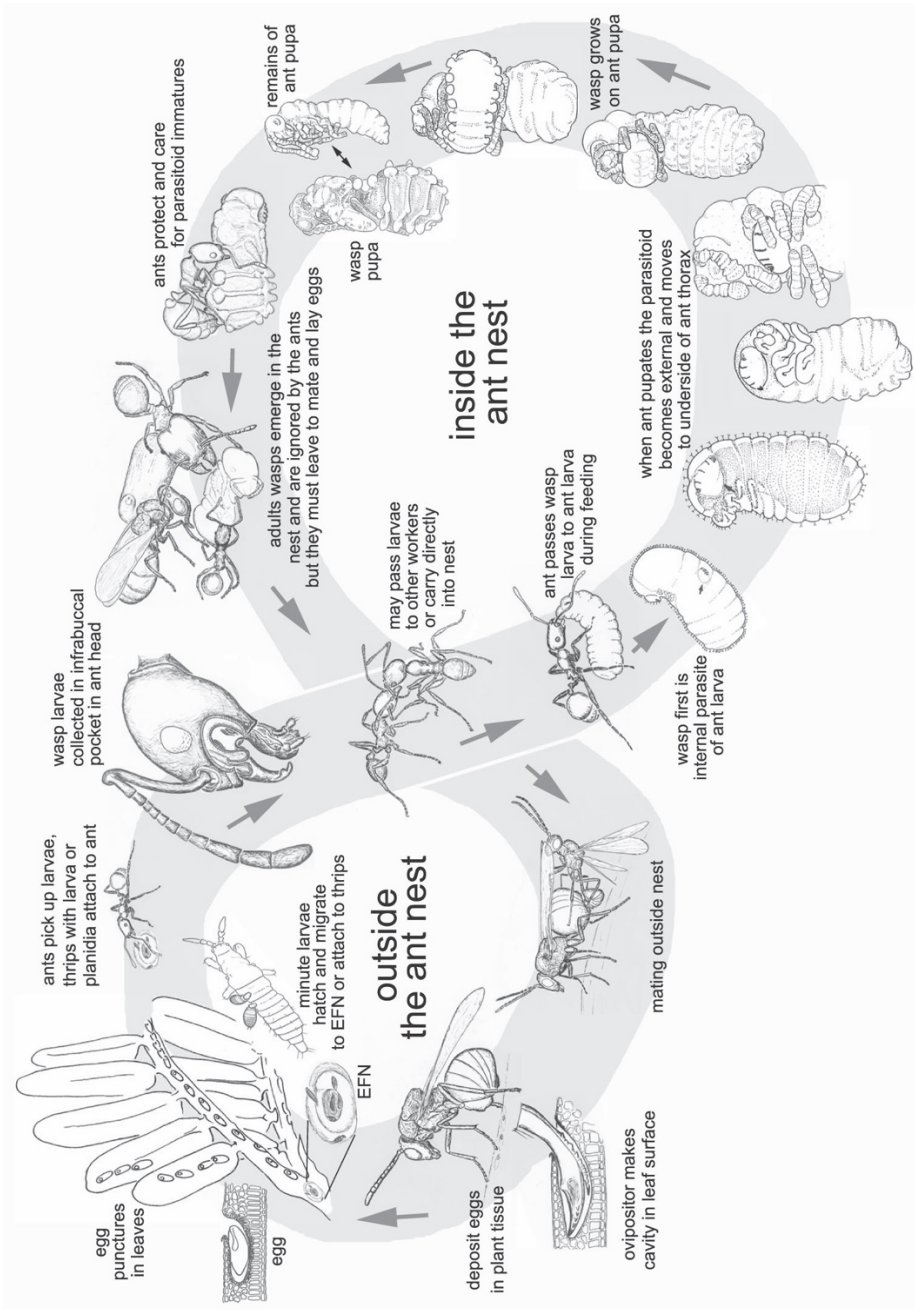


Figure 1.1: The lifecycle of a typical orasemine wasp. On the left: behaviors occurring outside the ant nest; mating, oviposition, and planidial acquisition by the ants (EFN: extrafloral nectary). On the right: behaviors occurring within the ant nest; attachment to the ant larva, development on the ant pupa, pupation, and eclosion.

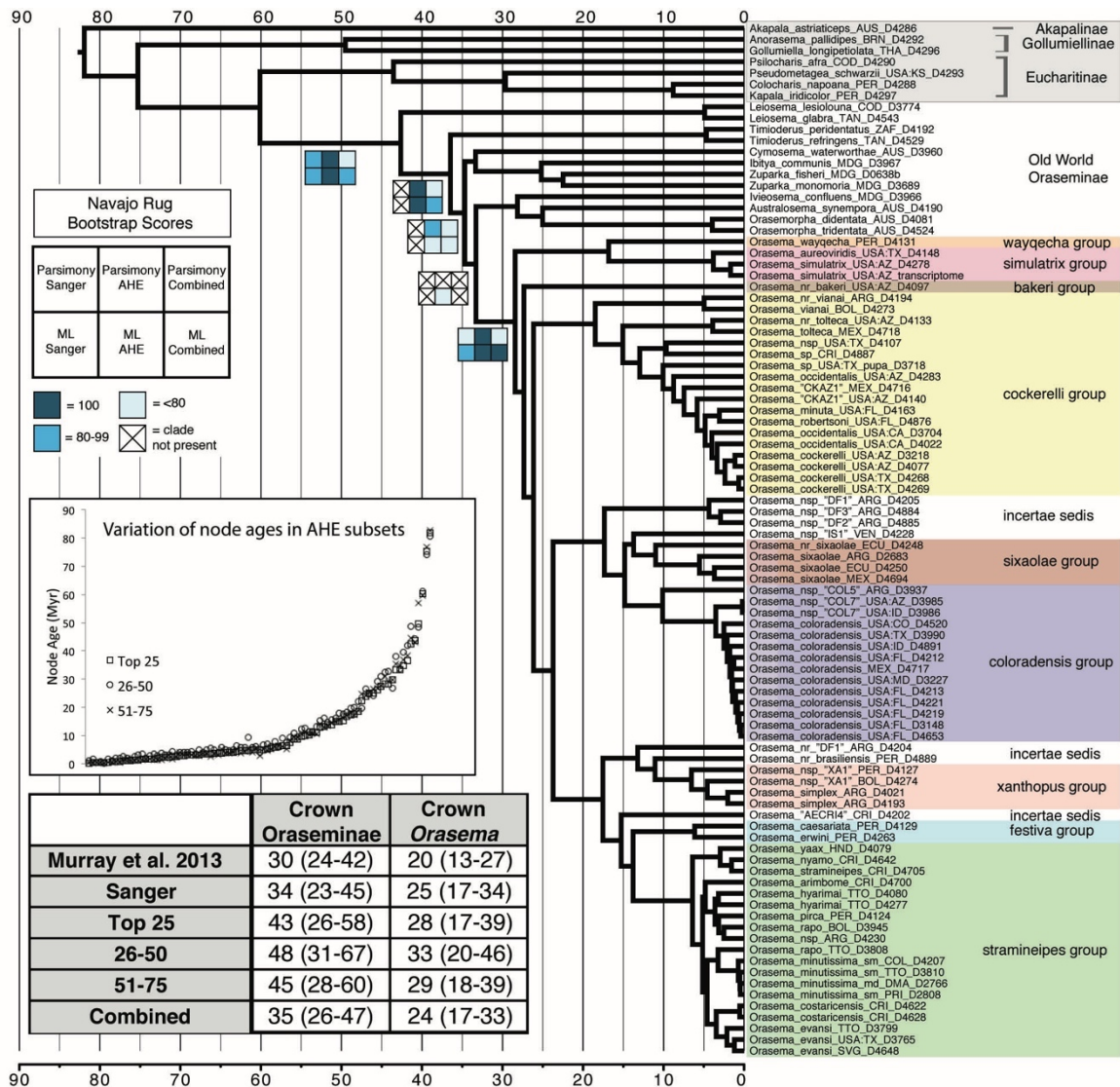


Figure 1.3: BEAST chronogram of Top 25 AHE loci using a fixed topology (AHE ML tree). Species groups of *Orasema* shown in color. Bootstrap support values are summarised as a Navajo Rug pattern, with darker squares showing higher support (values reported in supplementary documents). The variation in age estimates at each node for the AHE data subsets is shown in a scatterplot; the same node in each analysis is plotted on the same x-axis. Comparison of all dating analyses, including Murray et al. 2013, for the crown age of Oraseminae (minimum estimated date for specialization on Myrmicinae) and the crown age of *Orasema* (minimum estimated date for dispersing into the New World). Mean dates shown first with 95% HPD range in brackets.

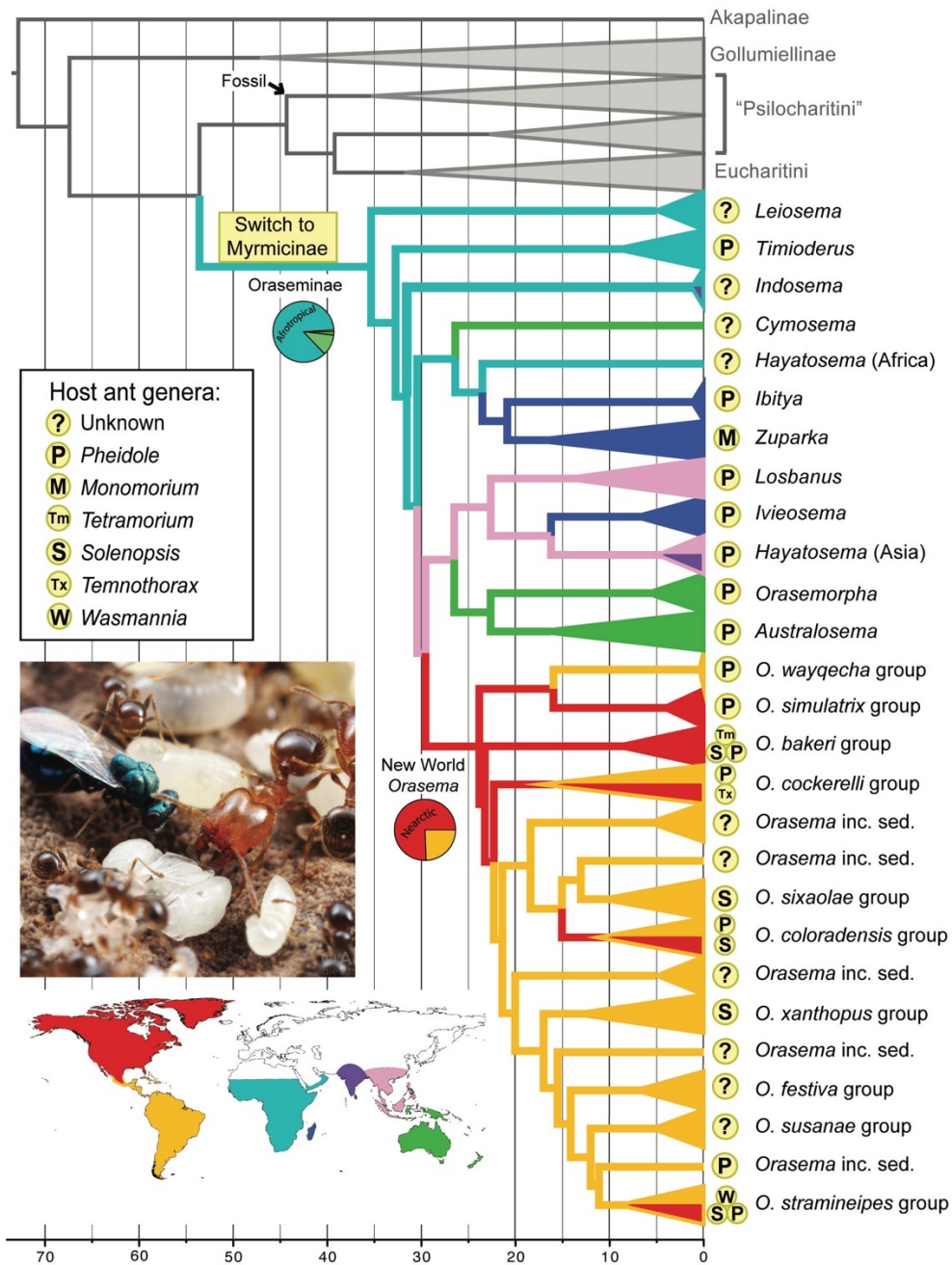


Figure 1.4: BEAST analysis of the Combined dataset with species collapsed into higher taxa (outgroup Eucharitidae to subfamily or tribe, Old World Oraseminae to genus, and *Orasema* to species group). Clades and branches colored by biogeographic area relating to the map. Biogeographic reconstruction summarised from DEC+J analysis with the two pie charts summarizing probabilities for the stem of Oraseminae and *Orasema*. Host ant records for Oraseminae are mapped to the tips of the tree. Photograph by Alexander Wild.

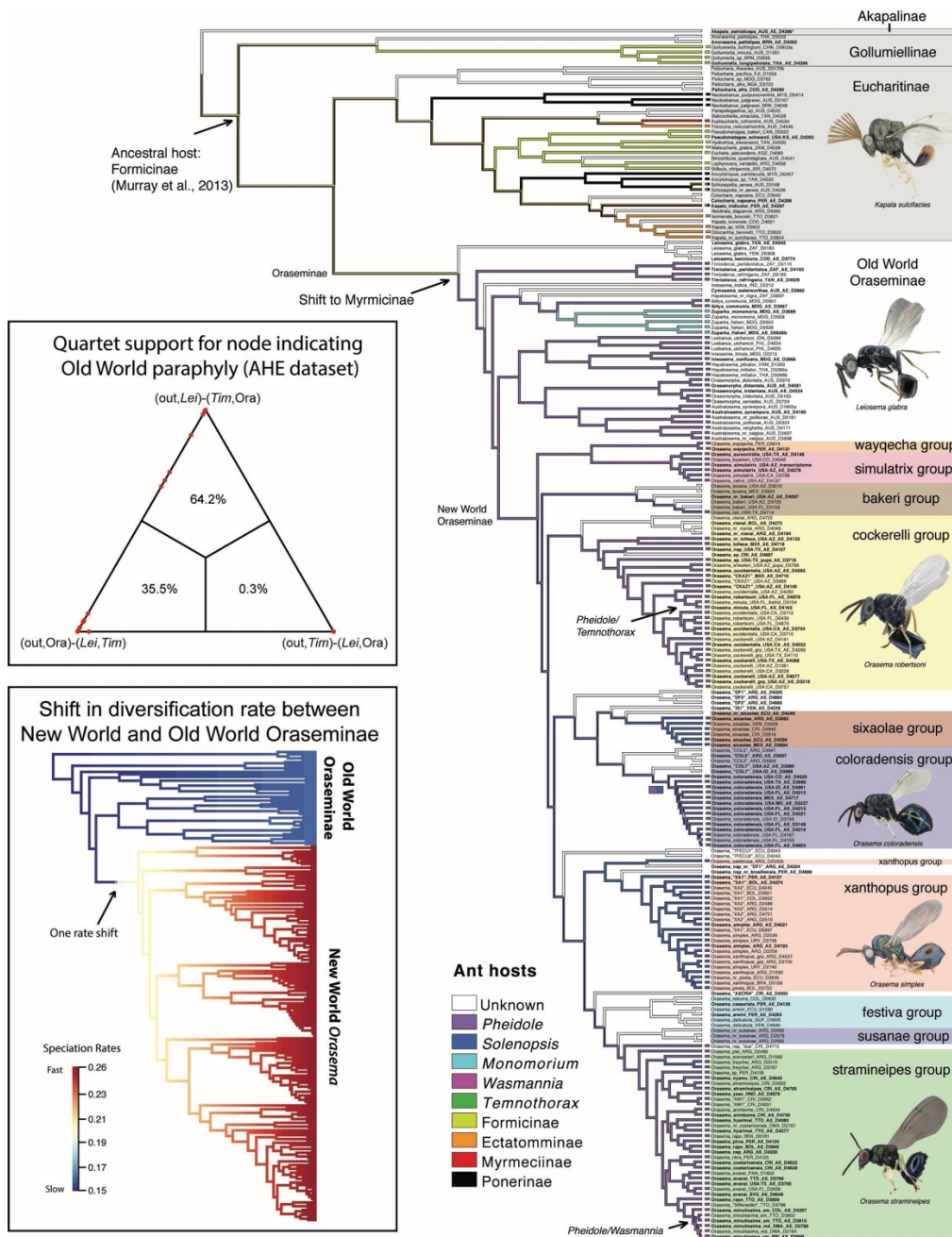
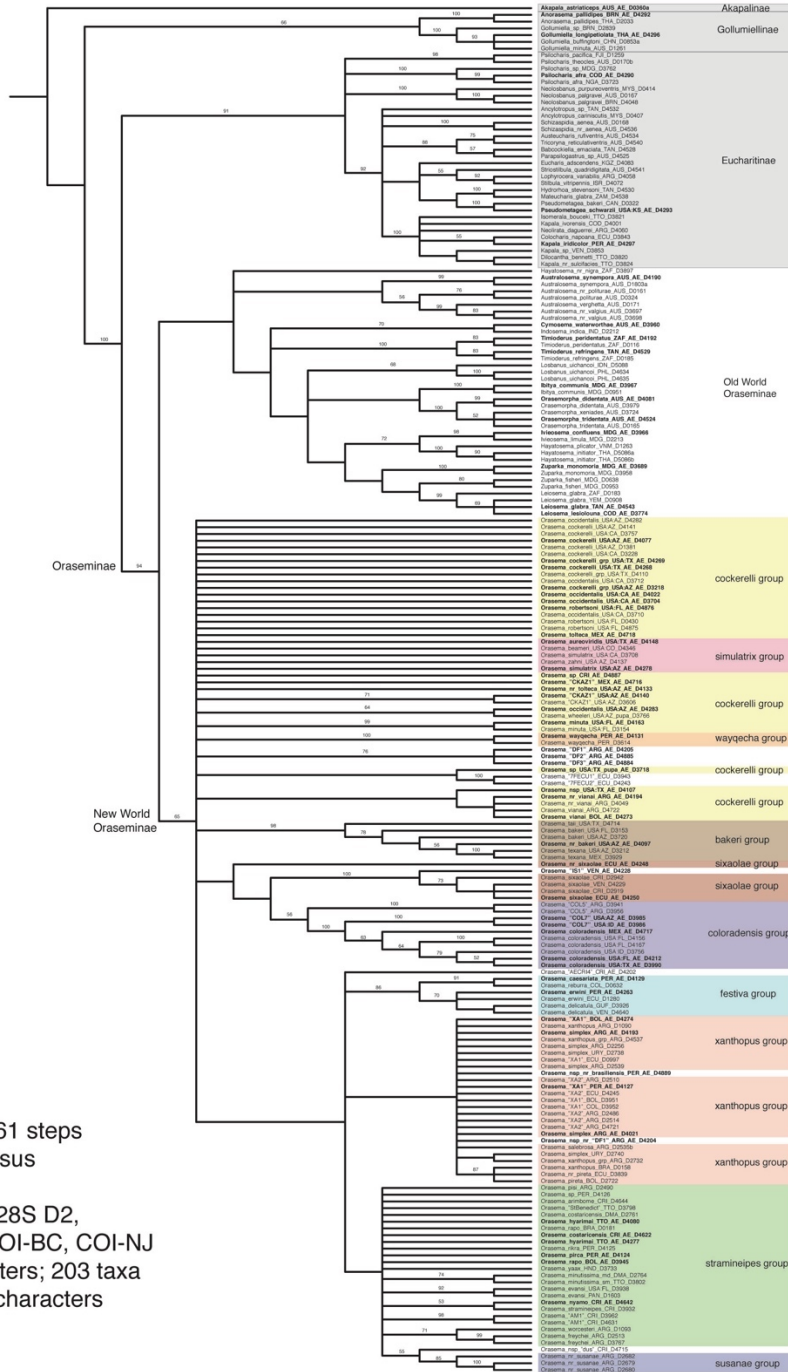


Figure 1.5: Additional phylogenetic comparative methods. Main figure: parsimony reconstruction of ancestral ant hosts on the Combined dated tree (Fig. 1.15) using Mesquite. Top inset: quartet support for the *Leiosema* sister relationship to the remaining Oraseminae using the AHE dataset from TREE-PUZZLE. Bottom inset: diversification analysis of Oraseminae (outgroups pruned off) using the Combined dated tree from BAMM showing the single most highly supported rate shift configuration from the Bayesian credible set (42 configurations) with a posterior probability of 0.3.

Strict consensus maximum parsimony tree (Sanger)



20 trees; 4,161 steps
 Strict consensus
 RI: 0.7280
 Loci: 18S-2, 28S D2,
 28S D3-5, COI-BC, COI-NJ
 3,046 characters; 203 taxa
 Unweighted characters
 TNT v.1.1

Figure 1.6: Strict consensus of 20 most parsimonious trees of the Sanger dataset from TNT (4,161 steps). Bootstrap support values are indicated unless lower than 50. Taxa in bold have been sampled for AHE genes.



Figure 1.7: Single most parsimonious tree of the AHE dataset from PAUP* (412,925 steps). Bootstrap support values are indicated unless lower than 50.

Strict consensus maximum parsimony tree (Combined)

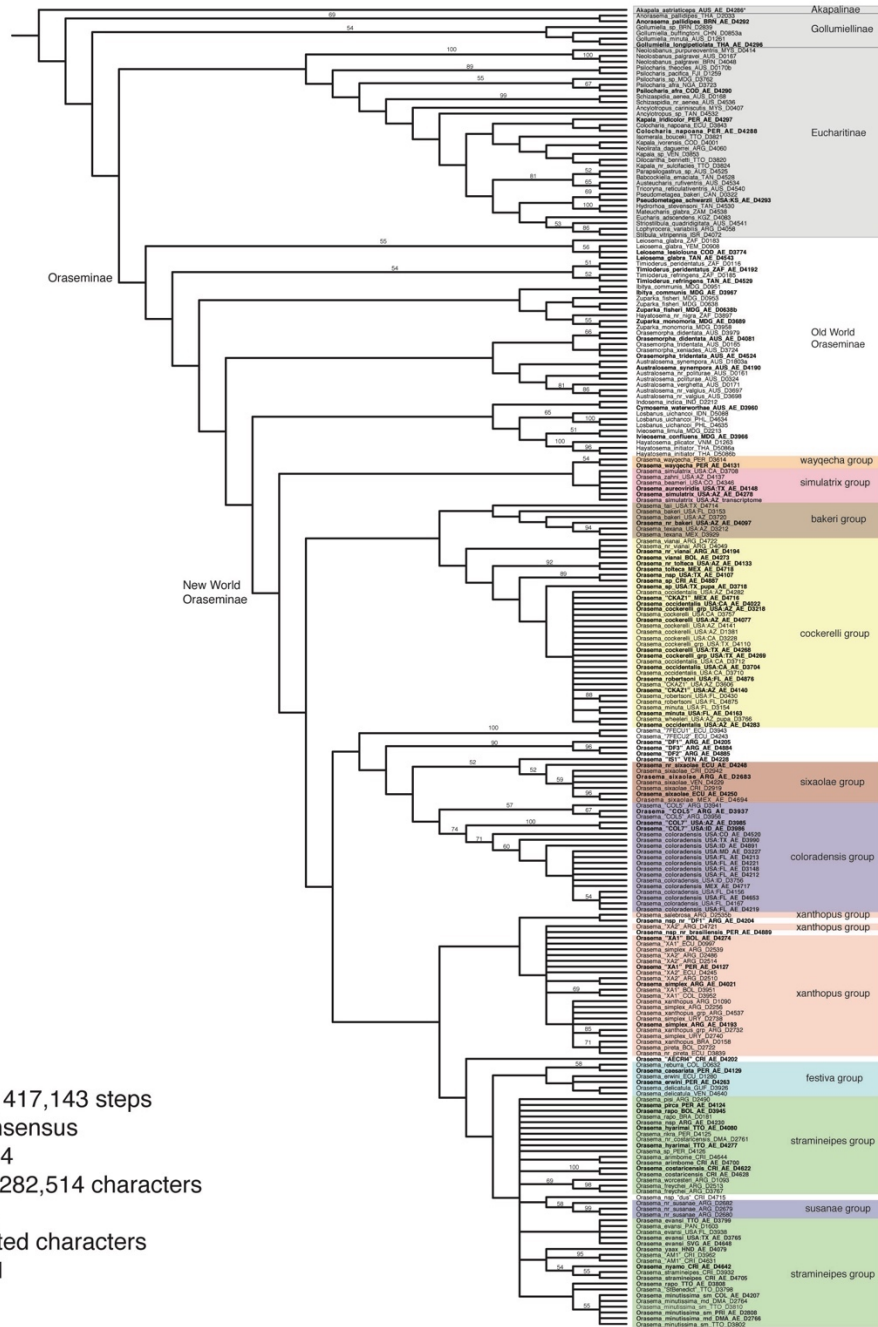


Figure 1.8: Strict consensus of 25 most parsimonious trees of the Combined dataset from TNT (417,143 steps). Bootstrap support values are indicated unless lower than 50. Taxa in bold have been sampled for AHE genes.

Maximum likelihood tree (Sanger)

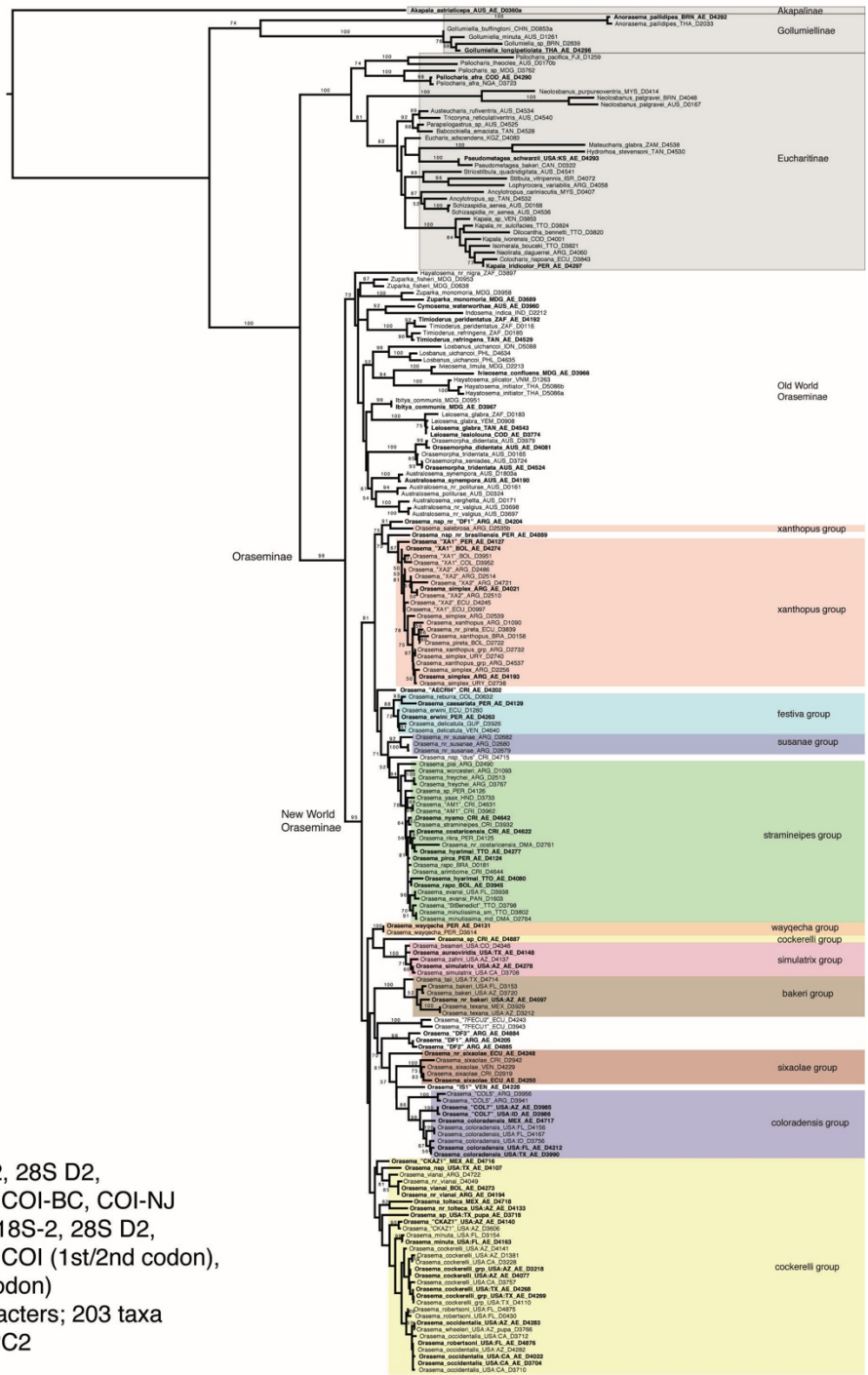


Figure 1.9: Maximum likelihood tree of the Sanger dataset from RAXML. Ribosomal genes partitioned by sequenced region and mitochondrial genes partitioned by codon position. Bootstrap support values are indicated unless lower than 50. Taxa in bold have been sampled for AHE genes.

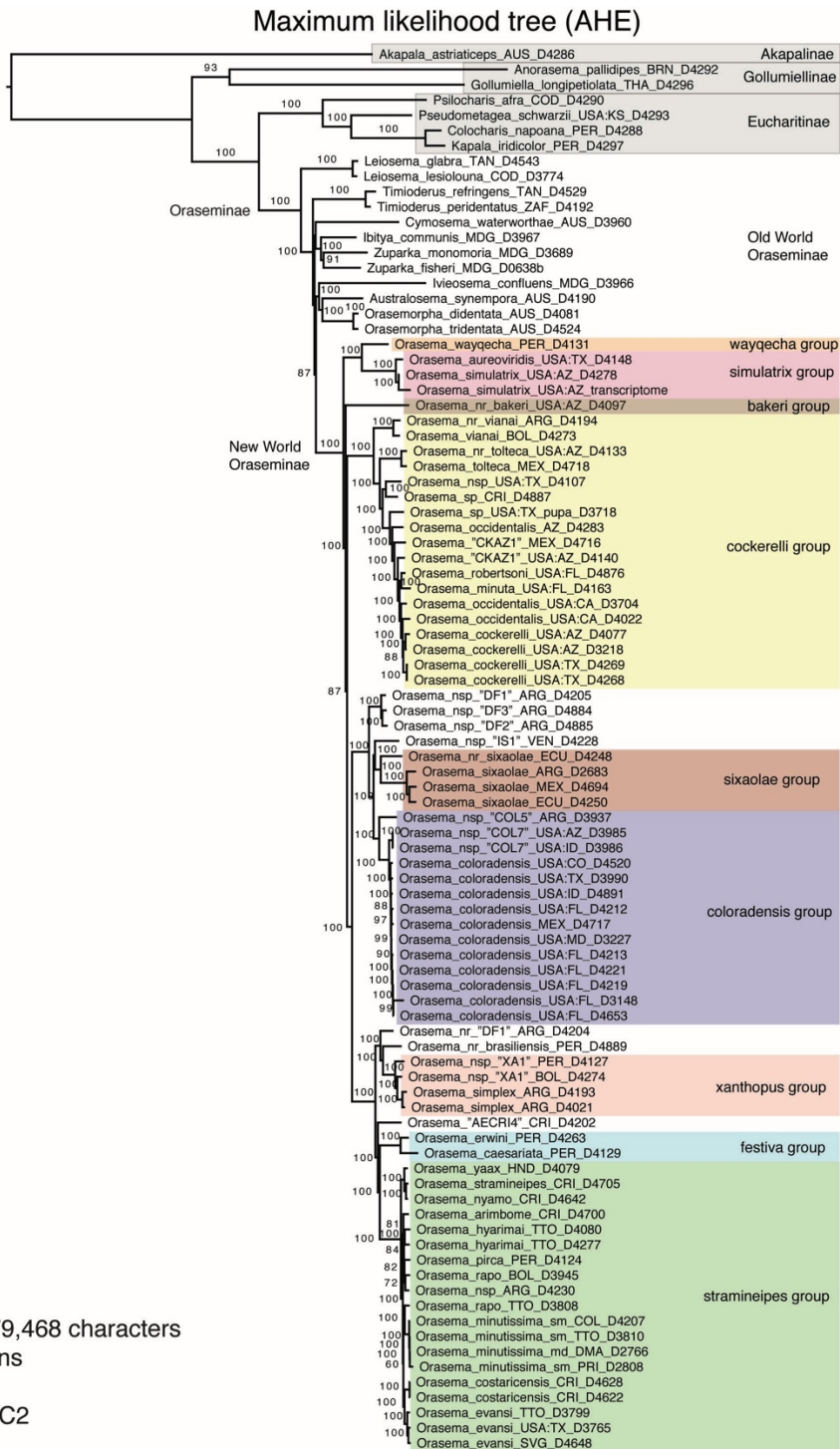


Figure 1.10: Maximum likelihood tree of the AHE dataset from RAXML. Genes partitioned by locus. Bootstrap support values are indicated unless lower than 50.

Maximum likelihood tree (Combined)

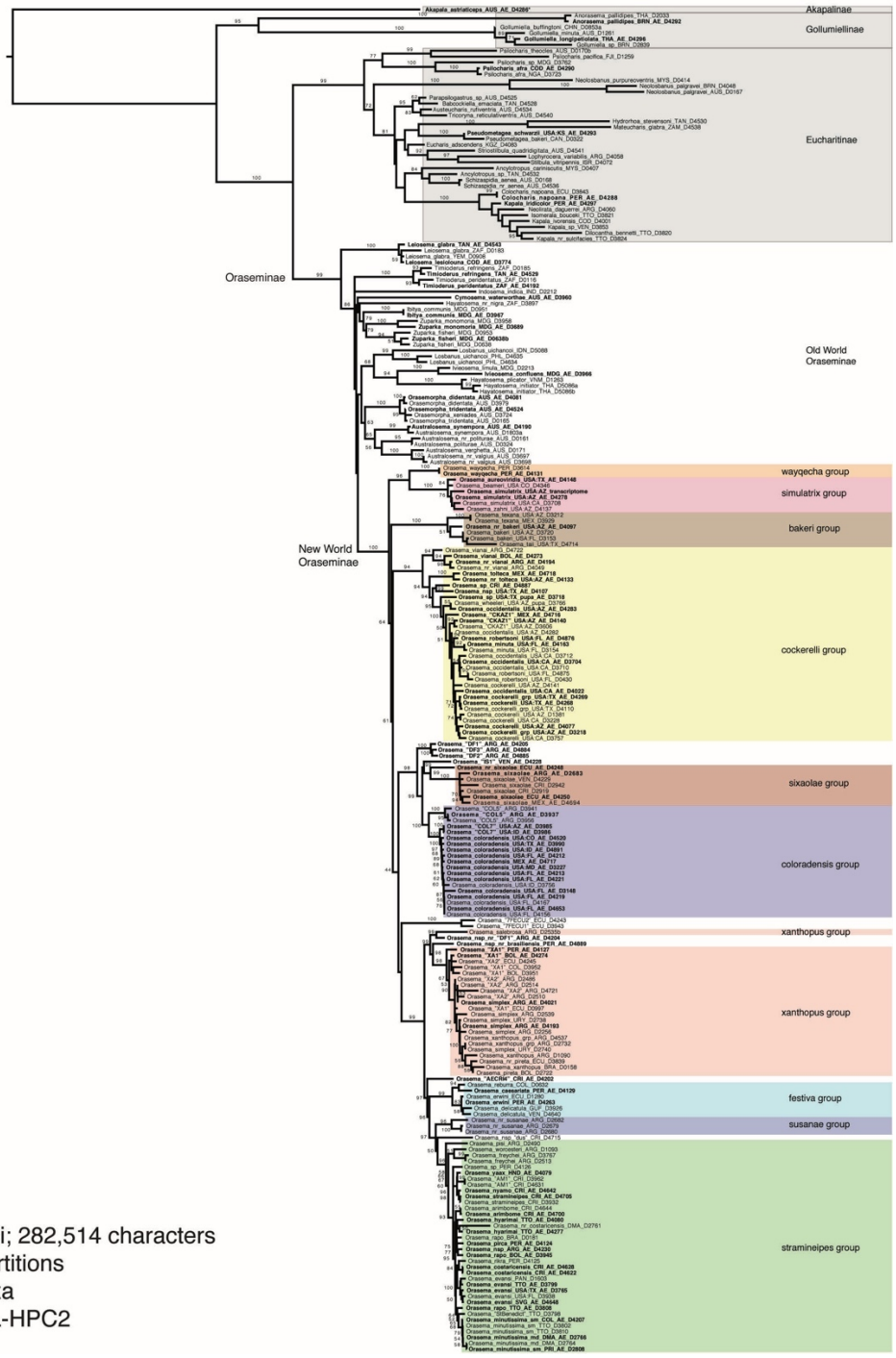


Figure 1.11: Maximum likelihood tree of the Combined dataset from RAXML. Sanger and AHE gene regions partitioned the same way as in Figs 1.9 and 1.10, respectively. Bootstrap support values are indicated unless lower than 50. Taxa in bold have been sampled for AHE genes.

Chronogram (Sanger)

5 loci; 3,046 characters
 203 taxa
 Relaxed clock log normal
 2 runs; 500 mil. gen/run
 Sample frequency=50,000
 ESS posterior=135

Priors

- ★ = ingroup constraint
- ★ = Psilocharis stem:
- log normal,
- M=8.08, S=1.0, O=39.2

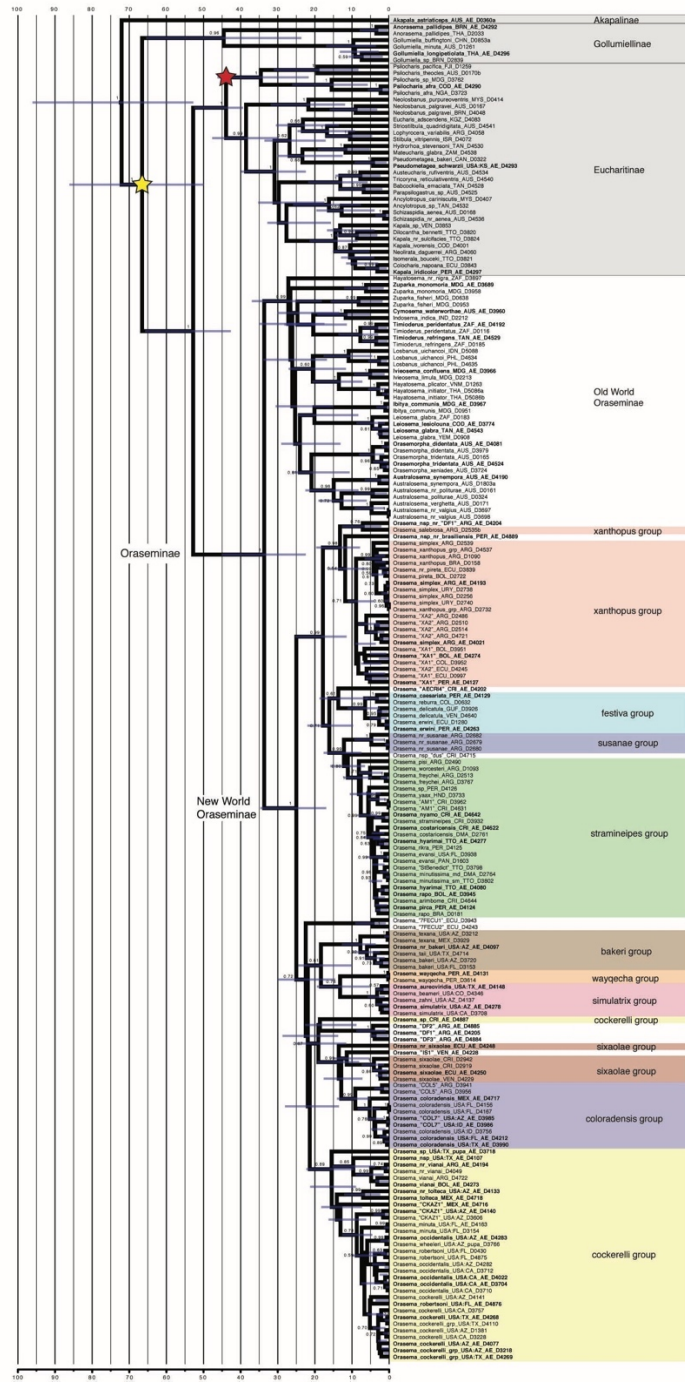
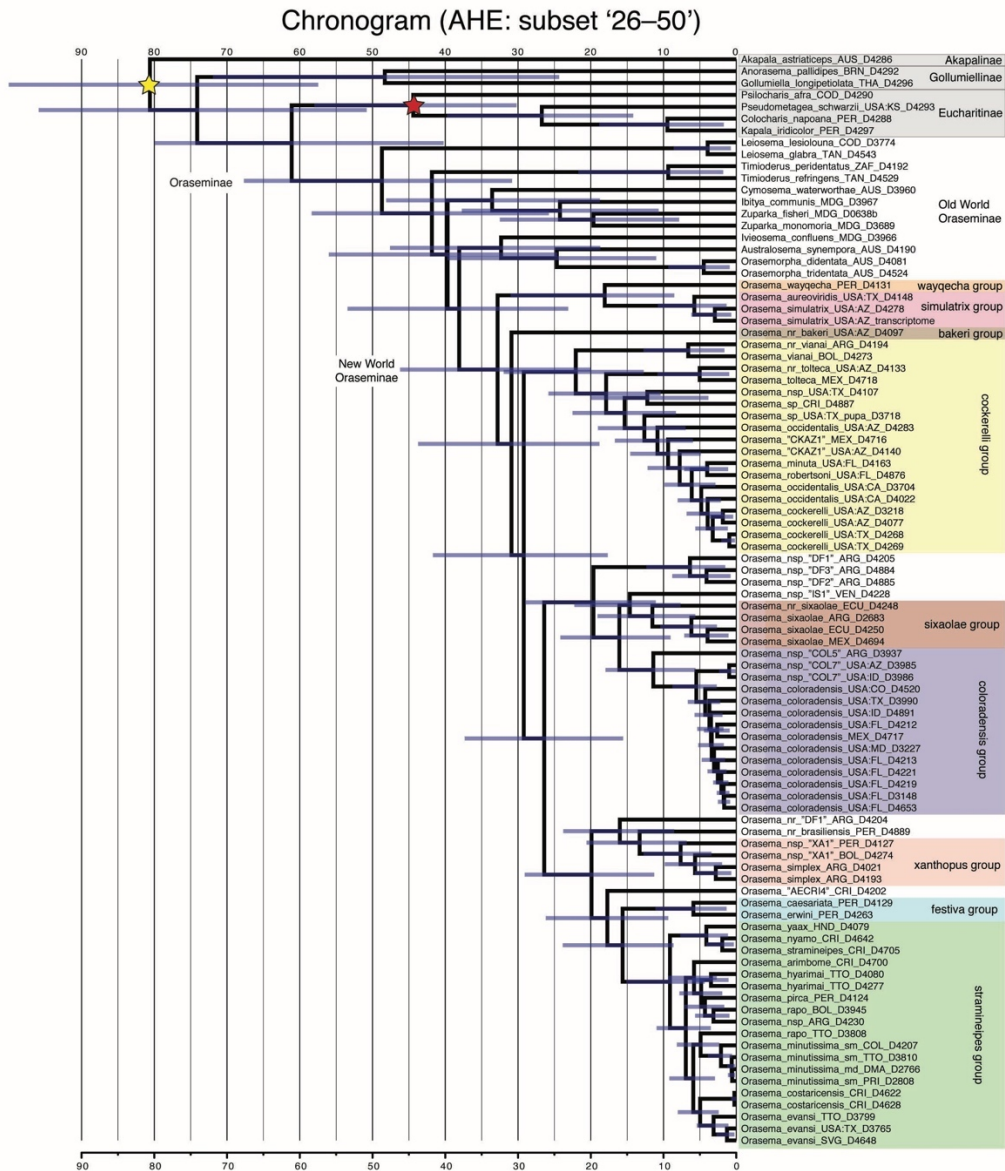


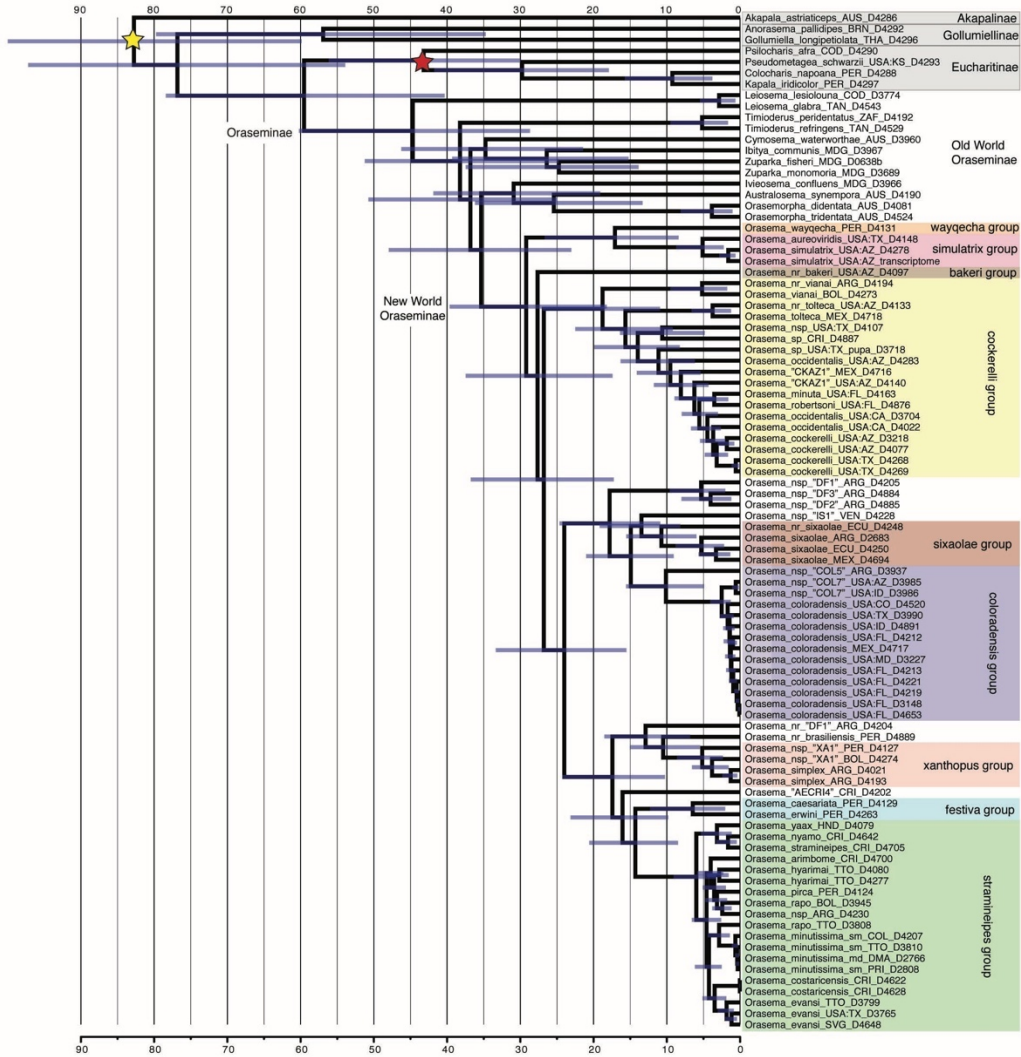
Figure 1.12: Maximum clade credibility chronogram of the Sanger dataset from BEAST2. Posterior probability support values are indicated unless lower than 50. Taxa in bold have been sampled for AHE genes. 95% HPD indicated by blue bars on nodes. Time scale is in millions of years.



25 AHE loci; 24,716 characters; 92 taxa
 Fixed tree topology (Fig.1.10); relaxed clock log normal
 150 million generations; sample frequency=20,000
 ESS posterior=158

Figure 1.13: Maximum clade credibility chronogram for loci ranked 26–50 of the AHE dataset from BEAST2 using a fixed topology (RAxML tree for all AHE loci; Fig. 1.10). Rankings are based on a PhyDesign analysis of the phylogenetic informativeness of the AHE loci (Table S1.4). 95% HPD indicated by blue bars on nodes. Time scale is in millions of years.

Chronogram (AHE: subset '51–75')



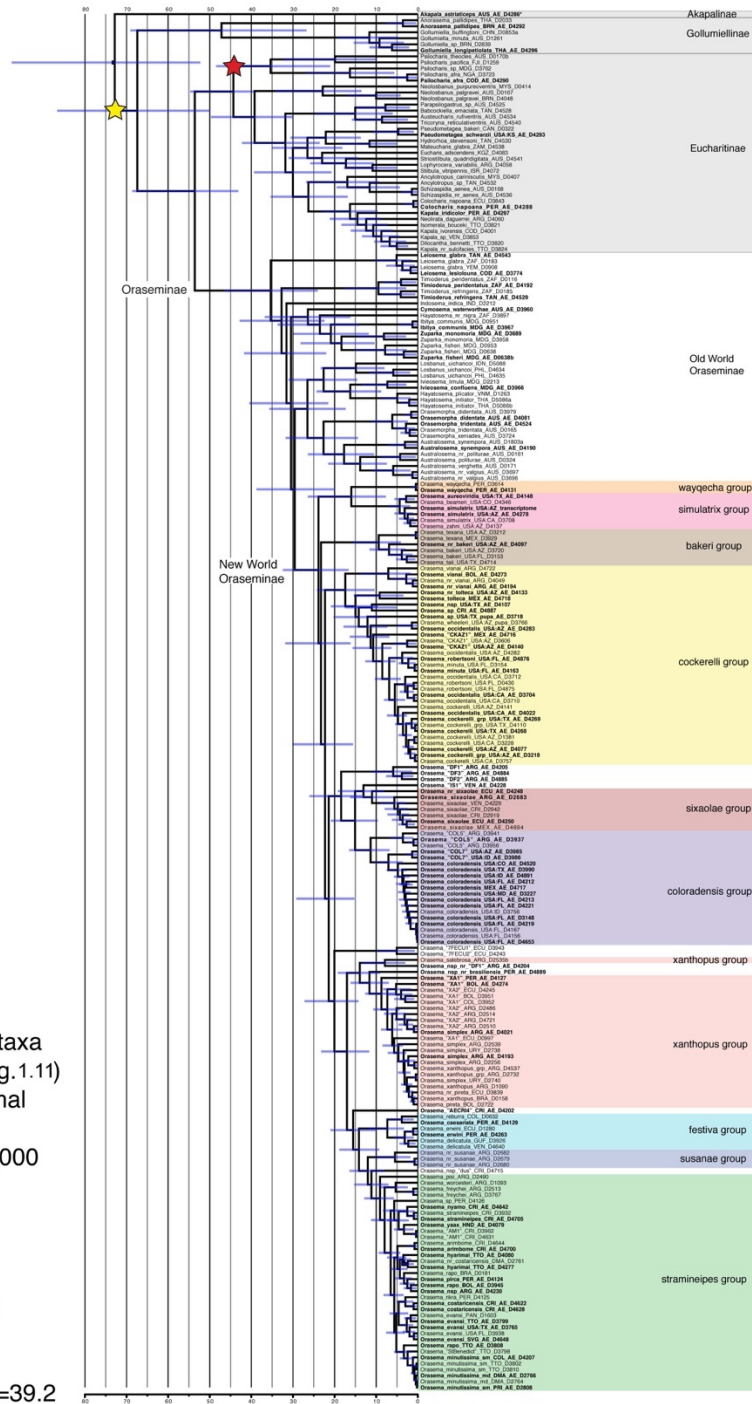
25 AHE loci; 26,127 characters; 92 taxa
 Fixed tree topology (Fig.1.10); relaxed clock log normal
 61 million generations; sample frequency=20,000
 ESS posterior=319

Priors

- ★ = root age constraint:
uniform, 45–100
- ★ = Eucharitinae crown secondary:
normal, M=52, S=7.8, O=0.95

Figure 1.14: Maximum clade credibility chronogram for loci ranked 51–75 of the AHE dataset from BEAST2 using a fixed topology (RAxML tree for all AHE loci; Fig. 1.10). Rankings are based on a PhyDesign analysis of the phylogenetic informativeness of the AHE loci (Table S1.4). 95% HPD indicated by blue bars on nodes. Time scale is in millions of years.

Chronogram (Combined)



5 Sanger loci
 3,046 characters; 229 taxa
 Fixed tree topology (Fig. 1.11)
 Relaxed clock log normal
 50 million generations
 Sample frequency=50,000
 ESS posterior=386

Priors
 ★ = ingroup constraint
 ★ = Psilocharis stem:
 log normal,
 M=8.08, S=1.0, O=39.2

Figure 1.15: Maximum clade credibility chronogram of the Combined dataset from BEAST2 using a fixed topology (RAxML tree of Combined dataset; Fig. 1.11) and using only the Sanger genes. 95% HPD indicated by blue bars on nodes. Time scale is in millions of years.

DEC tree (Combined)

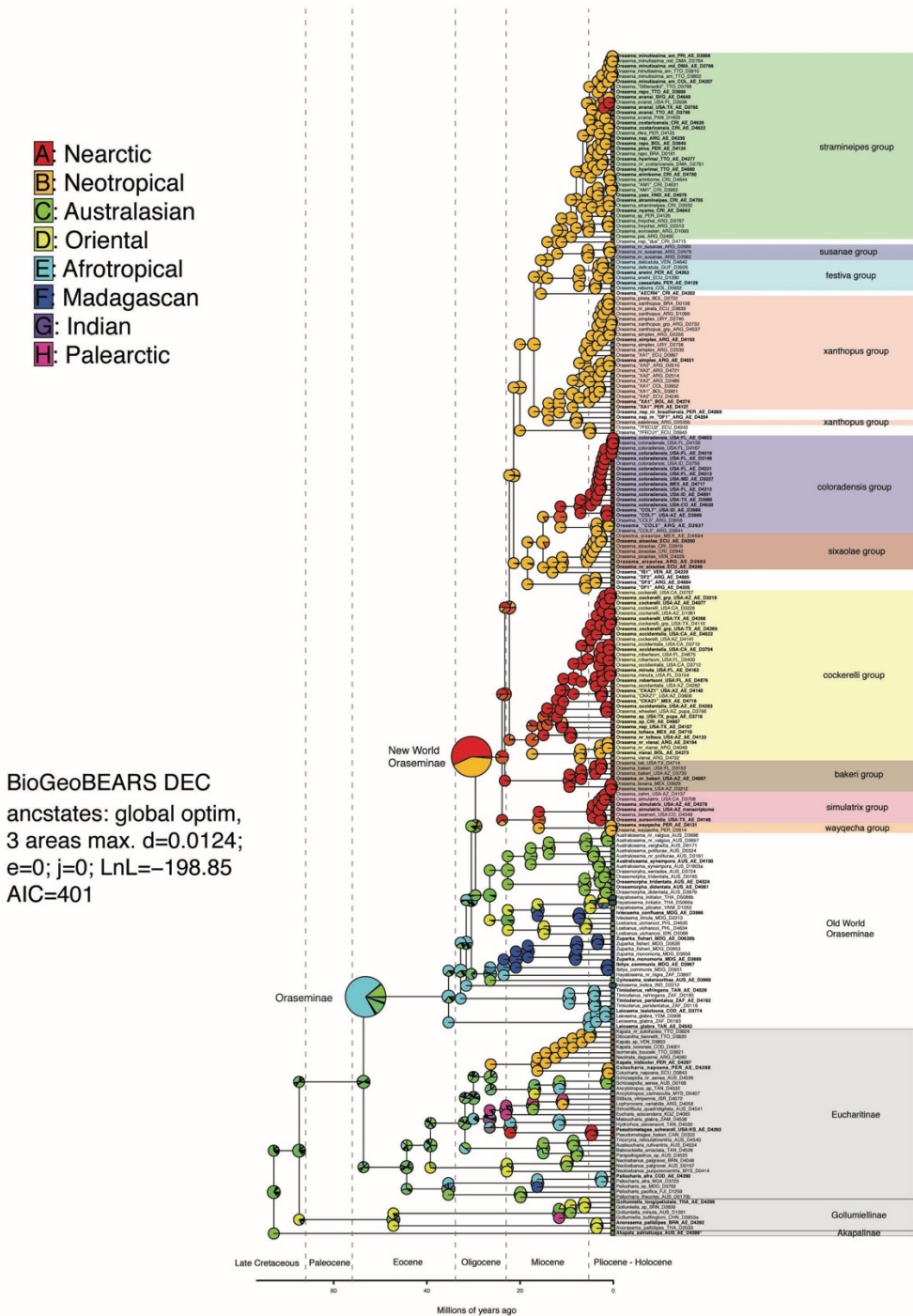


Figure 1.16: Dispersal, extinction, cladogenesis (DEC) analysis of the biogeography of the Combined dated tree (Fig. 1.15). Areas include: Nearctic, Neotropical, Australasian, Oriental, Afrotropical, Madagascan, Indian, and Palearctic. Dispersal rates were set by the position of the continents during historical epochs (Table S1.5).

DEC+J tree (Combined)

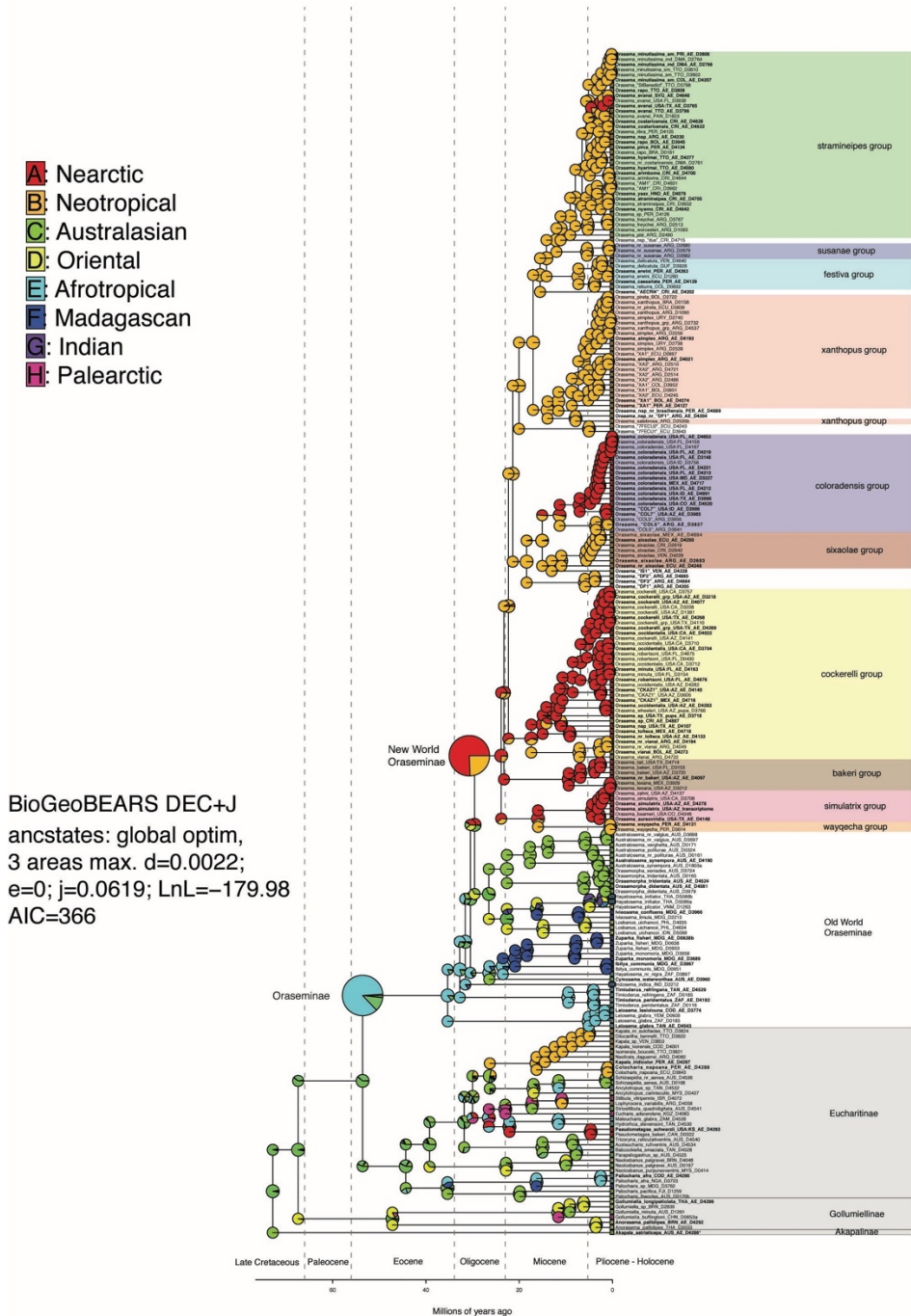


Figure 1.17: Dispersal, extinction, cladogenesis with jump dispersal (DEC+J) analysis of the biogeography of the Combined dated tree (Fig. 1.15). Areas include: Nearctic, Neotropical, Australasian, Oriental, Afrotropical, Madagascan, Indian, and Palearctic. Dispersal rates were set by the position of the continents during historical epochs (Table S1.5).

ASTRAL tree (AHE)

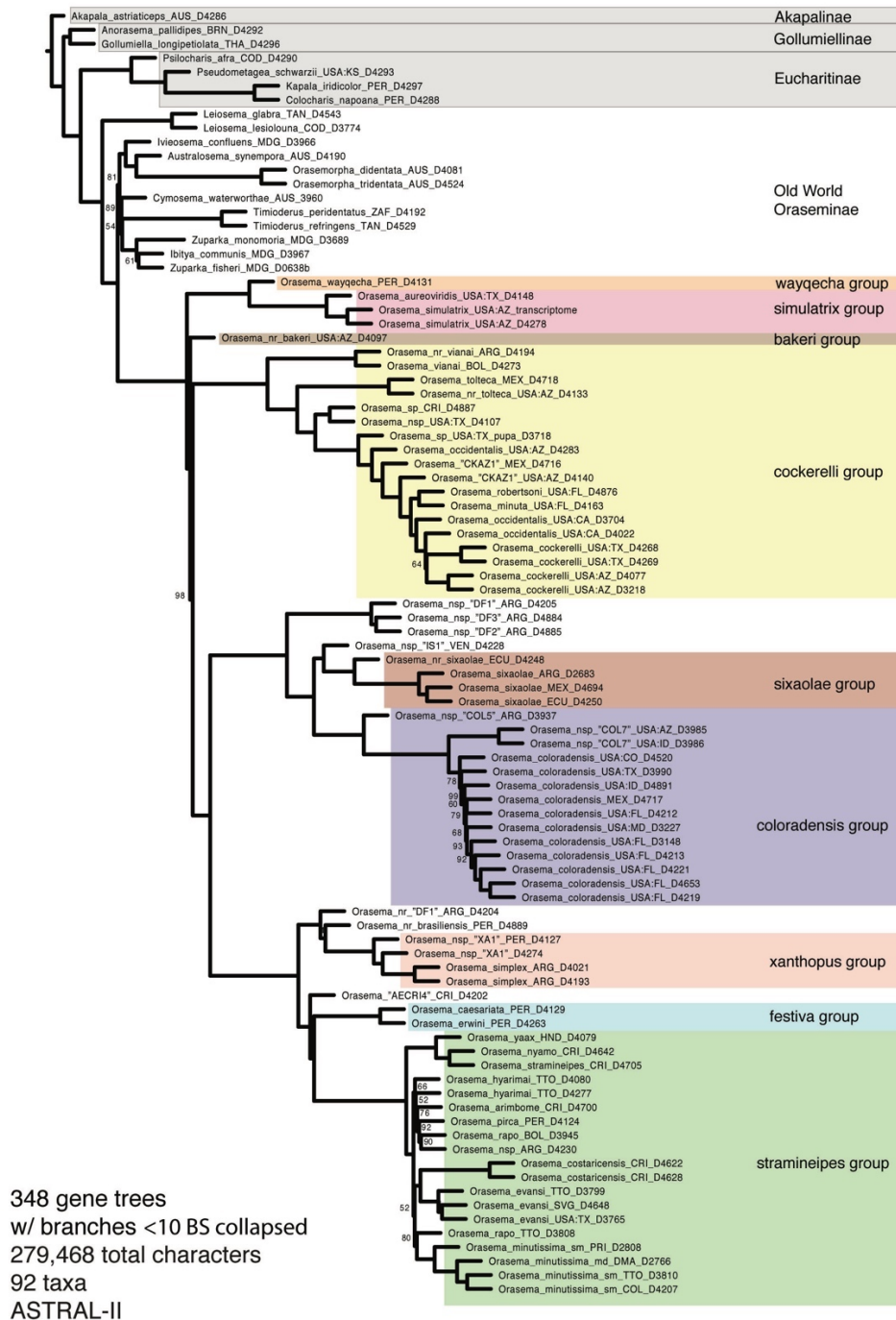


Figure 1.18: Coalescence species tree of Oraseminae from the AHE dataset using the program ASTRAL. 348 input trees (one for each AHE locus) were created in RAxML with clades supported by bootstrap values of 10 or less collapsed into polytomies. Support values are shown as local posterior probabilities (Sayyari & Mirarab, 2016); only values below 100 are shown.

Table 1.1: Oraseminae ant and plant host records								
Genus	Species Group	Species	Author	Ant Host	Reference	Plant Host	Plant Structure	Reference
<i>Australosema</i>		<i>valgus</i>	(Walker)	<i>Pheidole</i> sp.	Girault 1913	Santalaceae: <i>Exocarpos</i> sp.	spicule	Heraty 2000
<i>Hayatosema</i>		<i>assectator</i>	(Kerrich)	<i>Pheidole</i> sp.	Das 1963, Kerrich 1963	Theaceae: <i>Camellia sinensis</i> (L.) Kuntze	leaves	Das 1963, Kerrich 1963
<i>Hayatosema</i>		<i>initiator</i>	(Kerrich)			Theaceae: <i>Camellia sinensis</i> (L.) Kuntze	leaves	Kerrich 1963
<i>Ibitya</i>		<i>communis</i>	(Risbec)	<i>Pheidole veteratrix</i> Forel	Burks et al. 2017			
<i>Iviosema</i>		<i>fraudulenta</i>	(Reichensperger)	<i>Pheidole megacephala</i> (Fab.)	Reichensperger 1913			
<i>Losbanus</i>		<i>uichancoi</i>	(Heraty)			Fagaceae: <i>Celtis philippensis</i> Blanco, Leguminosae: <i>Leucaena leucocephala</i> (Lam.) de Wit	leaves	Ishii 1932
<i>Losbanus</i>		"sp. nr. <i>rugulosa</i> "		<i>Pheidole</i> sp.	Heraty 1990			
<i>Orasema</i>	bakeri	<i>taii</i>	Chien & Heraty	<i>Solenopsis geminata</i> (Fab.) X <i>xyloni</i> McCook hybrid	Heraty 1990, Chien & Heraty 2018	Leguminosae: <i>Acacia</i> sp., Fabaceae: <i>Vachellia</i> sp.	stems & leaves	Heraty 1990, Chien & Heraty 2018
<i>Orasema</i>	bakeri	<i>texana</i>	Gahan			Asteraceae: <i>Aster</i> sp.	bracts	Heraty 1990
<i>Orasema</i>	bakeri	"sp. 2 nr. <i>bakeri</i> "		<i>Pheidole</i> nr. <i>californica</i> Mayr, <i>P.</i> nr. <i>clementensis</i> Gregg, <i>Phieole</i> sp., <i>Tetramorium</i> sp.	Heraty 1990			
<i>Orasema</i>	cockerelli	<i>cockerelli</i>	Gahan			Leguminosae: <i>Acacia</i> sp.	stem, leaves	Heraty 1990

<i>Orasema</i>	cockerelli	<i>minuta</i>	Ashmead	<i>Pheidole</i> nr. <i>tetra</i> , <i>Temnothorax</i> <i>allardycei</i> (Mann)	Heraty 1990			
<i>Orasema</i>	cockerelli	<i>occidentalis</i>	Ashmead	<i>Pheidole</i> <i>pilifera</i> (Roger)	Wheeler & Wheeler 1986			
<i>Orasema</i>	cockerelli	<i>robertsoni</i>	Gahan	<i>Pheidole</i> <i>dentata</i> Mayr	Van Pelt 1950			
<i>Orasema</i>	cockerelli	<i>tolteca</i>	Mann	<i>Pheidole</i> <i>hirtula</i> Forel	Mann 1914	Asteraceae: <i>Melampodium</i> sp., Buddlejaceae: <i>Buddleja</i> sp., Fabaceae: <i>Dalea</i> sp., Malvaceae: <i>Sphaeralcea</i> sp., Verbenaceae: <i>Lippia</i> sp.	bracts	Heraty 1990
<i>Orasema</i>	cockerelli	<i>vianai</i>	Gemignani					
<i>Orasema</i>	cockerelli	<i>viridis</i>	Ashmead	<i>Pheidole</i> <i>tepicana</i> Pergande	Wheeler 1907	Asteraceae: <i>Haplopappus</i> sp., <i>Viguiera</i> sp., Malvaceae: <i>Sphaeralcea</i> sp.	bracts	Johnson et al. 1986
<i>Orasema</i>	cockerelli	<i>wheeleri</i>	Wheeler	<i>Pheidole</i> <i>ceres</i> Wheeler, <i>P.</i> <i>tepicana</i> Pergande	Wheeler 1907, Gahan 1940	Asteraceae: <i>Machaeranthera</i> sp.	bracts	Heraty 1990
<i>Orasema</i>	cockerelli	"nr. <i>cockerelli</i> "				Boraginaceae: <i>Cordia</i> sp.	flower stem	Heraty 1990
<i>Orasema</i>	cockerelli	"sp. 1 nr. <i>viridis</i> "				Verbenaceae: <i>Lantana</i> sp.	bracts?	Heraty 1990
<i>Orasema</i>	cockerelli	"sp. 2 nr. <i>viridis</i> "				Fabaceae: <i>Parkinsonia</i> sp., Lamiaceae: <i>Salvia</i> sp., Rhamnaceae: <i>Condalia</i> sp.	bracts, flower stem	Heraty 1990

<i>Orasema</i>	coloradensis	coloradensis	Wheeler	<i>Pheidole bicarinata</i> Mayr, <i>Solenopsis molesta</i> Emery, <i>Formica subnitens</i> Creighton (questionable)	Wheeler 1907, Johnson et al. 1986	Asteraceae: <i>Ericameria nauseosa</i> (Pall. ex Pursh) G.L. Nesom & G.I. Baird, Fabaceae: <i>Chamaecrista fasciculata</i> (Michx.) Greene, Gramineae	leaf blade	Johnson et al. 1986, Heraty 1990
<i>Orasema</i>	simulatrix	aureoviridis	Gahan			Asteraceae: <i>Psilostrophe</i> sp., Fabaceae: <i>Prosopis grandulosa</i> Torr.	leaves, bracts	Herreid 2015, Heraty 1990
<i>Orasema</i>	simulatrix	beameri	Gahan			Salicaceae: <i>Populus angustifolia</i> James	leaves	Herreid 2015
<i>Orasema</i>	simulatrix	simulatrix	Gahan	<i>Pheidole desertorum</i> Wheeler	Carey et al. 2012	Bignoniaceae: <i>Chilopsis linearis</i> (Cav.) Sweet	leaves	Carey et al. 2012
<i>Orasema</i>	simulatrix	zahni	Herreid			Fabaceae: <i>Prosopis grandulosa</i> Torr., <i>P. velutina</i> Wooton	leaves	Herreid 2015
<i>Orasema</i>	sixaolae	sixaolae	Wheeler & Wheeler	<i>Solenopsis tenuis</i> Mayr	Wheeler & Wheeler 1937			
<i>Orasema</i>	stramineipes	achkola	Burks, Heraty & Dominguez	<i>Pheidole dentata</i> Mayr	Heraty 1994			
<i>Orasema</i>	stramineipes	costaricensis	Wheeler & Wheeler	<i>Pheidole flavens</i> Roger, <i>P. vallifica</i> Forel	Wheeler & Wheeler 1937, Kempf 1972	Anacardiaceae: <i>Mangifera</i> sp., Calophyllaceae: <i>Callophyllum</i> ?, Rubiaceae: <i>Coffea</i> sp.	leaves	Heraty & Darling 1984, Heraty 1990, Burks et al. 2018
<i>Orasema</i>	stramineipes	evansi	Burks, Heraty & Dominguez	<i>Pheidole dentata</i> Mayr	Burks et al. 2018	Musaceae: <i>Musa</i> sp., Euphorbiaceae: <i>Alchornea costaricensis</i> Pax and K. Hoffm., Fagaceae: <i>Quercus nigra</i> L.	leaves, banana fingers	Kerrich 1963, Heraty 1990, Burks et al. 2018

<i>Orasema</i>	stramineipes	<i>freychei</i>	(Gemignani)	<i>Solenopsis quiquecuspis</i> Forel	Varone et al. 2010	Aquifoliaceae: <i>Ilex paraguariensis</i> A.St.-Hil., Bignoniaceae: <i>Tecoma stans</i> (L.) Juss. ex Kunth, <i>Amphilophium carolinae</i> (Lindl.) L.G. Lohmann, Oleaceae: <i>Olea europaea</i> L., Ericaceae: <i>Vaccinium corymbosum</i> L., Polygonaceae: <i>Muehlenbeckia sagittifolia</i> Meissn, Passifloraceae: <i>Passiflora caerulea</i> L., Ranunculaceae: <i>Clemantis</i> sp.	leaves	Burks et al. 2018, Nicolini 1950, Varone et al. 2010
<i>Orasema</i>	stramineipes	<i>minutissima</i>	Howard	<i>Pheidole</i> sp., <i>Wasmannia auropunctata</i> (Roger), <i>W. sigmoidea</i> (Mayr)	Mann 1918, Heraty 1994, Wetterer & Porter 2003, Burks et al. 2018	Cyathaceae: <i>Cyathea tenera</i> (J. Sm. ex Hook) T. Moore, Nephrolepidaceae: <i>Nephrolepis biserrata</i> (Sw.) Schott, Thelypteridaceae: <i>Thelypteris opposita</i> (Vahl) Ching, Polygonaceae: <i>Coccoloba uvifera</i> L., Simaroubaceae: <i>Simarouba amara</i> Aubl., Fabaceae: <i>Zapoteca ?formosa</i> (Kunth) H.M. Hern., Poaceae: <i>Gynerium sagittatus</i> (Aubl.) P.Beauv., Rubiaceae	leaves	Burks et al. 2018
<i>Orasema</i>	stramineipes	<i>rapo</i>	(Walker)	<i>Eciton quadriglume</i> (Haliday) (questionable)	Heraty 1990			

<i>Orasema</i>	stramineipes	<i>stramineipes</i>	Cameron			Piperaceae: <i>Piper multiplinervium</i> C. DC., <i>Piper sanctifelicis</i> Trel., Nephrolepidaceae: <i>Nephrolepis biserrata</i> (Sw.) Schott, Lauraceae: <i>Nectandra membranaceae</i> (Sw.) Griseb., Rubiaceae: <i>Pentagonia monocaulis</i> C.M. Taylor	leaves	Burks et al. 2018
<i>Orasema</i>	stramineipes	<i>woolleyi</i>	Burks, Heraty & Dominguez			Malvaceae: <i>Byttneria aculeata</i> (Jacq.) Jacq.	leaves	Burks et al. 2018
<i>Orasema</i>	stramineipes	<i>worcesteri</i>	(Girault)	<i>Pheidole nitidula</i> Emery, <i>P. radoszkowskii</i> Mayr	Gemignani 1933, Heraty et al. 1993			
<i>Orasema</i>	stramineipes	"AM1"		<i>Pheidole</i> sp.				
<i>Orasema</i>	susanae	<i>susanae</i>	Gemignani	<i>Pheidole</i> nr. <i>tetra</i>	Heraty 1990			
<i>Orasema</i>	wayqecha	<i>wayqecha</i>	Herreid	<i>Pheidole</i> sp.	Herreid 2015	Primulaceae: <i>Myrsine</i> sp.	leaves	Herreid 2015
<i>Orasema</i>	xanthopus	<i>pireta</i>	Heraty	<i>Solenopsis</i> sp.	Varone et al. 2010			
<i>Orasema</i>	xanthopus	<i>salebrosa</i>	Heraty	<i>Solenopsis invicta</i> Buren, <i>S. richteri</i> Forel	Heraty et al. 1993, Varone et al. 2010			

<i>Orasema</i>	xanthopus	<i>simplex</i>	Heraty	<i>Solenopsis invicta</i> Buren, <i>S. macdonaghi</i> Santschi, <i>S. quinquecupis</i> Forel, <i>S. richteri</i> Forel	Heraty et al. 1993, Varone et al. 2010	Smilacaceae: <i>Smilax campestris</i> Griseb, Poaceae: <i>Paspalum unispicatum</i> (Scribn. & Merr.) Nash, <i>P. denticulatum</i> Trin., <i>P. notatum</i> Fluegge, <i>P. dilatatum</i> Poir, Asteraceae: <i>Grindelia pulchella</i> Dann., <i>Stevia</i> aff. <i>entrierensis</i> Hieron, <i>Eupatorium</i> aff. <i>laevigatum</i> L., Fabaceae: <i>Sesbania virgata</i> (Cav.) Pers., Apocynaceae: <i>Asclepias curassavica</i> L., Verbenaceae: <i>Verbena montevidensis</i> Spreng., Malvaceae: <i>Sida rhombifolia</i> L., Scrophulariaceae: <i>Stemodia</i> aff. <i>lanceolata</i> Benth	leaves	Varone & Briano 2009
<i>Orasema</i>	xanthopus	<i>xanthopus</i>	(Cameron)	<i>Solenopsis invicta</i> Buren, <i>S. quinquecupis</i> Forel, <i>S. richteri</i> Forel, <i>S. sp.</i> (<i>saevisima</i> complex)	Silveira-Guido et al. 1964, Heraty et al. 1993, Varone et al. 2010			
<i>Orasemorpha</i>		<i>didentata</i>	(Girault)			Buxaceae: <i>Buxus sempervirans</i> L., Myrtaceae: <i>Melaleuca</i> sp.	leaves	Heraty 2000
<i>Orasemorpha</i>		<i>eribotes</i>	(Walker)	<i>Pheidole</i> sp.	Boucek 1988			
<i>Orasemorpha</i>		<i>myrmicae</i>	(Girault)	<i>Pheidole</i> sp.	Heraty 1994			

<i>Orasemorpha</i>		<i>tridentata</i>	(Girault)	<i>Pheidole proxima</i> Mayr	Brues 1934			
<i>Orasemorpha</i>		<i>xeniades</i>	(Walker)	<i>Pheidole tasmaniensis</i> Mayr	Heraty 1994			
<i>Timioderus</i>		<i>acuminatus</i>	Heraty	<i>Pheidole capensis</i> Mayr	Heraty 2000			
<i>Timioderus</i>		<i>peridentatus</i>	Heraty			Fabaceae: <i>Aspalathus</i> sp.	spicule	Heraty 2000
<i>Zuparka</i>		<i>monomoria</i>	(Heraty)	<i>Monomorium</i> sp.	Heraty 2000			

Chapter 2: A revision of the New World ant parasitoid genus *Orasema*

(Hymenoptera: Eucharitidae)

Abstract

Orasema Cameron (Eucharitidae) is a widespread New World genus of myrmicine ant parasitoids ranging from northern Argentina to southern Canada. At least 16 species groups can be recognized, but a comprehensive identification key to these groups has not been available. We revise several species groups, provide keys to species groups and species, and discuss the detailed life histories of several well-documented species. The *Orasema coloradensis* species group includes four species: *O. coloradensis* Wheeler, *O. iridescens* **n. sp.**, *O. scaura* **n. sp.**, and *O. violacea* Ashmead. The *Orasema bakeri* species group includes six species: *O. bablyi* **n. sp.**, *O. bakeri* Gahan, *O. dubitata* **n. sp.**, *O. polymyrmex* **n. sp.**, *O. taii* Chien & Heraty, and *O. texana* Gahan. The *Orasema tolteca* species group includes two species: *O. castilloae* **n. sp.** and *O. tolteca* Mann. The *Orasema sixaolae* species group is newly described and includes four species: *O. brachycephala* **n. sp.**, *O. nebula* **n. sp.**, *O. sixaolae* Wheeler & Wheeler, and *O. tinalandia* **n. sp.** The *Orasema acuminata* species group is newly described and includes two species: *O. acuminata* **n. sp.** and *O. cerulea* **n. sp.** The *Orasema hippocephala* species group is newly described and includes two species: *O. chrysozona* **n. sp.** and *O. hippocephala* **n. sp.** The *Orasema johnsoni* group is newly described and includes two species: *O. johnsoni* **n. sp.** and *O. spyrogaster* **n. sp.** The *Orasema heacoxi* group is newly described and includes two species: *O. heacoxi* **n. sp.** and *O. masonicki* **n. sp.**

Several unplaced species are described: *O. brasiliensis* (Bréthes), *O. cirrhocnemis* **n. sp.**, *O. monstrosa* **n. sp.**, *O. mutata* **n. sp.**, *O. psarops* **n. sp.**, and *O. roppai* **n. sp.** Species concepts and relationships are based on morphology and a recently published molecular phylogeny.

Introduction

Eucharitidae (Hymenoptera: Chalcidoidea) is the largest known hymenopteran clade of obligate parasitoids of immature ants (Clausen, 1940, 1941; Heraty, 1985, 2002; Lachaud & Pérez-Lachaud, 2012). The subfamily Oraseminae has a worldwide distribution and are known to parasitize only myrmicine ants (Baker et al., 2020). Old World Oraseminae are now treated as 12 different genera (Burks, Heraty, Mottern, Dominguez, & Heacox, 2017). *Orasema* Cameron is now restricted to the New World and currently comprises 72 described species. Several species groups of *Orasema* s.s. (New World) have been revised, including the *xanthopus* group (Heraty, Wojcik, & Jouvenaz, 1993), *festiva* group (Burks, Mottern, & Heraty, 2015), *simulatrix* and *wayqecha* groups (Herreid & Heraty, 2017), *stramineipes* group (Burks, Heraty, Dominguez, & Mottern, 2018), and *lasallei* group (Heraty & Baker, In Press), but several other species groups require revision or even recognition. With the large amount of phylogenetic information now available (Baker et al., 2020), we can approach the remaining species group designations and revisions with increased confidence.

Orasema is a monophyletic genus within a grade of Old World genera of Oraseminae (Fig. 2.1). Baker et al. (2020) proposed a single dispersal event for Oraseminae may have occurred across a Beringian Land Bridge into the New World approximately 24–30 MYA. Dispersal into the New World was accompanied by a tremendous radiation of species and adaptations from the ancestral host, *Pheidole* Westwood, to new host ant genera including *Solenopsis* Westwood, *Temnothorax* Mayr, and *Wasmannia* Forel. Along with this radiation, *Orasema* has become one of the most commonly collected genera of Eucharitidae in the New World, suggesting that it is not only diverse but relatively numerically abundant (Baker et al., 2020: figs 4, 5). Support along the backbone of the *Orasema* phylogeny is weak in the most taxon-inclusive maximum likelihood phylogeny but is in concordance with the highly-supported backbone of the Anchored Enrichment-only maximum likelihood phylogeny (Baker et al., 2020: figs S6 and S5, respectively). Their topology shows the *wayqecha+simulatrix* groups sister to the remaining *Orasema*, with the *bakeri* and *cockerelli* (= *cockerelli+heacoxi+tolteca+vianai*) groups paraphyletic and basal to the remaining species groups (Fig. 2.1). The Nearctic species groups (except *coloradensis* group) are distributed on the phylogeny, such that biogeographic analyses suggest a Nearctic-first dispersal followed by several Neotropical radiations (Baker et al., 2020: figs S11 and S12).

Orasema all have a strongly curved, apically swollen, and serrated ovipositor (Fig. 2.28F) to carve cavities into the leaves (Fig. 2.2D), stems (Fig. 2.2E), and involucre bracts of plants, in which single eggs are deposited per oviposition. These punctures

cause evident plant damage, and in several cases, species of *Orasema* have been regarded as minor agricultural pests (Heraty, 1994, 2000). Eggs hatch into planidial first-instar larvae that gain access to the host ant nest by phoretic attachment to foraging ant workers. An association with immature thrips (Fig. 2.2A), in which ants likely collect prey with attached planidia, has been observed in the *Orasema bakeri*, *cockerelli*, and *coloradensis* species groups (Chien & Heraty, 2018; Johnson, Miller, Heraty, & Merickel, 1986). An association of planidia with extrafloral nectaries (Fig. 2.2B) where ants feed has been observed in both the *Orasema simulatrix* and *wayqecha* species groups (Carey, Visscher, & Heraty, 2012; Herreid & Heraty, 2017). The exact means by which planidia enter the nest has not been verified, but they are likely transported in the infrabuccal pouch of the foraging ant. However, we have not found planidia in the mouthparts of their known myrmicine host genera, *Pheidole* or *Solenopsis*, but they have been found in the mouthparts (specifically the infrabuccal pouch) of *Formica* and *Camponotus* foraging on the same plants (Herreid & Heraty, 2017; Johnson et al., 1986), which they cannot parasitize. Given the small size of the worker caste of the ants *Orasema* can parasitize (*Pheidole*, *Solenopsis*, *Wasmannia*, and *Temnothorax*), it is possible that planidia develop exclusively on larval soldiers, males, and queens (Wheeler, 1907). However, it is also possible that *Orasema* can adapt to the size of its host and the quantity of food available, which has been inferred from the size polymorphism in *Orasema minutissima* Howard (Burks et al., 2018), or that parasitism by the planidium may be affecting growth of the host larva (Heraty, 1990). Once in the nest, planidia transfer to the ant larvae, likely during trophallaxis. A planidium will feed on an ant larva, sometimes engorging itself to

several times its unfed size (Fig. 2.2C) but will only continue to development during the host's prepupal or pupal stage (Clausen, 1941; Wheeler, 1907). While on the host larva, the planidium is usually located dorsally on the host's thorax, and they transect the host's body wall with the parasitoid's posterior end exposed externally, making them effectively endoparasitic (Heraty & Murray, 2013; Wheeler & Wheeler, 1937). During the host's pupal stage, the planidium (and later instars) take a completely external position on the ventral region of the thorax, and because myrmicine ants do not have a pupal cocoon, the parasitoid is exposed in the brood pile. Once the immature wasp finishes developing through its three larval instars and pupal stage, the adult wasp can leave the nest unhindered by the ants because of the similar hydrocarbon profile it acquires from close association with its hosts (Vander Meer, Jouvenaz, & Wojcik, 1989). If the adult wasp fails to leave the nest within a few days, it can be eviscerated by the ants (Heraty, 1994).

This work completes revisions of all major species groups of *Orasema* with the exception of the *susanae* group (which we are treating here as three separate species: *O. argentina* Gemignani, *O. deltae* Gemignani, and *O. susanae* Gemignani; from Argentina), *vianai* group (South America), and *cockerelli* group (North America). Herein, we revise the *Orasema coloradensis* species group, the *Orasema bakeri* species group, and the *Orasema tolteca* species group. We describe five new species groups: the *Orasema sixaolae* species group, the *Orasema acuminata* species group, the *Orasema hippocephala* species group, the *Orasema johnsoni* species group, and the *Orasema heacoxi* group. We also describe six unplaced taxa: *O. brasiliensis* (Bréthes), *O. cirrhocnemis* n. sp., *O. monstrosa* n. sp., *O. mutata* n. sp., *O. psarops* n. sp., and *O.*

roppai n. sp. A key to all species groups of *Orasema* is provided, and keys to the species in the groups being revised herein are provided.

Methods and Materials

Specimens. Material was examined from the following collections: ABS, Archbold Biological Station, Lake Placid, FL; AEIC, American Entomological Institute, Gainesville, FL; AMNH, American Museum of Natural History, New York, NY; ANSP, Academy of Natural Sciences, Philadelphia, PA; BMNH, Natural History Museum, London, United Kingdom; CASC, California Academy of Sciences, San Francisco, CA; CMNH, Carnegie Museum of Natural History, Pittsburgh, PA; CNC, Canadian National Collection of Insects, Arachnids and Nematodes, Ottawa, ON; DEFS, Universidade de São Paulo, São Paulo, Brazil; EMEC, Essig Museum of Entomology, Berkeley, CA; FSCA, Florida State Collection of Arthropods, Gainesville, FL; IFML, Instituto Fundación Miguel Lillo, Tucumán, Argentina; INBIO, Instituto Nacional de Biodiversidad, Costa Rica; INPA, Coleção Sistemática da Entomologia, Amazonas, Brazil; LACM, Los Angeles County Museum of Natural History, Los Angeles, CA; MACN, Museo Argentina de Ciencias Naturales, Buenos Aires, Argentina; MCZ, Museum of Comparative Zoology, Cambridge, MA; MEM, Mississippi State University, Mississippi, MS; MTEC, Montana State University, Bozeman, MT; MUCR, Museo de Insectos, Universidad de Costa Rica, San Jose, Costa Rica; MZLU, Lund University, Lund, Sweden; NMW, Naturhistorisches Museum Wien, Wien, Austria; ROME, Royal

Ontario Museum, Toronto, Canada; SAMC, Iziko Museum of Cape Town, Cape Town, South Africa; SDEI, Senckenberg Deutsches Entomologisches Institut, Müncheberg, Germany; SEMC, Snow Entomological Museum, Lawrence, KS; TAMU, Texas A&M University, College Station, TX; UAIC, University of Arizona, Tucson, AZ; UBC, Spencer Museum, Vancouver, Canada; UCDC, R.M. Bohart Museum of Entomology, Davis, CA; UCFC, University of Central Florida, Orlando, FL; UCLA, University of California, Los Angeles, CA; UCRC, Entomology Research Museum, University of California, Riverside, CA; UFES, Coleção Entomologica, Vitória, Brazil; UMMZ, Museum of Zoology, Ann Arbor, MI; USNM, National Museum of Natural History, Washington, DC; WFBM, W.F. Barr Entomological Collection, Moscow, ID; WSU, Maurice T. James Entomological Collection, Pullman, WA.

All specimens have a unique identification barcode label that includes the codon for the museum deposition, and specimens were databased using FileMaker Pro v.17.0 (© FileMaker, Inc.). Specimens for molecular sequencing have unique voucher identification labels; all vouchers were non-destructively sampled and deposited in their associated museums. Georeference points for specimens that were inferred from Google Earth v.7.3 (© Google, LLC) are denoted in italics. Images were taken with a Leica Imaging System (© Leica Microsystems) with a Z16 APO A microscope and stacked with Zerene Stacker v.1.04 (© Zerene Systems, LLC). Measurements were taken with an eyepiece micrometer for as many male and female specimens as were available up to a maximum of 10 specimens per sex.

Species were recognized and delimited based on a combination of molecular phylogenetic results from Baker et al. (2020) and observed morphological differences. The major challenge for delimiting species of *Orasema* is recognizing highly polymorphic species (e.g. *Orasema coloradensis* Wheeler and *Orasema minutissima*) versus multiple closely-related species. Species are presumed to have small amounts of polymorphism unless genetic sampling shows minimal variation between sampled individuals. We did not use objective cutoff values for genetic distance to delimit species because different species groups show varying amounts of genetic distance correlated to their morphological diversity, and delimitation decisions were made on a case-by-case basis.

Descriptions were initially generated using species description software written by Roger Burks in FileMaker Pro. Species group descriptions were generated by consolidating all invariable characters coded for species in that group and each species description reduced to only those features differing between species within a group. Morphological terms, including sculpture and abbreviations, follow Burks et al. (2018) and Heraty, Burks, Mbanyana, and Van Noort (2018). Examples of sculpture with terminology are provided (Fig. 2.3) and are largely based on the descriptions by Eady (1968) and Harris (1979).

Abbreviations used for measurements (see Figs 2.4C, 2.6): EH, eye height; F2L, second flagellomere length; F2W, second flagellomere width; F3L, third flagellomere length; FL, flagellum length; FWL, fore wing length; FWW, fore wing width; HCL, hind coxa length; HCW, hind coxa width; HFL, hind femur length; HFW, hind femur width;

HH, head height; HW; head width; IOD, interocular distance; MH, mesosoma height; ML, mesosoma length; MS, malar space; PTL, petiole length; PTW, petiole width. Palpomere formula follows a maxillary:labial format, and mandibular tooth count follows a right:left format.

Additional abbreviations used in figures (see Figs 2.3, 2.4, 2.6, 2.19, 2.33, and 2.34): acs, acrosternite; acy, anteclypeus; anl (F1), anellus (flagellomere 1); apc, anterior petiolar carina; ax, axilla; axs, axillular sulcus; bsa, basal area; cal, callus; cc, costal cell; clv, clava; cly, clypeus; cp, caudal pad; dor, dorsal view; dv, second (dorsal) valvula; F2/Fu1–F8/Fu7, flagellomeres 2–8 or funiculars 1–7; frl, frenal line; frn, frenum; lbr, labrum; llm, lateral lobe of mesoscutum; lp, labial palp; man, mandible; mlm, midlobe of mesoscutum; mp, maxillary palp; mv, marginal vein; not, notaulis; ped, pedicel; pet, petiole; pg, postgena; pmv, postmarginal vein; ppd, propodeum; pre, prepectus; pst, parastigma; sca, supraclypeal area; scd, mesoscutellar disc; scp, scape; smv, submarginal vein; spc, speculum; sss, scutoscutellar sulcus; stv, stigmal vein; TI–TXII, tergum 1–12; tpl, tergopleural line; ven, ventral view; vlf, valvifer; vv, first (ventral) valvula; wd, wing disc.

All phylogenetic analyses reported herein are from Baker et al. (2020).

Results

Key to the species groups of *Orasema*

- 1) Male and female antenna with 6 funicular segments (Fig. 2.42 D, E); mesoscutum and mesoscutellum rugose-areolate; scutoscutellar sulcus crossed by strong carinae (Fig. 2.42F); male antennal clava highly reduced (Fig. 2.42E)
..... *Orasema mutata* n. sp.
- Antenna with more than 6 funicular segments; mesoscutum and mesoscutellum with various sculpture; scutoscutellar sulcus usually with weaker carinae; male antennal clava not reduced 2
- 2) Male and female antenna with 7 funicular segments (Fig 2.6E: Fu1–Fu7); labrum with 4 digits (except some specimens of *O. scaura* (*Orasema coloradensis* group; up to 9 digits) which is the only species with 4 tarsomeres) 3
- Male and female antenna with 8–9 funicular segments (Fig. 2.18 D, E); labrum with 4 or more digits 17

Funicle 7-segmented

- 3) Midlobe of mesoscutum evenly reticulate (Fig. 2.3D) 4
- Midlobe of mesoscutum smooth (Fig. 2.3H) or with coarse irregular sculpture (Fig. 2.3 A, C, E, I), including rugose-reticulate (Fig. 2.3F) 10

Midlobe of mesoscutum reticulate

- 4) Postgena expanded over labiomaxillary complex (Fig. 2.31D)
..... *Orasema simulatrix* group; key provided in Herreid and Heraty (2017)
– Postgena not expanded, labiomaxillary complex visible (Fig. 2.4A) 5
- 5) Anterior margin of prepectus lacking carina and gradually sloping under margin
of pronotum (Fig. 2.13C) *Orasema bakeri* group, page 121
– Anterior margin of prepectus with carina (Fig. 2.18C) 6
- 6) Body size small (females 1.5–2.1 mm; males 1.5–2 mm); body color dark with
some iridescence; antenna (male and female) pedunculate with funicular segments
broader than long (Fig. 2.24 D,E)
..... (*Orasema sixaolae* Wheeler & Wheeler) *Orasema sixaolae* group, page 155
– Body size variable (females and males usually >2 mm); body color most often
strongly green or blue-green iridescent, but if dark, female antenna not
pedunculate and funicular segments longer than broad 7
- 7) Fore wing with one row of setae on the posterior end of the basal area; fore wing
disc with dense, long setae; female antennal funicular segments generally longer
than or as long as wide, width consistent from F3 to the clava (Fig. 2.4B)
..... *Orasema xanthopus* group (in part; undescribed species)

- Fore wing without only one row of setae in apical basal area, or if setae present, fore wing disc not densely setose, setae minute; female antennal funicular segments generally broader than long, width increasing from F3 to clava (Fig. 2.36D) **8**

 - 8)** Female face elongate (HW:HH 0.7–1 female; Fig. 2.37B); mesosoma elongate (ML:MH 1.4–1.6)
 (*Orasema masonicki* **n. sp.**) *Orasema heacoxi* group, page 186
 - Female face subtriangular (HW:HH 1–1.2); mesosoma tall (ML:MH 1–1.2) **9**

 - 9)** Nearctic distribution *Orasema cockerelli* group*
 - Neotropical distribution *Orasema vianai* group*
- * These two groups cannot be reliably differentiated morphologically, but they represent molecularly distinct lineages (Fig. 2.1).

Midlobe of mesoscutum not reticulate

- 10)** Body size large (male 3.8 mm); mandibular formula 2:2; mandibles and labrum reduced in size (Fig. 2.41B); antenna long (FL:HH 2) (female unknown)
 *Orasema monstrosa* **n. sp.** (unplaced to group)
- Body size variable (males typically <3.8 mm); mandibular formula 3:2; mandibles and labrum of normal size; antenna shorter (FL:HH typically <1.5) **11**

- 11)** Face, mesoscutal lateral lobe, axilla, mesoscutellum, and frenum sculpture smooth (Fig. 2.33F); face and eyes densely setose (Fig. 2.33B); length 2.1–2.9 mm; antenna with 8 funicular segments, but partial fusion between F2–F3 or F3–F4 giving appearance of 7 funiculars
 (*Orasema johnsoni* n. sp.) *Orasema johnsoni* group, page 180
- Sculpture distinct on at least some of the above-mentioned parts; if smooth, face and eyes lightly setose (Fig. 2.25B) and length approximately 1.4 mm; antenna with 7 funiculars **12**
- 12)** Midlobe of mesoscutum rugose-reticulate (Fig. 2.36F); female antennal flagellum progressively wider toward the apex (Fig. 2.36D); male antenna pedunculate, funiculars with semi-erect, curved setae (Fig. 2.36E)
 (*Orasema heacoxi* n. sp.) *Orasema heacoxi* group, page 186
- Midlobe of mesoscutum transversely costate (Fig. 2.3A), imbricate (Fig. 2.3E), rugose (Fig. 2.3I), or rugose-areolate (Fig. 2.3C); female antennal flagellum generally equal in width from F3–F8; male antenna rarely pedunculate, but if so (Fig. 2.27E), then setae not semi-erect, curved **13**
- 13)** Mesoscutum and mesoscutellum rugose-areolate (Fig. 2.27F); curvature of lateral lobes of mesoscutum (as seen dorsally) discontinuous with curvature of midlobe; antecostal sulcus smooth (Fig. 2.28E) *Orasema acuminata* group, page 167

- Midlobe of mesoscutum rarely rugose-areolate (i.e. either costate, imbricate, or rugose-reticulate); curvature of lateral lobes either continuous or discontinuous with curvature of midlobe; antecostal sulcus usually foveate, but if smooth, then other characters not matching **14**

- 14)** Body size small (females 1.4–2.2 mm; males 1.5–2 mm); body dark brown to black with some iridescence; midlobe of mesoscutum imbricate (Fig. 2.22E) or weakly transverse costate (Fig. 2.25E); head subcircular (Fig. 2.22B)
..... *Orasema sixaolae* group (in part), page 155

- Body size average (females 2.3–4.2 mm; males 2.1–3.4 mm); body usually with strong blue or green iridescence; midlobe of mesoscutum strongly costate (Fig. 2.6F) or rugose-areolate (Fig. 2.10F); head subtriangular (Fig. 2.8B) or elongate (Fig. 2.31B) **15**

- 15)** Face rugose-reticulate (Fig. 2.39B); funicular segments longer than broad (Fig. 2.39 D, E); femora yellow with at most a medial light brown patch (Fig. 2.39A) ...
..... *Orasema brasiliensis* (Bréthes) (unplaced to group)

- Face generally costate, but if rugose-reticulate, then funicular segments broader than long (Fig. 2.8D) and femora mostly dark brown with strong iridescence (Fig. 2.8A) **16**

- 16)** Mesosoma elongate (female ML:MH 1.6–2.2); head elongate (HW:HH 0.8–1.1) (Fig. 2.31B); occiput strongly curved (Fig. 2.31C)
 *Orasema hippocephala* group, page 173
- Mesosoma average (female ML:MH 1.2–1.7); head subtriangular (HW:HH 1.1–1.3) (Fig. 2.8B); occiput broadly curved (Fig. 2.10F)
 *Orasema coloradensis* group, page 103

Funicle 8–9 segmented

- 17)** Postgena expanded over labiomaxillary complex basally (Fig. 2.31D); fore wing with infuscations at least along cubital fold
 *Orasema wayqecha* group; key provided in Herreid and Heraty (2017)
- Postgena not expanded (Fig. 2.4A); fore wing completely hyaline **18**
- 18)** Face smooth; frons without any vertical costae (Fig. 2.33B) **19**
- Face sculptured (Fig. 2.18B), or if appearing mostly smooth, then frons with vertical costae (Fig. 2.4F) **20**
- 19)** Petiole with complete longitudinal carina on lateral margins (Fig. 2.4C); labrum with 8–10 digits; postmarginal vein on fore wing reaching near apex (Fig. 2.4D); lateral lobe of mesoscutum, axilla, mesoscutellar disc, and frenum with strong sculpture *Orasema festiva* group; key provided in Burks et al. (2015)

- Petiole without complete lateral longitudinal carina; labrum with 4 digits; postmarginal vein on fore wing short, not close to apex; lateral lobe of mesoscutum, axilla, scutellar disc, and frenum smooth (Fig. 2.33F)
..... *Orasema johnsoni* group, page 180

- 20)** Female and male with 9 funicular segments; fore wing basal area densely pilose; female femora completely yellow
..... *Orasema argentina* Gemignani (unplaced to group)

- Female with 8 funicular segments; male with 8 or 9 funicular segments; fore wing basal area bare to sparsely setose, never pilose; usually some femora medially dark **21**

- 21)** Fore wing costal cell with anteriorly expanded bare area (Fig 2.20H); face broad with reticulate sculpture (female MSP:EH 1–1.7; Fig. 2.20B); large body size (females 2.8–5.2 mm; usually >4 mm); males with 9 funiculars
..... *Orasema tolteca* group, page 146

- Fore wing without anteriorly expanded bare area of costal cell; face often subtriangular with reticulate or other sculpture (female MSP:EH 0.5–1.3, often <1); variable body size (females 1.2–5.8 mm, often <4 mm); males almost always with 8 funiculars **22**

- 22) Labrum with more than 6 digits, or if 4–6 digits, then having the following combination of characters: mesoscutum coarsely rugose-areolate; female funicular segments after F3 less than twice as long as broad to as broad as long; propodeum lacking median groove; eyes lacking setation 23
- Labrum usually with 4 digits, or if up to 6, then differing in at least one of the above characters 24
- 23) Labrum always with 4 digits; frons weakly imbricate, lower face weakly reticulate (Fig. 2.4E) *Orasema longinoi* Heraty & Baker (unplaced to group)
- Labrum usually with more than 6 digits, rarely with 4; frons strongly costate, lower face smooth (Fig. 2.4F), or entire face strongly reticulate
..... *Orasema lasallei* group; key provided in Heraty and Baker (In Press)
- 24) Female: fore and mid femora dark brown with iridescence, hind femur yellow; antennal funiculars same width throughout, slightly shorter apically; propodeum with a median carina within a median longitudinal groove (Fig. 2.4G); PTL:HCL 0.6–0.7; head and mesosoma dark green-blue iridescent; eyes bare. Male: only known from one heavily damaged molecular voucher, cannot be diagnosed
..... *Orasema deltae* Gemignani (unplaced to group)
- Characters at least partially disagreeing with above description 25

- 25) Eyes with setae longer than width of ommatidium, easily seen with low magnification (Fig. 2.44B); head relatively narrow (female HW:HH 1–1.1); frenum in dorsal view semicircular (Fig. 2.44F)
..... *Orasema roppai* **n. sp.** (unplaced to group)
- Eyes bare or with setae shorter than or equal to width of ommatidium, requiring high magnification to see; head usually more broad (female HW:HH 1–1.5, usually >1.1); frenum in dorsal view crescent-shaped or not visible (Fig. 2.40F) ...
..... **26**
- 26) Head broadly triangular with relatively small eyes (female MSP:EH ~1.2)
..... *Orasema susanae* Gemignani (unplaced to group)
- Head subtriangular with relatively larger eyes (female MSP:EH 0.5–1) (Fig. 2.40B) **27**
- 27) Antenna relatively short (female FL:HH 1–1.3); mesosoma relatively tall (ML:MH 1.1–1.3); large-bodied (females 3.7–4.6 mm) **28**
- Antenna usually long (female FL:HH 1–1.8, usually >1.3); mesosoma usually longer (ML:MH 1.1–1.6, usually >1.3); body size variable (females 1.2–5.1 mm, usually <4 mm) **29**
- 28) Legs past coxae tawny-orange; hind tibia greatly widened distally, about 3× as wide as metabasitarsus (Fig. 2.40E); stigmal vein slightly angled toward wing apex

- (Fig. 2.40A); female PTL:HCL 0.9–1.2; length 3.7 mm
 *Orasema cirrhocnemis* **n. sp.** (unplaced to group)
- Legs past coxae yellow; hind tibia normally widened distally, at most 2× as wide
 as metabasitarsus (Fig. 2.43E); stigmal vein slightly angled toward wing base
 (Fig. 2.43A); female PTL:HCL 1.4; length 4.2–4.6 mm
 *Orasema psarops* **n. sp.** (unplaced to group)
- 29)** Axillular groove usually anteriorly absent or narrowed; HW:HH 1–1.3; hind
 femora almost always yellow; first valvula of ovipositor with 4–5 teeth; male
 PTL:HCL 1.4–2.4
 *Orasema stramineipes* group; key provided in Burks et al. (2018)
- Axillular groove broad with a complete lateral carina; HW:HH 1.3–1.5; hind
 femora sometimes dark; first valvula of ovipositor with 7–10 teeth; male
 PTL:HCL 1–1.5
 *Orasema xanthopus* group; key provided in Heraty et al. (1993)

***Orasema coloradensis* species group**

(Figs 2.5–2.10)

Diagnosis. Recognized by the following combination of characters: a moderate to dense amount of setation on the head and mesosoma, transversely costate to areolate sculpture on the mesoscutal midlobe, elongate frenum in dorsal view, subquadrate head (length

approximately equal to width), 3:2 mandibular formula, antenna with 7 funicular segments, and 4–6 labral digits. While this group is easily recognized amongst other Nearctic taxa, the most distinctive features (setation and sculpture) become homoplastic when compared to some Neotropical and Old World taxa.

Description. Female. Length 2.4–4 mm. **Color.** Mandible, maxilla, and labium brown. Wing venation pale brown. **Head.** Head in frontal view subquadrate; longitudinal groove between eye and torulus absent; malar depression weakly impressed adjacent to mouth; clypeus smooth with shallow punctures; epistomal sulcus distinct; anterior tentorial pit strongly impressed; anteclypeus distinct, nearly straight. Mandibular formula 3:2; palpal formula 3:2. Occiput imbricate, shallowly emarginate in dorsal view; temples absent. Scape not reaching median ocellus. Flagellum with 7 funiculars; anellus disc-shaped; funiculars subequal in length distally, equal in width; clava subovate. **Mesosoma.** Notauli deep. Mesoscutellar disc as long as broad. Propleuron convex. Mesepisternum broadly rounded anterior to mid coxa; postpectal carina weak. Hind femur with even cover of short, dense setae. Fore wing basal area and speculum bare, costal cell and wing disc densely setose; marginal fringe relatively long; submarginal vein with several long setae; marginal vein with minute setae; stigmal vein slightly longer than broad, slightly angled toward wing apex. Hind wing costal cell with one or two irregular rows of setae. **Metasoma.** Antecostal sulcus foveate; acrosternite posteriorly rounded; apical setae of hypopygium present, minute.

Male. Length 2.2–3.4 mm. Lacking significant dimorphism except for slight differences in petiole length and a much smaller gaster.

Phylogenetics. All species except *O. violacea* have been molecularly sampled. Analyses using a few ribosomal and mitochondrial Sanger-sequenced loci, many Anchored Hybrid Enrichment (AHE) Illumina-sequenced loci, and a combination of both datasets resulted in a South American clade (*O. iridescens*) sister to a North American clade (*O. coloradensis* + *O. scaura*) (Baker et al., 2020). Monophyly of each of the three sampled species has been confirmed, with *O. coloradensis* thoroughly sampled across its geographic range, including specimens from Colorado, Idaho, Texas, Maryland, Florida, and northeastern Mexico; the crown age for this species is estimated to be *c.* 2–5 MY (varying between analyses) with an average of 5.3% sequence variation between AHE-sequenced specimens. The *coloradensis* species group is sister to the *sixaolae* species group + *O. monstrosa* (Fig. 2.1).

Discussion. Three trips were made to Idaho in 2013, 2015, and 2017 to collect *O. coloradensis* and *O. scaura*. Only a single specimen of *O. coloradensis* was collected among all three trips. Two additional trips were made to Hallelujah Junction, CA (near Reno, NV) to collect *O. scaura*, but no specimens were found. Two trips to Texas to collect *O. coloradensis* in 2014 and 2015 resulted in collecting several other species in the *bakeri*, *cockerelli*, and *simulatrix* groups but no *O. coloradensis*. Contrary to the other trips, collecting in Florida in 2014 resulted in an abundance of *O. coloradensis* specimens from multiple localities; however, no specimens that can be attributed to *O. violacea* have been collected since 1980. Low rates of collecting success in more arid locations has led

us to consider the following hypotheses: 1) these species are highly ephemeral, possibly only emerging as adults for a few days at a time, making targeted collecting difficult; or 2) these species are locally extinct or in very low densities, possibly due to changes in ant fauna as a result of the spread of invasive ant species, including *Solenopsis invicta* Buren and *Tetramorium caespitum* (L.) (cf. Chien & Heraty, 2018). While collecting in Hells Gate State Park, ID in 2013, James Johnson commented that the dominant ant in the area, *T. caespitum*, was not present when he was collecting in the 1980s, while the once-abundant proposed ant associate, *Formica subnitens*, was now extremely rare, and the host plant, gray rabbitbrush, was now largely absent from the area.

Key to species of the *Orasema coloradensis* species group

- 1) All legs with four tarsomeres (Fig. 2.9E); labrum with 4–11 digits (usually 6–7) that are often irregularly shaped (Fig. 2.9F); flagellum length shorter than height of the head (western Nearctic) *Orasema scaura* **n. sp.**
- All legs with five tarsomeres; labrum always with four digits and with regular symmetry; flagellum length as long as or longer than height of head **2**

- 2) Eyes bare (Fig. 2.8B); F2L:F2W 2–2.5 (female), 2.1–2.3 (male); PTL:PTW 2.1–3 (female), 3.4–4.2 (male) (Neotropical) *Orasema iridescens* **n. sp.**
- Eyes with sparse to moderate setation (Figs 2.6B, 2.10B); F2L:F2W 1.3–2 (female), 1.3–2.2 (male); PTL:PTW 0.9–2 (female), 2.2–3.3 (male) **3**

- 3) Coarsely areolate sculpture on the mesoscutal midlobe (Fig. 2.10F) (Florida)
 *Orasema violacea* Ashmead
- Transversely costate sculpture on the mesoscutal midlobe (Fig. 2.6F) (widespread
 Nearctic) *Orasema coloradensis* Wheeler

***Orasema coloradensis* Wheeler**

urn:lsid:zoobank.org:act:F03B755A-8EBA-4460-8F1D-ABD815B26DA5

(Figs 2.6, 2.7)

Orasema coloradensis Wheeler 1907: 12–14.

O. coloradensis; Gahan 1940: 441–442. Redescription and identification key.

Diagnosis. *Orasema coloradensis* is by far the most widespread and morphologically variable species in the *Orasema coloradensis* species group. It can be recognized from *Orasema scaura* by having five tarsomeres on all tarsi, a symmetrical labrum with four digits, and the length of the flagellum as long as or longer than the height of the head. It can be recognized from *Orasema iridescens* by having a shorter female petiole (PTL:PTW 1–2 in *O. coloradensis*; 2.1–3 in *O. iridescens*), having shorter/wider antennae (female F2L:F2W 1.4–2 in *O. coloradensis*; 2–2.5 in *O. iridescens*), and having setose compound eyes. This species is most similar to *O. violacea*, especially for some specimens collected in Florida and Texas, but can be recognized by the finer, more costate sculpture on the mesoscutal midlobe compared to the coarsely areolate sculpture in *O. violacea*. *Orasema violacea* also tends to have a larger body size than many, but not

all, specimens of *O. coloradensis*.

Description. Female. Length 2.4–3.7 mm (Fig. 2.6A). **Color.** Head and mesosoma a wide range of colors, typically blue, green, or both. Scape, pedicel, anellus, and flagellum brown. Coxae iridescent blue-green; femora mostly dark brown with iridescent reflections, tips pale; tibiae pale brown. Gaster same color as mesosoma. **Head** (Fig. 2.6B). HW:HH 1.1–1.3; face imbricate; eyes sparsely setose, IOD:EH 1.5–1.7; MS:EH 0.7–0.9; supraclypeal area as long as broad, equal to length of clypeus, smooth with shallow punctures. Labrum with 4 digits. Occiput with dorsal margin rounded. Pedicel globose, as broad as F1. FL:HH 1–1.4, F2L:F2W 1.4–2, F2L:F3L 1.2–1.8 (Fig. 2.6D). **Mesosoma** (Fig. 2.6 C, F). ML:MH 1.3–1.6. Mesoscutal midlobe transversely costate to areolate, densely setose; lateral lobe smooth to weakly imbricate. Axilla weakly sculptured; dorsally broadly rounded, mesoscutellum below dorsal margin of axilla; scutoscutellar sulcus narrow, regularly foveate, and broadly separated from transscutal articulation by deep foveae; mesoscutellar disc costate to areolate; frenal line regularly foveate; frenum weakly sculptured; axillular sulcus indicated by a weak longitudinal carina; axillula costate. Propodeal disc broadly rounded, without depression or carina, areolate-reticulate (Fig. 2.6G); callus weakly sculptured, costate anteriorly, densely setose. Propleuron weakly sculptured. Prepectus weakly sculptured. Mesepisternum weakly reticulate laterally, smooth ventrally. Upper mesepimeron weakly reticulate; lower mesepimeron smooth; transepimeral sulcus weakly impressed. Lateral metepisternum smooth medially with foveae posteriorly. HCL:HCW 1.4–1.9, weakly sculptured; HFL:HFW 4.6–5.7. FWL:FWW 2.3–2.5, FWL:ML 1.7–2.1; submarginal vein

with several long setae; postmarginal vein slightly longer than stigmal vein. **Metasoma.** Petiole cylindrical, linear in profile, PTL:PTW 1–2, PTL:HCL 0.6–1, areolate, lateral margin with longitudinal carina continuous with basal flange, ventral sulcus absent. First (ventral) valvula with 6–8 small, narrowly separated teeth, second (dorsal) valvula with 8–10 annuli that are broadly separated dorsally, carinae coalescing.

Male. Length 2.2–3.4 mm. HW:HH 1.2–1.3. Scape dark brown; FL:HH 1.3–1.6; anellus minute, difficult to distinguish; F2L:F2W 1.3–2.3 (Fig. 2.6E). Femora mostly dark brown with iridescence, tips pale; tibiae pale brown. PTL:PTW 2.2–3.4, PTL:HCL 1.1–1.5.

Egg. Described by Johnson et al. (1986).

Planidium. Described by Johnson et al. (1986).

Orasema coloradensis planidia have been extensively observed on immature thrips, *Sericothrips* sp., indicating that this may be a commonly used intermediate host for this species (Johnson et al., 1986). This may be a facultative relationship for *O. coloradensis* because they mostly oviposit into leaves (occasionally stems and buds) (Johnson et al., 1986) where immature thrips would not be expected to occur in high abundance, whereas other species oviposit exclusively into involucre bracts of unopened flower buds (where thrips density would be higher).

Ant hosts. Collected from nests of *Pheidole bicarinata* Mayr and *Solenopsis molesta* Emery in Colorado (Wheeler, 1907).

There is a record of *O. coloradensis* from the nest of *Formica subnitens* Creighton (Formicinae) (Johnson et al., 1986). We consider this record to be erroneous because

parasitized brood were never found; instead, the record was based on finding three *Orasema* adults in an emergence trap placed above a *Formica* mound, finding possible *Orasema* fragments within the nest, and finding one planidium attached to the maxilla of a *Formica* worker (Johnson et al., 1986). Colonies of *Solenopsis* parasitized by *O. coloradensis* have been observed in cleptobiosis with colonies of *Formica* (Wheeler, 1907), which may explain the observed association. It seems unlikely that *Orasema* could switch to another subfamily of ants with a pupal cocoon, which myrmicine ants lack. While other eucharitids can parasitize ants with pupal cocoons, and the maturing wasp pupa can be recovered from within the cocoon, this has never been observed within *Oraseminae*. Incidentally, an extensive two-year survey of *Formica subnitens* in Westbank, British Columbia, a locality where *O. coloradensis* has been collected, did not report finding *O. coloradensis* among the insects in or near the ant nests nor among the prey items of the ants (Ayre, 1957, 1958, 1959).

Plant hosts. Gray rabbitbrush (Asteraceae: *Ericameria nauseosa* (Pall ex. Pursh) G.L. Nesom & Baird), green rabbitbrush (Asteraceae: *Chrysothamnus viscidiflorus* (Hook.) Nutt.), and milkweed (Apocynaceae: *Asclepias* sp.) in Idaho (specimen records; Johnson et al., 1986); western ragweed (Asteraceae: *Ambrosia psilostachya* DC), partridge pea (Fabaceae: *Chamaecrista fasciculata* (Michx.) Greene), and rushfoil (Euphorbiaceae: *Croton* sp.) in Texas (specimen records); sidebeak pencilflower (Fabaceae: *Stylosanthes biflora* (L.) Britton, Sterns & Poggenb.) and New Jersey tea (Rhamnaceae: *Ceanothus americanus* L.) in Virginia (specimen records); and partridge pea, poorjoe (Rubiaceae: *Diodia teres* Walter), European turkey oak (Fagaceae: *Quercus*

ceris L.), and sandlace (Polygonaceae: *Polygonum dentroceras* T.M. Schust. & Reveal) in Florida (specimen records). Of these plant records, only *Ericameria* in Idaho and *Chamaecrista* in Florida have been independently confirmed as hosts, with *O. coloradensis* observed ovipositing into the leaves and stems of both of these plants.

Distribution (Fig. 2.5). Canada: AB, BC, MB, ON; United States: AZ, CA, CO, FL, GA, ID, IL, IN, IA, KS, LA, MD, MO, MT, NE, NV, NJ, NM, NC, OK, OR, SC, TX, UT, VA, WA, WY; Mexico: NL, PU, SL, VZ. Collected June–August.

Material examined. Lectotype: USA: CO: El Paso Co., Ute Pass, viii.1903 [1♀ (female specimen with head intact) **by present designation** for nomenclatorial stability, deposited in AMNH: UCRCENT00238021]. **Paralectotypes: USA: CO:** El Paso Co., Broadmoor, near Colorado Springs, 11.viii.1903 [3♀, 1♂, 15 pupae, AMNH: UCRCENT00238017–19]; Ute Pass, viii.1903 [1♀ (headless specimen), 1♂, AMNH: UCRCENT00238021]. **Larval slides: USA: ID:** Nez Perce Co., Hells Gate St. Pk., 293m, 46°21'24"N, 117°03'3"W, 14.vii.1983, T.D. Miller, *Ericameria nauseosa* [1?, UCRC: UCRCENT00499476]. **TX:** Kerr Co., Kerrville St. Pk., 500m, 30°00'12"N, 99°07'42"W, 24.vii.1988, Heraty, ovip. Grass [1?, UCRC: UCRCENT00499475].

Additional material examined: 736 specimens, see supplementary material.

There is some confusion regarding the type specimen of *Orasema coloradensis*. Wheeler (1907) was under the impression that *O. coloradensis* had already been described by Ashmead, which is made evident by attributing the binomen to Ashmead as well as the identification. Johnson et al. (1986) attribute the binomen to Gahan, but as Gahan (1940) points out, Wheeler (1907) was in fact the first to publish this name. This

confusion may be why the type material for this species is ambiguous. Wheeler (1907) did not directly designate type material, but he did provide a date (August, 1903) and locations (Manitou, Broadmoor, Beaver Ranch – all near Colorado Springs, CO) for material that he examined. The specimen currently designated as type (USNMENT00809501, type no. 27294) cannot actually be the type because this specimen was from a series collected by C.F. Baker. There are four series of card-mounted specimens that we recognize as the syntypes collected by Wheeler in August, 1903 from Broadmoor (UCRCENT00238017–19) and Ute Pass, CO (UCRCENT00238021). Because the syntype series is from multiple hosts, we raise one of the female specimens to lectotype status (UCRCENT00238021: there are three *Orasema* specimens on this card mount; the lectotype is the female with the intact head, which is placed above the other two specimens when viewed with the anterior end pointed left) while the remaining syntypes are now paralectotypes.

Discussion. There is a large amount of color and size variation in this species. In Texas, collection records show an enormous discrepancy in size (Fig. 2.7: D, E), while in Florida, color varies to a large degree (Fig. 2.7: H–J), and in Mexico, specimens have a slightly different head shape; however, despite this, all molecularly sampled specimens came out in a single highly-supported clade with little genetic variation (Baker et al., 2020).

***Orasema iridescens* n. sp.**

(Fig. 2.8)

Diagnosis. Recognizable from other members of the *O. coloradensis* species group by having bare compound eyes, longer petiole (PTL:PTW 2.1–3 for females; 3.4–4.3 for males), and a longer/thinner antenna (F2L:F2W 2–2.5 for females; 2.1–2.4 for males).

Description. Female. Length 2.6–4 mm (Fig. 2.8A). **Color.** Head and mesosoma black with green, blue, and purple iridescence. Scape pale brown; pedicel and anellus yellowish brown; flagellum brown. Coxae dark brown with iridescence; femora mostly brown, tips pale; tibiae pale. Gaster brown. **Head** (Fig. 2.8B). HW:HH 1.1–1.3; face imbricate; eyes bare, IOD:EH 1.4–1.6; MS:EH 0.6–0.8; supraclypeal area about as long as broad, shorter than clypeus, smooth. Labrum with 4 digits. Occiput with dorsal margin abrupt. Pedicel globose, as broad as F1. FL:HH 1.4–1.6; anellus disc-shaped but prominent; F2L:F2W 2–2.5, F2L:F3L 1.2–1.4 (Fig. 2.8D). **Mesosoma** (Fig. 2.8 C, F). ML:MH 1.5–1.7. Mesoscutal midlobe transversely costate, sparsely setose; lateral lobe smooth. Axilla smooth; dorsally rounded, on roughly same plane as mesoscutellum; scutoscutellar sulcus narrow, regularly foveate, broadly separated from transscutal articulation; mesoscutellar disc smooth; frenal line as smooth band; frenum smooth; axillular sulcus distinct and foveate; axillula costate. Propodeal disc broadly rounded, without depression or carina, rugose (Fig. 2.8G); callus smooth, with a few small setae. Propleuron smooth. Prepectus weakly sculptured medially. Mesepisternum weakly rugose-reticulate medially, smooth anteriorly and ventrally. Upper and lower

mesepimeron smooth; transepimeral sulcus distinct. Metepisternum laterally smooth. HCL:HCW 1.4–1.8, smooth to weakly sculptured; HFL:HFw 4.4–5.3. FWL:FWW 2.3–2.6, FWL:ML 1.9–2.1; submarginal vein with several long setae; postmarginal vein longer than stigmal vein. **Metasoma.** Petiole cylindrical, linear in profile, PTL:PTW 2.1–3, PTL:HCL 0.9–1.3, areolate, lateral margin rounded, ventral sulcus present, margins broadly separated. First (ventral) valvula without teeth, second (dorsal) valvula with 8–10 annuli that are narrowly separated dorsally, carinae coalescing.

Male. Length 2.7–3.4 mm. HW:HH 1.2–1.4. Scape pale brown; FL:HH 1.6–1.8; anellus disc-shaped but prominent; F2L:F2W 2.1–2.4 (Fig. 2.8E). Femora and tibiae pale yellow. PTL:PTW 3.4–4.3, PTL:HCL 1.5–1.8.

Ant hosts. Unknown.

Plant hosts. Unknown.

Distribution (Fig. 2.5). Argentina: BA, CN; Brazil: ES. Collected February–April, October–November.

Material examined. Holotype: Argentina: Corrientes: Rt. 12 & Rio Sta. Lucia, N. of Goya, 29°05'0"S, 59°16'0"W, 18-21.xi.2003, D. Bickel, trunk sticky trap [1♀, deposited in CNC: UCRCENT00320816]. **Paratypes: Argentina: Buenos Aires:** Castelar, 34°39'9"S, 58°38'15"W, 28.ii-9.iv.2007, G. Logarzo, MT [1♀, UCRCENT00434627]. **Corrientes:** Rt. 12 & Rio Sta. Lucia, N. of Goya, 29°05'0"S, 59°16'0"W, 18-21.xi.2003, D. Bickel, trunk sticky trap [11♂ 4♀, CNC: UCRCENT00320813–15, UCRCENT00320825–36]. **Brazil: Espírito Santo:** Santa

Teresa Est. Biol. Santa Lúcia, $19^{\circ}58'1''S$, $40^{\circ}32'16''W$, 13.x.2006, Tavares, Azevedo et al., Malaise 18 [1♀, UFES: UFES00091947].

Etymology. From Latin meaning “rainbow-like colors” in reference to the iridescent color of the body.

***Orasema scaura* n. sp.**

(Fig. 2.9)

Diagnosis. Recognized from other members of the *Orasema coloradensis* species group by having tarsi with four segments on all legs; tarsomeres distinctly lobate with lobes broadly overlapping subsequent tarsomeres on the ventral side; and antennal flagellum length shorter than height of the head. This is the only eucharitid known to have the tarsus 4-segmented (Fig. 2.9E).

Description. Female. Length 3–3.4 mm (Fig. 2.9A). **Color.** Head and mesosoma iridescent blue-green. Scape, pedicel, anellus, and flagellum brown. Coxae iridescent blue-green; femora mostly brown with iridescence, tips pale; tibiae yellow. Gaster same as mesosoma. **Head** (Fig. 2.9B). HW:HH 1.2–1.3; face imbricate; eyes sparsely setose, IOD:EH 1.4–1.6; MS:EH 0.7–0.9; supraclypeal area slightly broader than long, weakly sculptured. Labrum with variable asymmetric digits with 4–9 setae (Fig. 2.9F). Occiput with dorsal margin rounded. Pedicel globose, not as broad as F1. FL:HH 0.8–1; F2L:F2W 1.1–1.4, F2L:F3L 1.3–1.8 (Fig. 2.9D). **Mesosoma** (Fig. 2.9 C, G). ML:MH 1.3–1.6. Mesoscutal midlobe imbricate, densely setose; lateral lobe smooth. Axilla

smooth; dorsally rounded, on roughly same plane as mesoscutellum; scutoscutellar sulcus narrow, regularly foveate, broadly separated from transscutal articulation; mesoscutellar disc smooth; frenal line irregularly foveate; frenum smooth; axillular sulcus distinct and foveate; axillula areolate-reticulate. Propodeal disc broadly rounded, with shallow medial depression, rugose-areolate (Fig. 2.9H); callus nearly smooth, densely setose. Propleuron imbricate. Prepectus weakly rugose. Mesepisternum reticulate laterally, smooth ventrally. Upper and lower mesepimeron smooth; transepimeral sulcus weakly impressed. Metepisternum laterally smooth. HCL:HCW 1.4–2, with weak dorsolateral sculpture; HFL:HFV 3.1–3.8. FWL:FVW 2.2–2.5, FWL:ML 1.8–2.1; submarginal vein with several long setae; postmarginal vein slightly longer than stigmal vein. **Metasoma.** Petiole cylindrical, linear in profile, PTL:PTW 1.2–1.6, PTL:HCL 0.7–0.9, areolate-reticulate, lateral margin rounded, ventral sulcus present. First (ventral) valvula with 6–8 small, narrowly separated teeth, second (dorsal) valvula with 6–7 annuli that are narrowly separated dorsally, carinae coalescing.

Male. Unknown.

Ant hosts. Unknown.

Plant hosts. Swept from *Ericameria nauseosa* (Asteraceae) in Idaho.

Distribution (Fig. 2.5). United States: AZ, CA, ID, NV. Collected June–August.

Material examined. Holotype: USA: ID: Butte Co., 6 mi S Howe, 43°42'0"N, 113°01'50"W, 28.vii-4.viii.1983, M.P. Stafford, host plant: *Ericameria nauseosa* [1♀, deposited in WFBM: UCRCENT00407525]. **Paratypes: USA: AZ:** Cochise Co., Cave Ck. Cyn. Chiricahua Mts, 6 mi W Portal, 2042m, 31°55'0"N, 109°15'0"W, 11.vii.1981,

H.A. Hespenheide [1♀, UCLA: UCRCENT00414825]. Coconino Co., Hwy 180 SE Valle, 1850m, 35°37'13"N, 112°05'45"W, 26.vii.2008, S. Triapitsyn [1♀, UCRC: UCRCENT00264701]. Amedee, 40°16'12"N, 120°09'36"W, 4.vii.1947, T.F. Leigh [1♀, EMEC: UCRCENT00236340]. CA: Lassen Co., Hallelujah Junction, 1440m, 39°47'0"N, 120°04'0"W, 1-3.vii.1992, D. Carmean, 73 [1♀, UCDC: UCRCENT00416100]. Hallelujah Junction, 1440m, 39°47'0"N, 120°04'0"W, 29-30.vi.2006, M.F. Sherriffs, 060 [1♀, UCDC: UCRCENT00477664]. ID: Butte Co., 6 mi S Howe, 43°42'0"N, 113°01'50"W, 28.vii-4.viii.1983, M.P. Stafford, host plant: *Ericameria nauseosa* [45♀, WFBM: UCRCENT00403564–75, UCRCENT00403577–78, UCRCENT00403581–82, UCRCENT00403585, UCRCENT00407501–02, UCRCENT00407504–12, UCRCENT00407514–20, UCRCENT00407522–24, UCRCENT00407526–28, UCRCENT00407531, UCRCENT00407533–34, UCRCENT00407537]. 6 mi. S Howe, 43°41'24"N, 113°01'48"W, 4.viii.1983, N.P. Stafford [1♀, WFBM: UCRCENT00003619]; 22.vii.1982, J.B. Johnson, host plant: *Ericameria nauseosa* [5♀, WFBM: UCRCENT00403576, UCRCENT00403583, UCRCENT00403604, UCRCENT00407521, UCRCENT00407561] Canyon Co., 15 mi S Nampa, 43°18'47"N, 116°36'11"W, 21.vi.1977, J.M. Domek [1♀, WFBM: UCRCENT00403580]. Cassia Co., 9 mi E Malta, 42°18'25"N, 113°11'28"W, 14.vii.1981, R.P. Wight [1♀, WFBM: UCRCENT00403584]. Nez Perce Co., Hells Gate St. Pk., 293m, 46°21'24"N, 117°03'3"W, 14.vii.1983, J.B. Johnson, host plant: *Ericameria nauseosa* [3♀, WFBM: UCRCENT00407478, UCRCENT00407494–95]. Twin Falls Co., Rogerson, 42°13'5"N, 114°35'38"W, 20.vii.1961, R.E. Stecker, host plant: *Chrysothamnus* [1♀, WFBM:

UCRCENT00403579]. NV: Carson City, 39°09'49"N, 119°46'3"W, 6.vii, Baker [6♀, USNM: UCRCENT00247968–70, UCRCENT00248316–18]. Nye Co., Mercury, 36°39'39"N, 115°59'40"W, 5.viii.1964 [2♀, USNM: UCRCENT00248383–84]. Washoe Co., S end of Pyramid Lake, 1140m, 39°50'35"N, 119°26'49"W, 8.vii.1982, D.E. Russell [2♀, UCDC: UCRCENT00404586, UCRCENT00404588]; L.D. French [2♀, UCDC: UCRCENT00404585, UCRCENT00404587]; P. Timper [2♀, UCDC: UCRCENT00404583, UCRCENT00416064]. Verdi, 39°31'5"N, 119°59'20"W, 12.vii.1974, B. Villegas [1♀, UCDC: UCRCENT00404584].

Etymology. Latin, meaning “swollen ankles,” which refers to the thick, lobate tarsomeres.

Discussion. Because the large number of specimens have been collected for this species (75 examined) are all female, it seems likely that this species is parthenogenetic. Attempts to sequence *Wolbachia* from two point-mounted specimens collected in 1983 and 2008 were negative.

***Orasema violacea* Ashmead**

urn:lsid:zoobank.org:act:B4A7D285-5759-413D-AF1D-97C8CD7E450C

(Figs 2.7, 2.10)

Orasema violacea Ashmead 1888: 187–188.

O. violacea; Gahan 1940: 445–446. Redescription and identification key.

Diagnosis. Recognized from *Orasema scaura* by having five tarsomeres and the length

of the flagellum as long as or longer than the height of the head. It can be recognized from *Orasema iridescens* by having a shorter female petiole (PTL:PTW 0.9–1.2 in *O. violacea*; 2.1–3 in *O. iridescens*), having shorter/wider antennae (female F2L:F2W 1.3–1.6 in *O. coloradensis*; 2–2.5 in *O. iridescens*), and having setose compound eyes. This species is most similar to *O. coloradensis*, but can be recognized by having more coarsely areolate sculpture on the mesoscutal midlobe compared to the costate sculpture in *O. coloradensis* and other members of the group. *Orasema violacea* also tends to have a larger body size than most, but not all, specimens of *O. coloradensis*.

Description. Female. Length 3.3–3.8 mm (Fig. 2.10A). **Color.** Head and mesosoma blue, green, or combined. Scape, pedicel, anellus, and flagellum brown. Coxae iridescent blue-green; femora mostly brown with iridescence, tips pale; tibiae yellow. Gaster same as mesosoma or brown with iridescent reflections. **Head** (Fig. 2.10B). HW:HH 1.1–1.2; face rugose-reticulate; eyes sparsely setose, IOD:EH 1.5–1.6; MS:EH 0.7–0.8; supraclypeal area as long as broad, equal to length of clypeus, weakly rugose. Labrum with 4 digits. Occiput with dorsal margin abrupt. Pedicel globose, as broad as F1. FL:HH 1–1.2; F2L:F2W 1.3–1.6, F2L:F3L 1.3–1.5 (Fig. 2.10D). **Mesosoma** (Fig. 2.10 C, F). ML:MH 1.2–1.4. Mesoscutal midlobe rugose-areolate to areolate-reticulate, sparsely setose; lateral lobe rugose-reticulate. Axilla areolate-reticulate, dorsally rounded, on roughly same plane as mesoscutellum; scutoscutellar sulcus broad, irregularly foveate, and broadly separated from transscutal articulation; mesoscutellar disc areolate-reticulate; frenal line irregularly foveate; frenum areolate-reticulate; axillular sulcus distinct and foveate; axillula areolate-reticulate. Propodeal disc flat, rugose-areolate, without median

carina (Fig. 2.10G); callus areolate-reticulate, densely setose. Propleuron reticulate. Prepectus areolate-reticulate. Mesepisternum, upper-, and lower mesepimeron reticulate; transepimeral sulcus weakly impressed. Metepisternum laterally reticulate. HCL:HCW 1.5–1.8, reticulate; HFL:HFW 4.4–4.8. FWL:FWW 2.2–2.4, FWL:ML 1.6–1.7; submarginal vein with several long setae; postmarginal vein slightly longer than stigmal vein. **Metasoma.** Petiole broad, linear in profile, PTL:PTW 0.9–1.2, PTL:HCL 0.7–0.8, areolate-reticulate, lateral margin with longitudinal carina continuous with basal flange, ventral sulcus absent. First (ventral) valvula with 6–8 small, narrowly separated teeth, second (dorsal) valvula with 8–10 annuli that are narrowly separated dorsally, carinae coalescing.

Male. Length 2.8–3.1 mm. HW:HH 1.1–1.3. Scape brown; FL:HH 1.3; anellus disc-shaped; F2L:F2W 1.3–1.5 (Fig. 2.10E). Femora mostly brown, tips pale; tibiae yellow. PTL:PTW 1.7–2.3, PTL:HCL 1–1.3.

Ant hosts. Unknown.

Plant hosts. Unknown.

Distribution (Fig. 2.5). United States: FL. Collected June–July.

Material examined. Holotype: USA: FL: Eastern Florida [1♀, deposited in USNM: USNMENT00809466, type images: <http://n2t.net/ark:/65665/3b0c20be4-0882-4c1b-ad6a-a0987be4f0ce>]. **Additional material examined: USA: FL:** Franklin Co., St. George State Park, 29°44'46"N, 84°52'8"W, 13.vi.1980, L. Stange [1♂, FSCA: UCRCENT00411767]. Levy Co., 29°19'12"N, 82°44'24"W, 22.vi.1957, H.V. Weems, Jr. [3♂, FSCA: UCRCENT00411765, LACM: UCRCENT00305126, USNM:

UCRCENT00248390]; 3.vii.1954 [2♀, USNM: UCRCENT00248392–93]; 3.vii.1958 [1♀, FSCA: UCRCENT00411754]; 7.vii.1955 [1♀, FSCA: UCRCENT00411756].

Discussion. *Orasema coloradensis* specimens from Florida show a large amount of morphological variation with some specimens quite similar overall to *O. violacea*, making the two species occasionally difficult to distinguish (Fig. 2.7B). This may imply that *O. violacea* should be the senior synonym of *O. coloradensis*, or that some introgression between species may have taken place in Florida. Without molecular data for *O. violacea* to confirm or reject these hypotheses, it seems inappropriate at this time to synonymize these species. The few specimens examined that were determined to be *O. violacea* were mostly collected in the 1950's with a single specimen collected in 1980. Multiple recent failed attempts were made to collect fresh specimens, which, given the context of the changing ant fauna in Florida (especially *Solenopsis*, one of the hosts for *O. coloradensis*), may imply extinction of the species.

***Orasema bakeri* species group**

(Figs 2.11–2.16)

Diagnosis. Recognized by the following combination of characters: anterior margin of prepectus lacking a carina and gradually sloping under margin of pronotum (Fig. 2.13C), female petiole generally short (PTL:PTW <1.5), face and mesoscutal midlobe reticulate, 7 funicular segments, 4 labral digits. This group can be difficult to distinguish from the

Orasema cockerelli group, with the anterior edge of the prepectus often the only consistent difference between groups.

Description. Female. Length 2.2–3.5 mm. **Color.** Antennal flagellum brown. Mandible brown. Coxae brown with iridescence; femora mostly brown, tips pale. Gaster brown with iridescence. **Head.** Face reticulate; longitudinal groove between eye and torulus absent; malar depression weakly impressed adjacent to mouth; clypeus weakly sculptured; anterior tentorial pit strongly impressed. Labrum with 4 digits. Mandibular formula 3:2. Occiput imbricate, emarginate in dorsal view; temples present, rounded. Scape not reaching median ocellus. Flagellum with 7 funiculars; anellus disc-shaped; funiculars subequal in length distally, equal in width; clava subovate. **Mesosoma.** Mesoscutal midlobe, frenum, propodeal disc, and propleuron reticulate. Prepectus reticulate. Mesepisternum reticulate, broadly rounded anterior to mid coxa. Hind coxa reticulate. Hind wing costal cell with a broad bare area. **Metasoma.** Antecostal sulcus foveate; acrosternite posteriorly rounded; apical setae of hypopygium with several long hairs on each side of the midline. First (ventral) valvula with 6–8 small, narrowly separated teeth.

Male. Length 1.7–3 mm. Scape brown with iridescence; flagellum with 7 funiculars, anellus disc-shaped. Femora mostly brown, tips pale.

Phylogenetics. Four species in the *Orasema bakeri* group have been molecularly sampled for Sanger-sequenced genes: *O. texana*, *O. bakeri*, *O. taii*, and *O. dubitata*; only *Orasema bakeri* has been sequenced with AHE. Specimens of *O. bakeri* and *O. dubitata*

from Baker et al. (2020) were misidentified: “*Orasema_nr_bakeri_USA:AZ_AE_D4097*” is *Orasema bakeri* (UCRCENT00411576); “*Orasema_bakeri_USA:AZ_D3720*” and “*Orasema_bakeri_USA:FL_D3153*” are *Orasema dubitata* (UCRCENT00352479, UCRCENT00292550, respectively). The *bakeri-taii-dubitata* clade consists of the most difficult species to delimit in the *bakeri* group. *Orasema dubitata* was first recognized as distinct from *O. bakeri* by a number of differences in Sanger sequenced genes (18S rDNA has one nucleotide difference; 28S D2 rDNA two differences; 28S D3–5 rDNA four differences; COI-BC (cytochrome oxidase I barcoding) mtDNA six amino acid changes and at least 15 unambiguous nucleotide differences; COI-NJ (cytochrome oxidase I NJ) mtDNA has one amino acid change and three unambiguous nucleotide differences), and *O. taii* has only a small number of differences from *O. dubitata* (28S D2 has one difference; COI-NJ has no amino acid changes but at least 13 nucleotide changes). Because of difficulty separating the species in this group morphologically, references to the GenBank sequences from Baker et al. (2020) are provided at the end of the materials examined; *Orasema taii* (UCRCENT00243359; D4717) sequences are: 28S D2 (MH247391), 28S D3–5 (MH247544), COI-NJ (MH247756).

Key to species of the *Orasema bakeri* species group

- 1) Female petiole generally wider than long (PTL:PTW 0.6–1.3), male PTL:PTW 1.5–3; head wide (HH:IOD 1–1.2); notauli relatively deep, making mesoscutal lateral lobes appear discontinuous with curvature of midlobe in dorsal view (Figs 2.12F, 2.16F) **2**

- Female petiole generally longer than wide (PTL:PTW 0.8–1.5), male PTL:PTW 0.8–4.9; head more triangular (HH:IOD 1.2–1.5); notauli relatively shallow, making mesoscutal lateral lobes appear continuous with curvature of midlobe in dorsal view (Figs 2.13F, 2.14F, 2.15F) **3**

- 2)** Midlobe of mesoscutum with medial impression, lateral lobes reticulate to finely imbricate on dorsal surface (Fig. 2.16F); upper mesepisternum reticulate (Fig. 2.16C); female scape yellow (Fig. 2.16D); male antenna with setae semi-erect, curved (Fig. 2.16E); propodeum with medial carina (Fig. 2.16G) (southern Nearctic) *Orasema texana* Gahan

- Midlobe of mesoscutum without medial impression, lateral lobes reticulate with smooth patch on dorsal surface (Fig. 2.12F); upper mesepisternum smooth (Fig. 2.12C); female scape dark brown with iridescence (Fig. 2.12D); male antenna with setae closely appressed, straight (Fig. 2.12E); propodeum without medial carina (Fig. 2.12G) (Texas, North Carolina, South Carolina)
..... *Orasema bablyi* **n. sp.**

- 3)** Clava with a distinct ventral notch that separates two proximal clavomeres on ventral side (dorsally fused) (cf. figure 8 from Chien & Heraty (2018)) (Texas)
..... *Orasema taii* Chien & Heraty

- Clava without ventral notch, clavomeres completely fused **4**

- 4) Fore wing with marginal fringe always present; female often with medial, differentially-colored depression on mesoscutellum (Fig. 2.15F); male petiole often short (PTL:PTW 0.8–2.7) (central to southern Mexico) *Orasema polymyrmex* **n. sp.**
- Fore wing with marginal fringe sometimes absent; female without medial, differentially-colored depression on mesoscutellum; male petiole long (PTL:PTW 2.8–5) **5**
- 5) Generally with a slightly larger body size (3–3.5 mm females, 2.4–3 mm males); body generally with more green coloration (Fig. 2.13A) (widespread Nearctic) *Orasema bakeri* Gahan
- Generally with a smaller body size (2.2–3.2 mm females, 1.7–2.8 mm males); body generally with more violaceous or blue coloration (Fig. 2.14A) (widespread Nearctic) *Orasema dubitata* **n. sp.**

***Orasema bablyi* n. sp.**

(Fig. 2.12)

Diagnosis. Recognized from the other members of the *O. bakeri* group by having a dark, almost black body coloration and mesoscutum with lateral lobes dorsally smooth. It is most similar to *O. texana* but lacks a depression in the midlobe of the mesoscutum, lacks a medial carina on the propodeum, and has a smooth upper mesepimeron.

Description. Female. Length 2.2–2.8 mm (Fig. 2.12A). **Color.** Head and mesosoma dark bluish-black. Scape dark brown with iridescence; pedicel and dark brown. Maxilla and labium brown. Tibiae light brown. Fore wing venation pale brown. **Head** (Fig. 2.12B). Head in frontal view subquadrate; HW:HH 1.1–1.4; scrobal depression shallow, laterally rounded, with transverse striae; eyes sparsely setose, IOD:EH 1.7–1.9; MS:EH 0.7–0.9; supraclypeal area about as long as broad, shorter than clypeus, smooth; epistomal sulcus distinct and sharply defined; anteclypeus distinct, broadly rounded. Palpal formula 3:2. Occiput with dorsal margin evenly rounded. Pedicel small and globose. FL:HH 1–1.1; F2L:F2W 0.8–1.2, F2L:F3L 1–1.2 (Fig. 2.12D). **Mesosoma** (Fig. 2.12 C, F). ML:MH 1.2–1.4. Mesoscutal midlobe bare; lateral lobe dorsally smooth; notauli deep. Axilla smooth to lightly reticulate, dorsally rounded, on roughly same plane as mesoscutellum; scutoscutellar sulcus narrow, irregularly foveate, narrowly separated from transscutal articulation; mesoscutellar disc as long as broad, reticulate; frenal line as smooth band, foveate posteriorly; axillular sulcus anteriorly absent, narrow and foveate posteriorly; axillula areolate-reticulate. Propodeal disc flat, without depression or carina (Fig. 2.12G); callus reticulate, bare; callar nib absent. Propleuron nearly flat. Postpectal carina weak. Upper mesepimeron smooth; lower mesepimeron reticulate; transepimeral sulcus distinct. Metepisternum laterally reticulate. HCL:HCW 1.4–1.9; HFL:HFW 4.1–5.8, with even cover of short, dense setae. FWL:FWW 2.1–2.5, FWL:ML 1.9–2.1; basal third of wing bare, wing disc setose; marginal fringe minute; submarginal vein with minute setae; marginal vein with minute setae; stigmal vein about twice as long as broad, slightly angled toward wing apex; postmarginal vein slightly longer than stigmal vein.

Metasoma. Petiole broad, linear in profile, PTL:PTW 0.6–1.3, PTL:HCL 0.4–0.8, reticulate, lateral margin with longitudinal carina continuous with basal flange, ventral sulcus absent. Subapical carina absent; second (dorsal) valvula with 8–10 annuli that are narrowly separated dorsally, carinae coalescing.

Male. Length 2–2.4 mm. HW:HH 1.2–1.3. FL:HH 1.2–1.4, F2L:F2W 1–1.2 (Fig. 2.12E). Tibiae light brown. PTL:PTW 1.6–2.3, PTL:HCL 0.8–1.3.

Ant hosts. Unknown.

Plant hosts. Some specimens from Charlotte, North Carolina were collected from wild carrot (*Daucus carota* L.; Apiaceae), specimens from Bangs, Texas were collected from a peach orchard, and one other specimen from Texas was swept from *Gaillardia* (blanket flower; Asteraceae); none are associated with observing oviposition.

Distribution (Fig. 2.11). United States: NC, SC, TX. Collected April–July.

Material examined. Holotype: USA: NC: Mecklenburg Co., Charlotte, Beverly Woods, $35^{\circ}13'48''N$, $80^{\circ}51'0''W$, 18.vi.1964, P.P. Bably [1♀, deposited in ZSM: UCRCENT00245271]. **Paratypes: USA: NC:** Charlotte, Beverly Woods, $35^{\circ}08'2''N$, $80^{\circ}50'46''W$, 3.vi.1964, P.P. Bably [2♀, BMNH: UCRCENT00309301, UCRCENT00309380]; 5.vi.1964 [1♂, BMNH: UCRCENT00309300]; 10.vi.1964 [2♀, BMNH: UCRCENT00309374, UCRCENT00309453]; 11.vi.1964 [3♀, ZSM: UCRCENT00245265, UCRCENT00245297, UCRCENT00245311]; 13.vi.1964 [2♀, ZSM: UCRCENT00245286–87]; 15.vi.1964 [1♀, ZSM: UCRCENT00245313]; 17.vi.1964 [1♀, ZSM: UCRCENT00245312]; 18.vi.1964 [1♀, ZSM: UCRCENT00245270]; 2.vi.1964 [1♀, ZSM: UCRCENT00245272]; 3.vi.1964 [10♀,

BMNH: UCRCENT00309378, ZSM: UCRCENT00245288–96]; 4.vi.1964 [1♂ 6♀,
 ZSM: UCRCENT00245279–85]; 5.vi.1964 [3♂ 13♀, BMNH: UCRCENT00309370–72,
 ZSM: UCRCENT00245298–310]; 6.vi.1964 [1♀, ZSM: UCRCENT00245316];
 7.vi.1964 [2♀, BMNH: UCRCENT00309379, ZSM: UCRCENT00245318]; 8.vi.1964
 [3♀, BMNH: UCRCENT00309373, ZSM: UCRCENT00245315, UCRCENT00245317];
 9.vi.1964 [2♀, BMNH: UCRCENT00309375, ZSM: UCRCENT00245314]. **SC:** Oconee
 Co., Seneca, 289m, *34°41'8"N, 82°57'12"W*, 26.v.1962, R.O. Eikenbary, on pine [1♀,
 USNM: UCRCENT00416723]. **TX:** C.F. Baker, 2513 [1♀, USNM:
 UCRCENT00248504]. Brazos Co., Jones rd. 1.6 mi n. HWY 60, *30°34'48"N,*
96°23'24"W, 1.vi.1975, S.J. Merritt [1♀, TAMU: UCRCENT00426206]. Brown Co.,
 Bangs, peach orchard, *31°43'2"N, 99°07'57"W*, 8.vi.1938, Christenson, 10280 [4♀,
 USNM: UCRCENT00247934–37]; 10281 [1♂, USNM: UCRCENT00247939]; 9704
 [1♀, USNM: UCRCENT00247938]. Leon Co., 7.6 mi N Normangee, *31°08'6"N,*
96°07'16"W, 12.vi.1976, S.J. Merritt [1♀, TAMU: UCRCENT00243109]. Live Oak Co.,
 10 mi. south George West, *28°10'48"N, 98°06'36"W*, 22.iv.1978, D.W Plitt, ex pasture
 [1♂, TAMU: UCRCENT00426207]. Mills Co., 23 mi. w. Goldthwaite, *31°27'0"N,*
98°57'36"W, 24.iv.1971, V.V Board [1♀, UCRC: UCRCENT00311974]. Montague Co.,
 Bowie Lake, 8 mi N Bowie, *33°39'3"N, 97°55'24"W*, 13.vi.1972, R.W. Thorp [1♀,
 UCDC: UCRCENT00416059]. Robertson Co., 3 mi. South of Camp Creek Lake,
31°00'36"N, 96°18'0"W, 17.v.1970, J. C. Schaffner [1♀, TAMU: UCRCENT00243110].

Etymology. Named in honor of the collector of a large series of specimens from
 North Carolina, P.P. Bably.

***Orasema bakeri* Gahan**

urn:lsid:zoobank.org:act:6D47ACA9-C78B-47B9-9D0A-DBB3659B3624

(Fig. 2.13)

Orasema bakeri Gahan 1940: 452–453.

Diagnosis. Recognized from other members of the *O. bakeri* group from the combination of following characters: mesoscutal midlobe and lateral lobes reticulate without any depressions, relatively long petiole (PTL:PTW 0.8–1.3 in females, 3.5–4.9 in males), male antenna with setae long and broadly curved anteriorly, and a larger average body size. This species is difficult to diagnose from *O. dubitata* but is generally less violaceous and has a larger average body size.

Description. Female. Length 3–3.5 mm (Fig. 2.13A). **Color.** Head and mesosoma blue-green iridescent occasionally with violaceous patches. Scape, pedicel, and anellus pale brown; maxilla and labium pale brown. Tibiae light brown. Fore wing venation pale brown, nearly white. **Head** (Fig. 2.13B). Head in frontal view subtriangular; HW:HH 1.1–1.3; scrobal depression shallow, laterally rounded, with transverse striae; eyes bare, IOD:EH 1.5–1.9; MS:EH 0.7–1; supraclypeal area slightly broader than long, weakly reticulate; epistomal sulcus distinct and sharply defined; anteclypeus distinct, nearly straight. Palpal formula 3:2. Occiput with dorsal margin evenly rounded. Pedicel globose, broader than F1. FL:HH 0.9–1.1; F2L:F2W 1.3–2, F2L:F3L 1.1–1.5 (Fig. 2.13D). **Mesosoma** (Fig. 2.13 C, F). ML:MH 1.2–1.4. Mesoscutal midlobe bare; lateral lobe reticulate to nearly smooth; notauli deep. Axilla reticulate, dorsally rounded, on roughly

same plane as mesoscutellum; scutoscutellar sulcus narrow, regularly foveate, broadly separated from transscutal articulation; mesoscutellar disc as long as broad, reticulate; frenal line as smooth band; axillular sulcus indicated by a weak longitudinal carina; axillula reticulate. Propodeal disc broadly rounded, without depression or carina (Fig. 2.13G); reticulate; callus reticulate, bare; callar nib absent. Propleuron strongly convex, protruding ventrally. Postpectal carina weak. Upper and lower mesepimeron reticulate; transepimeral sulcus distinct. Metepisternum laterally reticulate. HCL:HCW 1.4–2; HFL:HFW 4.6–6, with even cover of short, dense setae. FWL:F2W 2.1–2.5, FWL:ML 1.9–2.2; basal third of wing bare, costal cell sparsely setose, wing disc with minute sparse setae; marginal fringe short to absent; submarginal vein with minute setae; marginal vein with sparse minute setae; stigmal vein about twice as long as broad, perpendicular to anterior wing margin; postmarginal vein longer than stigmal vein. **Metasoma.** Petiole cylindrical, linear in profile, PTL:PTW 0.8–1.3, PTL:HCL 0.5–0.8, reticulate, lateral margin rounded, ventral sulcus absent. Ovipositor with subapical carina present; second (dorsal) valvula with 6–7 annuli that are narrowly separated dorsally, carinae coalescing.

Male. Length 2.4–3 mm. HW:HH 1.2–1.3; FL:HH 1.2–1.3, F2L:F2W 1–1.4 (Fig. 2.13E). Tibiae light brown. PTL:PTW 3.5–4.9, PTL:HCL 1.3–1.7.

Ant hosts. Unknown.

Plant hosts. Swept from Fabaceae and *Chrysothamnus* sp. (Asteraceae) in Arizona, *Larrea* sp. (Zygophyllaceae) in New Mexico, *Heracleum mantegazzianum* Sommier & Levier (Apiaceae) in Colorado (Gahan, 1940).

Distribution (Fig. 2.11). Mexico: DF; United States: AZ, CO, ID, MN, NB, NM, OK, TX, UT, WY. Collected June–August.

Material Examined. Holotype: USA: CO: Larimer Co., Fort Collins, $40^{\circ}34'58''N$, $105^{\circ}05'5''W$, 13.vi.1895, C.F. Baker, 1563 [1♀, deposited in USNM:

USNMENT01524341, type images: <http://n2t.net/ark:/65665/3e5a194bb-aca0-4751-8a0c-1def5010f856>]. **Allotype: USA: CO:** Larimer Co., Fort Collins, $40^{\circ}34'58''N$,

$105^{\circ}05'5''W$, 13.vi.1895, C.F. Baker, 1563 [1♂, USNM: UCRCENT00247804].

Paratypes: USA: AZ: Pinal Co., Oracle, $32^{\circ}36'39''N$, $110^{\circ}46'14''W$, 7.vi.1898, Hubbard & Schwarz [1♀, USNM: UCRCENT00247813]. **CO:** Archuleta Co., Pagosa Springs,

$37^{\circ}15'55''N$, $107^{\circ}00'46''W$, C.F. Baker [1♂, USNM: UCRCENT00247812]. Larimer Co.,

Fort Collins, $40^{\circ}34'58''N$, $105^{\circ}05'5''W$, 13.vi.1895, C.F. Baker, 1563 [6♀, USNM:

UCRCENT00247805–10]; vi, wild parsnip bloom, 1086 [1♀, USNM:

UCRCENT00247811]. **Additional material examined:** 49 specimens, see

supplementary material. **GenBank sequences:** UCRCENT00411576 (D4097): 18S

(KR632468.1), 28S D2 (KR632393.1), 28S D3–5 (KR632432.1), COI-BC

(KR733117.1), COI-NJ (KR733149.1).

Discussion. This species is morphologically similar to *O. dubitata*, *O. taii*, and *O. polymyrmex*. While there is some molecular support for *O. dubitata* and *O. taii* as separate species, *O. polymyrmex* failed sequencing attempts. Due to the cryptic nature of this 4-species complex, it requires more thorough molecular sequencing across populations in separate geographic areas to be able to confidently associate morphological differences with phylogenetic differences.

***Orasema dubitata* n. sp.**

(Fig. 2.14)

Diagnosis. Recognized from other members of the *O. bakeri* group by the combination of following characters: mesoscutal midlobe and lateral lobes reticulate without any depressions, relatively long petiole (PTL:PTW 1–1.4 in females, 2.8–4.6 in males), and male antenna with setae long and broadly curved anteriorly (Fig. 2.14E). This species is difficult to diagnose from *O. bakeri* but is generally more blue-purple colored (as opposed to blue-green in *O. bakeri*) and has a smaller average body size.

Description. Female. Length 2.2–3.2 mm (Fig. 2.14A). **Color.** Head and mesosoma iridescent blue-purple. Scape, pedicel, and anellus pale brown. Maxilla and labium pale brown. Tibiae yellow. Fore wing venation clear to light brown. **Head** (Fig. 2.14B). Head in frontal view subtriangular; HW:HH 1.1–1.3; scrobal depression deep, laterally rounded, reticulate; eyes bare; IOD:EH 1.6–1.9; MS:EH 0.7–1; supraclypeal area as long as broad, equal to length of clypeus, smooth to weakly reticulate; epistomal sulcus distinct; anteclypeus distinct, nearly straight. Palpal formula 3:2. Occiput with dorsal margin evenly rounded. Pedicel globose, broader than F1. FL:HH 0.9–1.2; F2L:F2W 1–1.7, F2L:F3L 1–1.7 (Fig. 2.14D). **Mesosoma** (Fig. 2.14 C, F). ML:MH 1.2–1.4. Mesoscutal midlobe sparsely setose; lateral lobe reticulate; notauli deep. Axilla reticulate, dorsally rounded, on roughly same plane as mesoscutellum; scutoscutellar sulcus narrow, irregularly foveate, narrowly separated from transscutal articulation; mesoscutellar disc slightly longer than broad, reticulate; frenal line irregularly foveate; axillular sulcus

indicated by a strong longitudinal carina; axillula reticulate. Propodeal disc broadly rounded, without depression or carina (Fig. 2.14G); callus reticulate, bare; callar nib absent. Propleuron convex. Postpectal carina weak. Upper mesepimeron reticulate to smooth; lower mesepimeron reticulate; transepimeral sulcus distinct. Metepisternum laterally reticulate. HCL:HCW 1.4–1.9, reticulate; HFL:HFW 4.8–5.9, sparsely setose. FWL:F2W 2.3–2.6, FWL:ML 1.8–2.3; basal area and speculum bare, costal cell and wing disc sparsely setose; marginal fringe minute to absent; submarginal vein bare; marginal vein with sparse minute setae; stigmal vein about twice as long as broad, perpendicular to anterior wing margin; postmarginal vein longer than stigmal vein.

Metasoma. Petiole broad, linear in profile, PTL:PTW 1–1.4, PTL:HCL 0.6–0.9, reticulate, lateral margin rounded, ventral sulcus present with margins narrowly separated. Ovipositor with subapical carina present; second (dorsal) valvula with 6–7 annuli that are narrowly separated dorsally, carinae coalescing.

Male. Length 1.7–2.8 mm. HW:HH 1.1–1.3; FL:HH 1.1–1.5, F2L:F2W 1.1–1.8 (Fig. 2.14E). Tibiae yellow. PTL:PTW 2.8–4.6, PTL:HCL 1.2–1.8.

Ant hosts. Taken from the nest of *Pheidole californica* Mayr in California.

Plant hosts. Oviposits on the underside of the leaves of *Desmodium* sp. (Fabaceae) in Florida. Swept from *Chamaecrista fasciculata* (Michx.) Greene (Fabaceae) in Florida and *Chilopsis linearis* (Cav.) Sweet (Bignoniaceae) in New Mexico.

Distribution (Fig. 2.11). Mexico: VE; United States: AZ, CA, FL, KS, NM, TX. Collected March–November.

Material Examined. Holotype: USA: FL: Highlands Co., Archbold Biol. Sta. Lk. Placid, Trail 1 SSo, $27^{\circ}10'54''N$, $81^{\circ}21'6''W$, 25.vii.1986, M. Deyrup, Malaise Trap [1♀, deposited in USNM: UCRCENT00471759]. **Paratypes: Mexico: Veracruz:** 28 km SE Jalapa, $19^{\circ}24'39''N$, $96^{\circ}40'31''W$, 7.vii.1984, G. Gordh [1♂ UCRC: UCRCENT00435191]. **USA: AZ:** Cochise Co., 6.8 mi. SE Apache Tr. mouth Skeleton Cyn., 1371m, $31^{\circ}35'39''N$, $109^{\circ}04'8''W$, 14.viii.1982, G.Gibson [1♂ 2♀, CNC: UCRCENT00415343–45]. Skeleton Canyon, 8 mi. E Apache., $31^{\circ}35'39''N$, $109^{\circ}04'8''W$, 2.ix.1991, E.E. Grissell, creekside vegetation, sweep [1♂, USNM: UCRCENT00247964]. Box Canyon Road, 1203m, $31^{\circ}46'56''N$, $110^{\circ}51'2''W$, 26.vii.2009, J. Mottern, dry wash, sweep, M09-018 [1♀, UCRC: UCRCENT00352479]. IBP. Sta. Rita Destr. Site, 917m, $31^{\circ}51'3''N$, $110^{\circ}58'58''W$, 12.viii.1970, CEPA, D. Vac [1♂, UAZ: UCRCENT00403886]. Pima Co., Santa Rita Mtns., Box Cyn., 1700m, $31^{\circ}47'54''N$, $110^{\circ}46'37''W$, 3.viii.1996, M.W Gates, G96/045 [1♂, UCRC: UCRCENT00414167]. Pinal Co., Oracle, 1371m, $32^{\circ}36'39''N$, $110^{\circ}46'14''W$, 25.viii.1934, Ian Moore [1♂, SDNH: UCRCENT00242772]. **CA:** Pinon Flat, San Jacinto Mts., $33^{\circ}34'48''N$, $116^{\circ}27'36''W$, 27.v.1939, J.G. Shanafelt [1♀, LACM: UCRCENT00305136]. Lassen Co., Hallelujah Jct, $39^{\circ}46'30''N$, $120^{\circ}02'19''W$, 13.vii.1972, R.M. Bohart [2♀, UCDC: UCRCENT00416118–19]. Hallelujah Junction, 1440m, $39^{\circ}47'0''N$, $120^{\circ}04'0''W$, 30.vi.2006, P.S. Ward, ex *Pheidole californica* nest, 15622 [2♀, UCDC: UCRCENT00352480–81]. **FL:** Alachua Co., 5.5 mi West Gainesville, $29^{\circ}36'57''N$, $82^{\circ}24'22''W$, L.R Davis Jr [1♀, UCRC: UCRCENT00311927]. 5.5 Mi. W. Gainesville, T10S R19E Section 4, Castlegate Mobile Home Park,

29°39'14"N, 82°24'7"W, 21.viii.1985, Lloyd R. Davis. Jr., on *Cassia fasciculata* [1♂,
 FSCA: UCRCENT00322556]. Gainesville, 29°39'6"N, 82°19'29"W, 4.v.1937, L.J.
 Bottimer [1♂, USNM: UCRCENT00416654]. Highlands Co., Archbold Biol. Sta.,
 middle gate, 60m, 27°09'5"N, 81°21'16"W, 15.vii.2011, J.Heraty, oak scrub, swp, H11-
 095 [1♂, UCRC: UCRCENT00292549]. Archbold Biol. Sta. Lk. Placid, Trail 1 SSo,
 27°10'54"N, 81°21'6"W, 11.vi.1986, M. Deyrup, Malaise Trap [1♀, ABS:
 UCRCENT00421641]; 12.iii.1986 [1♀, ABS: UCRCENT00421654]; 14.viii.1986 [1♂
 1♀, ABS: UCRCENT00421652–53]; 16.iii.1983 [2♂, ABS: UCRCENT00421635–36];
 18.iv.1986 [1♂ 1♀, ABS: UCRCENT00421642–43]; 19.v.1986 [1♀, ABS:
 UCRCENT00421638]; 21.iii.1986 [1♂, ABS: UCRCENT00421649]; 21.xi.1986 [1♂,
 ABS: UCRCENT00421648]; 19.iii.1986 [1♀, ABS: UCRCENT00305344]; 14.v.1986
 [1♂ 1♀, ABS: UCRCENT00305372, UCRCENT00421632]; 21.iv.1986 [4♂ 1♀, ABS:
 UCRCENT00305331, UCRCENT00305367–70]; 22.vii.1985 [1♀, ABS:
 UCRCENT00305366]; 26.v.1986 [2♂ 2♀, ABS: UCRCENT00421624–26,
 UCRCENT00421629]; 28.iv.1986 [2♂, ABS: UCRCENT00305336,
 UCRCENT00421650]; 3.vi.1985 [1♂, ABS: UCRCENT00421657]; 30.v.1986 [2♀,
 ABS: UCRCENT00305326, UCRCENT00421659]; 30.vi.1986 [1♀, ABS:
 UCRCENT00421620]; 4.vi.1986 [1♀, ABS: UCRCENT00421631]; 7.iv.1986 [3♂ 2♀,
 ABS: UCRCENT00305339–43]; 9.vi.1986 [2♀, ABS: UCRCENT00421627–28];
 23.vi.1986 [1♂, ABS: UCRCENT00421622]; Trail 2 SSo, 20.iv.1986 [1♂ 1♀, ABS:
 UCRCENT00421646–47]; 23.iv.1986 [1♂ 1♀, ABS: UCRCENT00421639–40];
 24.iii.1986 [1♂, ABS: UCRCENT00421656]; 28.iii.1986 [1♂, ABS:

UCRCENT00421655]; 7.iv.1986 [1♂, ABS: UCRCENT00421645]. 11.viii.1984 [1♂, UCDC: UCRCENT00477673]; 12.v.1986 [1♀, ABS: UCRCENT00305346]; 16.vi.1986 [2♂, ABS: UCRCENT00305337–38]; 19.v.1986 [1♂, ABS: UCRCENT00305335]; 26.v.1986 [1♀, ABS: UCRCENT00305345]; 28.v.1986 [1♀, ABS: UCRCENT00421633]; 30.vi.1986 [1♀, ABS: UCRCENT00421619]; 31.iii.1986 [2♂ 1♀, ABS: UCRCENT0030533–34]; 7.v.1986 [1♂, ABS: UCRCENT00305371]; 10.iv.1986 [1♂ 1♀, ABS: UCRCENT00305327–28]; 7.vii.1986 [1♀, FSCA: UCRCENT00411879]; 25.iv.1986 [2♂ 2♀, ABS: UCRCENT00305358–61]; 30.iv.1986 [2♂ 2♀, ABS: UCRCENT00305362–65]; 4.iv.1986 [4♂ 2♀, ABS: UCRCENT00305347–48, UCRCENT00305350–53]; 9.iv.1986 [2♂ 1♀, ABS: UCRCENT00305354, UCRCENT00305356–57]. Archbold Biol. Sta.; middle gate, 60m, 27°09'5"N, 81°21'16"W, 15.vii.2011, J. Mottern, southern ridge sandhill, sweep, M11-021 [1♀, UCRC: UCRCENT00292550]. Archbold Biol. Sta., 27°10'54"N, 81°21'06"W, 26.iv–1.v.1968, D. Wahl, MT [1♀ UCRC: UCRCENT00436388]. Marion Co., 9mi SSW Ocala (KCE), 20-30m, 29°03'55"N, 82°11'36"W, 4-10.ix.1975, J.Wiley, malaise trap [1♀, UCRC: UCRCENT00311928]. Orange Co., Wekiwa Springs State Park, Burn Zone 43/31, 28°44'32"N, 81°30'33"W, 13.v.2001, P.J. Russell and S.M. Fullerton, Longleaf Pine - Turkey Oak, Malaise Trap [1♂, UCFC: UCFC00105176]; 18.viii.2001 [1♀, UCFC: UCFC00113078]; 23.vi.2001 [1♂, UCFC: UCFC00106282]; 26.v.2001 [1♀, UCFC: UCFC00105910]; 7.vii.2001 [1♀, UCFC: UCFC00107110]. Polk Co., Tiger Ck. Preserve Babson Pk.; NE of Pfundstein Rd, 27°48'36"N, 81°29'1"W, 23.v.2007, B. Pace-Aidana, A. Peterson, Sandhill/ Xeric Oak Hammock, Malaise [1♂, EMEC:

UCRCENT00236101]; 5.v.2007 [1♂, EMEC: UCRCENT00236099]. Putnam Co., 2mi W Interlachen , 29°38'14"N, 82°00'17"W, 30.v.1991, G. Zolnerwich [1♂, UCRC: UCRCENT00436362]. **ID:** Owyhee Co., Murphy, 43°12'54"N, 116°33'04"W, 21.vi.1977, D.M. Kirkbride [1♂, WFBM: UCRCENT00403630]. **KS:** Clark Co., Sitka, 37°10'30"N, 99°39'5"W, 12.vi.1960, W.T. Van Velzen [1♀, MEM: UCRCENT00242498]. **NM:** Dona Ana Co., nr. Whitesands, 1539m, 32°24'47"N, 106°32'52"W, 25.vi.2014, A. Baker & S. Heacox, sweep *Chilopsis*, AB14.025 [1♂, UCRC: UCRCENT00436482]. 14.9 km W Animas, 1326m, 31°56'13"N, 108°57'10"W, 26-30.vii.1982, G. Gibson [1♂, CNC: UCRCENT00415374]. 9.3 mi W Animas, 1308m, 31°56'14"N, 108°56'45"W, 26-30.vii.1982, G Gibson [3♂, CNC: UCRCENT00415376–78]. Hidalgo Co., Grat Ranch, Whitewater Mtns, nr border obelisk #61, 31°20'22"N, 108°35'59"W, 5.viii.2002, Gates/George [1♂, UCRC: UCRCENT00414036]. Gray Ranch, Animas Mtns., Culberson Camp, 31°23'08"N, 108°37'53"W, 2.viii.2002, M. Gates [1♂ UCRC: UCRCENT00408496]. **TX:** Brewster Co., Big Band Nat'l Pk, Glenspring Pond in 0.5 mi., 914m, 29°12'60"N, 103°15'59"W, 9.vii.1982, G. Gibson [1♂, CNC: UCRCENT00415392]. Erath Co., 5 mi. north Stephenville, 397m, 32°17'40"N, 98°11'23"W, 1-6.vi.1980, P. T. Riherd, ex Malaise trap [2♂ 2♀, TAMU: UCRCENT00243111, UCRCENT00426202–04]; 27-30.v.1980 [1♂, TAMU: UCRCENT00243112, UCRCENT00426511]. Presidio Co., Big Bend Ranch, 1.6 km NE McGuirks Tanks, 1318m, 29°28'56"N, 103°48'14"W, 19.vi.1990, J.B Woolley, 90/020 [1♂, UCRC: UCRCENT00312086]. **GenBank sequences:** UCRCENT00292550 (D3153): 18S (MH231641), 28S D2 (MH247293), 28S D3–5 (MH247458), COI-NJ

(MH247668); UCRCENT00352479 (D3720): 18S (KR632485.1), 28S D2 (KR632424.1), 28S D3–5 (KR632463.1), COI-BC (KR733142.1), COI-NJ (KR733178.1).

Etymology. From Latin *dubi* meaning “doubtful” in reference to the difficulty distinguishing this species from *Orasema bakeri* and the mistaken identifications in Baker et al. (2020).

***Orasema polymyrmex* n. sp.**

(Fig. 2.15)

Diagnosis. Recognized from other members of the *O. bakeri* group by the following combination of characters: short male petiole (PTL:PTW 0.8–1.2), female mesoscutellum often with a medial depression that is differentially colored, fore wings always with marginal fringe, mesoscutal midlobe rarely with an indication of a depression, mesoscutal lateral lobes reticulate, and clypeal margin generally broadly rounded. This species is most similar to *O. bakeri* and *O. dubitata*, but can be distinguished by the short male petiole and scutellar depression.

Description. Female. Length 2.3–3.4 mm (Fig. 2.15A). **Color.** Head and mesosoma dark blue-green. Scape yellow; pedicel and anellus light brown. Maxilla and labium light brown. Tibiae yellow. Fore wing venation pale brown to white. **Head** (Fig. 2.15B). Head in frontal view subtriangular; HW:HH 1.1–1.2; scrobal depression shallow, laterally rounded, reticulate; eyes bare, IOD:EH 1.5–1.9; MS:EH 0.7–1; supraclypeal area slightly

broader than long, mostly reticulate, becoming smooth medially; epistomal sulcus narrow but shallow; anteclypeus distinct, broadly rounded. Palpal formula 3:2. Occiput with dorsal margin evenly rounded. Pedicel globose, as broad as F1. FL:HH 0.9–1.1; F2L:F2W 1.1–1.6, F2L:F3L 1.1–1.6 (Fig. 2.15D). **Mesosoma** (Fig. 2.15 C, F). ML:MH 1.1–1.3. Mesoscutal midlobe bare; lateral lobe reticulate; notauli shallow. Axilla reticulate, dorsally rounded, on roughly same plane as mesoscutellum; scutoscutellar sulcus broad, irregularly foveate, broadly separated from transscutal articulation; mesoscutellar disc as long as broad, reticulate, often with a median depression having a lighter color; frenal line present as a short smooth line; axillular sulcus indicated by a weak longitudinal carina; axillula reticulate to areolate-reticulate. Propodeal disc broadly rounded, without depression or carina, slightly rugose medially (Fig. 2.15G); callus reticulate, bare; callar nib absent. Propleuron convex. Postpectal carina weak. Upper and lower mesepimeron reticulate; transepimeral sulcus weakly impressed. Metepisternum laterally reticulate. HCL:HCW 1.6–2; HFL:HFW 4.2–5.3, with even cover of short, dense setae. FWL:F2W 2.3–2.8, FWL:ML 2–2.3; basal third of wing bare, including speculum, wing disc with minute sparse setae; marginal fringe relatively long; submarginal vein and marginal vein with minute setae; stigmal vein about twice as long as broad, slightly angled toward wing apex; postmarginal vein longer than stigmal vein. **Metasoma**. Petiole broad, linear in profile, PTL:PTW 0.6–1.5, PTL:HCL 0.4–0.8, areolate-reticulate, lateral margin with longitudinal carina continuous with basal flange, ventral sulcus absent. Subapical carina present; second (dorsal) valvula with 8–10 annuli that are narrowly separated dorsally, carinae coalescing.

Male. Length 2–2.5 mm. HW:HH 1.1–1.3; FL:HH 1.1–1.4, F2L:F2W 1.3–1.6 (Fig. 2.15E). Tibiae yellow. PTL:PTW 0.8–2.7, PTL:HCL 0.5–1.4.

Ant hosts. Collected from a nest of *Pheidole* sp. in Jalisco and *Solenopsis* sp. in Neuvo Leon. In the Jalisco series of specimens, there is one damaged specimen of *Tetramorium* sp. pinned with *Orasema polymyrmex* (UCRCENT00416802); given that this would be the only instance of *Tetramorium* parasitism in *Orasema*, it seems unlikely that this is a true host and more likely that it was collected in the *Pheidole* nest as well.

Plant hosts. Swept from acacia-thorn scrub and oak-acacia grassland.

Distribution (Fig. 2.11). El Salvador: CU, LI; Guatemala: JA; Honduras: AT; Mexico: CM, CL, GR, HG, JA, MI, NL, OA, TM, VE. Collected April–August, November.

Material Examined. Holotype: Mexico: Oaxaca: 5.0 Km NW Jct 135/195, 1783m, $17^{\circ}19'8''N$, $96^{\circ}55'39''W$, 20.vii.1987, Heraty, oak-Acacia woodland [1♀, deposited in UCRC: UCRCENT00311872]. **Paratypes: Mexico: Campeche:** Cd. Del Carmen, $18^{\circ}39'11''N$, $91^{\circ}47'34''W$, 30.vii.1984, G. Gordh [1♀, UCRC: UCRCENT00435193]. **Colima:** Manzanillo, $19^{\circ}05'18''N$, $104^{\circ}18'31''W$, 31.vii.1965, H.E. Evans [1?, MCZ: UCRCENT00322662]. 4 mi. W Chilpancingo, $17^{\circ}32'24''N$, $99^{\circ}33'36''W$, 15.vii.1984, J.B Woolley [1♀, TAMU: UCRCENT00243107]. 4.5 mi NW El Ocotito, 690m, $17^{\circ}17'7''N$, $99^{\circ}34'1''W$, 7.vii.1987, Woolley and Zolnerowich, 87/018 [1♀, TAMU: UCRCENT00243102]. **Hidalgo:** Guanajuato, 2 mi W Dolores, $21^{\circ}09'0''N$, $100^{\circ}57'36''W$, 5.vii.1985, J. Woolley and G. Zolnerowich, 85/026 [1♀, TAMU: UCRCENT00243105]. 2mi. W Dolores, $21^{\circ}09'0''N$, $100^{\circ}57'36''W$, 5.vii.1985, J.Woolley and G. Zolnerowich,

85/026 [1♀, TAMU: UCRCENT00243106]. Chapala, 20°17'46"N, 103°11'28"W, 21.iv.1977, W.F. Barr [1♀, WFBM: UCRCENT00403625]. **Jalisco:** Cocula, 1348m, 20°21'55"N, 103°49'22"W, xi.1923, W.M. Mann [8♂ 1♀ 6?, USNM: UCRCENT00416796–810]. Plan de Barrancas, 21°03'29"N, 104°12'37"W, 3.v.1953, R.C. Bechtel & E.I. Schlinger [1♀, EMEC: UCRCENT00404885]. **Michoacan:** 11 mi. E Apatzingan, 19°02'44"N, 102°12'54"W, 20.viii.1954, E.G. Linsley, J.W. MacSwain & R.F. Smith [2♀, EMEC: UCRCENT00404877–78]. 30 mi S of Neuva Italia, 18°34'48"N, 102°04'48"W, 8.viii.1978, Plitt & Schaffner [1♀, TAMU: UCRCENT00243222]. **Nuevo Leon:** Monterrey, 540m, 25°40'0"N, 100°19'0"W, 20.viii.1995, A. Gonzalez, *Solenopsis* nest [2♀, UCRC: UCRCENT00278213, UCRCENT00278215]. 11 mi. n. Matias Romero, 17°01'48"N, 95°01'48"W, 6.vii.1971, Clark, Murray, Hart, Schaffner [1♀, TAMU: UCRCENT00426201]. 46.8 km E Potchula, 24m, 15°49'12"N, 96°03'45"W, 13.vii.1987, J. Heraty, Acacia-thorn scr. [4♀, UCRC: UCRCENT00311870, UCRCENT00311878–79, TAMU: UCRCENT00243103]. **Oaxaca:** Temascal, 43m, 18°14'28"N, 96°24'9"W, 30.vi.1964, A.G. Raske [6♀, EMEC: UCRCENT00404876, UCRCENT00404879–83]. **Tamaulipas:** Tampico, 22°15'19"N, 97°52'7"W, E. A. Schwarz [1♀, USNM: UCRCENT00416811]. **Veracruz:** Coyame, Lake Catemaco, 336m, 18°23'45"N, 95°04'13"W, 14.vii.1971, Clark, Murray, Hart, Schaffner [2♀, TAMU: UCRCENT00243098, UCRCENT00243045]. Nogales, 18°50'53"N, 97°10'30"W, vii.1955, N.L.H. Kraus [1♀, BPBM: UCRCENT00422379]. Paso de San Juan, 19°12'8"N, 96°19'26"W, 24.iv.1953, R.C. Bechtel & E.I. Schlinger [1?, EMEC: UCRCENT00404884]. **Additional material examined: El Salvador: Cuscutlan:**

Colima, $14^{\circ}03'36''N$, $89^{\circ}08'04''W$, 24.vi.1958, L.J. Bottimer [4♀, USNM: UCRCENT00248629–32]. **La Libertad:** Quezaltpeque, $13^{\circ}49'53''N$, $89^{\circ}16'49''W$, 21.vi.1961, M.E. Irwin [1♀, UCDC: UCRCENT00243427]; 500m, 5.vii.1963, D.Q. Cavagnaro & M.E. Irwin [2♀, 1♂, CAS: UCRCENT00417321, UCRCENT00417329–30]. **Guatemala: Jalapa:** 3 km S. Jalapa, 1300m, $14^{\circ}36'00''N$, $89^{\circ}58'48''W$, 12–13.ix.1987, Sharkey [1♀, CNC: UCRCENT00505455]. **Honduras: Atlántida:** Lancetilla, Tela, $15^{\circ}43'00''N$, $87^{\circ}27'00''W$, 31.viii.1995, R. Cave, MT [1♀ MZLU: UCRCENT00242600]. **Mexico: Guerrero:** 8 mi. S.E. Iguala, $18^{\circ}15'55''N$, $99^{\circ}28'2''W$, 22.viii.1958, H.F. Howden [1♀, CNC: UCRCENT00415449]. 100 km S. Zihuatanejo, $17^{\circ}10'12''N$, $100^{\circ}43'48''W$, 6.viii.1984, G. Gordh [2♂, UCRC: UCRCENT00435201–02].

Etymology. From Greek *poly* meaning “many” and *myrmex* meaning “ant” in reference to the multiple host ant genera implicated for this species.

Discussion. There may be more cryptic species diversity within this taxon considering the range of host records. The males from Guerrero, Mexico (UCRCENT00435201–02) and El Salvador (UCRCENT00417321) have a significantly longer petiole (PTL:PTW 2.6–2.7) than the males from Jalisco, Mexico (PTL:PTW 0.8–1.2; UCRCENT00416799–800, UCRCENT00416804–07, UCRCENT00416809–10), which is a trait that tends not to vary this much in other species. Lacking molecular data for this clade, we feel that it is premature to split this into further species at this time.

***Orasema texana* Gahan**

urn:lsid:zoobank.org:act:0A70BCAC-F58C-463C-B4D1-63307176C805

(Fig. 2.16)

Orasema texana Gahan 1940: 440–441.

Diagnosis. Recognized from other members of the *O. bakeri* group by generally having a broad medial depression in the mesoscutal midlobe, mesoscutal mid- and lateral lobes angulate at the notaulus anteriorly, and a callar nib. Other combinations of features that help diagnose *O. texana* include: petiole short/wide (PTL:PTW 0.6–1 in females; 1.6–3.2 in males), female scape yellow; propodeum often with median longitudinal carina, mesoscutal side lobes often with shallow depression dorsally, and axillular sulcus poorly defined to absent.

Description. Female. Length 2.5–3.4 mm (Fig. 2.16A). **Color.** Head and mesosoma dark, iridescent blue-green. Scape, pedicel, and anellus yellow. Maxilla and labium brown. Tibiae yellow. Fore wing venation pale brown. **Head** (Fig. 2.16B). Head in frontal view subquadrate; HW:HH 1.1–1.3; scrobal depression shallow, laterally rounded, reticulate; eyes bare, IOD:EH 1.5–2; MS:EH 0.6–1; supraclypeal area broader than long, smooth; epistomal sulcus distinct but shallow; anteclypeus distinct, broadly rounded. Palpal formula 2:2. Occiput with dorsal margin abrupt. Pedicel globose, broader than F1. FL:HH 0.9–1.1; F2L:F2W 1–1.6, F2L:F3L 1.2–1.8 (Fig. 2.16D). **Mesosoma** (Fig. 2.16 C, F). ML:MH 1.1–1.4. Mesoscutal midlobe bare; lateral lobe weakly reticulate to imbricate with an irregular dorsal impression; notauli deep. Axilla weakly rugose-

reticulate, dorsally well above mesoscutellum; scutoscutellar sulcus broad, irregularly foveate, reaching transscutal articulation; mesoscutellar disc as long as broad, areolate-reticulate; frenal line irregularly foveate; axillular sulcus absent; axillula areolate-reticulate. Propodeal disc flat, with median carina (Fig. 2.16G); callus smooth, bare; callar nib present. Propleuron nearly flat. Postpectal carina absent. Upper and lower mesepimeron smooth anteriorly, reticulate posteriorly; transepimeral sulcus weakly impressed. Metepisternum laterally smooth. HCL:HCW 1.4–2; HFL:HFW 3.7–5.9, with even cover of short setae. FWL:F2W 2.2–2.5, FWL:ML 1.9–2.2; basal third of wing sparsely setose, including speculum and costal cell, wing disc setose; marginal fringe relatively long; submarginal vein bare; marginal vein with minute setae; stigmal vein about the same length as width, slightly angled toward wing apex; postmarginal vein longer than stigmal vein. **Metasoma.** Petiole cylindrical, linear in profile, PTL:PTW 0.6–1, PTL:HCL 0.4–0.6, reticulate, lateral margin with longitudinal carina continuous with basal flange, ventral sulcus absent. Ovipositor with subapical carina present; second (dorsal) valvula with 6–7 annuli that are narrowly separated dorsally, carinae coalescing.

Male. Length 2.3–2.7 mm. HW:HH 1.2–1.5; FL:HH 1.1–1.3, F2L:F2W 1.1–1.6 (Fig. 2.16E). Tibiae yellow. PTL:PTW 1.6–3.2, PTL:HCL 0.8–1.4.

Planidium. Length 0.16 mm. Head with two pairs of dorsal cranial setae. Antenna, labial plates, and tergopleural line absent. Tergites I and II separate. Tergites I, II, and III with dorsal setae. Tergites II and VI with lateral setae. Tergites I, III, V, and VII with ventral setae. Tergites IV–VIII with posteriorly pointing ventral projections. Tergite IX

with separated leaflike ventral plate. Caudal pad present; caudal cerci present, about as long as tergites XI+XII.

Ant hosts. Unknown.

Plant hosts. Observed ovipositing into huisatch (*Vachellia farnesiana*; Fabaceae) in Texas. Swept from *Chilopsis linearis* (Bignoniaceae) and *Vachellia vernicosa* in Arizona, *Chilopsis linearis* in California, and *Vachellia constricta* in New Mexico.

Distribution (Fig. 2.11) Mexico: BC, BS, HG, NA, OA, SI, TM; United States: AZ, CA, NM, TX. Collected March–November.

Material Examined. Holotype: USA: TX: Grayson Co., Denison, $33^{\circ}45'0''N$, $96^{\circ}31'48''W$, 26.viii.1937, Christenson & Jones, sweep, C-3511 [1♀, deposited in USNM: USNMENT1520795, type images: <http://n2t.net/ark:/65665/3f8507c59-e9c9-4b8e-9bc7-6d9b34e9b034>]. **Larval slides: USA: TX:** San Patricio Co., Welder Wildlife Ref. near Vena Mills, 3m, $28^{\circ}06'42''N$, $97^{\circ}24'24''W$, 26.vi.1989, J. Heraty, Aster [5?, UCRC: UCRCENT00513224–28]. **Additional material examined:** 265 specimens, see supplementary material. **GenBank sequences:** UCRCENT00292561 (D3212): 18S (MH231711), 28S D2 (MH247394), 28S D3–5 (MH247546), COI-NJ (MH247760); UCRCENT00412495 (D3929): 18S (KR632475.1), 28S D2 (KR632406.1), 28S D3–5 (KR632445.1), COI-BC (KR733127.1).

***Orasema tolteca* species group**

(Figs 2.17–2.20)

Diagnosis. Recognized by the following combination of characters: generally large body size (among the largest of all *Orasema*), anterior margin of fore wing costal cell with bare area (Fig. 2.20H), head with face flat and with relatively small eyes, antenna with 8 funicular segments in females and 9 segments in males, mesoscutal midlobe not reticulate and sparsely setose, petiole cylindrical, postmarginal vein at most slightly longer than stigma vein, and mesosoma relatively tall, broad, and short longitudinally.

Description. Female. Length 2.8–5.2 mm. **Color.** Flagellum dark brown. Mandible, maxilla, and labium brown. Coxae iridescent green; tibiae yellow. Fore wing hyaline, venation pale brown. Petiole same as mesosoma. **Head.** Head in frontal view subtriangular to broadly triangular; face reticulate often with elongate reticulations between the eye and scrobe; scrobal depression shallow, laterally rounded, with transverse striae; longitudinal groove between eye and torulus absent; eyes sparsely setose; malar depression weakly impressed between mouth and eye margin; supraclypeal area longer than broad, weakly reticulate; clypeus weakly reticulate; epistomal sulcus vaguely defined; anterior tentorial pit strongly impressed; anteclypeus distinct, straight. Mandibular formula 3:2; palpal formula 3:3. Occiput imbricate, shallowly emarginate in dorsal view, dorsal margin evenly rounded; temples present, rounded. Scape reaching median ocellus. Pedicle small and globose. Flagellum with 8 funiculars; anellus disc-shaped; funiculars subequal in length distally, successively shorter; clava subovate. **Mesosoma.** Mesoscutal midlobe rugose-areolate to rugose reticulate, sparsely setose;

lateral lobe costate dorsally, rugose laterally; notauli shallow. Axilla dorsally rounded, on roughly same plane as mesoscutellum; scutoscutellar sulcus broad, irregularly foveate, narrowly separated from transscutal articulation; mesoscutellar disc as long as broad, rugose; frenal line foveate; frenum areolate. Propodeal disc flat, without depression or carina; callus with a few small setae. Propleuron convex, strigate. Prepectus triangular dorsally, strongly narrowed ventrally. Mesepisternum reticulate laterally, areolate-reticulate anteriorly, broadly rounded anterior to mid coxa; postpectal carina prominent. Lower mesepimeron rugose-reticulate; transepimeral sulcus distinct. Metepisternum laterally rugose-reticulate. Hind coxa reticulate laterally, smooth ventrally; hind femur with even cover of setae; hind tibia densely setose. Fore wing with basal area and speculum bare, costal cell mostly setose but with bare area near margin, wing disc densely setose; marginal fringe minute; submarginal vein with several long setae; marginal vein setose; stigma vein about as long as broad, slightly angled toward wing apex; postmarginal vein as long as stigma vein or slightly longer. Hind wing costal cell with broad, bare area. **Metasoma.** Petiole cylindrical, linear in profile, anterior carina strong, lateral margin with longitudinal carina continuous with basal flange. Antecostal sulcus foveate; acrosternite posteriorly rounded; apical setae of hypopygium with one pair of setae much longer than the others. Ovipositor with subapical carina present; first (ventral) valvula with 10–11 small, closely-spaced teeth.

Male. Length 3.5–4.6 mm. Scape dark brown with green iridescence; flagellum with 9 funiculars; anellus disc-shaped. Tibiae yellow.

Phylogenetics. Both species are represented in the analyses from Baker et al. (2020): *Orasema tolteca*, and *Orasema castilloae* (referred to as “Orasema_nr_tolteca_USA:AZ_AE_D4133”). These two species are sister groups in all analyses with AHE sequence data and were treated as part of the *cockerelli* species group despite *O. tolteca* being treated as its own group by Heraty (2000). In molecular analyses they rendered the remaining *cockerelli* group species paraphyletic by being more closely related to Nearctic *cockerelli* group than the Neotropical *cockerelli* group. We treat the *tolteca* group independently here, but to maintain a cladistic classification, we also split off and revise the *heacoxi* group and split off the Neotropical *vianai* group for future revisionary work. The split between *O. tolteca* and *O. castilloae* is estimated to have occurred 5–15 MYA.

Key to species of the *Orasema tolteca* species group

- 1) Labrum with 4–6 digits; hind femur with dark iridescent patch along at least 3/4 of length and all the way to base (Fig. 2.20A); male FL:HH 2.1–2.6 (central to southern Mexico) *Orasema tolteca* Mann
- Labrum always with 4 digits (Fig. 2.18B); hind femur with dark iridescent patch along 2/3 of length and light-colored near the base (Fig. 2.18A); male FL:HH 1.8–2 (Arizona to northern Mexico) *Orasema castilloae* **n. sp.**

***Orasema castilloae* n. sp.**

(Fig. 2.18)

Diagnosis. This species can be recognized from *O. tolteca* by having only 4 labral digits, generally greater proportion of yellow on the femora, and a male antenna with shorter/wider flagellar segments.

Description. Female. Length 2.8–5.2 mm (Fig. 2.18A). **Color.** Head and mesosoma iridescent blue-green. Scape yellow to partially brown with iridescence; pedicel and anellus brown. Femora dark brown with iridescence on basal two-thirds, fading to yellow on distal third. Gaster dark brown with strong green-blue iridescence. **Head** (Fig. 2.18B). HW:HH 1.1–1.4; IOD:EH 1.8–2.1; MS:EH 1–1.5. Labrum with 4 digits. FL:HH 1.2–1.5; F2L:F2W 1.2–1.5, F2L:F3L 1–1.4 (Fig. 2.18D). **Mesosoma** (Fig. 2.18 C, F). ML:MH 1–1.2. Axilla rugose; axillular sulcus weak and foveate; axillula areolate to areolate-reticulate. Propodeal disc areolate (Fig. 2.18G); callus areolate-reticulate. Propleuron rugose-reticulate. Upper mesepimeron reticulate. HCL:HCW 1.4–1.8; HFL:HFw 4.8–6.3. FWL:FWW 2.2–2.6, FWL:ML 2.1–2.4. **Metasoma.** PTL:PTW 1.1–1.9, PTL:HCL 0.6–1.2, reticulate, ventral sulcus absent. Ovipositor with second (dorsal) valvula with 6–7 annuli that are narrowly separated dorsally, carinae coalescing.

Male. Length 3.6–4 mm. HW:HH 1.2–1.3. FL:HH 1.8–2, F2L:F2W 1.6–2 (Fig. 2.18E). Femora dark brown medially, tips yellow. PTL:PTW 4.2–6.5, PTL:HCL 2–2.2.

Ant hosts. Unknown.

Plant hosts. Observed ovipositing in *Baccharis salicifolia* (Ruiz & Pav.) Pers. (Asteraceae). Swept from desert willow (*Chilopsis linearis* (Cav.) Sweet; Bignoniaceae), *Gossypium thurberi* Tod. (Malvaceae), and *Phacelia* sp. (Boraginaceae).

Distribution (Fig. 2.17). Mexico: SO; United States: AZ. Collected April–September.

Material examined. Holotype: USA: AZ: Santa Cruz Co., Flux Canyon Rd, 1445m, 31°29'46"N, 110°45'32"W, 12.viii.2014, Paul Masonick, oak savannah, swp, H14-100 [1♀, deposited in UCRC: UCRCENT00412574]. **Paratypes: Mexico: Sonora:** Nogales POE, 31°19'48"N, 110°56'24"W, 7.iv.1968, A. Kumlin, on vegetables [1♀, USNM: UCRCENT00416870]. 20 mi. S. Estacion Llano, 30°04'19"N, 111°06'12"W, 17.viii.1964, M.E. Irwin [1♀, UCRC: UCRCENT00413311]. **USA: AZ:** 1856, C.F. Baker [1♂ 1♀, USNM: UCRCENT00416866, UCRCENT00416869]. Cochise Co., 6 mi. W. of Montezuma Ps., Huachuca Mts., 31°20'24"N, 110°22'48"W, 19.viii.1940, J.J. DuBois [1♀, EMEC: UCRCENT00404902]. Bisbee (1429 Franklin St.), 31°24'26"N, 109°55'59"W, 16.vii.1995, A.S. & N. Menke [1♀, USNM: UCRCENT00416662]. Douglas, 1188m, 31°20'40"N, 109°32'43"W, 29.vii.1946, H.A. Scullen [1♀, ORSU: UCRCENT00403960]. Harshaw Ck, 31°29'37"N, 110°41'0"W, 18.viii.1999, J. George, ovipositing in *Baccharis salicifolia* [2♀, UCRC: UCRCENT00175176, UCRCENT00278220]. Gila Co., Globe, 1188m, 33°23'38"N, 110°47'14"W, 6.viii.1946, H.A. Scullen [1♀, ORSU: UCRCENT00403959]; vii.1930, Parker [1♂ 2♀, MCZ: UCRCENT00318643–44, CASC: UCRCENT00417524]; 10.ix.1917, C.H.T. Townsend, on *Thurberia thespesioides* [1♀, USNM: UCRCENT00416868]; 13.ix.1945, R.A. Flock

[1♀, UCRC: UCRCENT00413316]. Six Shooter Canyon, nr. Globe, 33°22'51"N, 110°46'12"W, 17.viii.1958, R.L. Westcott [1♀, LACM: UCRCENT00305151]. Graham Co., Pinal Mts., 32°42'3"N, 109°52'18"W, 3.vii.1932 [1♀, UCRC: UCRCENT00413317]. Maricopa Co., Canon L., 33°32'24"N, 111°26'24"W, 1933, Parker [1?, CASC: UCRCENT00417398]. Baboquivari Mts., Elkhorn Ranch, 31°47'24"N, 111°34'12"W, 21.iv.1962, M.L. Noller, on *Phacelia* [1♀, UAZ: UCRCENT00403767]. Continental, 31°51'0"N, 110°58'12"W, 14.vi.1955, G.D. Butler, desert willow [1♀, UAZ: UCRCENT00403766]. Organ Pipe Cactus Nat. Mon., 32°05'15"N, 112°54'21"W, 6.viii.1955, G.D. Butler & F.G. Werner [1♀, UAZ: UCRCENT00403783]. Sycamore Cn., nr. Ruby, 31°55'12"N, 110°47'24"W, 16-17.viii.1961, Werner and Bequaert [1♀, UAZ: UCRCENT00403774]. Pima Co., Tucson, 32°13'12"N, 110°55'48"W, 28.iv.1940, S.L. Green [1♀, UAZ: UCRCENT00403764]; 24.iv.1940 [1♀, UAZ: UCRCENT00403770]; 745m, 11.viii.1924, E.P. Van Duzee [1♀, CASC: UCRCENT00417399]; v.1960, F.G. Werner [1♀, UAZ: UCRCENT00403775]; Wickham [1♂, USNM: UCRCENT00416867]. Pinal Co., Vic. Mammoth, 1005m, 32°43'21"N, 110°38'26"W, 9.viii.1977, Olson and Hetz [1♀, UAZ: UCRCENT00403773]. Santa Cruz Co., 12 mi. E. Nogales, 31°20'24"N, 110°43'48"W, 1.viii.1961, Werner and Nutting [1♀, UAZ: UCRCENT00403771]. Apache Rd, 1623m, 31°25'34"N, 110°41'48"W, 13.viii.2014, J.Heraty, meadow, swp, H14-102 [2♀, UCRC: UCRCENT00412584, UCRCENT00412674]. Harshaw Creek ~7mi. SE Patagonia, 31°31'3"N, 110°41'36"W, 5.vii.1996, Carey [1♀, USNM: UCRCENT00416655]. Nogales, 1183m, 31°20'25"N, 110°56'3"W, 16.viii.1968, R.M. Bohart [1♀, UCDC:

UCRCENT00415615]; 28.viii.1982, J. LaSalle [1♀, CNC: UCRCENT00505429]. Patagonia Mtns. ~4 mi. S.E. Patagonia Harshaw, 31°31'2"N, 110°41'36"W, 23.vii.2000, J. George [2♀, UCRC: UCRCENT00414045–46]; Harshaw Ck ~7mi. SE Patagonia, 17.viii.1999, M. Gates & J. George, *Baccharis salicifolia*, sweep [1♂ 1♀ 2?, USNM: UCRCENT00248215–16, UCRCENT00248263, UCRCENT00416634]. Patagonia Mts., Summit, Lochiel Rd., Sta, 31°21'0"N, 110°25'48"W, 5.ix.1964, F. Werner [1♀, UAZ: UCRCENT00403765]. Patagonia, 31°32'24"N, 110°45'36"W, 26.vii.1962, Noller [1♀, UAZ: UCRCENT00403768]; Werner, Bequaert, and Noller [1♀, UAZ: UCRCENT00403772]. Sycamore Cyn., Hank and Yank Spr., 1280m, 31°55'12"N, 110°47'24"W, 7-8.viii.1982, G. Gibson [1♂, TAMU: UCRCENT00243185].

Etymology. Named in honor of Stephanie Castillo, a fellow entomology graduate student.

***Orasema tolteca* Mann**

urn:lsid:zoobank.org:act:F048E1C6-69F7-42FA-8FBB-F05717784453

(Figs 2.19, 2.20)

Orasema tolteca Mann 1914: 183–184.

O. tolteca; Gahan 1940: 444–445. Redescription and identification key.

Diagnosis. This species can be recognized from *O. castilloae* by having generally more labral digits (4–8), generally a dark patch that takes up a larger proportion of the femora and extending to the base, and a male antenna with longer/thinner flagellar segments.

Description. Female: Length 3.4–4.9 mm (Fig. 2.20A). **Color.** Head and mesosoma range from black to dull green to bright iridescent green. Scape brown with strong iridescence; pedicel and anellus dark brown. Femora mostly dark brown with iridescence, yellow distally. Gaster green to dark brown with strong iridescence. **Head** (Fig. 2.20B). HW:HH 1.2–1.3; IOD:EH 2–3; MS:EH 1.1–1.7. Labrum with 4–8 digits. FL:HH 1.2–1.6; F2L:F2W 1.3–2, F2L:F3L 0.9–1.3 (Fig. 2.20D). **Mesosoma** (Fig. 2.20 C, F). ML:MH 1–1.3. Axilla areolate-rugose; axillular sulcus vaguely indicated by a longitudinal carina; axillula areolate. Propodeal disc areolate-reticulate (Fig. 2.21G); callus reticulate. Prepectus weakly reticulate. Upper mesepimeron rugose-reticulate. HCL:HCW 1.1–2; HFL:HFV 5.4–7. FWL:FWW 2.3–2.6, FWL:ML 2.1–2.5. **Metasoma.** PTL:PTW 1.4–2.5, PTL:HCL 0.8–1.2, rugose-reticulate, ventral sulcus present with margins widely separated. Ovipositor with second (dorsal) valvula with 8–10 annuli that are broadly separated dorsally, carinae weakly coalescing.

Male. Length 3.5–4.6 mm. HW:HH 1.1–1.3. FL:HH 2.1–2.6; F2L:F2W 1.6–2.4 (Fig. 2.20E). Femora mostly dark brown, yellow distally. PTL:PTW 3.7–9.2, PTL:HCL 1.5–2.5.

Planidium. Length 0.18 mm (Fig. 2.19 A–C). Head with two pairs of dorsal cranial setae. Antenna, labial plates absent. Tergopleural line vaguely indicated. Tergites I and II separate. Tergites I, II, and III with dorsal setae. Tergites II and VI with lateral setae. Tergites I, III, V, and VII with ventral setae. Tergites IV–VII with posteriorly pointing ventral projections. Tergite IX with separated leaflike ventral plate. Caudal pad present; caudal cerci present, about as long as tergites X+XI+XII.

Pupa. (Fig. 2.19D). Fits the general description for Oraseminae pupae provide by Heraty (1994), with the three large tubercles along the dorsal margin of the petiole and the prominent transverse abdominal ridges being the most diagnostic features of the subfamily. This species has a dorsal longitudinal ridge on the gaster as well as incomplete dorsolateral ridges on the apical segments. It lacks distinct sublateral processes on the gaster as well as distinct tubercles on the mesosoma.

Ant hosts. Collected from nest of *Pheidole hirtula* Forel (Mann, 1914).

Plant hosts. Oviposits into bracts of *Buddleia* (Loganiaceae), *Melanopodium* (Asteraceae), *Sphaeralcea* (Malvaceae), *Dalea* (Fabaceae), and *Lippia* (Verbenaceae) (Heraty, 1990). Swept from *Sphaeralcea angustifolia* (Cav.) G. Don (Malvaceae), *Eysenhardtia polystachya* (Ortega) Sarg. (Fabaceae), *Lantana* (Verbenaceae), acacia-cactus scrub.

Distribution (Fig. 2.17). Mexico: AG, CH, CO, DF, DG, GT, JA, MO, NL, OA, PU, QT, SI, SL, TM, VE, ZA. Collected March–November.

Material examined. Syntypes: Mexico: Hidalgo: San Miguel, 20°54'36"N, 100°44'24"W, W. M. Mann [3♀, deposited in USNM: UCRCENT00416732–33, UCRCENT00318645]. **Larval slides. Mexico: Oaxaca:** 4.8 km SE Matalan, 2015m, 16°49'59"N, 96°21'36"W, 17.vii.1987, J. Heraty, oak scrub-Lantana, host plant: *Lantana* [5?, UCRC: UCRCENT00436245–48, UCRCENT00436250]. **San Luis Potosi:** 7.2 mi E San Luis Potosi, 22°09'36"N, 100°52'12"W, 3.vii.1987, J. Heraty, host plant: *Sphaeralcea angustifolia* [8?, UCRC: UCRCENT00436233–39, UCRCENT00436243]. **Additional material examined:** 93 specimens, see supplementary material.

***Orasema sixaolae* species group**

(Figs 2.21–2.25)

Diagnosis. Recognized by the following combination of characters: small-bodied (1.4–2.2 mm); antenna with 7 funiculars (male and female), funicular segments wide and cup-shaped with a short peduncle; PTL:PTW 1.6–4.2 (female), 5–7.8 (male). Generally, this group has subcircular head shape, weak reticulate sculpture on the face and mesosoma, and dark body color.

Description. Female. Length 1.4–2.2 mm. **Color.** Scape, pedicel and anellus pale brown; flagellum brown. Maxilla and labium pale brown. Coxae brown. Wing venation pale brown. Gaster brown. **Head.** Scrobal depression shallow, laterally rounded, with transverse striae; anterior tentorial pit strongly impressed; anteclypeus distinct, broadly rounded. Occiput imbricate, emarginate in dorsal view. Scape not reaching median ocellus. Flagellum with 7 funiculars. **Mesosoma.** Notauli deep. Axilla dorsally rounded, on roughly the same plane as mesoscutellum; frenum and axillula smooth. Propodeal disc broadly rounded; callus smooth. Mesepisternum broadly rounded anterior to mid coxa. Upper and lower mesepimeron smooth; transepimeral sulcus distinct. Metepisternum laterally smooth. Propleuron convex. Postpectal carina weak. Hind coxa weakly reticulate. Fore wing marginal fringe relatively long; marginal vein pilose; stigmal vein slightly longer than broad. **Metasoma.** Petiole cylindrical, linear in profile.

Male. Length 1.5–2 mm. Scape pale brown; flagellum with 7 funiculars; anellus disc-shaped. Femora mostly brown, tips pale.

Phylogenetics. *Orasema sixaolae* and *O. nebula* (referred to as “nr. sixaolae”) are the only species molecularly sampled (Baker et al., 2020). Specimens of *O. sixaolae* sampled from Mexico, Costa Rica, Venezuela, and Ecuador are monophyletic with a crown age at *c.* 4–7 MY and an average of 9.3% sequence variation between AHE-sequenced specimens, and *O. nebula* from Ecuador is the sister species. This species group is sister to *O. monstrosa*, which seems to share very few morphological similarities with the *O. sixaolae* species group, warranting placement as its own group.

Key to species of the *Orasema sixaolae* species group

- 1) Curvature of eyes in frontal view appearing continuous with the curvature of the head (Figs 2.24B, 2.25B); female IOD:EYH >1.5; angle created by mesoscutellum, frenum, and propodeum less obtuse (closer to right angle) in lateral view (Figs 2.24C, 2.25C) **2**
- Curvature of eyes in frontal view discontinuous with curvature of head, eyes appear to be bulging from sides of head (Figs 2.22B, 2.23B); female IOD:EYH <1.5; angle created by mesoscutellum, frenum, and propodeum more obtuse in lateral view (Figs 2.22C, 2.23C) **3**

- 2) Face and mesoscutal midlobe distinctly reticulate (Fig. 2.24 B, F); frenum <25% length of mesoscutellum in dorsal view (Fig. 2.24F); female petiole longer/thinner (PTL:PTW 3.1–4.1) (widespread Neotropical)
..... *Orasema sixaolae* Wheeler & Wheeler

- Face smooth (Fig. 2.25B); mesoscutal midlobe imbricate anteriorly transitioning to smooth dorsally (Fig. 2.25E); frenum >25% length of mesoscutellum in dorsal view (Fig. 2.25E); female petiole shorter/wider (PTL:PTW 2.2) (Ecuador)
..... *Orasema tinalandia* **n. sp.**
- 3)** Flagellomeres 3–8 as wide as long (Fig. 2.23 D, E); female petiole longer than hind coxa (Costa Rica and Ecuador) *Orasema nebula* **n. sp.**
- All flagellomeres longer than wide (Fig. 2.22D); female petiole subequal in length to hind coxa (Brazil) *Orasema brachycephala* **n. sp.**

***Orasema brachycephala* n. sp.**

(Fig. 2.22)

Diagnosis. Recognized from other members of the *Orasema sixaolae* group by the relatively elongate flagellomeres on the antenna (F2L:F2W 1.8), including a relatively quadrate anellus (Fig. 2.22D). Recognized from *O. sixaolae* and *O. nebula* by the petiole being shorter in length than the hind coxa (female). Recognized from *O. tinalandia* by more coarsely, reticulately sculptured mesoscutal lateral lobes and axillae and by the wider/deeper anterior tentorial pits.

Description. Female. Length 2.2 mm (Fig. 2.22A). **Color.** Head and mesosoma dark brown with bluish iridescence. Mandible pale brown, darkened near edge. Femora and tibiae pale brown. **Head** (Fig. 2.22B). Head in frontal view subovoid; HW:HH 1.4; face

lightly reticulate, nearly smooth; longitudinal groove between eye and torulus absent; eyes sparsely setose, IOD:EH 1.4; MS:EH 0.5; malar depression weakly impressed adjacent to mouth; supraclypeal area slightly broader than long, nearly smooth; clypeus shallowly imbricate; epistomal sulcus distinct and sharply defined. Labrum with 4 digits. Mandibular formula not observed; palpal formula 2:2. Occiput with dorsal margin evenly rounded; temples absent. Pedicel globose, broader than F1. FL:HH 1.7; anellus large; F2L:F2W 1.8, F2L:F3L 1; following funiculars subequal in length, equal in width; clava subovate (Fig. 2.22D). **Mesosoma** (Fig. 2.22 C, E). ML:MH 1.7. Mesoscutal midlobe weakly reticulate, sparsely setose; lateral lobe weakly reticulate. Axilla weakly reticulate; scutoscutellar sulcus broad, irregularly foveate, broadly separated from transscutal articulation; mesoscutellar disc as long as broad, weakly reticulate to smooth; frenal line as smooth band; axillular sulcus indicated by a strong longitudinal carina. Propodeal disc areolate-reticulate, with irregular median carina, smooth laterally (Fig. 2.22F); callus with several long setae on dorsal margin. Propleuron weakly reticulate. Prepectus mostly smooth. Mesepisternum reticulate. HCL:HCW 2.2; HFL:HFW 4.2, with even cover of short, dense setae. FWL:FWW 2.1, FWL:ML 2.3; entirely setose, wing disc densely setose; submarginal vein with several long setae; stigmal vein perpendicular to anterior wing margin; postmarginal vein several times longer than stigmal vein. Hind wing costal cell with only 1 or 2 irregular rows of setae. **Metasoma**. PTL:PTW 1.7, PTL:HCL 0.7, areolate-reticulate, lateral margin rounded, ventral sulcus present with margins broadly separated. Antecostal sulcus foveate; acrosternite posteriorly rounded; apical setae of hypopygium with several long hairs on each side of midline. Ovipositor not visible.

Male. Unknown.

Ant hosts. Unknown.

Plant hosts. Unknown.

Distribution (Fig. 2.21). Brazil: RJ. Collected in January (one specimen)

Material examined. Holotype: Brazil: Rio de Janeiro: Gunabara Floresta de Tijuca, 22°55'48"S, 43°14'24"W, i.1974, M. Alvarenga [1♀, deposited in CNC: UCRCENT00247554].

Etymology. From Greek *brachy* meaning “short” and *cephal* meaning “head” in reference to the relatively short/wide face.

***Orasema nebula* n. sp.**

(Fig. 2.23)

Diagnosis. Recognized from *O. brachycephala* by having flagellomeres that are approximately as wide as they are long (cup-shaped) with distinct peduncles, a petiole (female) that is longer than the hind coxae, a propodeum with a medial carina but without areolate sculpture, and a shorter body length. Recognized from *O. tinalandia* by having more reticulate sculpture on the mesosoma and having a petiole that is longer than the hind coxae. This species is most similar to *O. sixaolae* but can be recognized by a longer body (female ML:MH 1.6 in *O. nebula*; 1.1–1.4 in *O. sixaolae*), smoother sculpture on the face, a generally smaller MSP:EYH (which gives the head a more circular, less triangular appearance), and a shorter/wider petiole (male and female).

Female. Length 1.8 mm (Fig. 2.23A). **Color.** Head and mesosoma brownish black with some blue-green iridescence. Mandible brown. Femora mostly brown, tips pale; tibiae pale brown. **Head** (Fig. 2.23B). Head in frontal view subovoid; HW:HH 1.3; face weakly reticulate, nearly smooth; longitudinal groove between eye and torulus present or absent; eyes sparsely setose, IOD:EH 1.5; MS:EH 0.6; malar depression weakly impressed adjacent to mouth; supraclypeal area slightly broader than long, smooth; clypeus smooth; epistomal sulcus distinct and sharply defined. Labrum with 4 digits. Mandibular formula not observed; palpal formula 3:2. Occiput with dorsal margin evenly rounded; temples absent. Pedicel globose, broader than F1. FL:HH 1.5; anellus disc-shaped; F2L:F2W 1.4, F2L:F3L 1.2; following funiculars subequal in length, gradually broader; clava subovate (Fig. 2.23D). **Mesosoma** (Fig. 2.23 C, F). ML:MH 1.6. Mesoscutal midlobe imbricate to reticulate, sparsely setose; lateral lobe irregularly finely reticulate. Axilla weakly reticulate; scutoscutellar sulcus broad, irregularly foveate, broadly separated from transscutal articulation; mesoscutellar disc slightly longer than broad, irregularly finely reticulate; frenal line thin and irregularly foveate; axillular sulcus indicated by a weak longitudinal carina. Propodeal disc smooth laterally, with irregular median carina (Fig. 2.23G); callus with several short setae on dorsal margin. Propleuron smooth. Prepectus smooth to weakly reticulate. Mesepisternum reticulate laterally, smooth ventrally. HCL:HCW 1.8; HFL:HFW 5.7, setose dorsally and laterally. FWL:FWW 2.3, FWL:ML 2.3; basal area and speculum bare, costal cell and wing disc densely setose; submarginal vein with small setae; stigmal vein slightly angled toward wing apex; postmarginal vein slightly longer than stigmal vein. Hind wing costal cell

entirely setose. **Metasoma.** PTL:PTW 2.8, PTL:HCL 1.2, areolate, lateral margin rounded, ventral sulcus absent. Antecostal sulcus smooth; acrosternite posteriorly angulate; apical setae of hypopygium with one pair of long setae. Ovipositor with subapical carina present; first (ventral) valvula with 6–8 small, narrowly separated teeth, second (dorsal) valvula with 8–10 annuli that are broadly separated dorsally by smooth area.

Male. Length 1.9 mm. HW:HH 1.3. FL:HH 1.6; F2L:F2W 1.6 (Fig. 2.23E). Tibiae pale brown. PTL:PTW 5, PTL:HCL 2.4.

Ant hosts. Unknown.

Plant hosts. Unknown.

Distribution (Fig. 2.21). Costa Rica: AL; Ecuador: OR. Collected in February, October, and December.

Material examined. Holotype: Ecuador: Orellana: Tiputini Biodiversity Station, nr Yasuni National Park, 220-250m, 0°37'55"S, 76°08'39"W, 8.ii.1999, T.L. Erwin et al., terre firme forest, Fogging, Lot# 2024 [1♀, deposited in USNM: UCRCENT00247795].

Paratype: Ecuador: Orellana: 1 km S. Onkone Gare Camp, Reserva Etnica Waorani, 216.3m, 0°39'25"S, 76°27'10"W, 8.x.1995, T.L. Erwin et al., terre firme forest, Fogging, Lot# 1259 [1♂, USNM: UCRCENT00247799].

Discussion. The collection events in Ecuador where specimens of *O. nebula* have been collected by canopy fogging also collected many more specimens of *O. sixaolae*, confirmed by molecular sequencing (Baker et al., 2020). Most of these *O. sixaolae*

specimens are distinct, but some bear a close resemblance to *O. nebula* (e.g. UCRCENT00247800, UCRCENT00311894).

Etymology. From Latin *nebula* meaning “cloud or fog” in reference to specimens being collected from canopy fogging.

***Orasema sixaolae* Wheeler & Wheeler**

urn:lsid:zoobank.org:act:4CB6983B-FC4A-4DCD-90D5-D4974A1AE2C1

(Fig. 2.24)

Orasema sixaolae Wheeler & Wheeler, 1937: 163–164.

Diagnosis. Recognized from *O. brachycephala* by having flagellomeres as wide as long (cup-shaped) with distinct peduncles and having a petiole much longer than the hind coxa. Recognized from *O. tinalandia* by having more coarsely reticulate sculpture on the mesoscutal midlobe and a petiole much longer than the hind coxa. This species is most similar to *O. nebula* but can be recognized by the more coarsely reticulate sculpture on the face, a generally larger MSP:EYH (which gives the head a more triangular, less circular appearance), and a longer/thinner petiole (male and female).

Description. Female. Length 1.5–2.1 mm (Fig. 2.24A). **Color.** Head and mesosoma dark with iridescence. Mandible brown; Femora mostly brown, tips pale; tibiae yellow.

Head (Fig. 2.24B). Head in frontal view subquadrate; HW:HH 1.1–1.2; face completely reticulate to slightly costate on frons; longitudinal groove between eye and torulus present; eyes bare, IOD:EH 1.5–1.8; MS:EH 0.6–0.9; malar depression absent;

supraclypeal area as long as broad, equal to length of clypeus, smooth; clypeus smooth to shallowly reticulate; epistomal sulcus vaguely defined. Labrum with 4–5 digits.

Mandibular formula 3:2; palpal formula 3:2. Occiput with dorsal margin evenly rounded; temples absent. Pedicel globose, broader than F1. FL:HH 1.1–1.3; anellus disc-shaped; F2L:F2W 1–1.5, F2L:F3L 1–1.2; following funiculars subequal in length, gradually broader; clava subovate (Fig. 2.24D). **Mesosoma** (Fig. 2.24 C, F). ML:MH 1.1–1.4.

Mesoscutal midlobe reticulate, bare or with very minute setae; lateral lobe smooth. Axilla smooth; scutoscutellar sulcus broad, irregularly foveate, narrowly separated from transscutal articulation; mesoscutellar disc slightly longer than broad, reticulate; frenal line regularly foveate; axillular sulcus indicated by a weak longitudinal carina. Propodeal disc with median carina, smooth laterally (Fig. 2.24G); callus with several short setae on dorsal margin. Prepectus, mesepisternum, and propleuron reticulate. HCL:HCW 1.7–2.3; HFL:HFW 6.1–7, with even cover of short, dense setae. FWL:FWW 2.3–2.5, FWL:ML 2.4–2.8; basal third of wing bare, including speculum and costal cell, wing disc densely setose; submarginal vein bare; stigmal vein perpendicular to anterior wing margin; postmarginal vein several times longer than stigmal vein. Hind wing costal cell with a broad bare area. **Metasoma**. PTL:PTW 3.1–4.2, PTL:HCL 1.1–1.4, areolate-reticulate, lateral margin rounded, ventral sulcus present with margins narrowly separated.

Antecostal sulcus foveate; acrosternite posteriorly rounded; apical setae of hypopygium present, minute. Ovipositor with subapical carina present; first (ventral) valvula with 6–8 small, narrowly separated teeth, second (dorsal) valvula with 6–7 annuli that are broadly separated dorsally by smooth area.

Male. Length 1.5–2 mm. HH:HW 1.2–1.3. FL:HH 1.3–1.5; F2L:F2W 1.2–1.4 (Fig. 2.24E). Tibiae yellow. PTL:PTW 6.2–7.8, PTL:HCL 1.7–2.5.

Planidium. Described by Wheeler and Wheeler (1937).

Pupa. Fits the general description for *Orasema* pupae provide by Heraty (1994), with the three large tubercles along the dorsal margin of the petiole and the prominent transverse abdominal ridges being the most diagnostic features of the subfamily. This species has stronger tubercles coming from the abdominal ridges than the pupa of *O. tolteca* (Fig. 2.19D).

Ant hosts. *Solenopsis tenuis* Mayr in Costa Rica (Wheeler & Wheeler, 1937) and *Solenopsis picea* Emery in Mexico.

Both species of *Solenopsis* make their nests in dead twigs, where parasitized brood and *Orasema* pupae were found. In southern Mexico, dead twigs were placed as baits at coffee plantations to monitor *Solenopsis* activity, and *O. sixaolae* were found in many of these plantations (de la Mora Rodríguez et al., unpublished).

Plant hosts. Unknown, but possibly coffee, *Coffea arabica* (L.) (Rubiaceae).

Distribution (Fig. 2.21). Argentina: BA, MN, SA; Belize: TO; Brazil: SP, MG; Costa Rica: AL, GU, HE, LI, PU; Ecuador: NA, OR; Honduras: OL; Mexico: CP, VE; Peru: MD; Trinidad: SL; Venezuela: BO. Specimens collected throughout the year.

Material examined. Syntype: Costa Rica: Limon: No. 375 Sixaola River, 9°32'N, 82°42'W, vii.1924, G.C. Wheeler [1♀, deposited in USNM: UCRCENT00248527].

Additional material examined: 62 specimens, see supplementary material.

Discussion. This species has the largest known distribution of any species in Oraseminae, even though it is far less morphologically diverse than *O. coloradensis*. Specimens of *O. sixaolae* have been collected at a fairly even rate throughout the year (49 records), indicating that tropical/subtropical species of *Orasema* are far less ephemeral than the temperate species found in the Nearctic. Despite their presence in previous collections, our sampling in Trinidad (2013) and Costa Rica (2016) failed to find any additional *O. sixaolae*.

***Orasema tinalandia* n. sp.**

(Fig. 2.25)

Diagnosis. Recognized from other species in the *Orasema sixaolae* species group by the smoother sculpture on the mesoscutal midlobe. Recognized from *O. sixaolae* and *O. nebula* by having a petiole that is shorter than the hind coxae. Recognized from *O. brachycephala* by having flagellomeres that are as wide as long.

Description. Female. Length 1.4 mm (Fig. 2.25A). **Color.** Head and mesosoma brown with bluish iridescence. Mandible brown. Femora mostly brown, tips pale; tibiae pale brown. **Head** (Fig. 2.25B). Head in frontal view subtriangular; HW:HH 1.2; face smooth; longitudinal groove between eye and torulus present; eyes sparsely setose, IOD:EH 1.6; MS:EH 0.6; malar depression absent; supraclypeal area slightly broader than long, smooth; clypeus smooth; epistomal sulcus distinct and sharply defined. Labrum with 4 digits. Mandibular formula not observed; palpal formula 3:2. Occiput with

dorsal margin abrupt; temples present, rounded. Pedicel globose, as broad as F1. FL:HH 1.2; anellus disc-shaped; F2L:F2W 0.8, F2L:F3L 0.8; following funiculars subequal in length, gradually broader; clava subconical (Fig. 2.25D). **Mesosoma** (Fig. 2.25 C, E). ML:MH 1.5. Mesoscutal midlobe weakly reticulate, nearly smooth, sparsely setose; lateral lobe smooth. Axilla smooth; scutoscutellar sulcus narrow, regularly foveate, broadly separated from transscutal articulation; mesoscutellar disc slightly longer than broad, smooth; frenal line regularly foveate; axillular sulcus distinct and foveate. Propodeal disc areolate, smooth laterally (Fig. 2.25F); callus with several short setae on dorsal margin. Propleuron smooth. Prepectus smooth. Mesepisternum smooth. HCL:HCW 1.9; HFL:HFW 6.3, sparsely setose. FWL:FWW 2.7, FWL:ML 2.5; basal third of wing bare, wing disc evenly setose; submarginal vein with 8 long setae dorsally; stigmal vein perpendicular to anterior wing margin; postmarginal vein same length as stigmal vein. Hind wing costal cell with a few setae. **Metasoma**. PTL:PTW 2.3, PTL:HCL 0.8, areolate, lateral margin with longitudinal carina continuous with basal flange, ventral sulcus not observed. Antecostal sulcus foveate; acrosternite posteriorly angulate; apical setae of hypopygium with one pair of long setae. Ovipositor with subapical carina weak; first (ventral) valvula with 10–11 small, closely spaced teeth, second (dorsal) valvula with 8–10 annuli that are broadly separated dorsally by smooth area.

Male. Unknown.

Ant hosts. Unknown.

Plant hosts. Unknown.

Distribution (Fig. 2.21). Ecuador: PC. Collected in February (one specimen).

Material examined. Holotype: Ecuador: Pichincha: Tinalandia, 850m, $0^{\circ}16'49''N$, $79^{\circ}06'37''W$, 2.ii.1983, Masner & Sharkey [1♀, deposited in CNC: UCRCENT00247522].

Etymology. Referring to the locality ‘Tinalandia’ in Ecuador where the specimen was collected.

***Orasema acuminata* species group**

(Figs 2.26–2.28)

Diagnosis. Recognized by the following combination of characters: antenna with 7 funicular segments; labrum with 4 digits; mesoscutum and mesoscutellum coarsely rugose-areolate; eyes bare; antecostal sulcus smooth (Fig. 2.28E).

Description. Female. Length 2.6–3.7 mm. **Color.** Scape yellow; anellus pale brown; flagellum dark brown. Mandible pale brown with dark edges; maxilla and labium pale brown. Coxae brown with iridescence; tibiae yellow. Fore wing hyaline; venation pale brown. Petiole same as mesosoma; gaster dark brown with iridescence. **Head.** Head in frontal view subtriangular; scrobal depression shallow, laterally rounded, with transverse striae; longitudinal groove between eye and torulus absent; eyes bare; clypeus smooth; epistomal sulcus vaguely defined; anterior tentorial pits deeply impressed. Labrum with 4 digits. Mandibular formula 3:2; palpal formula 3:2. Occiput imbricate, emarginate in dorsal view, dorsal margin rounded; temples present. Scape not reaching median ocellus.

Pedicle small and globose. Flagellum with 7 funiculars; anellus disc-shaped. **Mesosoma.** Mesoscutal midlobe rugose-areolate, moderately setose; lateral lobe rugose-areolate; notauli deep. Axilla rugose-areolate; scutoscutellar sulcus broad, regularly foveate; mesoscutellar disc as long as broad, rugose-areolate; frenum and axillula rugose-areolate. Propodeal disc flat, without depression or carina, areolate; callus areolate, with several long setae. Propleuron convex, imbricate. Prepectus triangular dorsally, strongly narrowed ventrally, rugose-areolate. Mesepisternum areolate, broadly rounded anterior to mid coxa; postpectal carina weak. Transepimeral sulcus distinct. Hind femur densely setose laterally. Fore wing with marginal fringe relatively long; marginal vein setose; stigmal vein slightly longer than broad; postmarginal vein several times longer than stigmal vein. Hind wing costal cell setose. **Metasoma.** Petiole cylindrical, linear in profile, rugose, ventral sulcus absent. Antecostal sulcus smooth; acrosternite posteriorly rounded (Fig. 2.28E).

Male. Length 2.6–3.2 mm. (Only known from *Orasema acuminata*).

Phylogenetics. Only one species, *Orasema acuminata*, has been sampled for molecular data (referred to as “*Orasema_nsp_nr_brasiliensis_PER_AE_D4889*”). This species was the sister to the majority of the *Orasema xanthopus* group in most analyses (Baker et al., 2020).

Key to species of the *Orasema acuminata* species group

- 1) Clava strongly pointed (Fig. 2.27 D, E); sculpture on face more rugose than reticulate (Fig. 2.27B); upper mesepimeron areolate (Fig. 2.27C); femora mostly light brown (Fig. 2.27A); body color green-blue-purple (Ecuador and Peru)
..... *Orasema acuminata* **n. sp.**
- Clava subovate (Fig. 2.28D); sculpture on face more reticulate than rugose (Fig. 2.28B); upper mesepimeron smooth (Fig. 2.28C); femora dark brown (Fig. 2.28A); body color dark blue (Honduras) *Orasema cerulea* **n. sp.**

***Orasema acuminata* n. sp.**

(Fig. 2.27)

Diagnosis. Recognized from *O. cerulea* by having the antennal clava strongly pointed, facial sculpture more rugose than reticulate, upper mesepimeron areolate, femora pale brown, and body color green-blue-purple.

Description. Female. Length 3.2–3.7 mm (Fig. 2.27A). **Color.** Head and mesosoma iridescent green-blue-purple. Pedicle brown. Femora pale brown, tips yellow. **Head** (Fig. 2.27B). HW:HH 1–1.2; face rugose-reticulate; IOD:EH 1.4–1.6; MS:EH 0.6–0.8; malar depression weakly impressed between mouth and eye margin; supraclypeal area longer than broad, weakly sculptured; anteclypeus distinct, nearly straight. FL:HH 0.9–1; F2L:F2W 1.6–1.8, F2L:F3L 1.1–1.2; funiculars subequal in length distally, equal in width; clava subconical (Fig. 2.27D). **Mesosoma** (Fig. 2.27 C, F, G) ML:MH 1.3–1.6.

Axilla dorsally rounded, on roughly the same plane as the mesoscutellum; scutoscutellar sulcus meeting transscutal articulation medially; frenal line indicated by a strong dorsal carina; axillular sulcus indicated by a strong longitudinal carina. Upper mesepimeron areolate; lower mesepimeron rugose-reticulate. Metepisternum rugose-areolate.

HCL:HCW 1.6–2, weakly reticulate; HFL:HFW 4.9–5.7. FWL:FWW 2.7–2.9, FWL:ML 2.1–2.4; basal area and speculum bare, costal cell and wing disc densely setose; submarginal vein with small setae; stigmal vein perpendicular to anterior wing margin.

Metasoma. PTL:PTW 2.2–2.4, PTL:HCL 1.1–1.3, lateral margin with weak longitudinal carina. Apical setae of hypopygium with several long setae on either side of the midline. Ovipositor not visible.

Male. Length 2.6–3.2 mm. HW:HH 1.1–1.2. Scape yellow; flagellum with 7 funiculars, FL:HH 1.1–1.4; anellus disc-shaped; F2L:F2W 1.2–1.7 (Fig. 2.27E). Femora pale brown, darker medially; tibiae yellow. PTL:PTW 5.5–6.5, PTL:HCL 2–2.4.

Ant hosts. Unknown.

Plant hosts. Unknown.

Distribution (Fig. 2.26). Ecuador: NA, ZC; Peru: CS, MD. Collected in February–August.

Material examined. Holotype: Ecuador: Zamora-Chinchi: Yacwambi, 3°35'42"S, 78°55'41"W, 3.iv.1965, Luis Peña [1♀, deposited in AEIC: UCRCENT00415025]. **Paratypes: Ecuador: Napo:** Limoncocha, on Rio Napo, 0°58'59"S, 77°49'1"W, 15.vii.1974, Boyce A. Drummond, III, Malaise Trap [1♀, FSCA: UCRCENT00411896]. **Peru: Cusco:** Quince Mil, 633m, 13°13'3"S, 70°43'40"W, 23-

31.viii.2012, J.A. Rafael; R.R. Cavichioli; D.M. Takiya, Malaise [1♂, INPA: UCRCENT00504574]. **Madre de Dios:** Rio Tambopata Res., 30 km (air) SW Puerto Maldonado, 290m, 12°50'0"S, 69°17'0"W, 1.iii.1982, T.L. Erwin et al. [1♂, USNM: UCRCENT00247953]; 25.ii.1984 [1♂, USNM: UCRCENT00247958]; 7.v.1984 [1♂, USNM: UCRCENT00247951, UCRCENT00247955, UCRCENT00247959].

Etymology. From Latin *acumin* meaning "pointed" in reference to the pointed clava.

***Orasema cerulea* n. sp.**

(Fig. 2.28)

Diagnosis. Recognized from *O. acuminata* by having the antennal clava subovate, facial sculpture more reticulate than rugose, upper mesepimeron smooth, femora dark brown, and body color dark blue.

Description. Female. Length 2.6–3 mm (Fig. 2.28A). **Color.** Head and mesosoma dark iridescent blue. pedicel pale brown. Femora mostly brown, tips pale. **Head** (Fig. 2.28B). HW:HH 1.1–1.2; face rugose-reticulate; IOD:EH 1.7–1.9; MS:EH 0.9–1; malar depression weakly impressed adjacent to mouth; supraclypeal area as long as broad, weakly rugose-reticulate; anteclypeus distinct, broadly rounded. FL:HH 1.3–1.4; F2L:F2W 2.1–2.8, F2L:F3L 1.1–1.3; following funiculars subequal in length, gradually broader; clava subovate (Fig. 2.28D). **Mesosoma** (Fig. 2.28 C, G, H). ML:MH 1.2–1.3. Axilla dorsally well above mesoscutellum; scutoscutellar sulcus narrowly separated from transscutal articulation; frenal line irregularly foveate; axillular sulcus weak and foveate.

Upper mesepimeron smooth; lower mesepimeron nearly smooth with weak carinae. Metepisternum weakly rugose-areolate. HCL:HCW 1.6–2.1, costate; HFL:HFw 6.6–8.9. FWL:FwW 2.5–2.7, FWL:ML 2.3–2.5; basal area sparsely setose, speculum bare, costal cell and wing disc setose; submarginal vein with several long setae; stigmal vein slightly angled toward wing base. **Metasoma.** PTL:PTW 5.4–6.5, PTL:HCL 2.1–2.4, lateral margin rounded. Apical setae of hypopygium with one pair of long setae. Ovipositor with subapical carina present; first (ventral) valvula with 6–8 small, narrowly separated teeth, second (dorsal) valvula with 6–7 annuli that are broadly separated dorsally by smooth area (Fig. 2.28F).

Male. Unknown.

Ant hosts. Unknown.

Plant hosts. Unknown.

Distribution (Fig. 2.26). Costa Rica: AL; Honduras: YO. Collected in February and September.

Material examined. Holotype: Honduras: Yoro: Palo de Comba, 15°11'0"N, 87°39'0"W, 27.ix.1995, R. Cave, mid elevation secondary forest, Malaise Trap [1♀, deposited in MZLU: UCRCENT00242604]. **Paratypes: Costa Rica: Alejuela:** Playuelas, RNVS Caño Negro, 20m, 10°57'13"N, 84°44'51"W, 1–18.ii.1994, K. Martinez [1♀, INBIO: INBIOCRI001746776]. **Honduras: Yoro:** Palo de Comba, 15°11'0"N, 87°39'0"W, 27.ix.1995, R. Cave, mid elevation secondary forest, Malaise Trap [2♀, MZLU: UCRCENT00242603, UCRCENT00242605].

Etymology. From Latin *cerule* meaning “blue” in reference to the body coloration.

***Orasema hippocephala* species group**

(Figs 2.29–2.31)

Diagnosis. Recognized by the following combination of characters: antenna with 7 funicular segments, a strongly curved occiput (Fig. 2.31C), which gives the head a crescent shape in dorsal view, a face that appears thinner and more elongate than most *Orasema*, which can be denoted by the IOD:HH (generally <0.7 , whereas most other species groups tend to be >0.7), postgena converging (Fig. 2.31D), mesoscutal midlobe costate to costate-reticulate, and mesosoma relatively elongate, which can be denoted by the MSL:MSH (generally >1.6 , whereas most other species groups tend to be <1.6).

Description. Female. Length 2.3–4.2 mm. **Color.** Scape yellow; flagellum brown. Mandible pale brown; maxilla and labium pale brown to yellow. Tibiae yellow. Wing venation pale brown. Gaster brown with iridescence. **Head.** Head in frontal view elongate. Face costate; scrobal depression deep, laterally rounded, with transverse striae; longitudinal groove between eye and torulus absent; eyes sparsely setose; supraclypeal area about as long as broad, shorter than clypeus; clypeus smooth; epistomal sulcus distinct; anterior tentorial pit strongly impressed; anteclypeus distinct, broadly rounded. Labrum with 4 digits. Mandibular formula 3:2. Occiput imbricate, deeply emarginate in dorsal view, dorsal margin abrupt. Scape not reaching median ocellus. Pedicel small and globose. Flagellum with 7 funiculars; anellus disc-shaped; following funiculars subequal in length, equal in width. **Mesosoma.** Mesoscutal lateral lobe smooth and shining; notauli deep. Axilla dorsally flat, on same plane as mesoscutellum; scutoscutellar sulcus narrowly separated from transscutal articulation; axillula areolate. Propodeal disc flat,

areolate, occasionally with irregular median carina; callus with several long setae. Propleuron convex, coriaceous. Prepectus areolate-reticulate. Mesepisternum reticulate laterally, smooth ventrally, straight anterior to mid coxa; postpectal carina weak. Upper mesepimeron smooth; lower mesepimeron weakly reticulate; transepimeral sulcus distinct. Metepisternum weakly reticulate. Hind coxa reticulate. Fore wing basal area and speculum bare, costal cell and wing disc densely setose; marginal fringe relatively long; submarginal vein with several long setae; marginal vein pilose; stigmal vein slightly longer than broad, slightly angled toward wing apex. **Metasoma.** Petiole cylindrical, linear in profile, lateral margin rounded, ventral sulcus present with margins broadly separated. Antecostal sulcus foveate; acrosternite posteriorly rounded; apical setae of hypopygium present, minute.

Male. Length 2.1–2.7 mm. (Only known from *Orasema chrysozona*).

Phylogenetics. The *Orasema hippocephala* group is placed sister to the clade containing the *coloradensis*-, *sixaolae*-, and *monstrosa* groups (Baker et al., 2020). Specimens sampled include one *Orasema hippocephala* (designated “Orasema_”DF1”_ARG_AE_D4205”), and two *Orasema chrysozona* (designated “Orasema_”DF2”_ARG_AE_D4885” and “Orasema_”DF3”_ARG_AE_D4884”). The decision to include “DF2” (UCRCENT00436599) and “DF3” (UCRCENT00169577) into the same species was partially the result of a small molecular distance between the two specimens when compared to other well-sampled species (e.g. *Orasema coloradensis* and *O. sixaolae*), despite these specimens having a large difference in body size.

Key to species of the *Orasema hippocephala* species group

- 1) Head and mesosoma generally bright iridescent green (Fig. 2.31A); femora all pale yellow (Fig. 2.31A); notauli and scutoscutellar sulcus with small, shallow punctures (Fig. 2.31G) (widespread Neotropical) *Orasema hippocephala* **n. sp.**
- Head and mesosoma generally darker iridescent green (Fig. 2.30A); femora with a medial dark patch (Fig. 2.30A); notauli and scutoscutellar sulcus with larger, more irregular, deep punctures (Fig. 2.30F) (widespread Neotropical)
..... *Orasema chrysozona* **n. sp.**

***Orasema chrysozona* n. sp.**

(Fig. 2.30)

Diagnosis. Distinguished from *O. hippocephala* by having usually all femora (at least hind femur) darkly colored medially, notauli and scutoscutellar sulcus with wide, deep foveae, and head and mesosoma with darker and more variable green-blue iridescent coloration.

Description. Female. Length 2.3–4.2 mm (Fig. 2.30A). **Color.** Head and mesosoma dark iridescent blue-green, sometimes with some purple iridescence. Pedicel and anellus yellow. Coxae dark brown with iridescence; fore and mid femora brown becoming pale distally; hind femur mostly brown, tips pale. **Head** (Fig. 2.30B). HW:HH 0.8–1.1; IOD:EH 1–1.7; MS:EH 0.7–0.9; malar depression absent or impressed between mouth and eye margin; supraclypeal area smooth, becoming costate laterally. Palpal formula

3:3. Temples present, rounded. FL:HH 1.2–1.4; F2L:F2W 1.1–1.9, F2L:F3L 1.1–1.3 (Fig. 2.30D); clava subovate. **Mesosoma** (Fig. 2.30 C, F, G). ML:MH 1.6–2.2.

Mesoscutal midlobe transversely costate, densely setose. Axilla mostly smooth with weak sculpture near the margins; scutoscutellar sulcus broad, irregularly foveate; mesoscutellar disc as long as broad, rugose; frenal line as smooth band with a lighter color than the mesoscutellum and frenum; frenum areolate-reticulate; axillular sulcus indicated by a strong longitudinal carina. Callus areolate-reticulate. HCL:HCW 1.4–2; HFL:HF_W 3.6–5, with short dense setae on the dorsal side, longer and sparser setae on ventral side. FWL:FW_W 2.4–2.7, FWL:ML 1.7–2.2; postmarginal vein slightly longer than stimal vein. Hind wing costal cell with only 1 or 2 irregular rows of setae. **Metasoma**.

PTL:PTW 1.5–2.5, PTL:HCL 0.7–1.2, areolate. Ovipositor not visible.

Male. Length 2.1–2.7 mm. HW:HH 1–1.1; scape yellow becoming brown distally; flagellum with 7 funiculars, FL:HH 1.3–1.5; anellus disc-shaped; F2L:F2W 1.3–1.7 (Fig. 2.30E). Fore and mid femora mostly brown becoming yellow distally; hind femur mostly brown with iridescence; tibiae yellow. PTL:PTW 3.3–4.3, PTL:HCL 1.4–1.7.

Ant hosts. Unknown.

Plant hosts. Unknown.

Distribution (Fig. 2.29). Argentina: CB, CT, SA, SE, TM; Bolivia: SC; Brazil: AM, SP; Paraguay: AS, CR. Collected in January–March, June, December.

Material examined. Holotype: Argentina: Santiago del Estero: E de Lavalle, 28°10'54"S, 65°02'57"W, 20 Feb 2010, J. Torr ns, T10-001 [1♀, deposited in IFML: UCRCENT00436599]. **Paratypes: Argentina: Catamarca:** RN 38 near La Merced,

869m, 28°12'0"S, 65°38'24"W, 18.iii.2003, J. Munro, roadside scrub and acacia, sweep [1♀, UCRC: UCRCENT00169639]. **Cordoba:** El Sauce, 31°06'0"S, 64°18'36"W, i.1954, Viana [1♀, AMNH: UCRCENT00424197]. **Salta:** Tartagal, 6 km a Lag. del Cielo, 22°26'6"S, 63°41'38"W, 20.xii.2003, P. Fidalgo [1♀, UCRC: UCRCENT00169651]. **Santiago del Estero:** 5 km Lavalle, 28°10'54"S, 65°02'57"W, 20.ii.2010, J. Torrén, T10-002 [1♀, IFML: UCRCENT00436514]. **Tucumán:** Las Cejas, 26°53'1"S, 64°44'3"W, 1-21.i.1968, C.C. Porter [1♀, MCZ: UCRCENT00322659]. Rio Nio, 26°26'17"S, 64°58'3"W, 26.xii.2003, P. Fidalgo - J. Torrén [1♀, UCRC: UCRCENT00169577]. Tapia, 26°33'24"S, 65°17'41"W, 28.ii.2016, J. Torrén, T16001 [1♀, UCRC: UCRCENT00439176]. **Bolivia: Santa Cruz:** Santa Cruz, 17°47'6"S, 63°10'41"W, J. Steinbach [1♂, MCZ: UCRCENT00316412]. **Brazil: Amazonas:** Barcelos, Rio Araca, Boca Rio Curuduri, 35m, 0°05'50"N, 63°17'22"W, 19.vi.2010, J.A. Rafael; P. Dias; R. Machado [1♀, INPA: UCRCENT00504581]. **São Paulo:** S. Bocaina, 1680m, 22°08'24"S, 48°31'12"W, iii.1973 [2♀, CNC: UCRCENT00425821, UCRCENT00505444]. Sao Carlos, Canchin Farm, 608m, 21°10'22"S, 47°52'56"W, 4-6.i.1996, M. Sharkey [5♀, UCR: UCRCENT00091320–24]. Ribeirão Grande, Parque Estadual Intervalles, 24°16'23"S, 48°25'21"W, 21.i.2011, N.W. Perioto e eq., Malaise [1♀, INPA: UCRCENT00504576]; 20.xii.2010 [1♀, INPA: UCRCENT00504580]; 22.i.2010 [3♀, INPA: UCRCENT00504577–79]. **Paraguay: Asunción:** 50-130m, 25°16'56"S, 57°38'6"W, 15-18.i.1972 [3♂, CNC: UCRCENT00320985–87]. **Cordillera:** S. Bernardino, 25°16'12"S, 57°19'12"W, i, Fiebrig [1♂, NMW: UCRCENT00423312].

Etymology. From Greek *chrys* meaning “gold” and *zon* meaning “belt” in reference to the golden-colored frenal line.

Discussion. This species shows a large amount of morphological diversity, which may suggest the need for future splitting of more species. Our choice to designate a single species is largely based on the similarity in molecular sequence data between two sampled specimens referred to as DF2 (UCRCENT00436599) and DF3 (UCRCENT00169577) by Baker et al. (2020). These two specimens have a large difference in total body size (3.2 and 2.3 mm body length, respectively), but they have less sequence divergence than *O. coloradensis* or *O. sixaolae*, which are two well-sampled species.

***Orasema hippocephala* n. sp.**

(Fig. 2.31)

Diagnosis. Recognized from *Orasema chrysozona* by the combination of having all femora pale yellow, having the notauli and scutoscutellar sulcus with small, shallow punctures, and having a head and mesosoma consistently bright iridescent green.

Description. Female. Length 3.3–3.6 mm (Fig. 2.31A). **Color.** Head and mesosoma bright green. Pedicel and anellus brown. Fore coxa yellow, mid and hind coxae iridescent green; femora yellow. **Head** (Fig. 2.31B–D). HW:HH 0.8–1; IOD:EH 1–1.2; MS:EH 0.5–0.7; malar depression absent; supraclypeal area smooth. Palpal formula 3:2. Temples present, angulate. FL:HH 0.9–1.1; F2L:F2W 1.4–2, F2L:F3L 1.4; clava subconical (Fig.

2.31F). **Mesosoma** (Fig. 2.31 E, G, H). ML:MH 1.7–2.1. Mesoscutal midlobe costate, sparsely setose. Axilla smooth; scutoscutellar sulcus narrow, regularly foveate; mesoscutellar disc slightly longer than broad, weakly costate-reticulate; frenal line irregularly foveate; smooth with scattered shallow depressions; axillular sulcus distinct and foveate. Callus areolate. HCL:HCW 1.6–2.1; HFL:HFW 4–4.8, with moderate cover of short setae. FWL:FWW 2.3–2.6, FWL:ML 1.8–2.1; postmarginal vein several times longer than stigmal vein. Hind wing costal cell with a broad bare area. **Metasoma**. PTL:PTW 2–2.7, PTL:HCL 0.9–1.2, rugose-reticulate. Ovipositor with subapical carina present; first (ventral) valvula with 6–8 small, narrowly separated teeth, second (dorsal) valvula with 8–10 annuli that are broadly separated dorsally, carinae coalescing.

Male. Unknown.

Ant hosts. Unknown.

Plant hosts. Unknown.

Distribution (Fig. 2.29). Argentina: CN, LR, SF, TM; Brazil: BA; Uruguay: CO.

Collected in January–April.

Material Examined. Holotype: Argentina: Tucumán: Las Tipas (Trancas), 1169m, 26°38'9"S, 65°24'58"W, 2-6 Jan 2009, E. Viria, malaise trap [1♀, deposited in UCRC: UCRCENT00434580]. **Paratypes: Argentina: Corrientes:** Hwy. 12, Arroyo Carumbe, 29°30'18"S, 57°52'48"W, 15.i.1989, C.W. & L.B. O'Brien & G. Wibmer [1♀, CASC: UCRCENT00417408]. **La Rioja:** Santa Cruz, 1637m, 28°40'45"S, 66°57'52"W, 15-31.iv.2007, C. Porter & P. Fidalgo, decid. for., malaise trap, H07-049 [1♀, UCRC: UCRCENT00161481]; Sta. V. Cruz, 28°35'8"S, 66°37'50"W, 15-31.iii.2003, D. Peralta,

MT [1♀, IFML: UCRCENT00436715]; 15.i.2007 [1♀, IFML: UCRCENT00436709];
28.ii.2007 [5♀, IFML: UCRCENT00436703–05, MACN: UCRCENT00436896–97];
31.i.2007 [6♀, IFML: UCRCENT00436707–08, MACN: UCRCENT00436899–900,
UCRC: UCRCENT00169650, UCRCENT00169656]. **Santa Fe:** 8 km. N Recreo, 24m,
31°25'2"S, 60°44'42"W, 31.i.1989, C.W. & L.B. O'Brien & G. Wibmer [1♀, CASC:
UCRCENT00417427]. **Brazil: Bahia:** Chapada, 1347m, *12°52'46"S, 41°24'13"W*, iv
[2♀, USNM: UCRCENT00247814, UCRCENT00416666]. **Tucumán:** btw Choromoto
& Higuera, 900m, *26°22'48"S, 65°22'12"W*, 9.i.1996, M.J. Sharkey [2♀, CNC:
UCRCENT00505442–43]. **Uruguay: Colonia:** 1 km. E. R.21, km. 184, *33°58'52"S,*
58°16'52"W, 9.ii.1989, C.W. & L. O'Brien & G. Wibmer [6♀, CASC:
UCRCENT00417415, UCRCENT00417417–21].

Etymology. From Greek *hipp* meaning “horse” and *cephal* meaning “head” in
reference to its elongated head.

***Orasema johnsoni* species group**

(Figs 2.32–2.34)

Diagnosis. Recognized by the following combination of characters: smooth but setose
head and mesosoma, strongly setose eyes, generally 8-segmented funicle (several
antennal mutations in specimens), and occiput typically emarginate in dorsal view, but
not strongly emarginate as in the *Orasema hippocephala* group.

Description. Female. Length 2.1–3.3 mm. **Color.** Head and mesosoma dark with green, blue, and purple iridescence. Pedicel, anellus, mandible, maxilla, and labium brown. Femora brown; tibiae yellow. Wing venation pale brown. Gaster brown with iridescence. **Head.** Head in frontal view subtriangular; scrobal depression shallow, laterally rounded, smooth; supraclypeal area slightly broader than long, smooth; clypeus smooth; epistomal sulcus vaguely defined; anterior tentorial pit strongly impressed; anteclypeus distinct, straight. Labrum with 4 digits. Palpal formula 3:2. Occiput imbricate, emarginate in dorsal view, dorsal margin abrupt. Scape not reaching median ocellus. Pedicle globose. Clava subovate. **Mesosoma.** Mesoscutal midlobe densely setose; lateral lobe smooth. Axilla smooth, dorsally rounded, on roughly same plane as mesoscutellum; scutoscutellar sulcus irregularly foveate, broadly separated from transscutal articulation; mesoscutellar disc as long as broad, smooth; frenum and axilla smooth. Propodeal disc areolate, with irregular median carina; callus mostly smooth with minute impressions, densely setose. Propleuron convex, smooth. Postpectal carina weak. Upper and lower mesepimeron smooth; transepimeral sulcus distinct. Metepisternum laterally smooth. Hind coxa smooth; hind femur with even cover of short, dense setae. Fore wing with marginal fringe relatively long; submarginal vein with several long setae; marginal vein with minute setae; stigmal vein slightly longer than broad, slightly angled toward wing apex; postmarginal vein longer than stigmal vein. **Metasoma.** Petiole cylindrical, linear in profile, areolate, ventral sulcus present with margins widely separated. Apical setae of hypopygium with several long hairs on each side of midline. Ovipositor with subapical carina present; first (ventral) valvula without teeth, second

(dorsal) valvula with 8–10 annuli that are narrowly separated dorsally, carinae coalescing.

Male. Unknown.

Phylogenetics. There is no molecular data for this species group. Having 8 funicular segments suggests that they may belong within the *xanthopus-festiva-lasallei-stramineipes* clade, which contains almost all 8-funicular taxa (with the exception of the *wayqecha* and *tolteca* groups). Alternatively, the general body shape and hairiness suggests that they may be within the *coloradensis-sixaolae-monstrosa* clade (Fig. 2.1).

Key to species of the *Orasema johnsoni* species group

- 1) Valvifer rounded (Fig. 2.33E); mesoscutal midlobe with weak costate sculpture (Fig. 2.33F); frenal line weak but complete (Fig. 33F) (Brazil and Uruguay)
..... *Orasema johnsoni* **n. sp.**
- Valvifer digitate (Fig. 2.34E); mesoscutal midlobe completely smooth (Fig. 2.34F); frenal line absent or incomplete medially (Fig. 2.34F) (Brazil)
..... *Orasema spyrogaster* **n. sp.**

***Orasema johnsoni* n. sp.**

(Fig. 2.33)

Diagnosis. Recognized from *O. spyrogaster* by having the valvifer rounded (Fig. 2.33E), mesoscutal midlobe with weak costate sculpture, and frenal line complete.

Description. Female. Length 2.1–2.9 mm (Fig. 2.33A). **Color.** Scape pale brown; flagellum brown. Fore coxa brown proximally, yellow distally; Mid and hind coxae brown with iridescence. **Head** (Fig. 2.33B). HW:HH 1.2–1.3; face smooth to lightly coriaceous; longitudinal groove between eye and torulus present, small; eyes densely setose, IOD:EH 1.5–1.7; MS:EH 0.6–0.8; malar depression weakly impressed between mouth and eye margin. Mandibular formula not observed. Temples present, rounded. Flagellum with 7–8 funiculars (first and second funicular partially fused on lateral side of one antenna for one specimen; second and third partially fused medially on both antennae of second specimen), FL:HH 1.3–1.5; anellus stout, about twice as broad as long; F2L:F2W 1.6–2, F2L:F3L 0.6–1.3; following funiculars subequal in length, equal in width (Fig. 2.33D). **Mesosoma** (Fig. 2.33 C, F). ML:MH 1.5–1.7. Mesoscutal midlobe transversely costate; notauli deep. Scutoscutellar sulcus broad; frenal line present as a shallow impression; axillular sulcus distinct and foveate. Propodeal disc flat (Fig. 2.33G). Prepectus weakly rugose to smooth. Mesepisternum weakly rugose laterally, smooth ventrally, broadly rounded anterior to mid coxa. HCL:HCW 1.6–1.9; HFL:HFW 4.3–5. FWL:FWW 2.5–2.7, FWL:ML 2–2.2; basal area bare; speculum, costal cell, and wing disc densely setose. Hind wing costal cell with only 1 or 2 irregular rows of setae.

Metasoma: PTL:PTW 1.6–2, PTL:HCL 0.9–1, lateral margin with longitudinal carina continuous with basal flange. Antecostal sulcus foveate; acrosternite posteriorly angulate.

Male. Unknown.

Ant hosts. Unknown.

Plant hosts. Unknown.

Distribution (Fig. 2.32). Argentina: BA; Brazil: SP; Uruguay: TA. Collected in February, November.

Material examined. Holotype: Uruguay: Tacuarembó: 40 km NW Tacuarembó, 200-300m, $31^{\circ}29'45''S$, $56^{\circ}18'8''W$, 2-9.ii.1963, J.K. Bouseman [1♀, deposited in AMNH: UCRCENT00238022]. **Paratype: Argentina: Buenos Aires:** San Isidro, $34^{\circ}28'15''S$, $58^{\circ}31'43''W$, iv.1958, J. Daguerra [1♀, USNM: UCRCENT00248388].

Brazil: São Paulo: Anhembi, 455m, $22^{\circ}42'6''S$, $48^{\circ}10'9''W$, 12.xi.2012, E.N.L. Ferreira, Malaise [1♀, DEFS: UCRCENT00439199].

Etymology. Named in honor of James (Ding) Johnson, entomologist and *Orasema* collector.

***Orasema spyrogaster* n. sp.**

(Fig. 2.34)

Diagnosis. Recognized from *Orasema johnsoni* by having the valvifer digitate (Fig. 2.34E), mesoscutal midlobe completely smooth, and a frenal line that is absent or incomplete medially.

Description. Female. Length 2.5–3.3 mm (Fig. 2.34A). **Color.** Scape brown; flagellum dark brown. Coxae brown with iridescence. **Head** (Fig. 2.34B). HW:HH 1.2–1.3; face smooth; eyes covered in long, erect setae, IOD:EH 1.3–1.4; MS:EH 0.6–0.7; malar depression absent. Mandibular formula 3:2. Temples present, angulate. Flagellum with 8 funiculars, FL:HH 1.6–1.7; anellus disc-shaped; F2L:F2W 2.3–2.6, F2L:F3L 1.3–1.4; following funiculars subequal in length, gradually broader (Fig. 2.34D). **Mesosoma** (Fig. 2.34 C, F). ML:MH 1.5–1.8. Mesoscutal midlobe smooth; notauli shallow. Scutoscutellar sulcus narrow; frenal line indistinct; axillular sulcus indicated by a strong longitudinal carina. Propodeal disc broadly rounded (Fig. 2.34G). Prepectus smooth. Mesepisternum weakly areolate laterally, smooth ventrally, nearly straight anterior to mid coxa. HCL:HCW 1.9–2; HFL:HFW 4.5–4.6. FWL:FWW 2.5–2.6, FWL:ML 2.1–2.2; entirely densely setose. Hind wing costal cell entirely setose. **Metasoma.** PTL:PTW 1.6–1.8, PTL:HCL 0.8–1, lateral margin rounded. Antecostal sulcus foveate to smooth posteriorly; acrosternite posteriorly rounded.

Male. Unknown.

Ant hosts. Unknown.

Plant hosts. Unknown.

Distribution (Fig. 2.32). Brazil: PA, RR. Collected in April, December.

Material examined. Holotype: Brazil: Roraima: Amajari, Serra do Tepequem, $3^{\circ}44'24''N$, $61^{\circ}45'0''W$, 1-15.iv.2016, Rafael et al., Malaise [1♀, deposited in INPA: UCRCENT00504573]. **Paratype: Brazil: Pará:** Utinga, Belem, $1^{\circ}25'12''S$, $48^{\circ}26'24''W$, xii.1966, S.J. Oliveira [1♀, AEIC: UCRCENT00251376].

Etymology. From Greek *spyr* meaning “basket” and *gaster* meaning “stomach” in reference to the odd basket-like structure of the valvifer.

Discussion. The valvifer is invariable in all other species of *Orasema* and is apically rounded with long thin setae covering the surface (Fig. 2.33E). The valvifer of *Orasema spyrogaster* has a unique morphology with thick cuticular projections (or digits) at the apex giving it a comb-like appearance as well as the long thin setae covering the surface (Fig. 2.34E).

***Orasema heacoxi* species group**

(Figs 2.35–2.37)

Diagnosis. Recognized by the following combination of characters: flagellum with 7 funiculars, labrum with 4 digits, basal third of fore wing bare, face reticulate, postpectal carina absent, propodeum areolate-reticulate, and petiole rugose-reticulate. This group is most similar to the *cockerelli* and *bakeri* species groups. It can be distinguished from the *cockerelli* group by having rugose-reticulate sculpture on the mesoscutal midlobe or, if reticulate, having an elongate face and semicircular frenum when viewed dorsally. It can be distinguished from the *bakeri* group by having a distinct anterior carina present on the prepectus.

Description. Female. Length 1.7–2.2 mm. **Color.** Head and mesosoma iridescent blue-green. Pedicel and anellus brown; flagellum dark brown. Maxilla and labium brown. Coxae brown with strong blue-green iridescence; tibiae yellow. Wing venation pale

brown. **Head.** Face reticulate; scrobal depression shallow, laterally rounded, with transverse striae; eyes bare; supraclypeal area longer than broad, weakly reticulate; clypeus weakly reticulate; anterior tentorial pit strongly impressed; anteclypeus distinct, broadly rounded. Labrum with 4 digits. Mandibular formula 3:2, palpal formula 3:2. Occiput imbricate-reticulate, dorsal margin evenly rounded; temples present, rounded. Scape not reaching median ocellus. Flagellum with 7 funiculars; anellus disc-shaped; following funiculars subequal in length, gradually broader; clava subconical. **Mesosoma.** Mesoscutal midlobe sparsely setose; lateral lobe reticulate; notauli deep. Axilla reticulate, dorsally rounded, on roughly the same plane as mesoscutellum; scutoscutellar sulcus regularly foveate; mesoscutellar disc slightly longer than broad, reticulate; frenal line indistinct; axillular sulcus weak and foveate. Propodeal disc broadly rounded, without depression or carina, areolate-reticulate; callus weakly reticulate, bare; callar nib absent. Propleuron convex, reticulate. Prepectus weakly reticulate. Mesepisternum straight anterior to mid coxa; postpectal carina absent. Hind femur sparsely setose. Fore wing with basal third of wing bare, costal cell sparsely setose, wing disc setose; marginal fringe relatively long; submarginal vein with small setae; marginal vein pilose; stigmal vein slightly longer than broad, slightly angled toward wing apex; postmarginal vein shorter than stigmal vein. Hind wing costal cell with a broad bare area. **Metasoma.** Petiole cylindrical, linear in profile, rugose-reticulate. Antecostal sulcus foveate; acrosternite posteriorly rounded. Ovipositor with subapical carina present; first (ventral) valvula with 10–11 small, closely spaced teeth, second (dorsal) valvula with 8–10 annuli that are broadly separated dorsally by smooth area.

Male. Length 1.8–2.1 mm. Flagellum with 7 funiculars; anellus disc-shaped. Femora mostly brown with iridescence, tips pale.

Phylogenetics. Both species are represented in the phylogenetic analyses of Baker et al. (2020). *Orasema heacoxi* (referred to as “*Orasema_nsp_USA:TX_D4107*”) and *O. masonicki* (referred to as “*Orasema_sp_CRI_D4887*”) are sister species in every analysis except the analyses only using Sanger sequencing data, which resulted in a very poorly resolved *cockerelli* group (parsimony) or split *O. masonicki* away from the *cockerelli* group (ML and BEAST). In analyses with AHE sequencing data, the sister relationship is supported with 99–100 bootstrap scores. This group was treated as part of a more inclusive *cockerelli* group by Baker et al. (2020), but we split it into its own group because the two species are fairly distinct compared to other Nearctic *cockerelli* group species, which themselves form a well-supported clade. The split between *O. heacoxi* and *O. masonicki* is estimated to have occurred 5–17 MYA; the split between the *heacoxi* group and *cockerelli* group is estimated to have occurred 10–20 MYA.

Key to species of the *Orasema heacoxi* species group

- 1) Face subtriangular to subcircular (Fig. 2.36B); mesoscutal midlobe, axilla, and mesoscutellar disc rugose-reticulate (Fig. 2.36F); petiole relatively short (PTL:PTW 1–2.1 female; 3.8–5.5 male); male antennal flagellomeres pedunculate with semi-erect, curved setae (Fig. 2.36E) (Texas) *Orasema heacoxi* **n. sp.**

- Face elongate (Fig. 2.37B); mesoscutal midlobe, axilla, and mesoscutellar disc reticulate (Fig. 2.37F); petiole relatively long (PTL:PTW 2.5–3.4 female; 5.5–7.5 male); male antennal flagellomeres closely spaced with straight, closely-appressed setae (Fig. 2.37E) (Costa Rica) *Orasema masonicki* **n. sp.**

***Orasema heacoxi* n. sp.**

(Fig. 2.36)

Diagnosis. Distinguished from *O. masonicki* by having the face subtriangular to subcircular but never elongate; the mesoscutal midlobe, axilla, and mesoscutellar disc rugose-reticulate; the petiole (male and female) shorter/wider; and the male antennal flagellomeres pedunculate with semi-erect, curved setae.

Description. Female. Length 1.7–2.2 mm (Fig. 2.36A). **Color.** Scape yellow to brown. Mandible yellowish brown. Femora brown with iridescence, tips pale. Gaster dark brown with iridescence. **Head** (Fig. 2.36B). Head in frontal view subtriangular; HW:HH 1–1.3; longitudinal groove between eye and torulus shallowly depressed; IOD:EH 1.2–1.5; MS:EH 0.5–0.8; malar depression weakly impressed between mouth and eye margin; epistomal sulcus vaguely defined. Occiput shallowly emarginate in dorsal view. Pedicel globose, broader than F1. FL:HH 0.8–1; F2L:F2W 1–1.8, F2L:F3L 0.8–1.5 (Fig. 2.36D). **Mesosoma** (Fig. 2.36 C, F, G). ML:MH 1.3–1.7. Mesoscutal midlobe rugose-reticulate. Scutoscuteellar sulcus narrow, broadly separated from transscutal articulation; frenum rugose-reticulate; axillula weakly reticulate. Mesepisternum reticulate laterally with

anterior smooth patch, smooth ventrally. Upper mesepimeron smooth; lower mesepimeron weakly reticulate; transepimeral sulcus distinct. Metepisternum laterally smooth. HCL:HCW 1.5–2.1, reticulate dorsally, becoming smooth ventrally; HFL:HFW 4.4–6.4. FWL:FWW 2.1–2.4, FWL:ML 1.8–2.2. **Metasoma.** PTL:PTW 1–2.1, PTL:HCL 0.8–1.1, lateral margin with longitudinal carina continuous with basal flange, ventral sulcus present with margins broadly separated. Apical setae of hypopygium with one pair of setae much longer than the others.

Male. Length 1.8–2.1 mm. HW:HH 1–1.1; scape dark brown; FL:HH 1.2–1.3, F2L:F2W 1.2–1.3 (Fig. 2.36E). Fore and mid tibiae yellow, hind tibia mostly yellow with medial brown patch. PTL:PTW 3.8–5.5, PTL:HCL 1.5–1.6.

Ant hosts. Unknown.

Plant hosts. Collected on *Salvia farinacea* Benth. (Lamiaceae).

Distribution (Fig. 2.35). United States: TX. Collected in June.

Material examined. Holotype: USA: TX: Kerr Co., Kerrville-Schreiner Pk, 30°00'7"N, 99°07'34"W, 20.vi.2015, A. Baker & P. Masonick, sweep sage, AB15.014A [1♀, deposited in UCRC: UCRCENT00414529]. **Paratypes: TX:** Kerr Co., Kerrville-Schreiner Park, 30°00'7"N, 99°07'34"W, 22.vi.2015, A. Baker & P. Masonick, sweep mesquite, AB15.017B [9♀, UCRC: UCRCENT00439287–95]; AB15.020B [1♀, UCRC: UCRCENT00439296]; sweep sage, AB15.017A [3♀, UCRC: UCRCENT00439274, UCRCENT00439280–81]; 20.vi.2015, AB15.014B [2♀, UCRC: UCRCENT00414530, UCRCENT00439286]; AB15.014A [1♂ 3♀, UCRC: UCRCENT00439275–78]; 22.vi.2015, AB15.020A [4♀, UCRC: UCRCENT00439282–85]; 494m, 30°00'14"N,

99°07'27"W, 29.vi.2014, S. Heacox & A. Baker, sweep sage, SH 20-14 [2♂ 3♀, UCRC: UCRCENT00436485, UCRCENT00498721–22, UCRCENT00498725, UCRCENT00498730]; 28.vi.2014, AB14.040 [1♀ 1?, UCRC: UCRCENT00498723, UCRCENT00498728]; 529m, 30°00'9"N, 99°07'34"W, AB14.038 [2♀, UCRC: UCRCENT00436483, UCRCENT00498724]; 29.vi.2014, SH 21-14 [4♀, UCRC: UCRCENT00498726–27, UCRCENT00498729, UCRCENT00498731]. Kerrville, 30°02'51"N, 99°08'25"W, 20.vi.1996, W.F. Chamberlain [1♂, TAMU: UCRCENT00426496].

Etymology. Named in honor of Scott Heacox, who assisted collecting some of the first specimens of this species and has been a valuable contributor to eucharitid research at UCR.

***Orasema masonicki* n. sp.**

(Fig. 2.37)

Diagnosis. Distinguished from *O. heacoxi* by having the face elongate; the mesoscutal midlobe, axillae, and mesoscutellar disc reticulate; the petiole (male and female) longer/thinner; and the male antennal flagellomeres more closely spaced with straight, closely-appressed setae.

Description. Female. Length 1.9–2.2 mm (Fig. 2.37A). **Color.** Scape brown. Mandible brown. Femora brown with strong iridescence. Gaster dark brown with strong blue-green iridescence. **Head** (Fig. 2.37B). Head in frontal view elongate; HW:HH 0.7–

1; longitudinal groove between eye and torulus absent; IOD:EH 1–1.1; MS:EH 0.3–0.6; malar depression weakly impressed adjacent to mouth; epistomal sulcus distinct and sharply defined. Occiput deeply emarginate in dorsal view. Pedicel small and globose. FL:HH 0.6–0.9; F2L:F2W 1–1.5, F2L:F3L 1 (Fig. 2.37D). **Mesosoma** (Fig. 2.37 C, F, G). ML:MH 1.4–1.6. Mesoscutal midlobe reticulate. Scutoscutellar sulcus broad, narrowly separated from transscutal articulation; frenum reticulate; axillula reticulate. Mesepisternum reticulate laterally, weakly reticulate ventrally. Upper mesepimeron weakly reticulate; lower mesepimeron reticulate; transepimeral sulcus weakly impressed. Metepisternum laterally reticulate. HCL:HCW 1.2–1.8, reticulate; HFL:HFW 4.6–6.3. FWL:FWW 2.2–3.9, FWL:ML 1.9–2.4. **Metasoma**. PTL:PTW 2.5–3.4, PTL:HCL 1.1–1.7, lateral margin rounded, ventral sulcus present with margins narrowly separated. Apical setae of hypopygium with several setae on each side of midline.

Male. Length 2–2.1 mm. HW:HH 0.9–1.1. Scape brown; FL:HH 0.9–1.2; F2L:F2W 0.8–1.4 (Fig. 2.37E). Tibiae yellow. PTL:PTW 5.5–7.5, PTL:HCL 2.2–3.3.

Ant hosts. Unknown.

Plant hosts. Unknown.

Distribution (Fig. 2.35). Costa Rica: AL, GU, HE. Collected January–May.

Material examined. Holotype: Costa Rica: Guanacaste: Est. Pitilla, 9 km S Santa Cecilia, P.N. Guanacaste, 700m, 10°59'28"N, 85°25'39"W, iii.1995, P. Rios, #4359 [1♀, deposited in INBIO: INBIOCRI02242095]. **Paratypes: Costa Rica: Alajuela:** Sect. San Ramon de Dos Rios, 620m, 10°52'54"N, 85°24'41"W, 16.i-3.ii.1995, F.A. Quesada, #4400 [1♂, INBIO: INBIOCRI02192938]; 20.ii-5.iii.1995, #4401 [4♂ 1?, INBIO:

INBIOCRI02138790, INBIOCRI02138802, INBIOCRI02138811, INBIOCRI02138832, INBIOCRI02138835]; C. Cano, #4396 [15♂ 4♀, INBIO: INBIOCRI02133093, INBIOCRI02133101–02, INBIOCRI02133144, INBIOCRI02133155–56, INBIOCRI02133159, INBIOCRI02133164–66, INBIOCRI02133183, INBIOCRI02133195, INBIOCRI02133204, INBIOCRI02133209, INBIOCRI02133213–15, INBIOCRI02133225, INBIOCRI02133227]; 20.ii-3.iii.1995, #4398 [10♂ 8♀, INBIO: INBIOCRI02174676–77, INBIOCRI02174679–80, INBIOCRI02174682, INBIOCRI02174686–87, INBIOCRI02174691, INBIOCRI02174714, INBIOCRI02174730, INBIOCRI02174755, INBIOCRI02174760, INBIOCRI02174776, INBIOCRI02174783, INBIOCRI02174787–88, INBIOCRI02174793, INBIOCRI02174800]; 11-15.iv.1994, C. Moraga, #2840 [1♂, INBIO: INBIOCRI01780190]; 13-28.iii.1994, K. Taylor, #2763 [4♂ 1♀, INBIO: INBIOCRI01712287, INBIOCRI01712554, INBIOCRI01712730, INBIOCRI01712733, INBIOCRI01760375]. **Guanacaste:** Est. Pitilla, 9 km S Santa Cecilia, P.N. Guanacaste, 700m, 10°59'28"N, 85°25'39"W, 2-19.iii.1992, P. Rios [1♀, INBIO: INBIOCRI00420518]. Sector Las Pailas, 800m, 10°46'31"N, 85°20'59"W, 12.iv-3.v.1995, K. Taylor, #4810 [2♂ 1♀, INBIO: INBIOCRI02425608, INBIOCRI02425621, INBIOCRI02425633]; 16-30.iii.1995, #4811 [8♂, INBIO: INBIOCRI02403459, INBIOCRI02403595, INBIOCRI02403602–03, INBIOCRI02403778, INBIOCRI02403840, INBIOCRI02403851, INBIOCRI02403878]. **Heredia:** Send. Terciopelo, Est. Magsaysay, P.N. Braulio Carrillo, 220m, 10°24'2"N, 84°02'53"W, 1991, malaise trap [1♂, INBIO: INBIOCRI01194079].

Etymology. Named in honor of Paul Masonick, an entomologist who has helped to collect specimens of *Orasema* including specimens in the *heacoxi* group.

Unplaced *Orasema* species

(Figs 2.38–2.44)

Discussion. Several species could not be confidently placed to species groups, especially those lacking molecular phylogenetic data. Placing these taxa into species groups described herein would make the species group key more difficult to use, so we prefer to treat them as unplaced until more data can be collected.

***Orasema brasiliensis* (Bréthes)**

urn:lsid:zoobank.org:pub:709CAB4E-6CDF-4EB2-B9A8-BA2A98AD0388

(Fig. 2.39)

Eucharomorpha (?) *brasiliensis* (Bréthes) 1927: 331–332.

Orasema brasiliensis; Heraty 2002: 50. Change of combination.

Diagnosis. Recognized from other *Orasema* by the following combination of characters: antenna with 7 funicular segments; labrum with 4 digits; eyes bare; femora entirely yellow, or at most with small light brown spot medially; face, mesoscutum, and mesoscutellum rugose-reticulate; supraclypeal area wider than long; femora relatively short and wide (female HFL:HFW 4.1–4.6).

Description. Female. Length 3.9–4.3 mm (Fig. 2.39A). **Color.** Head and mesosoma dark green. Scape brown; pedicel yellow; anellus pale brown; flagellum dark brown. Mandible brown; maxilla and labium pale brown. Coxae brown with green iridescence; femora and tibiae yellow. Fore wing hyaline; venation pale brown. Petiole same as mesosoma; gaster dark brown with iridescence. **Head** (Fig. 2.39B). Head in frontal view subtriangular; HW:HH 1.1–1.2; face rugose-reticulate; scrobal depression shallow, laterally rounded, with transverse striae; longitudinal groove between eye and torulus absent; eyes bare, IOD:EH 1.7–1.9; MS:EH 1–1.1; malar depression weakly impressed adjacent to mouth; supraclypeal area broader than long, weakly sculptured; clypeus weakly sculptured; epistomal sulcus distinct and sharply defined; anterior tentorial pit shallow; anteclypeus distinct, broadly rounded. Labrum with 4 digits. Mandibular formula 3:2; palpal formula 3:3. Occiput imbricate, shallowly emarginate in dorsal view, dorsal margin evenly rounded; temples absent. Scape not reaching median ocellus. Pedicle small and globose. Flagellum with 7 funiculars; FL:HH 1.3–1.4; anellus disc-shaped; F2L:F2W 2.2–2.5, F2L:F3L 1.5–1.7; following funiculars subequal in length, equal in width; clava subcylindrical (Fig. 2.39D). **Mesosoma** (Fig. 2.39 C, F). ML:MH 1.4–1.6. Mesoscutal midlobe rugose-reticulate, sparsely setose; lateral lobe rugose-reticulate; notauli deep. Axilla rugose-reticulate, dorsally rounded, on roughly the same plane as mesoscutellum; scutoscutellar sulcus broad, irregularly foveate, narrowly separated from transscutal articulation; mesoscutellar disc slightly longer than broad, rugose-areolate; frenal line indistinct dorsally with smooth carinae laterally; frenum rugose-reticulate; axillular sulcus indicated by a strong longitudinal carina; axillula

rugose-reticulate. Propodeal disc flat, without depression or carina, areolate (Fig. 2.39G); callus reticulate to smooth, with several long setae. Propleuron convex, weakly reticulate. Prepectus triangular dorsally, weakly narrowed ventrally, rugose-reticulate. Mesepisternum reticulate laterally, smooth ventrally, broadly rounded anterior to mid coxa; postpectal carina weak. Upper and lower mesepimeron reticulate. Metepisternum laterally reticulate. HCL:HCW 1.6–1.8, reticulate dorsally becoming smooth ventrally; HFL:HFW 4.1–4.6, with even cover of short, dense setae. FWL:FWW 2.4–2.7, FWL:ML 1.8–2; basal area and speculum bare, costal cell and wing disc densely setose; marginal fringe relatively long; submarginal vein with small setae; marginal vein setose; stigmal vein about twice as long as broad, perpendicular to anterior wing margin; postmarginal vein several times longer than stigmal vein. Hind wing costal cell sparsely setose.

Metasoma. Petiole cylindrical, linear in profile, PTL:PTW 1.6–2.5, PTL:HCL 0.8–1, rugose-reticulate, lateral margin with incomplete longitudinal carina, ventral sulcus absent. Antecostal sulcus foveate; acrosternite posteriorly rounded; apical setae of hypopygium with one pair of setae much longer than the others. Ovipositor with subapical carina present; first (ventral) valvula with 6–8 small, narrowly separated teeth, second (dorsal) valvula with 8–10 annuli that are narrowly separated dorsally, carinae coalescing.

Male. Length 2.5–3.2 mm. HW:HH 1–1.2. Scape yellow-brown; flagellum with 7 funiculars, FL:HH 1.5–1.6; anellus disc-shaped; F2L:F2W 1.8–2.2 (Fig. 2.39E). Femora mostly brown, tips pale; tibiae yellow. PTL:PTW 3.3–4.9, PTL:HCL 1.3–1.7.

Ant hosts. Unknown.

Plant hosts. Unknown.

Distribution (Fig. 2.38). Argentina: TM; Brazil: SP. Collected in January, October–December.

Material examined. Syntype: Brazil: São Paulo: São Paulo, 23°34'S, 46°38'W, 5.xi.1922, Melzer [1♀, deposited in SDEI: UCRCENT00439039]. **Additional material examined: Brazil: São Paulo:** São Paulo, 800m, 23°38'20"S, 46°36'58"W, 22.xii.1965, V.N. Alin [1♀, UCDC: UCRCENT00416052]; 12.i.1964 [2♂, AMNH: UCRCENT00238117–18]; 16.x.1965 [1♀, USNM: UCRCENT00248491].

Discussion. This species may be closely-related to *O. roppai* based on similar sculpture and size, however it differs in having 7 antennal funiculars (8 funiculars in *O. roppai*), bare eyes, and a wider supraclypeal area. We decided not to treat these two species as the same species group because the difference in funicular segments is not known to occur in other groups except the *xanthopus* species group.

***Orasema cirrhocnemis* n. sp.**

(Fig. 2.40)

Diagnosis. Recognized from other *Orasema* by the following combination of characters: antenna with 8 funiculars; labrum with 4–6 digits; legs beyond coxae entirely tawny-orange colored except for a small dark patch on the posterior fore and mid femora; mid and hind tibiae broadened apically (nearly as broad as femora) (Fig. 2.40E); mesoscutal

midlobe and mesoscutellum rugose-reticulate; malar depression strongly impressed between eye and mouth.

Description. Female. Length 3.7 mm (Fig. 2.40A). **Color.** Head and mesosoma iridescent blue-green. Scape, pedicel, and anellus brown; flagellum dark brown. Mandible dark brown; maxilla and labium brown. Coxae iridescent blue-green-purple; fore and mid femur mostly orange with iridescent brown patches laterally; hind femur and tibiae orange. Fore wing hyaline; venation pale brown to clear. Petiole same as mesosoma; gaster dark brown with iridescence. **Head** (Fig. 2.40B). Head in frontal view subtriangular; HW:HH 1.1–1.2; face reticulate; scrobal depression shallow, laterally rounded, with transverse striae; longitudinal groove between eye and torulus absent; eyes sparsely setose, IOD:EH 1.6–1.8; MS:EH 0.8–0.9; malar depression impressed between mouth and eye margin; supraclypeal area about as long as broad, shorter than clypeus, weakly reticulate to smooth; clypeus smooth; epistomal sulcus vaguely defined; anterior tentorial pit strongly impressed; anteclypeus distinct, straight. Labrum with 4–6 digits. Mandibular formula not observed; palpal formula 3:3. Occiput imbricate, shallowly emarginate in dorsal view, dorsal margin evenly rounded; temples present, rounded. Scape not reaching median ocellus. Pedicel small and globose. Flagellum with 8 funiculars; FL:HH 1–1.2; anellus disc-shaped; F2L:F2W 1.3–1.7, F2L:F3L 0.8–0.9; following funiculars subequal in width, successively shorter; clava subovate (Fig. 2.40D). **Mesosoma** (Fig. 2.40 C, F). ML:MH 1.1–1.2. Mesoscutal midlobe costate anteriorly, rugose-reticulate posteriorly, sparsely setose; lateral lobe reticulate dorsally, rugose laterally; notauli deep. Axilla reticulate, dorsally flat, on same plane as mesoscutellum;

scutoscutellar sulcus broad, irregularly foveate, narrowly separated from transscutal articulation; mesoscutellar disc as long as broad, rugose-reticulate; frenal line foveate; frenum areolate; axillular sulcus indicated by a weak longitudinal carina; axillula areolate-reticulate. Propodeal disc flat, areolate-reticulate, without medial depression or carina (Fig. 2.40G); callus areolate-reticulate, with a few small setae. Propleuron convex, reticulate. Prepectus triangular dorsally, strongly narrowed ventrally, rugose-reticulate. Mesepisternum rugose-reticulate, strigate-areolate posteriorly, broadly rounded anterior to mid coxa; postpectal carina weak. Upper and lower mesepimeron rugose-reticulate; transepimeral sulcus distinct. Metepisternum laterally weakly reticulate. HCL:HCW 1.2–1.8, reticulate dorsally, smooth ventrally; HFL:HFW 4.7–5, with even cover of short, dense setae. FWL:FWW 2.6, FWL:ML 1.8–2.2; entirely setose; marginal fringe relatively long; submarginal vein and marginal vein with minute setae; stigmal vein about as long as broad, slightly angled toward wing apex; postmarginal vein as long as stigmal vein. Hind wing costal cell sparsely setose. **Metasoma.** Petiole cylindrical, linear in profile, PTL:PTW 1.2–1.3, PTL:HCL 0.9–1.2, areolate-reticulate, lateral margin with longitudinal carina continuous with basal flange, ventral sulcus present, margins narrowly spaced. Antecostal sulcus foveate; acrosternite posteriorly angulate; apical setae of hypopygium with several pairs of setae on either side of the midline. Ovipositor not visible.

Male. Unknown.

Ant hosts. Unknown.

Plant hosts. Unknown.

Distribution (Fig. 2.38). Uruguay: CO. Collected in February (2 specimens).

Material examined. Holotype: Uruguay: Colonia Department: R. 2, km. 194, Arroyo S. Pedro, $32^{\circ}52'51''S$, $57^{\circ}58'20''W$, 8.ii.1989, C.W. & L. O'Brien & G. Wibmer [1♀, deposited in CASC: UCRCENT00417413]. **Paratype: Uruguay:** Colonia Department: R. 2, km. 194, Arroyo S. Pedro, $32^{\circ}52'51''S$, $57^{\circ}58'20''W$, 8.ii.1989, C.W. & L. O'Brien & G. Wibmer [1♀, CASC: UCRCENT00417412].

Etymology. From Greek *cirrho* meaning “tawny” and *cnemis* meaning “leg” in reference to the dark tawny-orange color of the legs.

Discussion. This species has been preliminarily placed in several different groups. The large body size, 8 funiculars, and sculpture on the body may suggest that it is close to the *tolteca* group, however, the face is not as broad, the femora are not darkly colored, and the fore wing costal cell lacks the bare anterior area.

***Orasema monstrosa* n. sp.**

(Fig. 2.41)

Diagnosis. Recognized from other *Orasema* by the following combination of characters: mandibles small with 2:2 dental formula, labrum greatly reduced in size, extremely setose head and mesosoma, 7-segmented funicle, coarsely areolate sculpture on the mesoscutal midlobe, and large male body size (female unknown).

Description. Male. Length 3.8 mm (Fig. 2.41A). **Color.** Head and mesosoma dark green with iridescence. Scape pale brown; pedicel, anellus, and flagellum brown.

Mandible, maxilla, and labium brown. Coxae brown with strong iridescence; femora brown; tibiae yellow. Wing venation yellowish. Gaster brown. **Head** (Fig. 2.41B). Head in frontal view subtriangular; HW:HH 1.3; face rugose; scrobal depression shallow, laterally rounded, areolate; longitudinal groove between eye and torulus absent; eyes densely setose, IOD:EH 1.5; MS:EH 0.7; malar depression absent; supraclypeal area longer than broad, convex, with scattered punctations; clypeus smooth; epistomal sulcus distinct and sharply defined; anterior tentorial pit shallow; anteclypeus distinct, broadly rounded. Labrum with 4 digits, very minute. Mandibular formula 2:2; palpal formula 3:2. Occiput imbricate, shallowly emarginate in dorsal view, dorsal margin abrupt; temples present, rounded. Scape not reaching median ocellus. Pedicel globose. Flagellum with 7 funiculars, FL:HH 2; anellus minute, difficult to distinguish; F2L:F2W 1.6, F2L:F3L 1.1; following funiculars subequal in length, equal in width; clava subcylindrical (Fig. 2.41D). **Mesosoma** (Fig. 2.41 C, E). ML:MH 1.5. Mesoscutal midlobe rugose, densely setose; lateral lobe finely rugose; notauli deep. Axilla weakly sculptured; dorsally rounded, on roughly same plane as mesoscutellum; scutoscutellar sulcus broad, irregularly foveate, broadly separated from transscutal articulation; mesoscutellar disc slightly longer than broad, areolate; frenal line as strong carina; frenum areolate; axillular sulcus absent; axillula rugose-areolate. Propodeal disc broadly rounded, without depression or carina, rugose (Fig. 2.41F); callus rugose, densely setose. Propleuron convex, weakly sculptured. Prepectus areolate. Mesepisternum areolate-reticulate, broadly rounded anterior to mid coxa; postpectal carina prominent. Upper mesepimeron smooth; lower mesepimeron smooth to reticulate; transepimeral sulcus weakly defined. HCL:HCW 2.2, with weak

dorsolateral sculpture; HFL:HFW 6.5, with even cover of elongate, semi-erect setae. FWL:FWW 2.5, FWL:ML 2.2; basal area and speculum sparsely setose, wing disc densely setose; marginal fringe relatively long; submarginal vein with several long setae; marginal vein setose; stigmal vein as long as broad, slightly angled toward wing apex; postmarginal vein 3.2× as long as stigmal vein. Hind wing costal cell entirely setose.

Metasoma. Petiole cylindrical, linear in profile, PTL:PTW 6.2, PTL:HCL 1.8, areolate, lateral margin rounded, ventral sulcus absent. Antecostal sulcus foveate to smooth posteriorly; acrosternite posteriorly angulate.

Female. Unknown.

Ant hosts. Unknown.

Plant hosts. Unknown.

Distribution (Fig. 2.38). Venezuela: BO. Collected in April (one specimen).

Material Examined. Holotype: Venezuela: Bolívar: Auyan Tepuy Camp, 2075m, 5°46'7"N, 62°31'56"W, 19-25 Apr 1994, L. Masner & J.L. Garcia, malaise trap [1♂, deposited in UCRC: UCRCENT00434585].

Etymology. From Latin *monstrum* meaning “monstrosity” and *-osus* meaning “full of” in reference to the large size and hairiness.

Phylogenetics. *Orasema monstrosa* (referred to as “*Orasema_nsp_*”IS1”_VEN_D4228”) is the only molecularly sampled unplaced taxon. It is sister to the *Orasema sixaolae* group (Baker et al., 2020). These two groups share very few morphological characters in common, therefore, this species was not included in the *sixaolae* group.

***Orasema mutata* n. sp.**

(Fig. 2.42)

Diagnosis. This is the only known species of *Orasema* with 6 funicular segments and males without a stigmal vein. Additionally, the following combination of characters are diagnostic: scutoscutellar sulcus with carinae that are continuous with the axilla and mesoscutellum, curvature of the mesoscutal lateral lobes discontinuous with the midlobe from dorsal view, male clava reduced to a single minute segment.

Description. Female. Length 2.1–2.2 mm (Fig. 2.42A). **Color.** Head and mesosoma dark brown with blue-purple iridescence. Scape yellow; pedicel and anellus pale brown; flagellum brown. Mandible brown with dark tips; maxilla and labium brown. Coxae brown with iridescence; femora mostly brown, tips pale; tibiae yellow. Fore wing hyaline; venation pale brown. Petiole same as mesosoma; gaster brown. **Head** (Fig. 2.42B). Head in frontal view subcircular; HW:HH 1.2–1.3; face rugose; scrobal depression shallow, laterally rounded, with transverse striae; longitudinal groove between eye and torulus absent; eyes bare, IOD:EH 1.5–1.6; MS:EH 0.7–0.8; malar depression absent; supraclypeal area about as long as broad, shorter than clypeus, weakly sculptured; clypeus weakly sculptured; epistomal sulcus distinct; anterior tentorial pit strongly impressed; anteclypeus distinct, broadly rounded. Labrum with 5 digits. Left mandible with 3 teeth, right mandible not observed; palpal formula 3:2. Occiput imbricate, emarginate in dorsal view, dorsal margin abrupt; temples present, rounded. Scape not reaching median ocellus. Pedicel globose, broader than F1. Flagellum with 6 funiculars;

FL:HH 1.2–1.3; anellus disc-shaped; F2L:F2W 2, F2L:F3L 1; following funiculars subequal in length, equal in width; clava subconical (Fig. 2.42D). **Mesosoma** (Fig. 2.42 C, F). ML:MH 1.3–1.4. Mesoscutal midlobe coarsely rugose-areolate, sparsely setose; lateral lobe transversely costate; notauli deep. Axilla areolate, dorsally rounded, on roughly same plane as mesoscutellum; scutoscutellar sulcus broad, crossed by carinae that extend into the axillar and scutellar sculpture, narrowly separated from transscutal articulation; mesoscutellar disc as long as broad, areolate; frenal line present as strong carina; frenum areolate; axillular sulcus indistinct; axillula rugose. Propodeal disc flat, without depression or carina, rugose-areolate (Fig. 2.42G); callus nearly smooth, with several long setae. Propleuron convex, nearly smooth. Prepectus evenly triangular, weakly reticulate dorsally, rugose ventrally. Mesepisternum rugose-areolate laterally, smooth ventrally, broadly rounded anterior to mid coxa; postpectal carina weak. Upper mesepimeron smooth; lower mesepimeron rugose; transepimeral sulcus weakly impressed. Metepisternum laterally nearly smooth. HCL:HCW 2.3, weakly rugose-reticulate; HFL:HFW 6.7–6.8, lightly setose. FWL:FWW 2.3–2.4, FWL:ML 2.3–2.4; basal area bare, speculum, costal cell, and wing disc densely setose; marginal fringe relatively long; submarginal vein setose; marginal vein setose; stigmal vein 1.5–2.0× as long as broad, slightly angled toward wing apex; postmarginal vein several times longer than stigmal vein. Hind wing costal cell with a broad bare area medially. **Metasoma**. Petiole cylindrical, linear in profile, PTL:PTW 3.8–3.9, PTL:HCL 1.3–1.4, rugose, lateral margin rounded, ventral sulcus absent. Antecostal sulcus smooth; acrosternite posteriorly angulate; apical setae of hypopygium with one pair of long setae. Ovipositor strongly

curved cephalad; subapical carina present; first (ventral) valvula with 6–8 small, narrowly separated teeth, second (dorsal) valvula with 8–10 annuli that are broadly separated dorsally by smooth area.

Male. Length 2.1–2.2 mm. HW:HH 1.3–1.4; scape yellow; flagellum with 6 funiculars, FL:HH 1.4–1.5; anellus disc-shaped; F2L:F2W 2.7–2.8 (Fig. 2.42E). Fore and mid femora yellow, hind femur pale brown with yellow tips; tibiae yellow. PTL:PTW 9, PTL:HCL 2.1–2.2.

Ant hosts. Unknown.

Plant hosts. Unknown.

Distribution (Fig. 2.38). Costa Rica: AL, LI. Specimens collected in April and October (2 specimens).

Material examined. Holotype: Costa Rica: Limón: Sector Cerro Cocori, Fca. de E. Rojas, 150m, 10°35'34"N, 83°42'52"W, x.1991, E. Rojas [1♀, deposited in INBIO: INBIOCRI00462110]. **Paratypes: Costa Rica: Alajuela:** San Carlos, P.N. Arenal, Sendero Pilón, 650m, 10°39'0"N, 84°21'0"W, 5.iii-20.iv.2001, G. Carballo, malaise, #62074 [1♂, INBIO: INB03983200].

Etymology. From Latin *muta* meaning “change” in reference to the mutated-looking antennae.

Discussion. This species was not going to be described at first because we believed that it was either a common species with a mutated antenna or a single strange specimen, but once we found a matching male and female from similar localities collected a decade apart, we realized that this likely represents a real species.

***Orasema psarops* n. sp.**

(Fig. 2.43)

Diagnosis. Recognized from other *Orasema* by the following combination of characters: antenna with 8 funicular segments; labrum with 4 digits; dorsal mesosoma entirely rugose-reticulate; legs past the coxae entirely yellow; large body size (females 4.2–4.6 mm); basal third of fore wing entirely bare except for a single posterior line of setae; stigmal vein angled toward the wing base; lower face with scattered, minute punctures.

Description. Female. Length 4.2–4.6 mm (Fig. 2.43A). **Color.** Head and mesosoma iridescent green-blue. Scape yellow; pedicel brown; anellus yellow; flagellum dark brown. Mandible yellow with teeth black at apex; maxilla and labium yellow. Coxae dark brown with green iridescence; femora and tibiae yellow (Fig. 2.43E). Fore wing hyaline; venation brown. Petiole same as mesosoma; gaster dark brown with iridescence. **Head** (Fig. 2.43B). Head in frontal view subtriangular; HW:HH 1.2–1.3; face reticulate with small scattered impressions; scrobal depression shallow, laterally rounded, with transverse striae; dorsal scrobal depressions absent; longitudinal groove between eye and torulus absent; eyes sparsely setose, IOD:EH 1.6–1.7; MS:EH 0.8–1; malar depression weakly impressed adjacent to mouth; supraclypeal area longer than broad, shorter than clypeus, weakly reticulate; clypeus smooth; epistomal sulcus distinct and sharply defined; anterior tentorial pit strongly impressed; anteclypeus distinct, broadly rounded. Labrum with 4 digits. Mandibular formula 3:2; palpal formula 3:3. Occiput imbricate, emarginate in dorsal view, dorsal margin evenly rounded; temples present, rounded. Scape not

reaching median ocellus. Pedicel small and globose. Flagellum with 8 funiculars; FL:HH 1.2–1.3; anellus disc-shaped; F2L:F2W 1.25, F2L:F3L 0.8–1; following funiculars subequal in width, successively shorter; clava subconical (Fig. 2.43D). **Mesosoma** (Fig. 2.43 C, F). ML:MH 1.1–1.3. Mesoscutal midlobe rugose-reticulate, sparsely setose; lateral lobe rugose-reticulate; notauli deep. Axilla rugose-reticulate, dorsally flat, on same plane as mesoscutellum; scutoscutellar sulcus broad, irregularly foveate, broadly separated from transscutal articulation; mesoscutellar disc as long as broad, rugose-reticulate; frenal line foveate; frenum areolate-reticulate; axillular sulcus vaguely indicated by carina; axillula areolate-reticulate. Propodeal disc flat, areolate-reticulate, without depression or carina (Fig. 2.43G); callus reticulate, with a few small setae. Propleuron convex, reticulate. Prepectus triangular dorsally, strongly narrowed ventrally, sculpture areolate-reticulate. Mesepisternum strigate-reticulate laterally, areolate-reticulate anteriorly, broadly rounded anterior to mid coxa; postpectal carina weak. Upper mesepimeron smooth; lower mesepimeron rugose-reticulate; transepimeral sulcus distinct. Metepisternum laterally reticulate. HCL:HCW 1.5, reticulate dorsally, smooth ventrally; HFL:HFW 5.8–6.3, with even cover of short, dense setae. FWL:FWW 2.5–2.8, FWL:ML 2.5–2.6; basal area and speculum bare, costal cell and wing disc densely setose; marginal fringe minute; submarginal vein with several long setae; marginal vein setose; stigmal vein slightly longer than broad, slightly angled toward base of wing; postmarginal vein longer than stigmal vein. Hind wing costal cell with a few setae apically. **Metasoma**. Petiole cylindrical, linear in profile, PTL:PTW 2.5, PTL:HCL 1.4, areolate-reticulate, lateral margin rounded, ventral sulcus present with margins broadly

separated. Antecostal sulcus foveate; acrosternite posteriorly rounded; apical setae of hypopygium with one pair of setae much longer than the others. Ovipositor not visible.

Male. Unknown.

Ant hosts. Unknown.

Plant hosts. Unknown.

Distribution (Fig. 2.38). Venezuela: TA. Collected in July (2 specimens).

Material examined. Holotype: Venezuela: Tachira: Pregonero, Camp. Siberia, Hospital, 1280m, $8^{\circ}00'56''N$, $71^{\circ}45'48''W$, 10-31.vii.1989, S. & J. Peck [1♀, deposited in UCRC: UCRCENT00434755]. **Paratype: Venezuela: Tachira:** Pregonero, Camp. Siberia, Hospital, 1280m, $8^{\circ}00'56''N$, $71^{\circ}45'48''W$, 10-31.vii.1989, S. & J. Peck [1♀, UCRC: UCRCENT00434753].

Etymology. From Greek *psaro* meaning “speckled” and *ops* meaning “face” in reference to the small punctures scattered across the face.

Discussion. This species has some similarities to another Venezuelan species, *Orasema chunpi* Burks, Heraty & Dominguez (*stramineipes* species group), however it is distinctly larger and its antennae do not closely resemble other *stramineipes* group species. The large body size and sculpture may suggest an affiliation with the *tolteca* species group, however, it lacks the distinctively broad face, dark femora, and bare anterior edge of the fore wing costal cell.

***Orasema roppai* n. sp.**

(Fig. 2.44)

Diagnosis. Recognized from other *Orasema* by the following combination of characters: antenna with 8 funicular segments; labrum with 4 digits; face, mesoscutum, and mesoscutellum entirely rugose-reticulate; eyes setose; axillular sulcus strong and complete; face more subquadrate than subtriangular (HW:HH 1–1.1).

Description. Female. Length 3.2–3.8 mm (Fig. 2.44A). **Color.** Head and mesosoma iridescent blue-green. Scape, pedicle, and anellus yellow; flagellum dark brown. Mandible yellowish brown; maxilla and labium pale brown. Coxae dark brown; femora entirely yellow or light brown proximally, yellow distally; tibiae yellow. Fore wing hyaline; venation pale brown. Petiole same as mesosoma; gaster dark brown with iridescence. **Head** (Fig. 2.44B). Head in frontal view subquadrate; HW:HH 1–1.1; face rugose-reticulate; scrobal depression shallow, laterally rounded, with transverse striae; longitudinal groove between eye and torulus absent; eyes densely setose, IOD:EH 1.4–1.6; MS:EH 0.7–0.9; malar depression weakly impressed adjacent to mouth; supraclypeal area slightly longer than broad, weakly sculptured; clypeus smooth; epistomal sulcus vaguely defined; anterior tentorial pit strongly impressed; anteclypeus distinct, nearly straight. Labrum with 4 digits. Mandibular formula not observed; palpal formula 3:3. Occiput imbricate, deeply emarginate in dorsal view, dorsal margin rounded; temples present. Scape not reaching median ocellus. Pedicle small and globose. Flagellum with 8 funiculars; FL:HH 1.1–1.4; anellus disc-shaped; F2L:F2W 1.5–2, F2L:F3L 1.1–1.4;

following funiculars subequal in length, equal in width; clava subovate (Fig. 2.44D).

Mesosoma (Fig. 2.44 C, F). ML:MH 1.4–1.7. Mesoscutal midlobe rugose-reticulate, densely setose; lateral lobe rugose-reticulate; notauli deep. Axilla rugose-reticulate, dorsally flat, on same plane as mesoscutellum; scutoscutellar sulcus broad, irregularly foveate, reaching transscutal articulation; mesoscutellar disc as long as broad, rugose-reticulate; frenal line regularly foveate; frenum rugose-reticulate; axillular sulcus indicated by a strong lateral carina; axillula rugose. Propodeal disc flat, without depression or carina, areolate-reticulate (Fig. 2.44G); callus rugose-reticulate, with several long setae. Propleuron convex, weakly reticulate. Prepectus triangular dorsally, strongly narrowed ventrally, rugose-reticulate. Mesepisternum reticulate laterally, smooth ventrally, broadly rounded anterior to mid coxa; postpectal carina weak. Upper and lower mesepimeron reticulate to smooth; transepimeral sulcus distinct. Metepisternum laterally reticulate. HCL:HCW 1.5–1.7, reticulate dorsally, becoming smooth ventrally; HFL:HFW 3.8–4.7, with short dense setae dorsally, and fewer longer setae ventrally. FWL:FWW 2.6–2.9, FWL:ML 1.9–2.2; basal area and speculum bare, costal cell and wing disc densely setose; marginal fringe relatively long; submarginal vein with small setae; marginal vein densely setose; stigmal vein about twice as long as broad, slightly angled toward wing apex; postmarginal vein several times longer than stigmal vein. Hind wing costal cell with a broad bare area. **Metasoma**. Petiole cylindrical, linear in profile, PTL:PTW 1.6–2, PTL:HCL 0.8–1, areolate-reticulate, lateral margin rounded, ventral sulcus absent. Antecostal sulcus foveate; acrosternite posteriorly rounded; apical setae of hypopygium with one pair of setae much longer than the others. Ovipositor not visible.

Male. Length 2.1–2.7 mm. HW:HH 1–1.2; scape yellow; flagellum with 8–9 funiculars (one specimen with complete antennae has a different count on either antenna), FL:HH 1.6–1.7; anellus disc-shaped; F2L:F2W 1.5–1.9 (Fig. 2.44E). Femora brown proximally, yellow distally; tibiae yellow. PTL:PTW 2.8–3.4, PTL:HCL 1.3–1.6.

Ant hosts. Unknown.

Plant hosts. Unknown.

Distribution (Fig. 2.38). Argentina: MN; Brazil: RS. Collected in November–December.

Material examined. Holotype: Brazil: Rio Grande do Sul: S. Augusto, 511m, 27°51'29"S, 53°46'49"W, Dec 1975, O. Roppa [1♀, deposited in CNC:

UCRCENT00415610]. **Paratypes: Argentina: Misiones:** Puerto Rico, 26°48'41"S, 55°01'39"W, 5-13.xi.1970, C. Porter & L. Stange, Malaise Trap [1♂, IFML:

UCRCENT00436518]. **Brazil: Rio Grande do Sul:** S. Augusto, 511m, 27°51'29"S, 53°46'49"W, 19.xii.1975, O. Roppa [1♂ 14♀, CNC: UCRCENT00321008–11,

UCRCENT00415379–84, UCRCENT00415608–09, UCRCENT00415611–12, ROME: UCRCENT00418056].

Etymology. Named in honor of the collector of most of the specimens of this species, “O. Roppa.”

Discussion. This species shares many similarities with *Orasema brasiliensis*, but has 8 funiculars rather than 7 and a different head shape. It has some similarities with the *stramineipes* species group, but the head shape and antenna shape do not match the other members of that group.

References

- Ayre, G.L. (1957) Ecological notes on *Formica subnitens* Creighton (Hymenoptera: Formicidae). *Insectes Sociaux*, **4**, 173–176.
- Ayre, G.L. (1958) Notes on insects found in or near nests of *Formica subnitens* Creighton (Hymenoptera: Formicidae) in British Columbia. *Insectes Sociaux*, **5**, 1–7.
- Ayre, G.L. (1959) Food habits of *Formica subnitens* Creighton (Hymenoptera: Formicidae) at Westbank, British Columbia. *Insectes Sociaux*, **4**, 105–114.
- Baker, A.J., Heraty, J.M., Mottern, J., Zhang, J., Hines, H.M., Lemmon, A.R. & Lemmon, E.M. (2020) Inverse dispersal patterns in a group of ant parasitoids (Hymenoptera: Eucharitidae: Oraseminae) and their ant hosts. *Systematic Entomology*, **45**, 1–19.
- Burks, R.A., Heraty, J.M., Dominguez, C. & Mottern, J.L. (2018) Complex diversity in a mainly tropical group of ant parasitoids: revision of the *Orasema stramineipes* species group (Hymenoptera: Chalcidoidea: Eucharitidae). *Zootaxa*, **4401**, 1–107.
- Burks, R.A., Heraty, J.M., Mottern, J., Dominguez, C. & Heacox, S. (2017) Biting the bullet: revisionary notes on the Oraseminae of the Old World (Hymenoptera, Chalcidoidea, Eucharitidae). *Journal of Hymenoptera Research*, **55**, 139–188.
- Burks, R.A., Mottern, J. & Heraty, J.M. (2015) Revision of the *Orasema festiva* species group (Hymenoptera: Chalcidoidea: Eucharitidae). *Zootaxa*, **3972**, 521–534.
- Carey, B., Visscher, K. & Heraty, J.M. (2012) Nectary use for gaining access to an ant host by the parasitoid *Orasema simulatrix* (Hymenoptera, Eucharitidae). *Journal of Hymenoptera Research*, **27**, 47–65.
- Chien, I. & Heraty, J.M. (2018) Come and gone: Description of a new species of Eucharitidae (Hymenoptera) attacking *Solenopsis* (Hymenoptera: Formicidae) in Texas. *Insect Systematics and Diversity*, **2**, 1–7.
- Clausen, C.P. (1940) The oviposition habits of the Eucharitidae (Hymenoptera). *Journal of the Washington Academy of Sciences*, **30**, 504–516.
- Clausen, C.P. (1941) The habits of the Eucharitidae. *Psyche (Cambridge)*, **48**, 57–69.
- Eady, R.D. (1968) Some illustrations of microsculpture in the Hymenoptera. *Proceedings of the Royal Entomological Society of London. Series A, General Entomology*, **43**, 66–72.

- Gahan, A.B. (1940) A contribution to the knowledge of the Eucharidae (Hymenoptera: Chalcidoidea). *Proceedings of the United States National Museum*, **88**, 425–458.
- Harris, R.A. (1979) A glossary of surface sculpturing. *Occasional Papers in Entomology*, **28**, 1–31.
- Heraty, J.M. (1985) A revision of the Nearctic Eucharitinae (Hymenoptera: Chalcidoidea: Eucharitidae). *Proceedings of the Entomological Society of Ontario*, **116**, 61–103.
- Heraty, J.M. (1990) Classification and evolution of the Oraseminae (Hymenoptera: Eucharitidae). Texas A&M University, Department of Entomology, thesis.
- Heraty, J.M. (1994) Classification and evolution of the Oraseminae in the Old World, including revisions of two closely related genera of Eucharitinae (Hymenoptera: Eucharitidae). *Life Sciences Contributions*, **157**, 1–174.
- Heraty, J.M. (2000) Phylogenetic relationships of Oraseminae (Hymenoptera: Eucharitidae). *Annals of the Entomological Society of America*, **93**, 374–390.
- Heraty, J.M. (2002) A revision of the genera of Eucharitidae (Hymenoptera: Chalcidoidea) of the world. *Memoirs of the American Entomological Institute*, **68**, 1–359.
- Heraty, J.M. & Baker, A.J. (In Press) New species of *Orasema* (Hymenoptera: Eucharitidae) from Central and South America. *Journal of Natural History*.
- Heraty, J.M., Burks, R.A., Mbanyana, N. & Van Noort, S. (2018) Morphology and life history of an ant parasitoid, *Psilocharis afra* (Hymenoptera: Eucharitidae). *Zootaxa*, **4482**, 491–510.
- Heraty, J.M. & Murray, E. (2013) The life history of *Pseudometagea schwarzii*, with a discussion of the evolution of endoparasitism and koinobiosis in Eucharitidae and Perilampidae (Chalcidoidea). *Journal of Hymenoptera Research*, **35**, 1–15.
- Heraty, J.M., Wojcik, D.P. & Jouvenaz, D.P. (1993) Species of *Orasema* parasitic on the *Solenopsis saevissima*-complex in South America (Hymenoptera: Eucharitidae, Formicidae). *Journal of Hymenoptera Research*, **2**, 169–182.
- Herreid, J.S. & Heraty, J.M. (2017) Hitchhikers at the dinner table: a revisionary study of a group of ant parasitoids (Hymenoptera: Eucharitidae) specializing in the use of extrafloral nectaries for host access. *Systematic Entomology*, **42**, 204–229.

- Johnson, J.B., Miller, T.D., Heraty, J.M. & Merickel, F.W. (1986) Observations on the biology of two species of *Oraesema* (Hymenoptera: Eucharitidae). *Proceedings of the Entomological Society of Washington*, **88**, 542–549.
- Lachaud, J.-P. & Pérez-Lachaud, G. (2012) Diversity of species and behavior of hymenopteran parasitoids of ants: a review. *Psyche*, **2012**, 1–24.
- Mann, W.M. (1914) Some myrmecophilous insects from Mexico. *Psyche*, **21**, 171–184.
- Vander Meer, R.K., Jouvenaz, D.P. & Wojcik, D.P. (1989) Chemical mimicry in a parasitoid (Hymenoptera, Eucharitidae) of fire ants (Hymenoptera, Formicidae). *Journal of Chemical Ecology*, **15**, 2247–2261.
- Wheeler, G.C. & Wheeler, E.W. (1937) New hymenopterous parasites of ants (Chalcidoidea: Eucharidae). *Annals of the Entomological Society of America*, **30**, 163–175.
- Wheeler, W.M. (1907) The polymorphism of ants, with an account of some singular abnormalities due to parasitism. *Bulletin of the American Museum of Natural History*, **23**, 1–90.

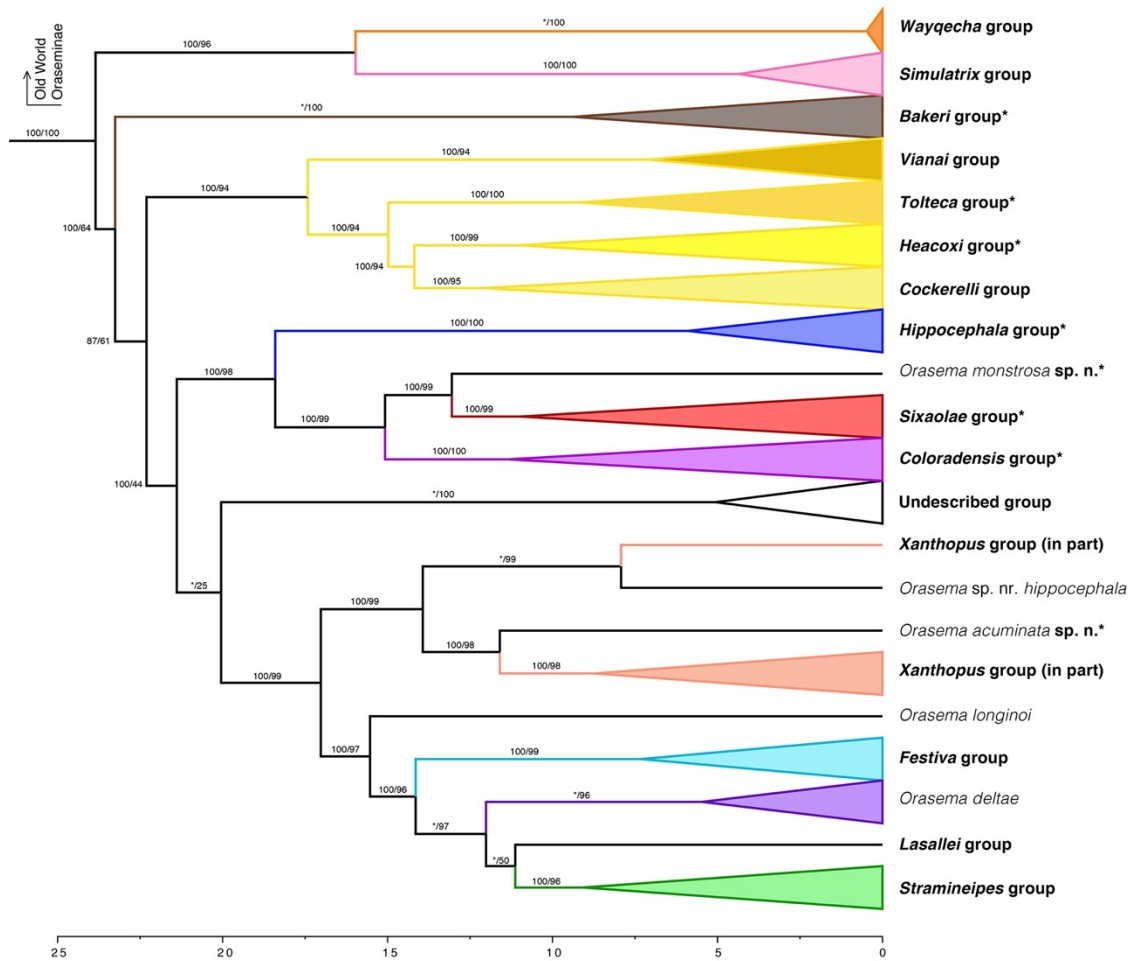


Figure 2.1: Time tree summarizing phylogenetic relationships of *Orasema* from Baker et al. (2020), with species groups collapsed. Support values show bootstrap support for the AHE-only maximum likelihood analysis followed by the combined AHE + Sanger maximum likelihood analysis. Time scale is calibrated in millions of years. Species groups or species being revised herein are denoted with asterisks.

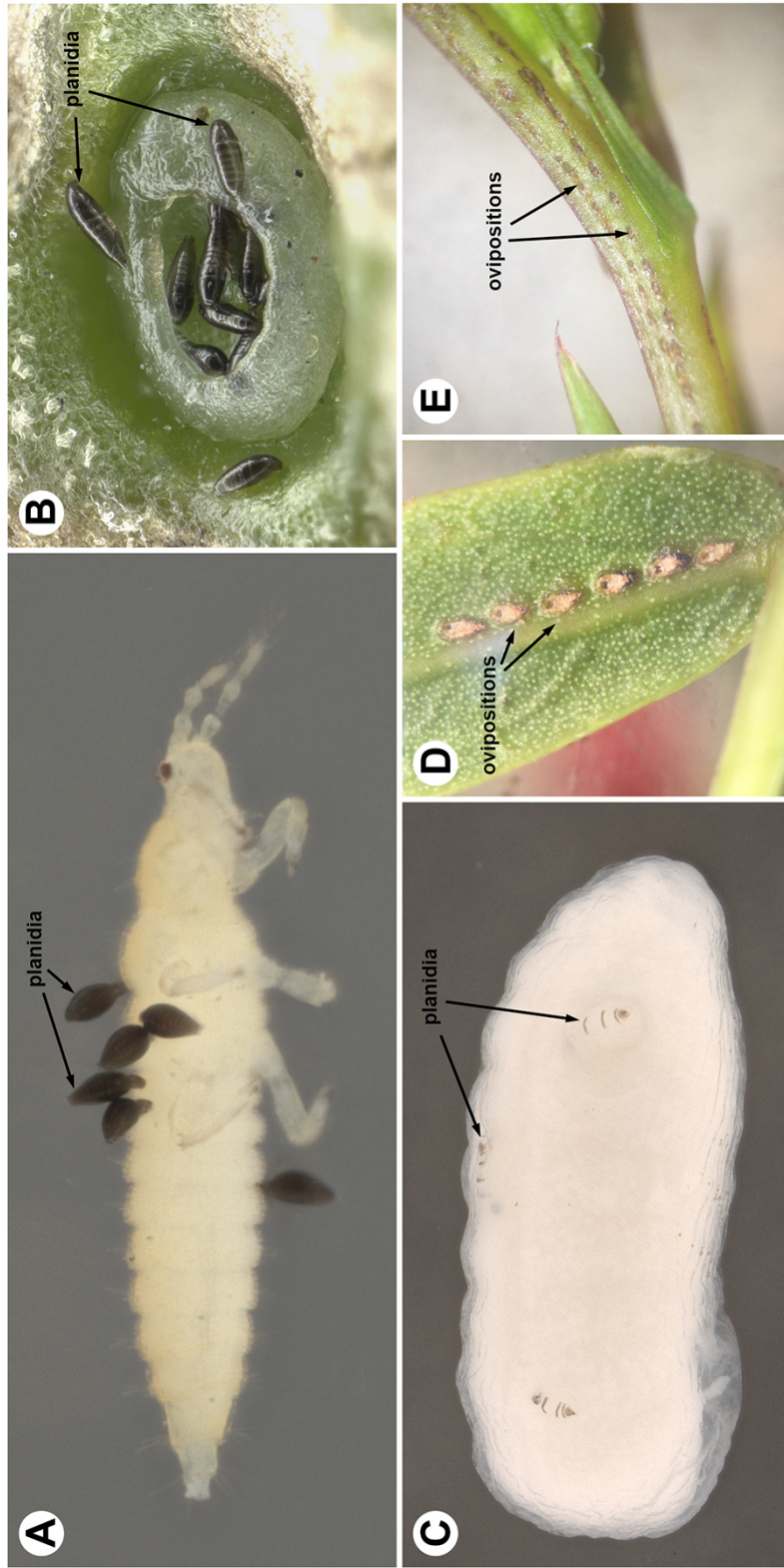


Figure 2.2: *Orasema* immature stages. **A**, immature thrips with unfed planidia of *O. coloradensis* phoretically attached; **B**, unfed planidia of *O. simulatrix* Gahan congregating in an extrafloral nectary of *Chilopsis linearis* (Herreid & Heraty, 2017); **C**, late-instar ant larva with several attached feeding planidia of an *O. stramineipes* group species; **D**, *Orasema aureoviridis* Gahan leaf ovipositions on *Prosopis glandulosa* Torr.; **E**, *Orasema coloradensis* stem ovipositions on *Chamaecrista fasciculata*.

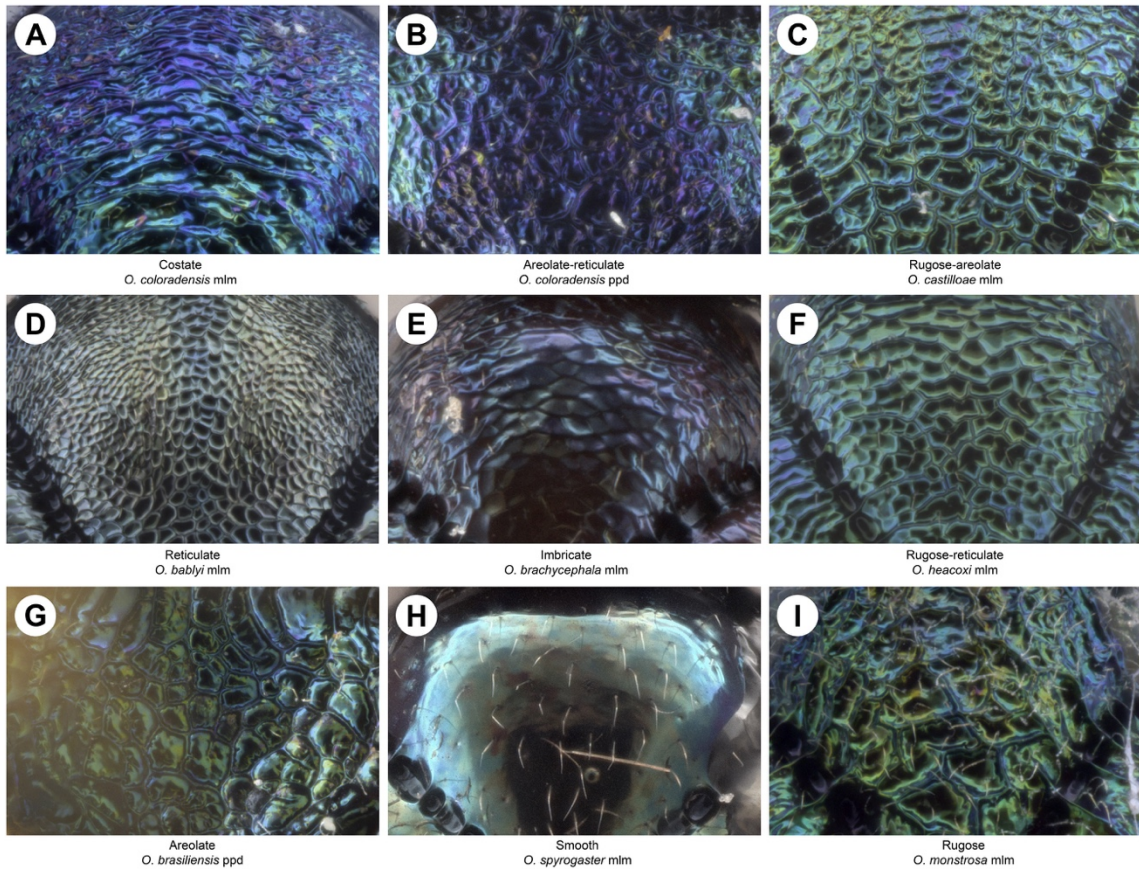


Figure 2.3: Comparison of surface sculpture in *Orasema*. **A**, costate: raised, mostly parallel ridges; **B**, areolate-reticulate: shallow reticulations within large areolae; **C**, rugose-areolate: strong ridges that occasionally form closed cells (areolae) but often have dead-ends; **D**, reticulate: small cells enclosed by raised ridges, similar in size and shape to surrounding cells; **E**, imbricate: cells that are raised above adjacent cells on one side, shingle-like; **F**, rugose-reticulate: small enclosed cells mixed with irregular raised ridges; **G**, areolate: large raised ridges forming large enclosed cells; **H**, smooth: no obvious sculpture, ridges, or patterns; **I**, rugose: large raised ridges that have dead-ends and do not enclose cells.

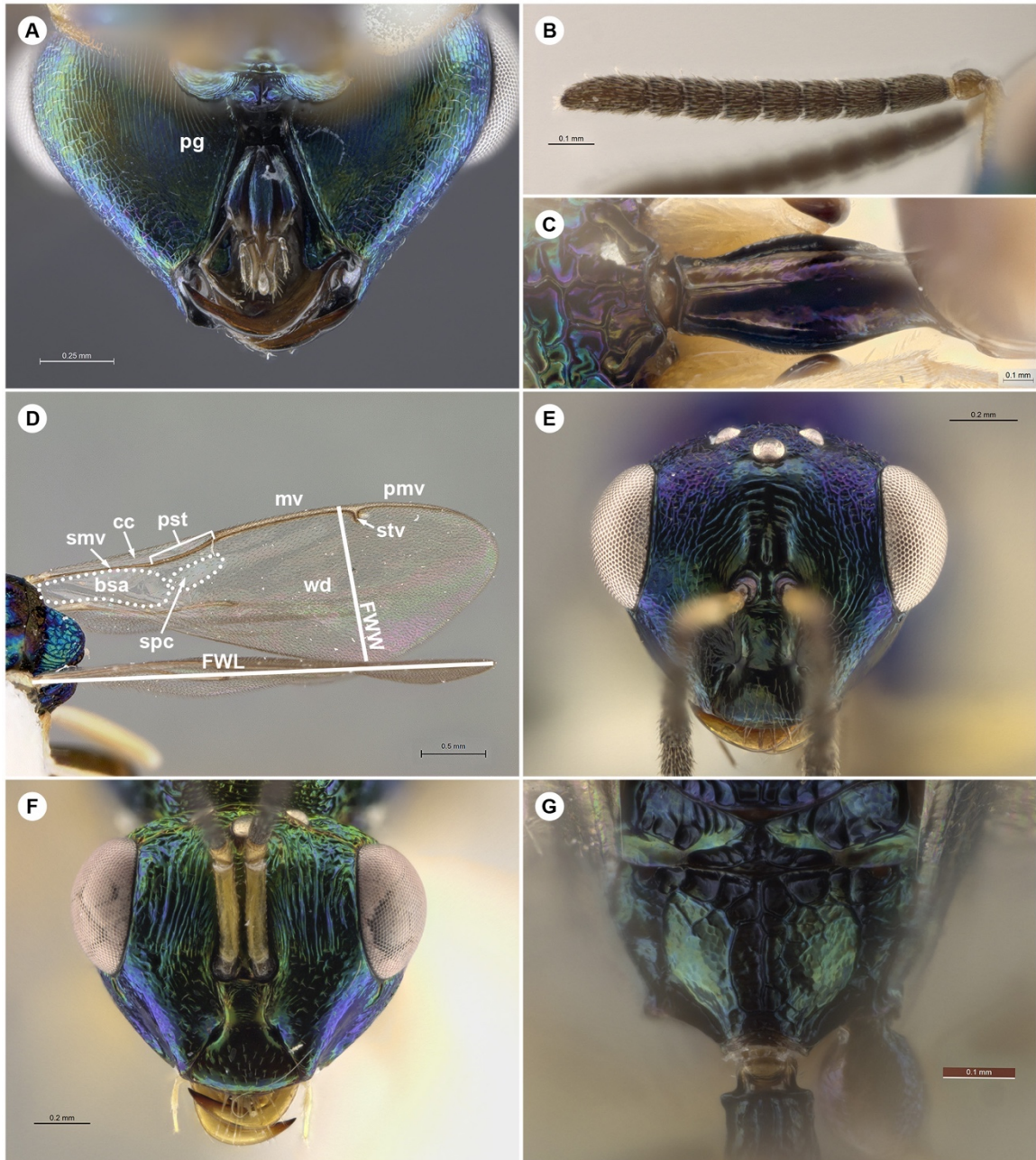


Figure 2.4: Diagnostic features for *Orasema*. *Orasema castilloae* (UCRCENT00412574): **A**, posterior head showing typical non-expanded post gena; *Orasema* undescribed xanthopus group species (UCRCENT00320847): **B**, female antenna; *Orasema delicatula* (UCRCENT00239436): **C**, petiole with complete longitudinal carinae on lateral sides; *Orasema delicatula* (UCRCENT00320683): **D**, fore wing with elongate postmarginal vein; *Orasema longinoi* (UCRCENT00491415): **E**, anterior face; *Orasema lasallei* (UCRCENT00242606): **F**, anterior face; *Orasema deltae* (UCRCENT00169600): **G**, propodeum with medial carina within medial longitudinal groove.



Figure 2.5: Distribution map of species in the *Orasema coloradensis* species group.

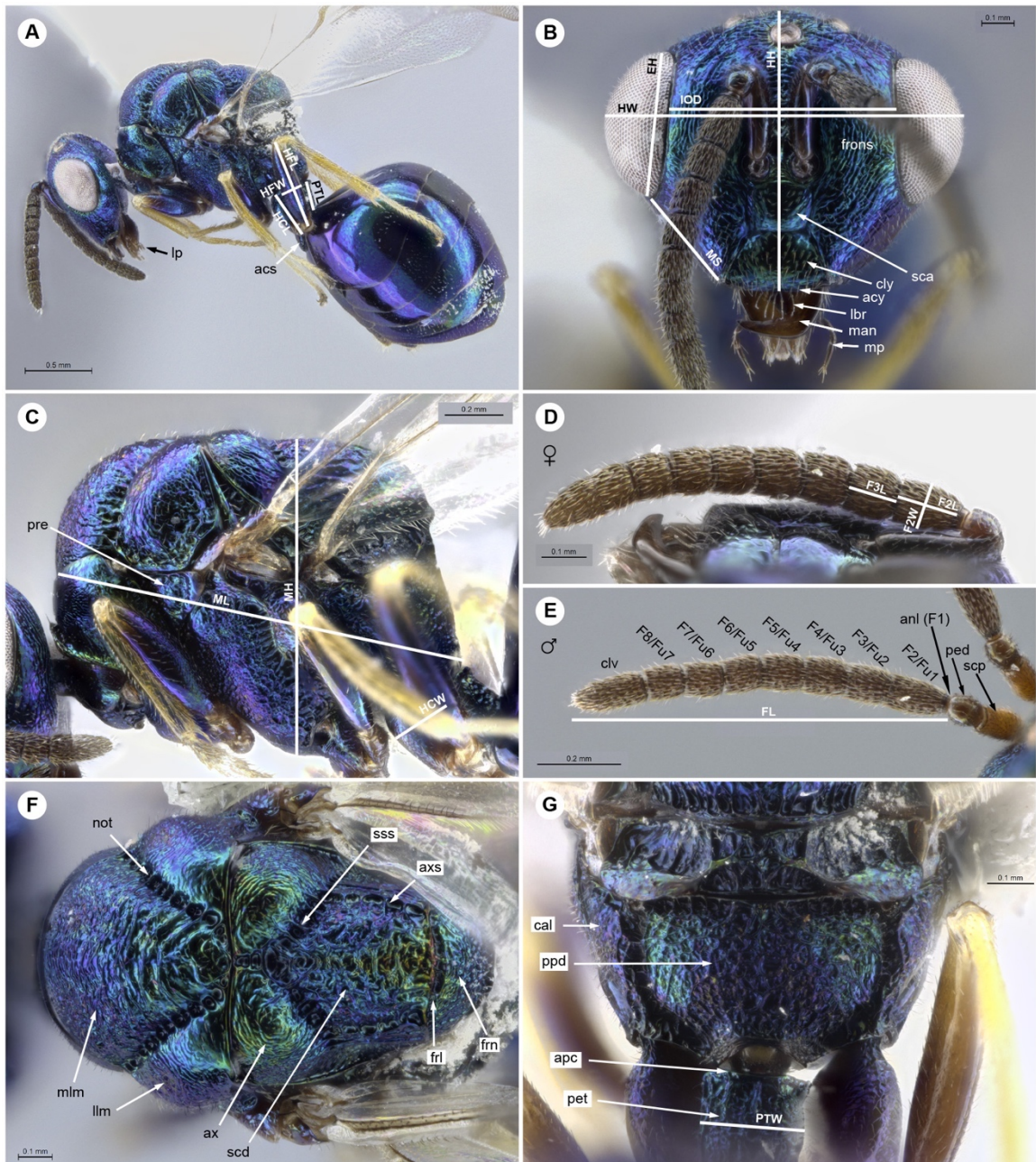


Figure 2.6: *Orasema coloradensis*. Female (UCRCENT00437137): **A**, habitus, lateral; **B**, head, anterior; **C**, mesosoma, lateral; **D**, antenna; **F**, mesosoma, dorsal. Female (UCRCENT00439136): **G**, propodeum, posterior. Male (UCRCENT00437137): **E**, antenna.

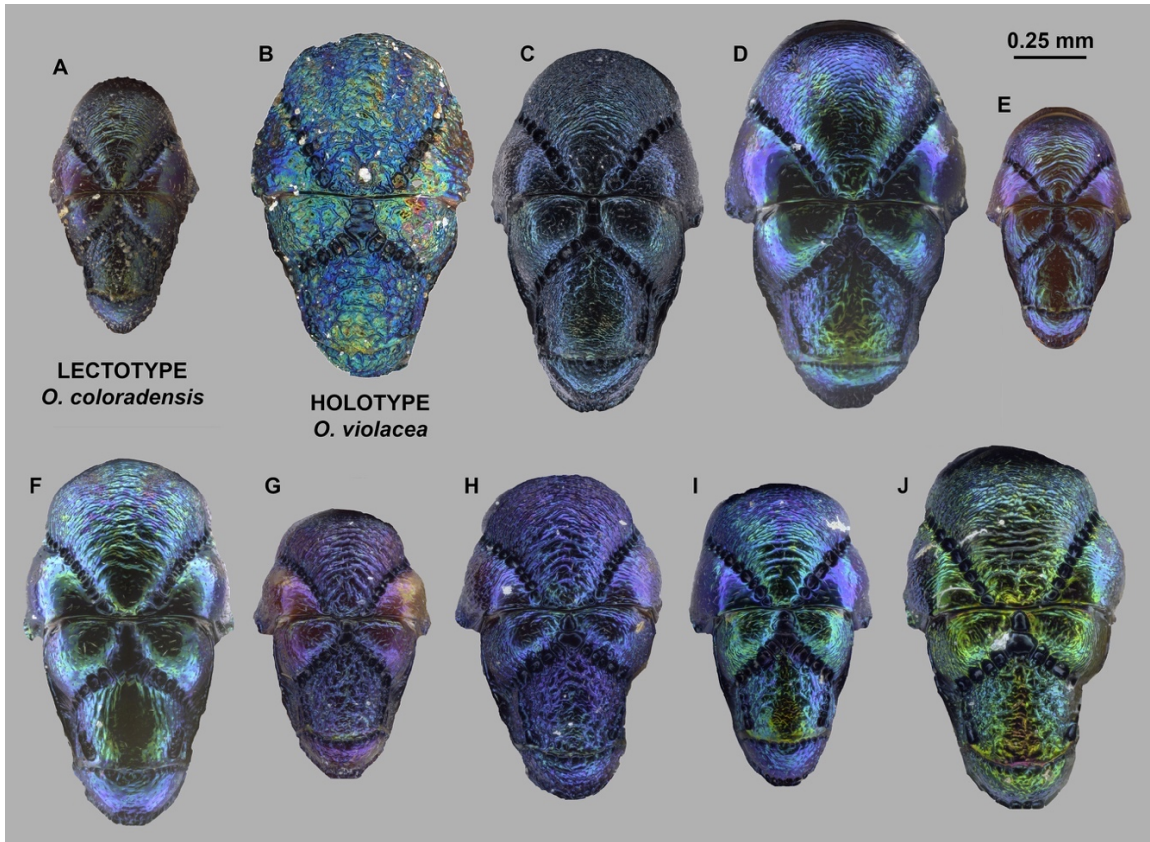


Figure 2.7: Comparison of the dorsal mesosoma of female *Orasema coloradensis*. All specimens scaled proportionately. **A**, *Orasema coloradensis* Lectotype from Colorado (UCRCENT00238021); **B**, *O. violacea* holotype from Florida (USNMENT00809466); **C**, *O. coloradensis* from Colorado (UCRCENT00444500); **D**, *O. coloradensis* from Texas (UCRCENT00320732); **E**, *O. coloradensis* from Texas (UCRCENT00397223); **F**, *O. coloradensis* from Idaho (UCRCENT00352500); **G**, *O. coloradensis* from Maryland (UCRCENT00414400); **H**, *O. coloradensis* from Florida (UCRCENT00411745); **I**, *O. coloradensis* from Florida (UCRCENT00139590); **J**, *O. coloradensis* from Florida (UCRCENT00404257).

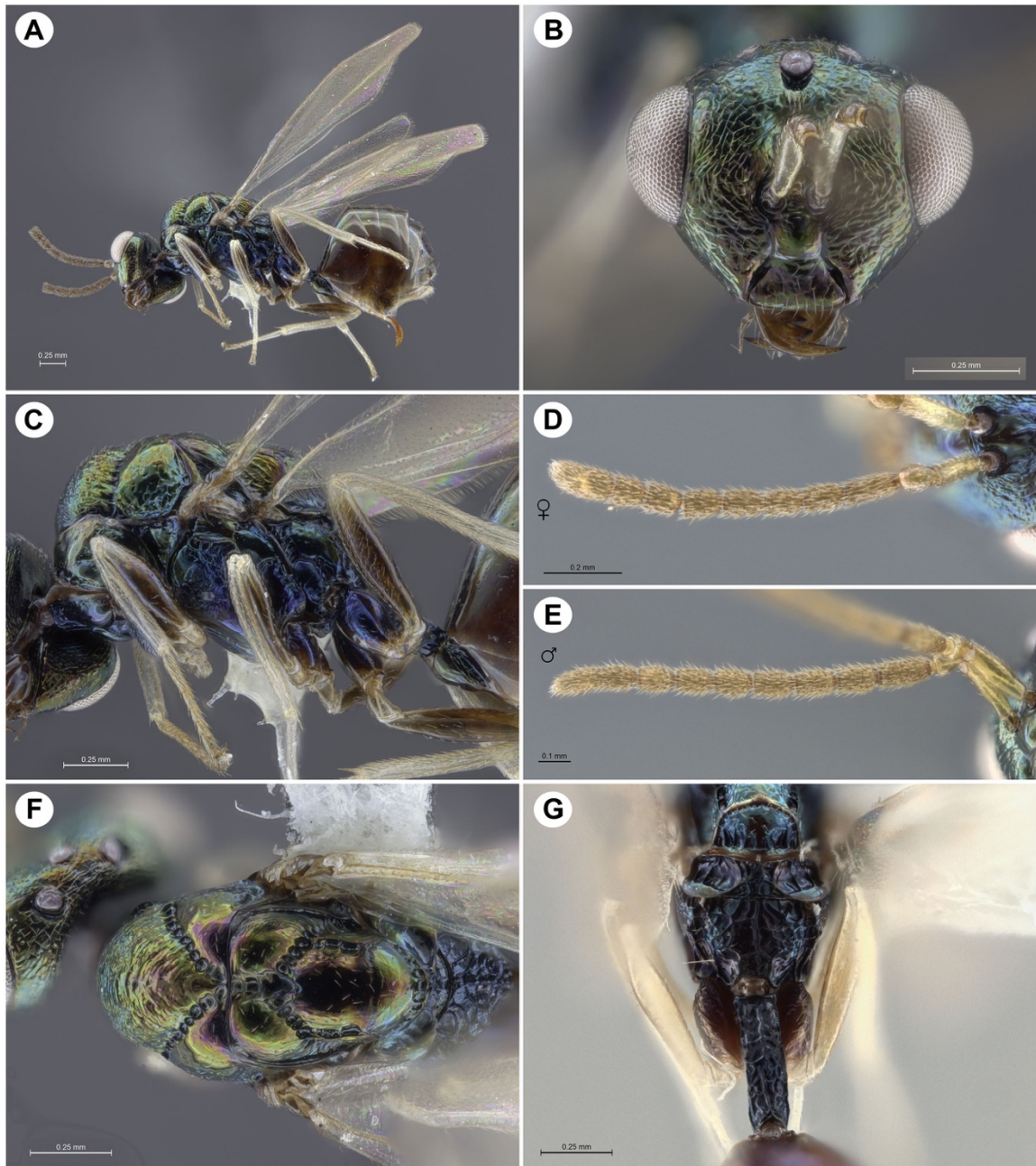


Figure 2.8: *Orasema iridescens*. Holotype female (UCRCENT00320816): **A**, habitus, lateral; **B**, head, anterior; **C**, mesosoma, lateral; **F**, mesosoma, dorsal; **G**, propodeum, posterior. Paratype female (UCRCENT00320829): **D**, antenna. Paratype male (UCRCENT00320835): **E**, antenna.

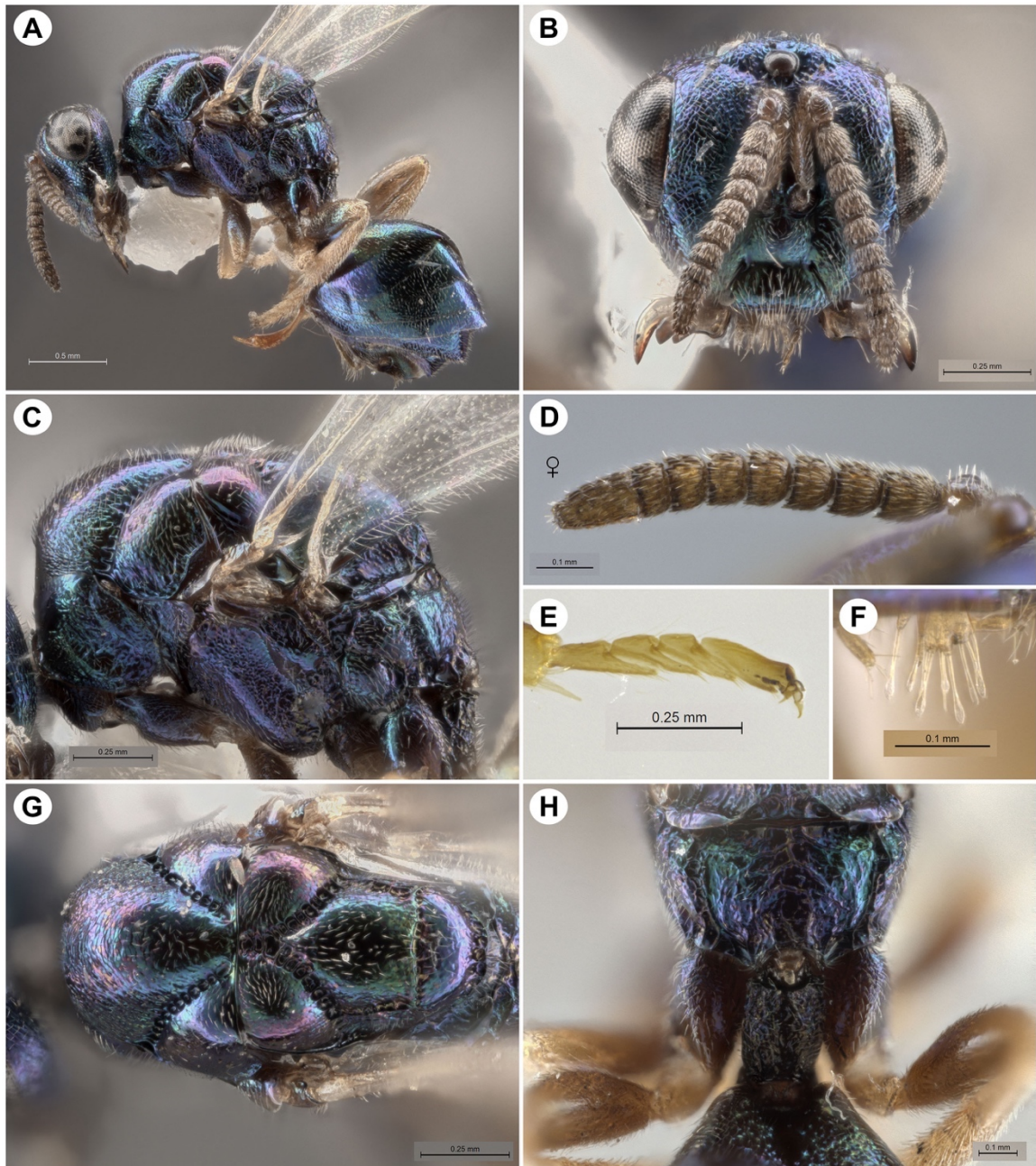


Figure 2.9: *Orasema scaura*. Holotype female (UCRCENT00407525): **A**, habitus, lateral; **B**, head, anterior; **C**, mesosoma, lateral; **D**, antenna; **G**, mesosoma, dorsal; **H**, propodeum, posterior. Female (UCRCENT00407508): **E**, tarsus. Paratype female (UCRCENT00407506): **F**, labrum.

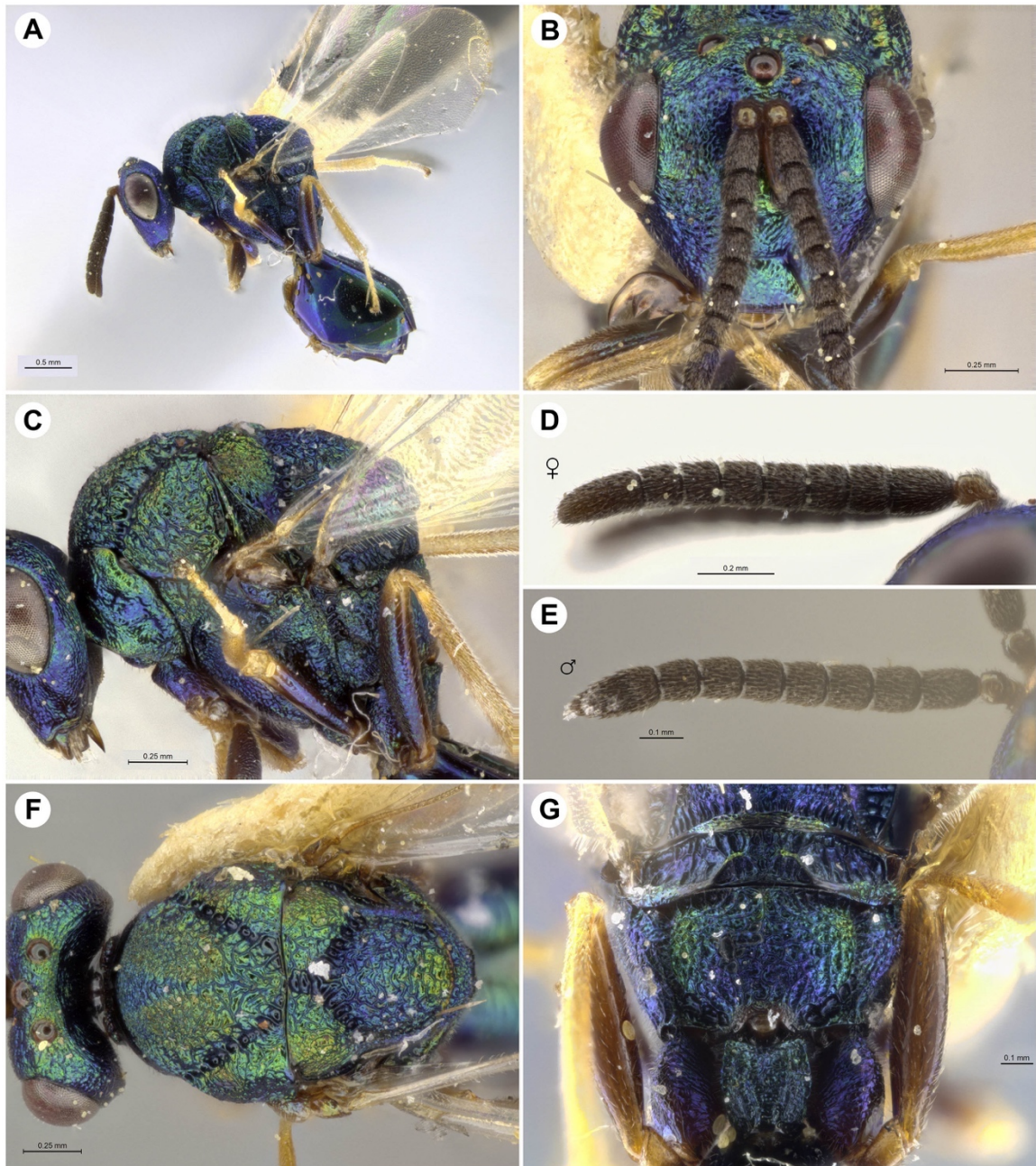


Figure 2.10: *Orasema violacea*. Female (UCRCENT00411756): **A**, habitus, lateral; **B**, head, anterior; **C**, mesosoma, lateral; **D**, antenna; **F**, mesosoma, dorsal; **G**, propodeum, posterior. Male (UCRCENT00248390): **E**, antenna.

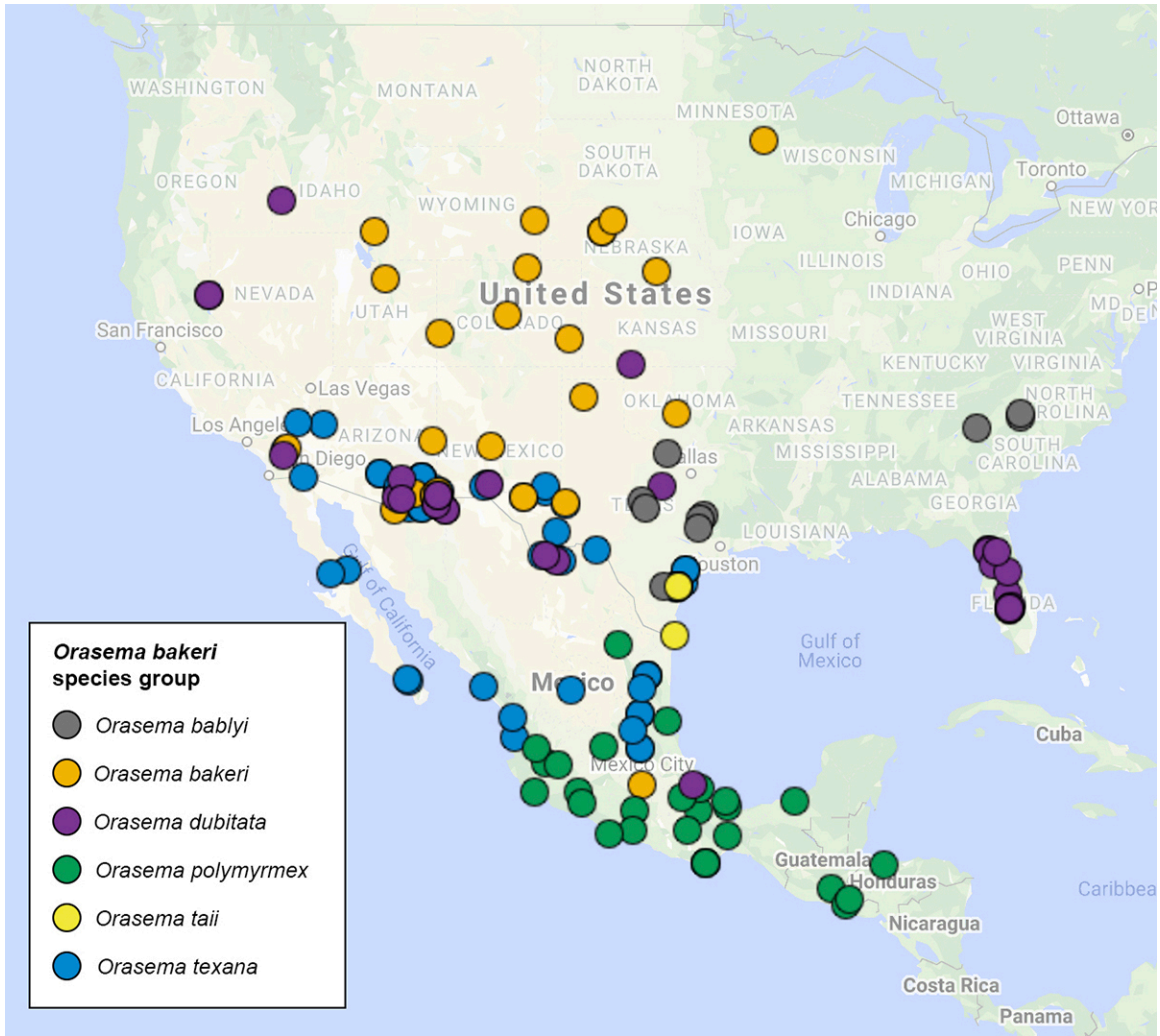


Figure 2.11: Distribution map of species in the *Orasema bakeri* species group.

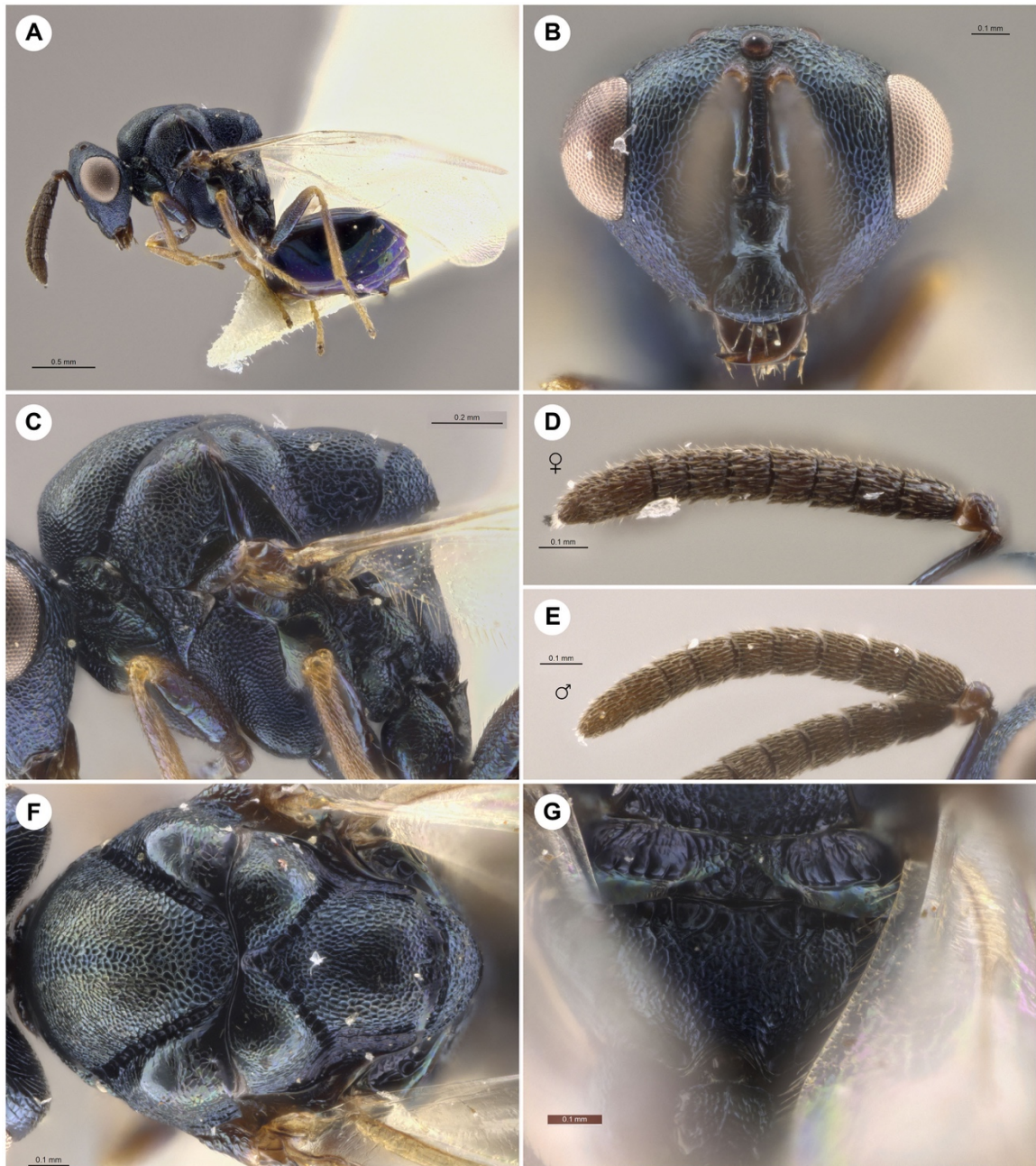


Figure 2.12: *Orasema bablyi*. Holotype female (UCRCENT00245271): **A**, habitus, lateral; **B**, head, anterior; **C**, mesosoma, lateral; **D**, antenna; **F**, mesosoma, dorsal; **G**, propodeum, posterior. Paratype male (UCRCENT00245279): **E**, antenna.

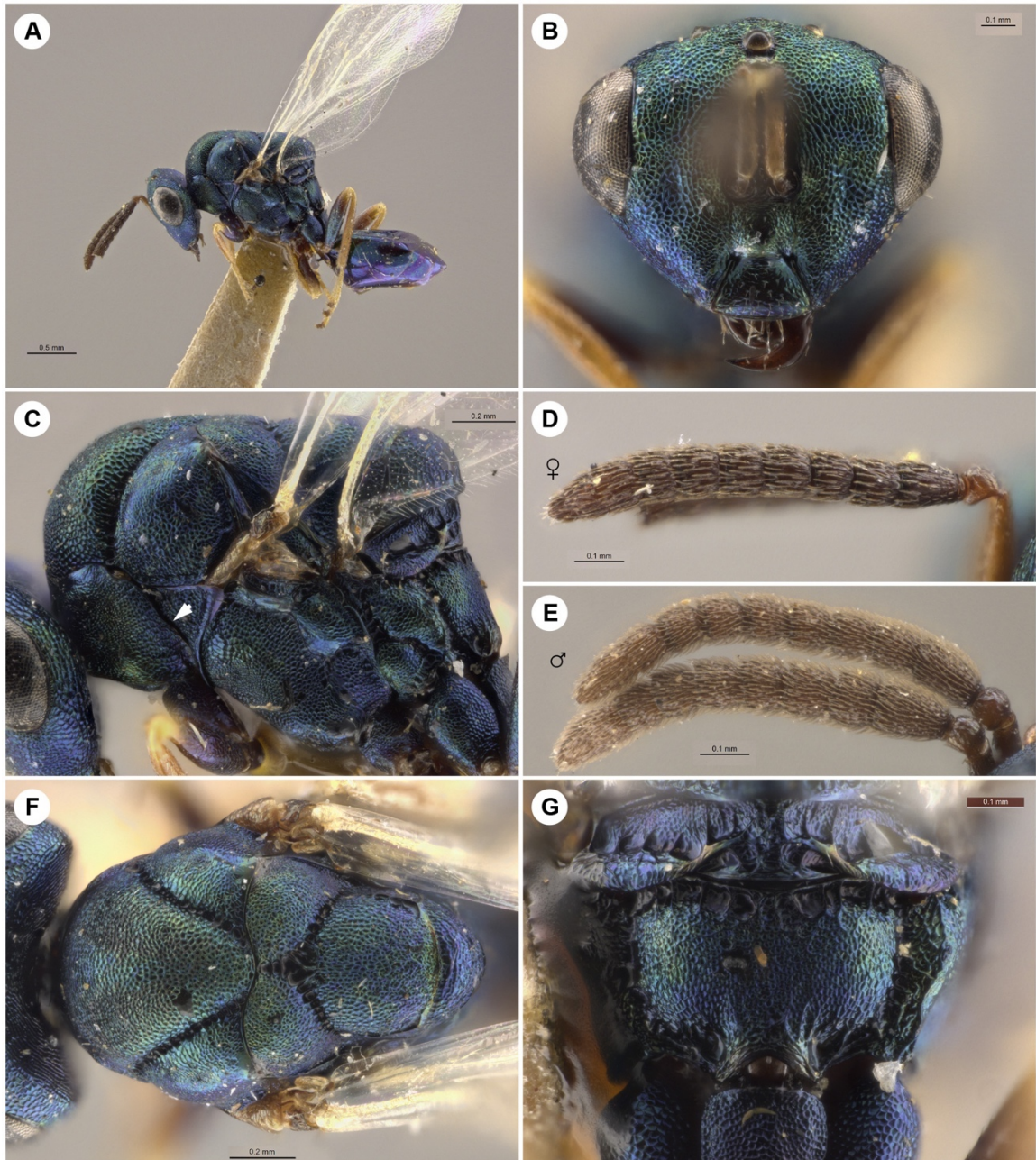


Figure 2.13: *Orasema bakeri*. Paratype female (UCRCENT00247810): **A**, habitus, lateral; **B**, head, anterior; **C**, mesosoma, lateral, arrow indicating lack of anterior prepectal carina; **D**, antenna; **F**, mesosoma, dorsal; **G**, propodeum, posterior. Allotype male (UCRCENT00247804): **E**, antenna.

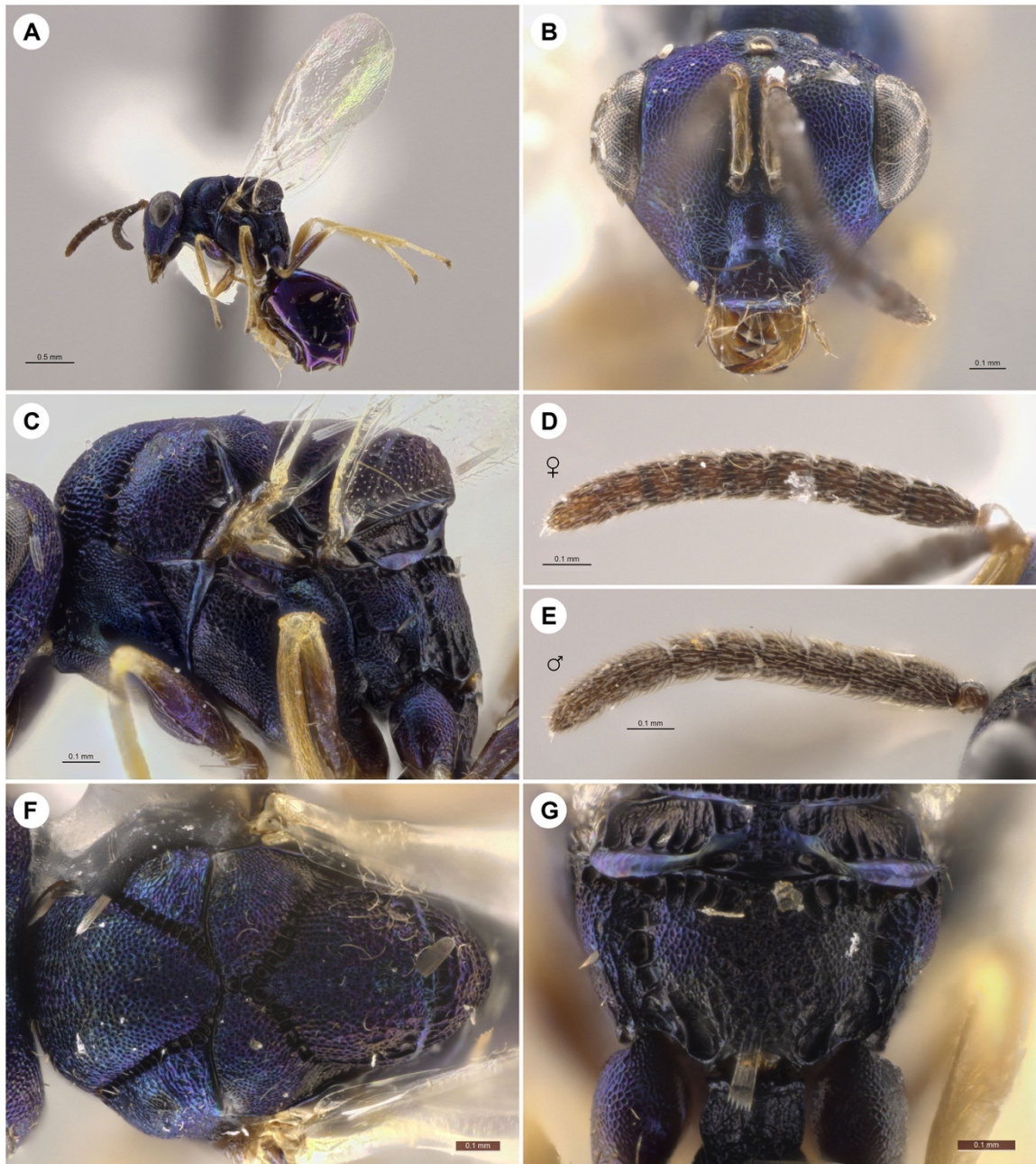


Figure 2.14: *Orasema dubitata*. Holotype female (UCRCENT00471759): **A**, habitus, lateral; **B**, head, anterior; **C**, mesosoma, lateral; **D**, antenna; **F**, mesosoma, dorsal; **G**, propodeum, posterior. Paratype male (UCRCENT00305342): **E**, antenna.

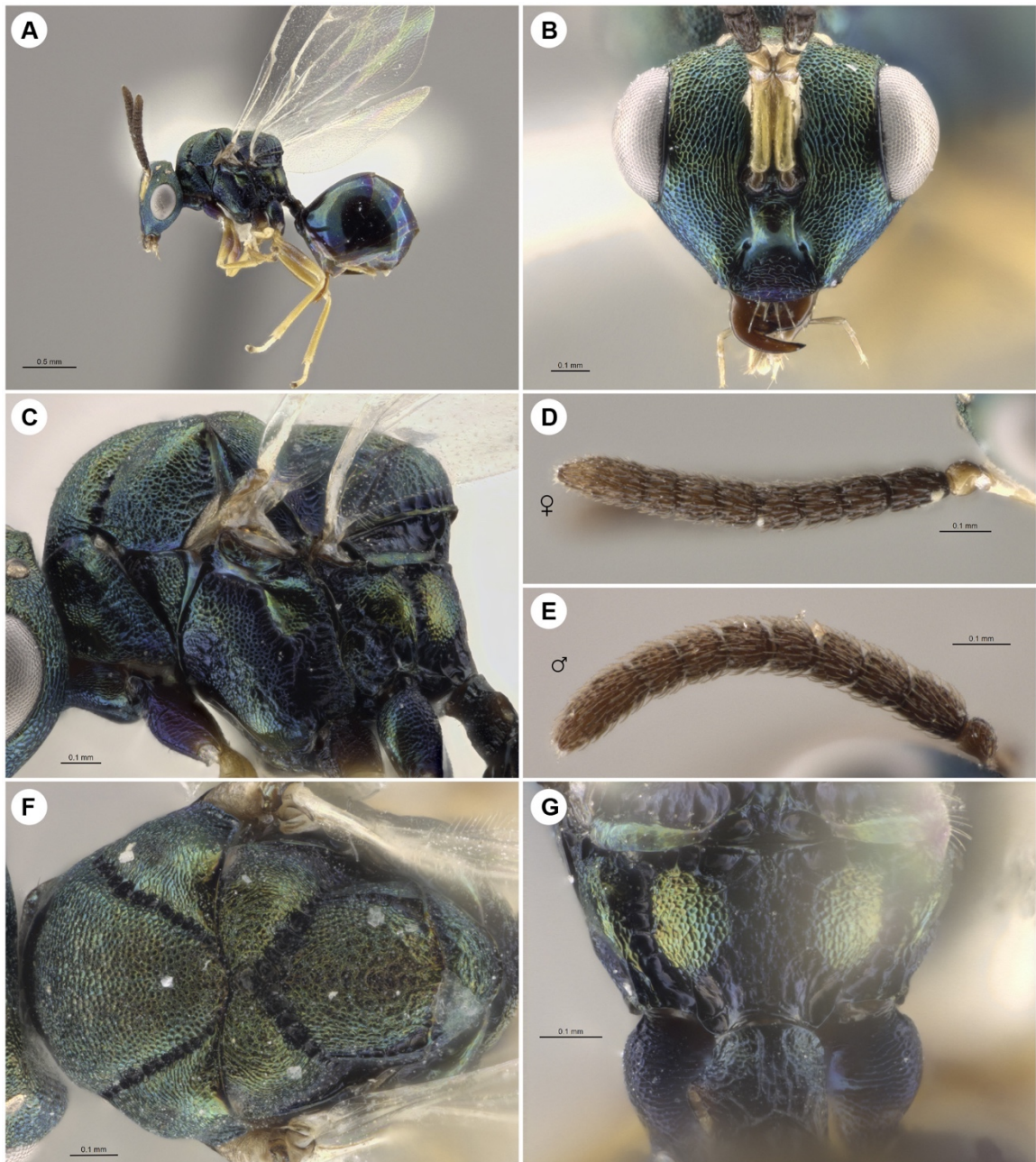


Figure 2.15: *Orasema polymyrmex*. Holotype female (UCRCENT00311872): **A**, habitus, lateral; **B**, head, anterior; **C**, mesosoma, lateral; **D**, antenna; **F**, mesosoma, dorsal; **G**, propodeum, posterior. Paratype male (UCRCENT00416800): **E**, antenna.

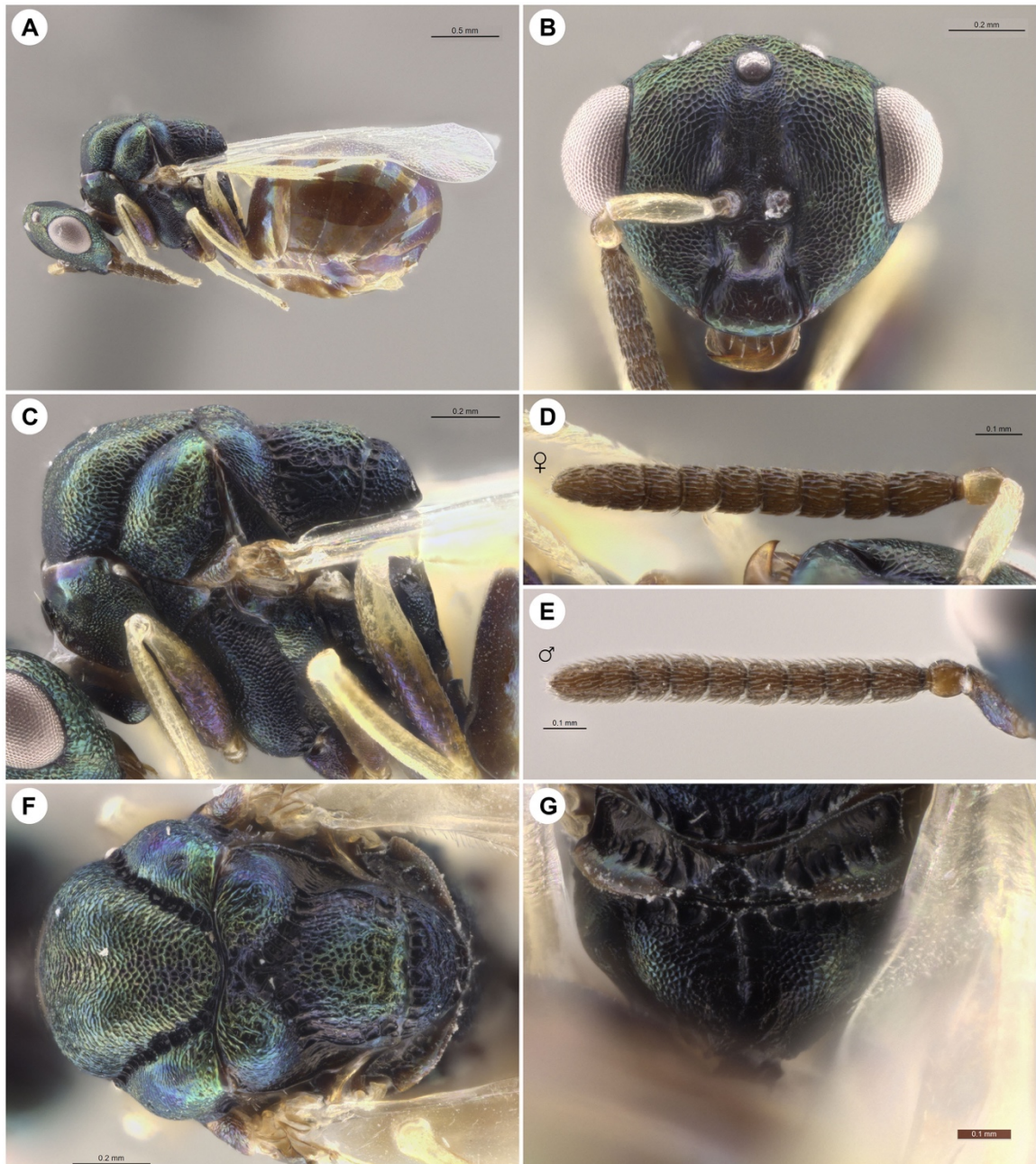


Figure 2.16: *Orasema texana*. Female (UCRCENT00412495): **A**, habitus, lateral; **B**, head, anterior; **C**, mesosoma, lateral; **D**, antenna; **F**, mesosoma, dorsal; **G**, propodeum, posterior. Male (UCRCENT00311934): **E**, antenna.

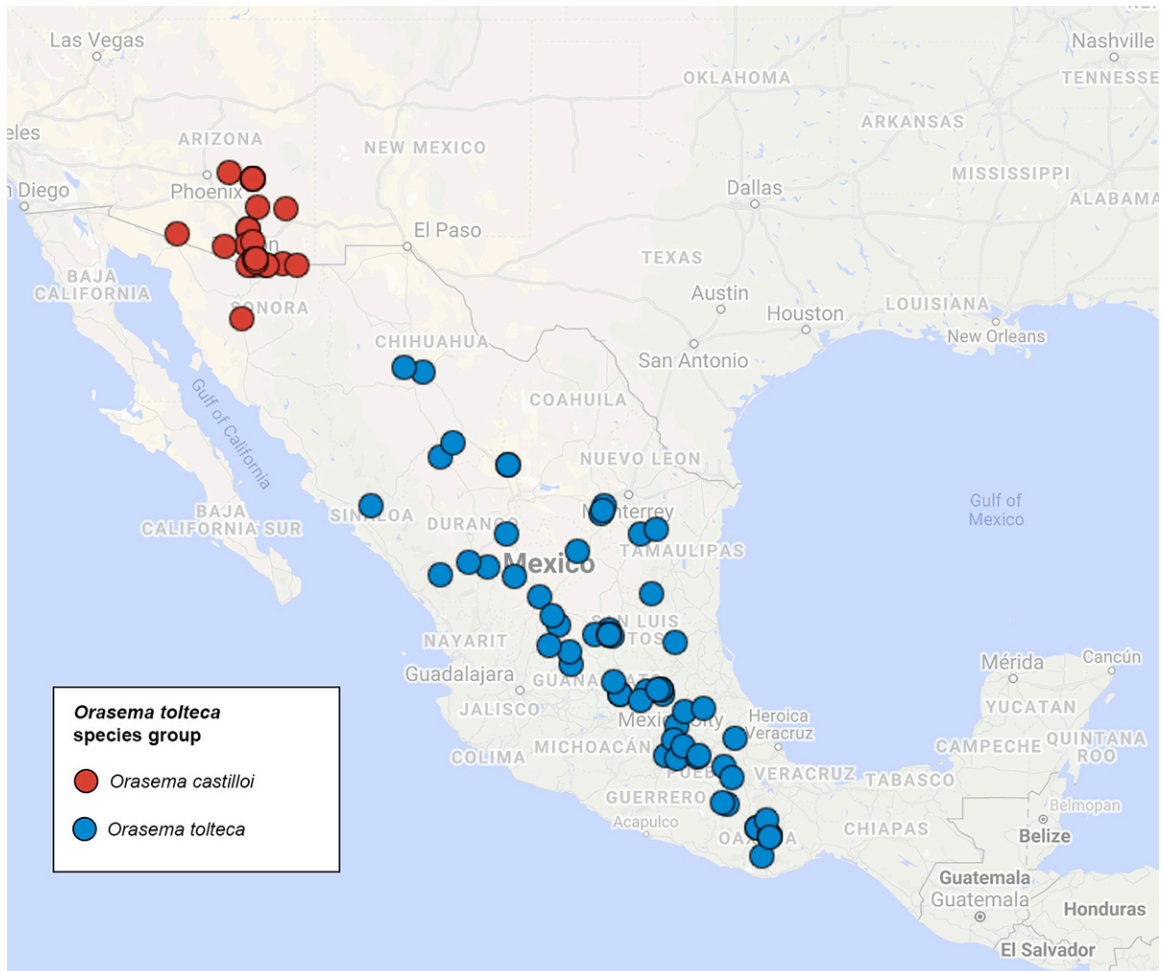


Figure 2.17: Distribution map of species in the *Orasema tolteca* species group.

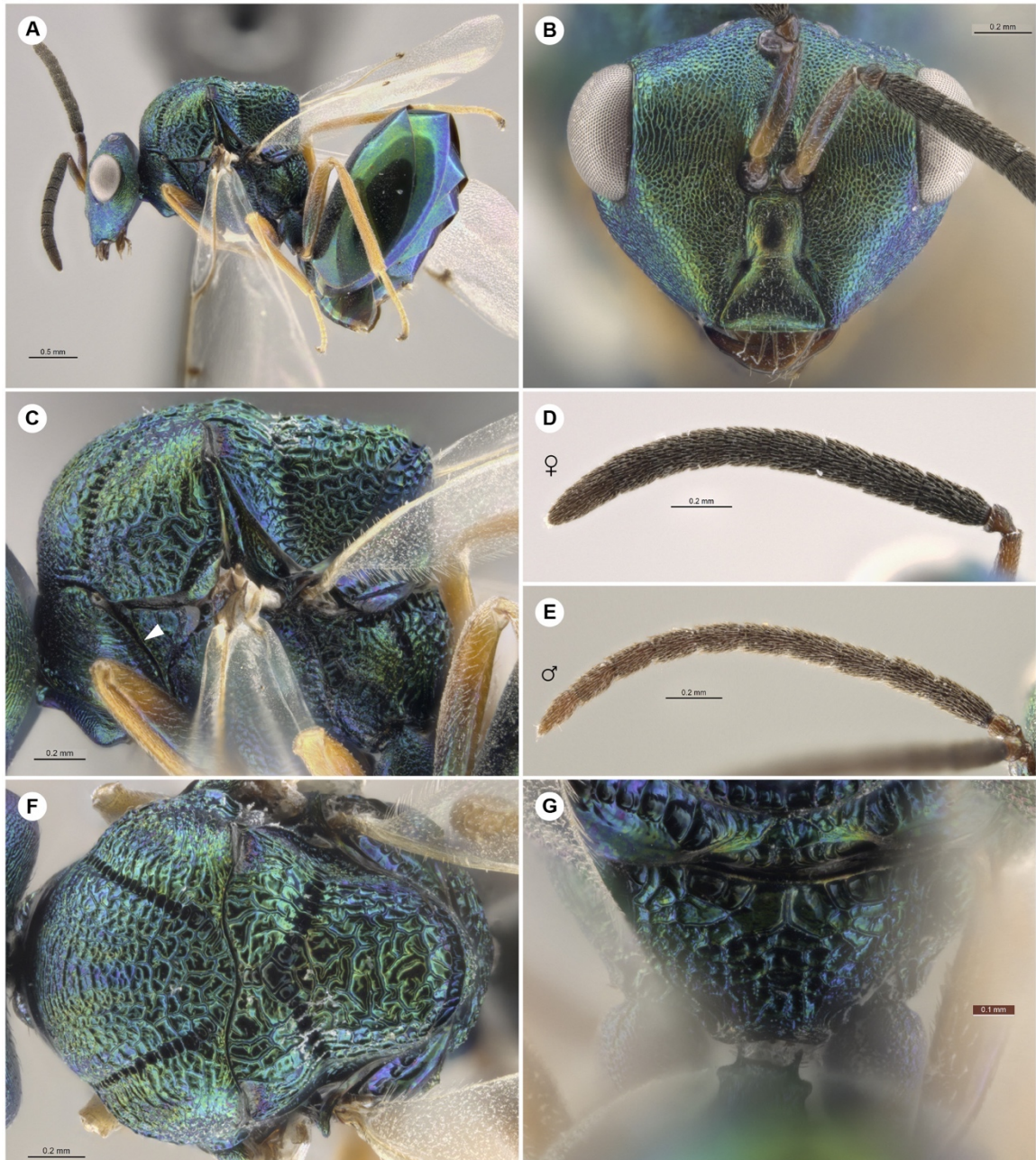


Figure 2.18: *Orasema castilloae*. Holotype female (UCRCENT00412574): **A**, habitus, lateral; **B**, head, anterior; **C**, mesosoma, lateral, arrow indicating presence of anterior prepectal carina; **D**, antenna; **F**, mesosoma, dorsal; **G**, propodeum, posterior. Paratype male (UCRCENT00416866): **E**, antenna.

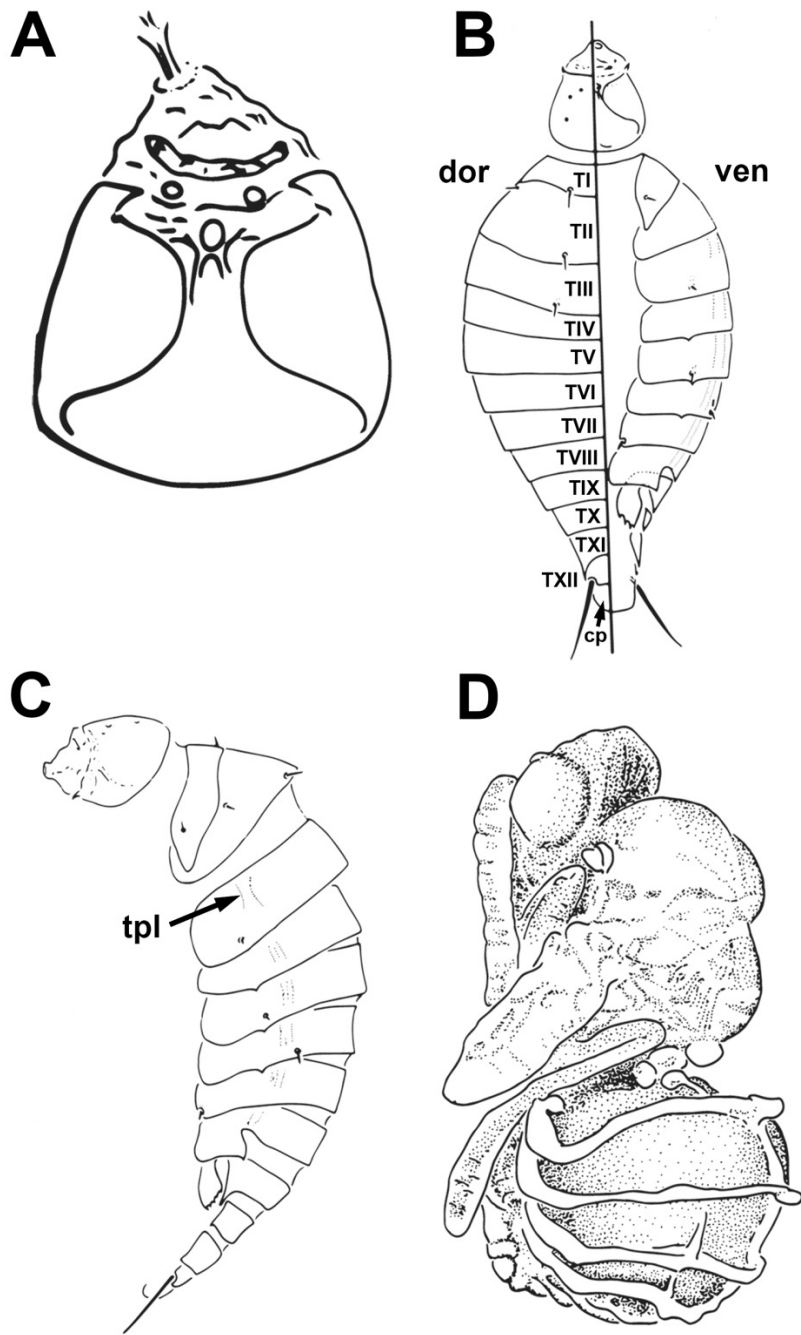


Figure 2.19: Immature stages of *Orasema toteca*. **A**, planidium head, ventral; **B**, planidium habitus (dorsal left and ventral right); **C**, planidium habitus, lateral. **D**, pupa habitus, dorsolateral. Modified from Heraty (1990).

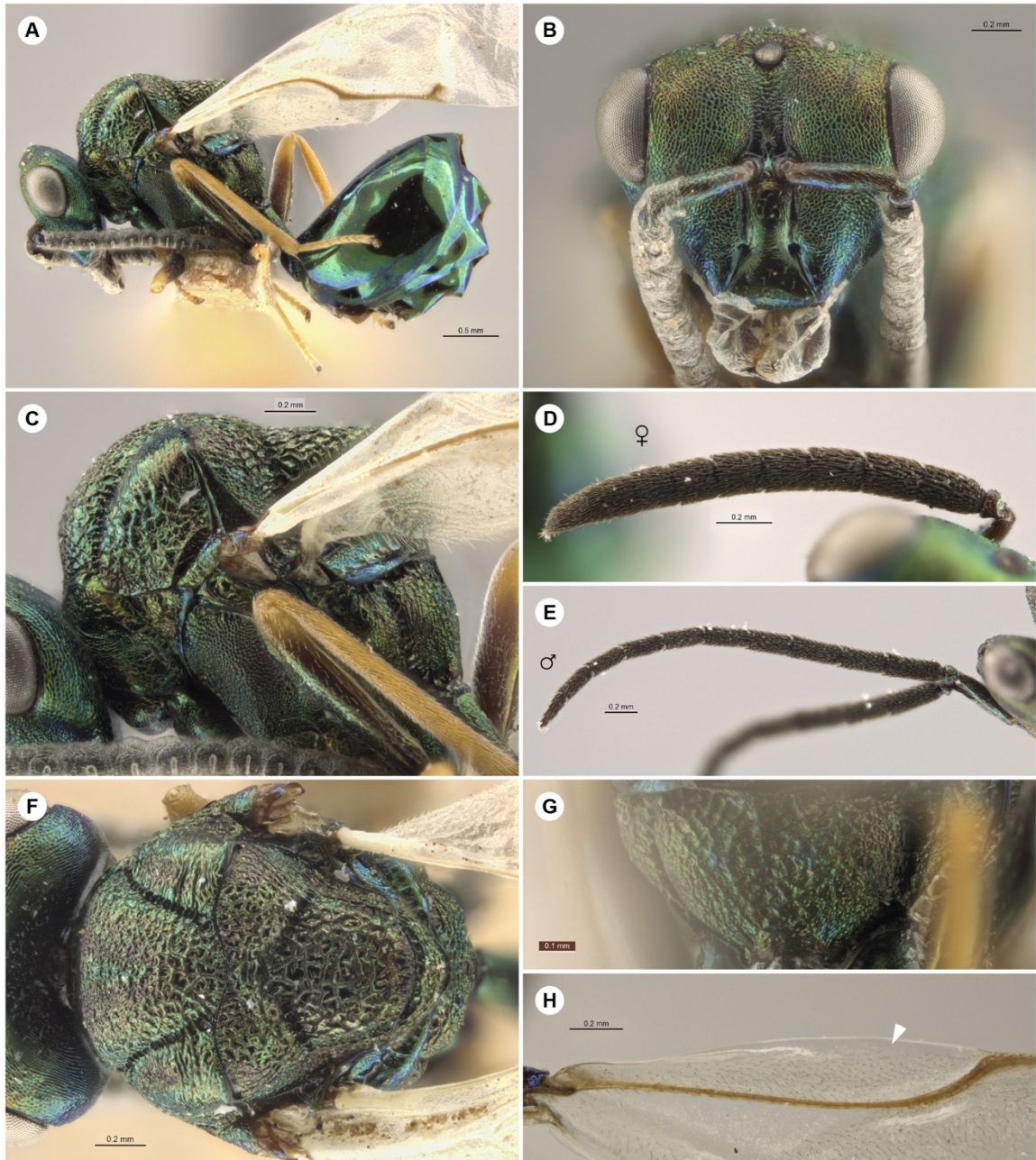


Figure 2.20: *Orasema tolteca*. Syntype female (UCRCENT00318645): **A**, habitus, lateral; **B**, head, anterior; **C**, mesosoma, lateral; **D**, antenna; **F**, mesosoma, dorsal; **G**, propodeum, posterior. Male (UCRCENT00417437): **E**, antenna. Female (UCRCENT00478756): **H**, fore wing costal cell, arrow indicating bare anterior area.



Figure 2.21: Distribution map of species in the *Orasema sixaolae* species group.



Figure 2.22: *Orasema brachycephala*. Holotype female (UCRCENT00247554): **A**, habitus, lateral; **B**, head, anterior; **C**, mesosoma, lateral; **D**, antenna; **E**, mesosoma, dorsal; **F**, propodeum, posterior.

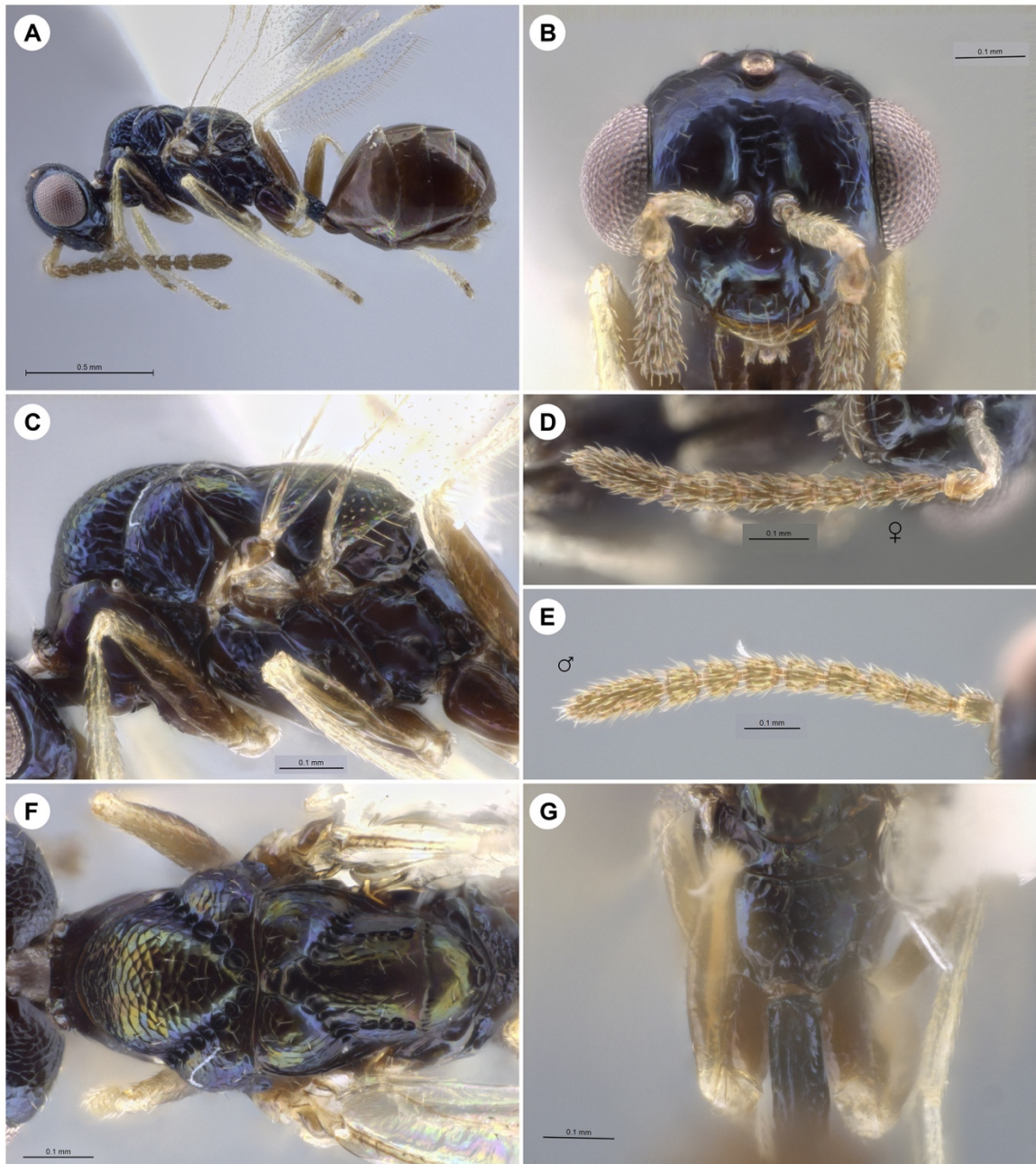


Figure 2.23: *Orasema nebula*. Holotype female (UCRCENT00247795): **A**, habitus, lateral; **B**, head, anterior; **C**, mesosoma, lateral; **D**, antenna; **F**, mesosoma, dorsal; **G**, propodeum, posterior. Paratype male (UCRCENT00247799): **E**, antenna.

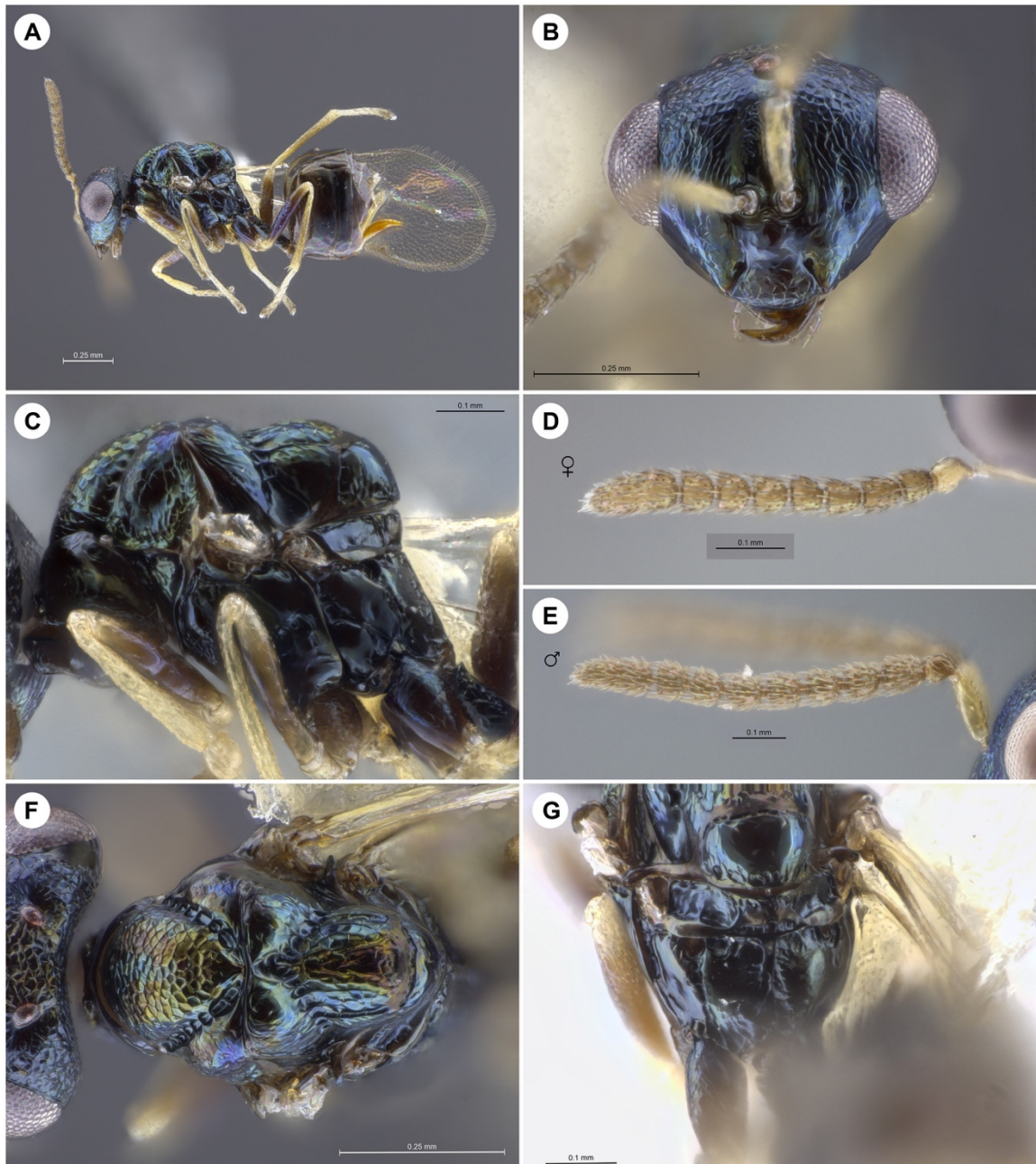


Figure 2.24: *Orasema sixaolae*. Female (UCRCENT00282692): **A**, habitus, lateral; **B**, head, anterior; **C**, mesosoma, lateral; **D**, antenna; **F**, mesosoma, dorsal; **G**, propodeum, posterior. Male (UCRCENT00247779): **E**, antenna.

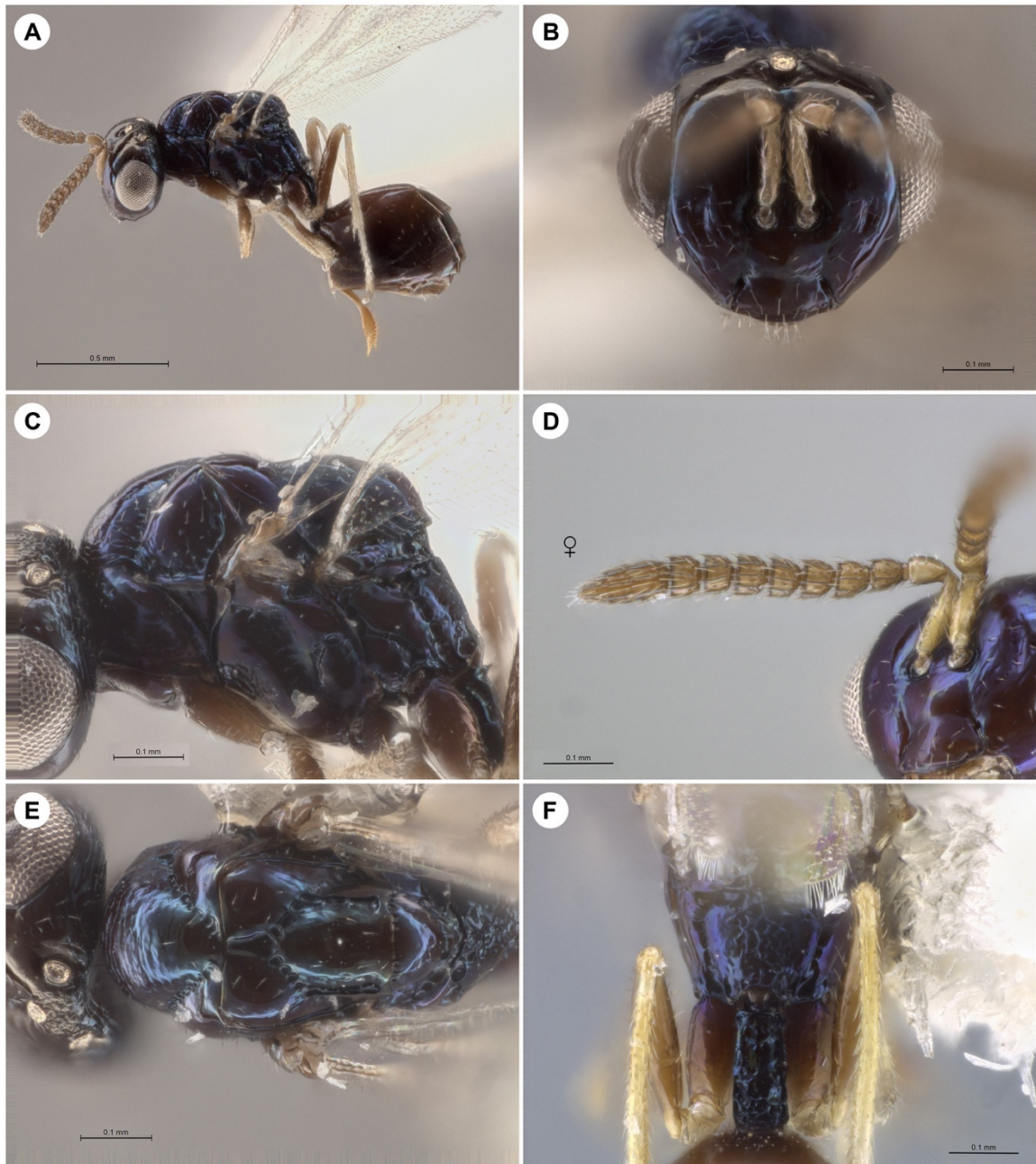


Figure 2.25: *Orasema tinalandia*. Holotype female (UCRCENT00247552): **A**, habitus, lateral; **B**, head, anterior; **C**, mesosoma, lateral; **D**, antenna; **E**, mesosoma, dorsal; **F**, propodeum, posterior.



Figure 2.26: Distribution map of species in the *Orasema acuminata* species group.

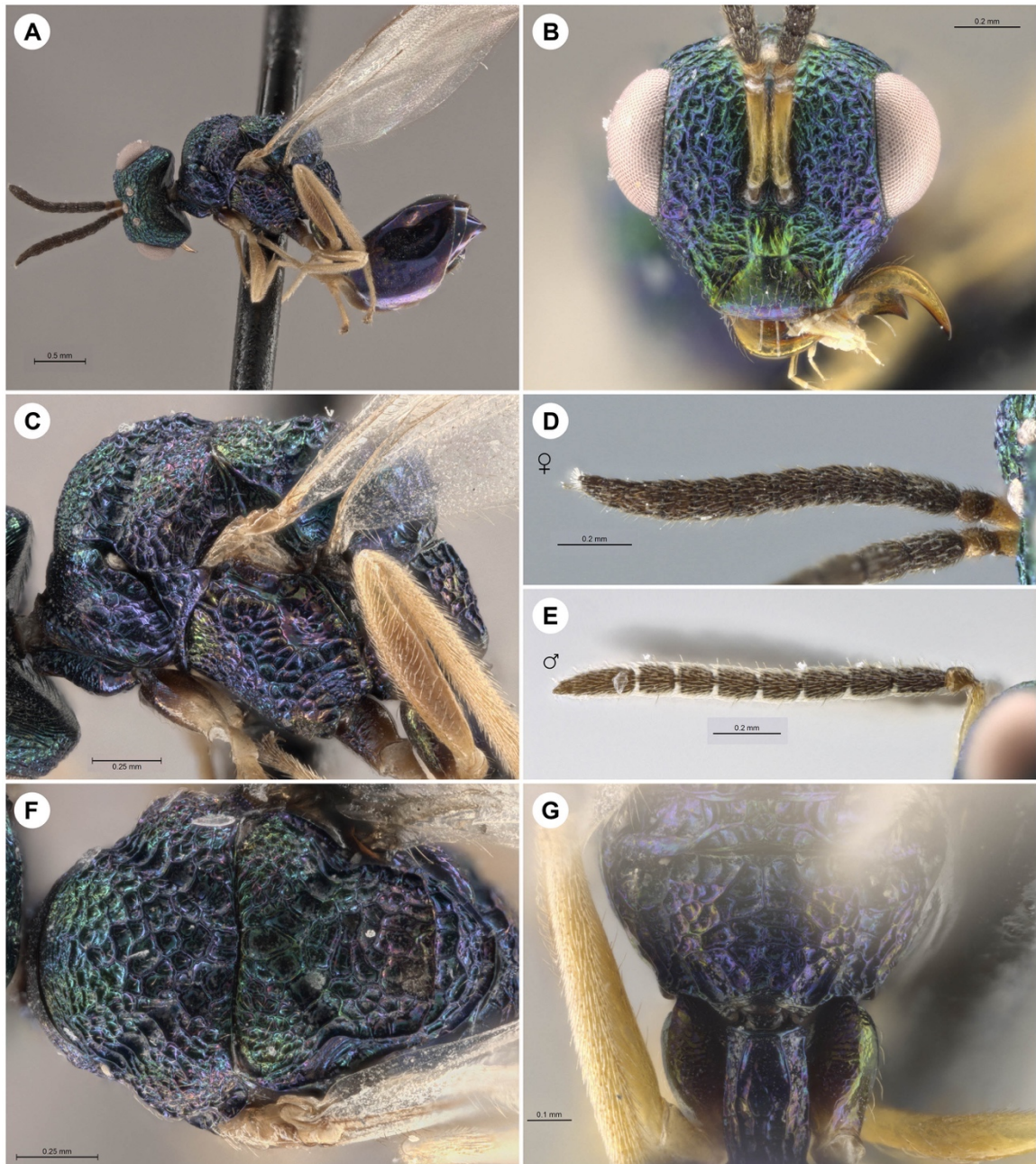


Figure 2.27: *Orasema acuminata*. Holotype female (UCRCENT00415025): **A**, habitus, lateral; **B**, head, anterior; **C**, mesosoma, lateral; **D**, antenna; **F**, mesosoma, dorsal; **G**, propodeum, posterior. Paratype male (UCRCENT00247959): **E**, antenna.

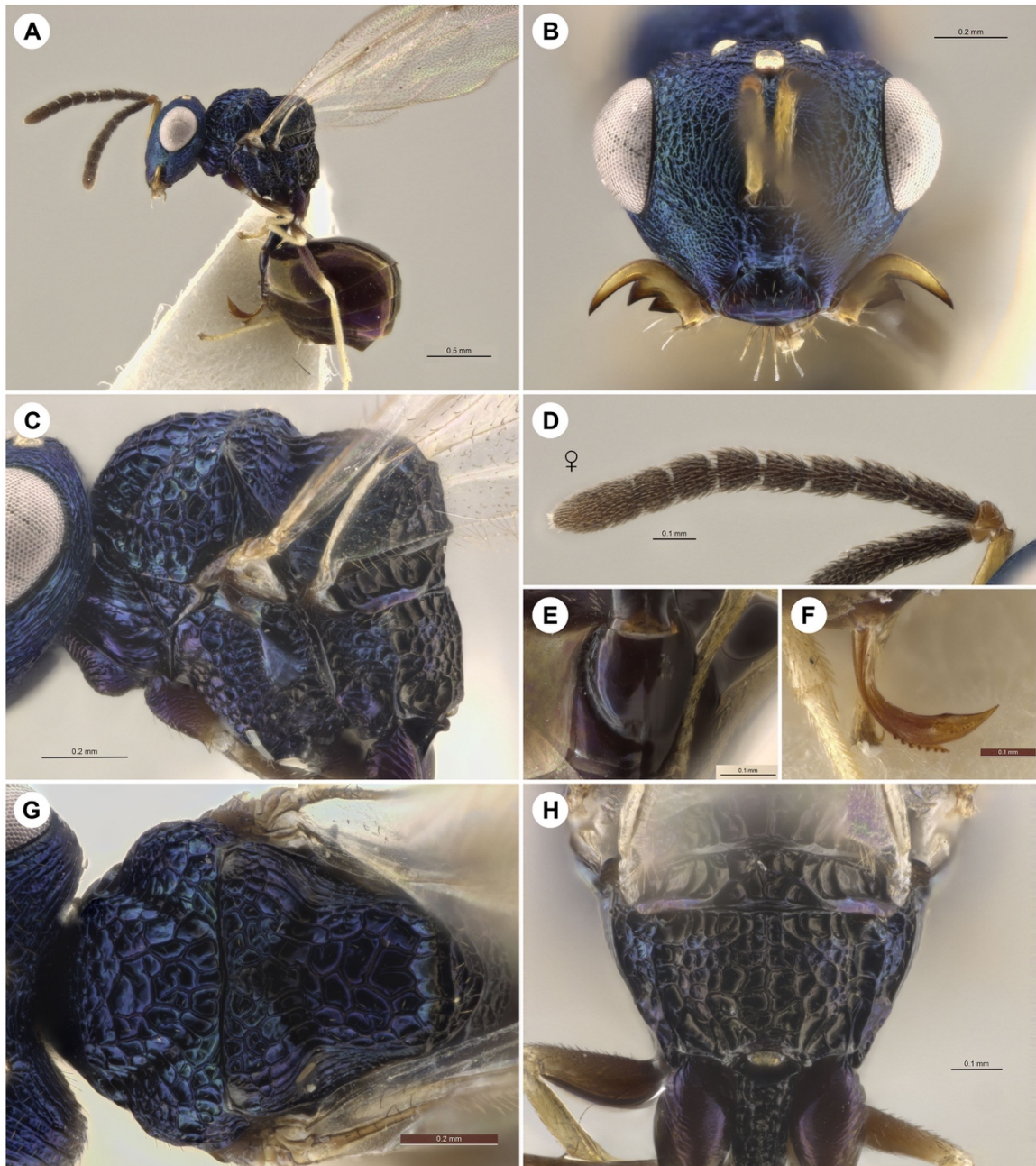


Figure 2.28: *Orasema cerulea*. Holotype female (UCRCENT00242604): **A**, habitus, lateral; **B**, head, anterior; **C**, mesosoma, lateral; **D**, antenna; **E**, acrosternite, anterior; **F**, ovipositor, lateral; **G**, mesosoma, dorsal; **H**, propodeum, posterior.



Figure 2.29: Distribution map of species in the *Orasema hippocephala* species group.

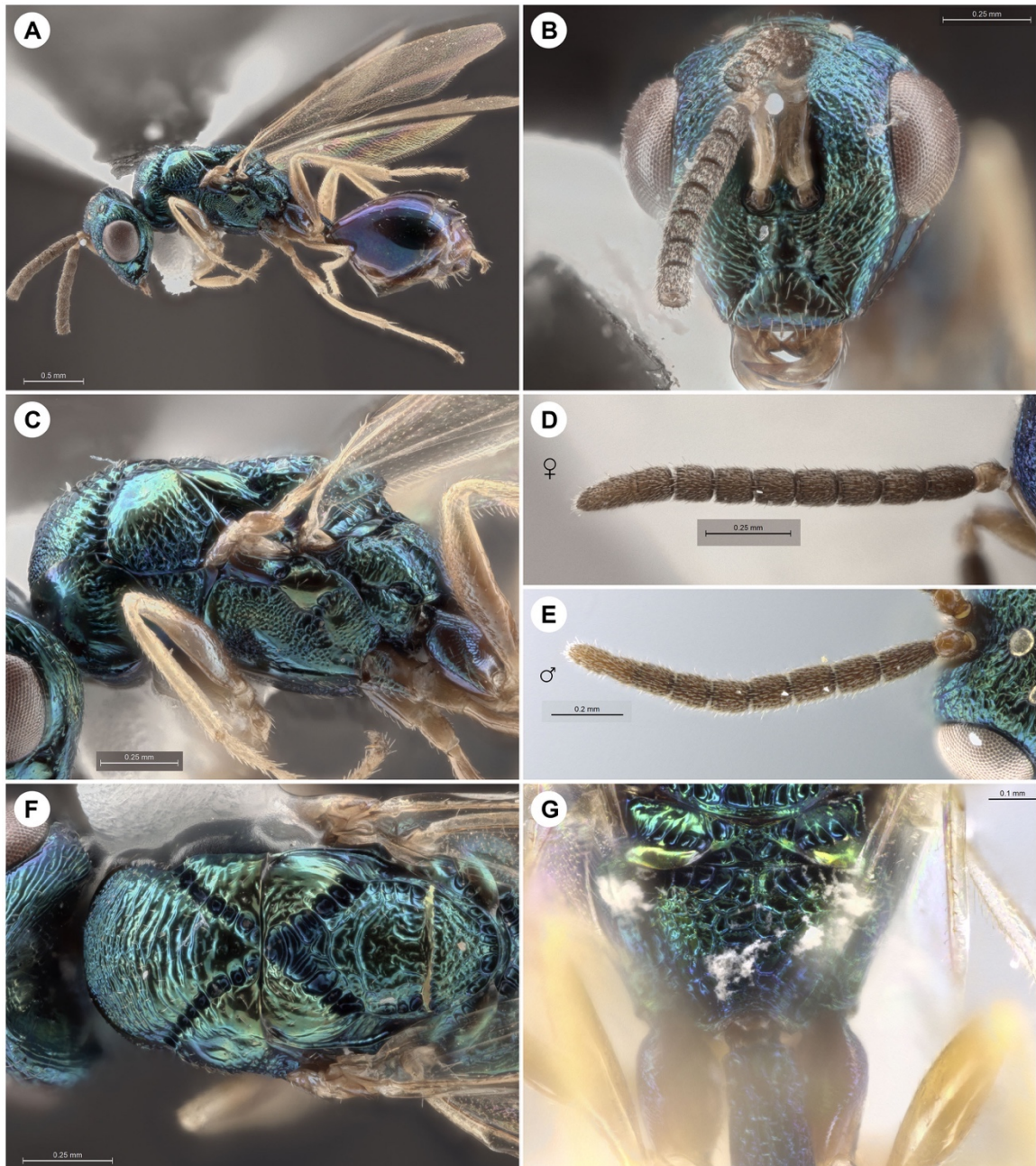


Figure 2.30: *Orasema chrysozona*. Holotype female (UCRCENT00436599): **A**, habitus, lateral; **B**, head, anterior; **C**, mesosoma, lateral; **F**, mesosoma, dorsal; **G**, propodeum, posterior. Paratype female (UCRCENT00169639): **D**, antenna. Paratype male (UCRCENT00320986): **E**, antenna.

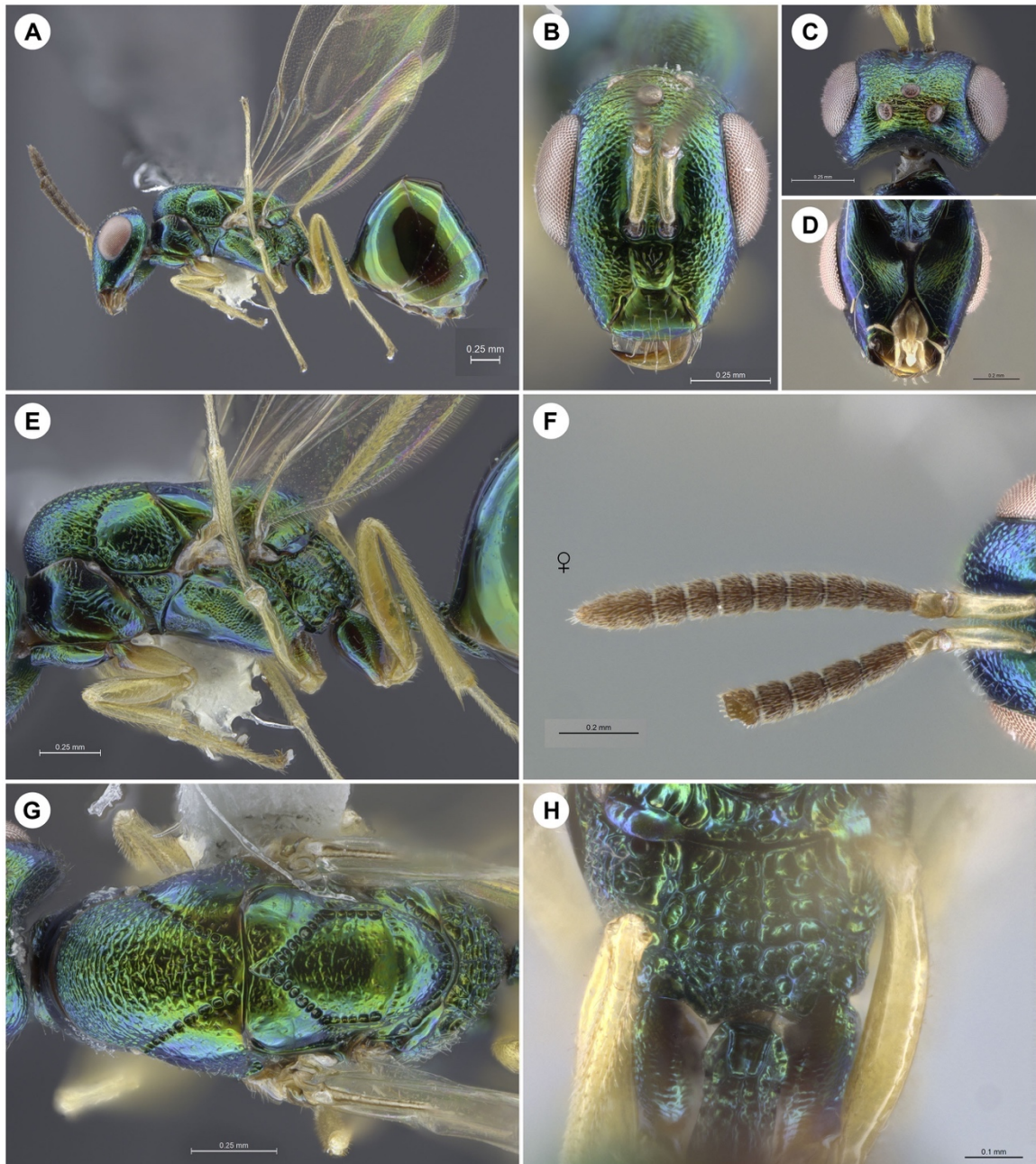


Figure 2.31: *Orasema hippocephala*. Holotype female (UCRCENT00434580): **A**, habitus, lateral; **B**, head, anterior; **E**, mesosoma, lateral; **F**, antenna; **G**, mesosoma, dorsal; **H**, propodeum, posterior. Paratype female (UCRCENT00161481): **C**, head, dorsal. Paratype female (UCRCENT00436704): **D**, head, posterior.



Figure 2.32: Distribution map of species in the *Orasema johnsoni* species group.

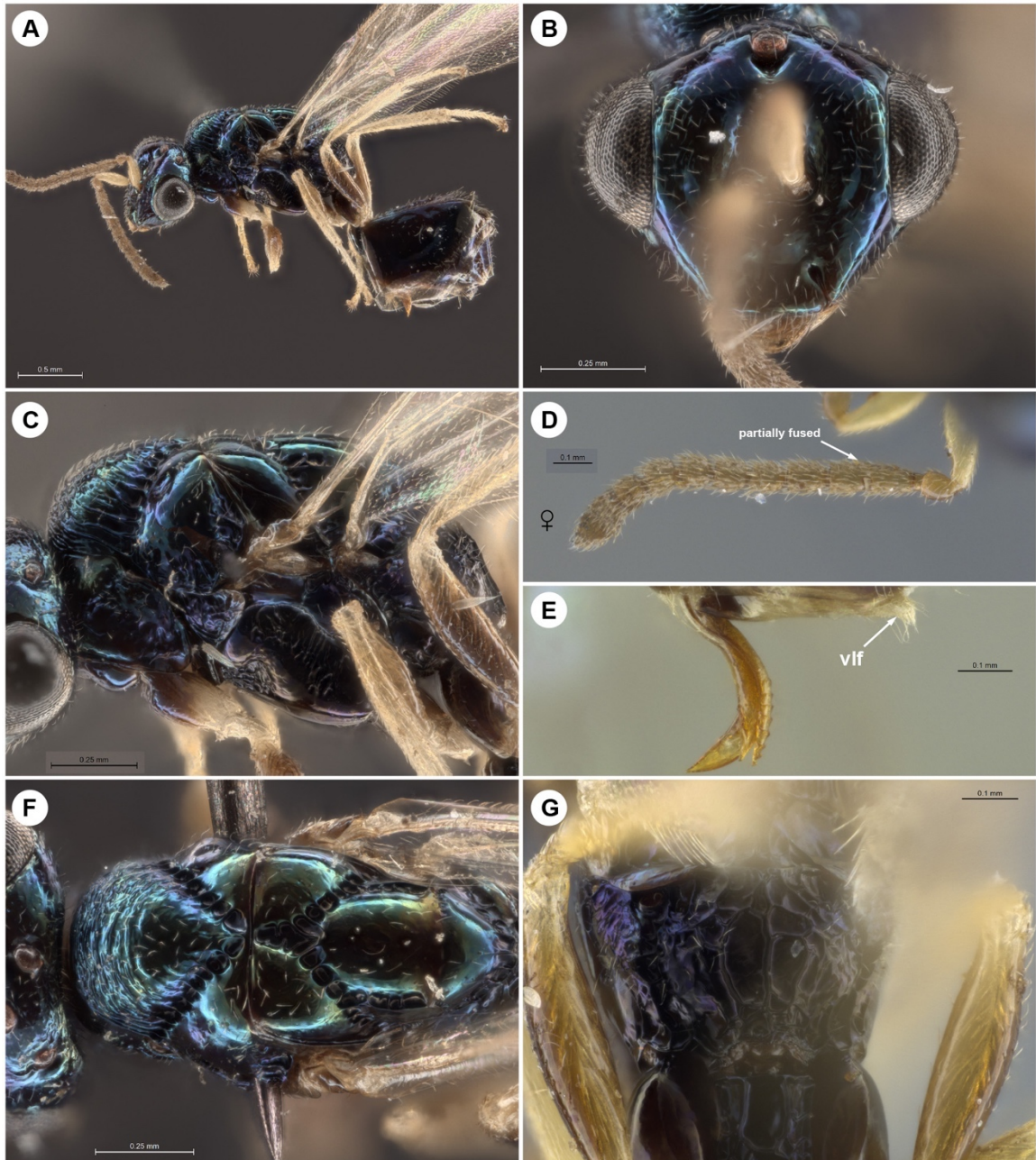


Figure 2.33: *Orasema johnsoni*. Holotype female (UCRCENT00238022): **A**, habitus, lateral; **B**, head, anterior; **C**, mesosoma, lateral; **D**, antenna showing partial fusion of F2 and F3; **F**, mesosoma, dorsal; **G**, propodeum, posterior. Paratype female (UCRCENT00439199): **E**, ovipositor and valvifer, lateral.

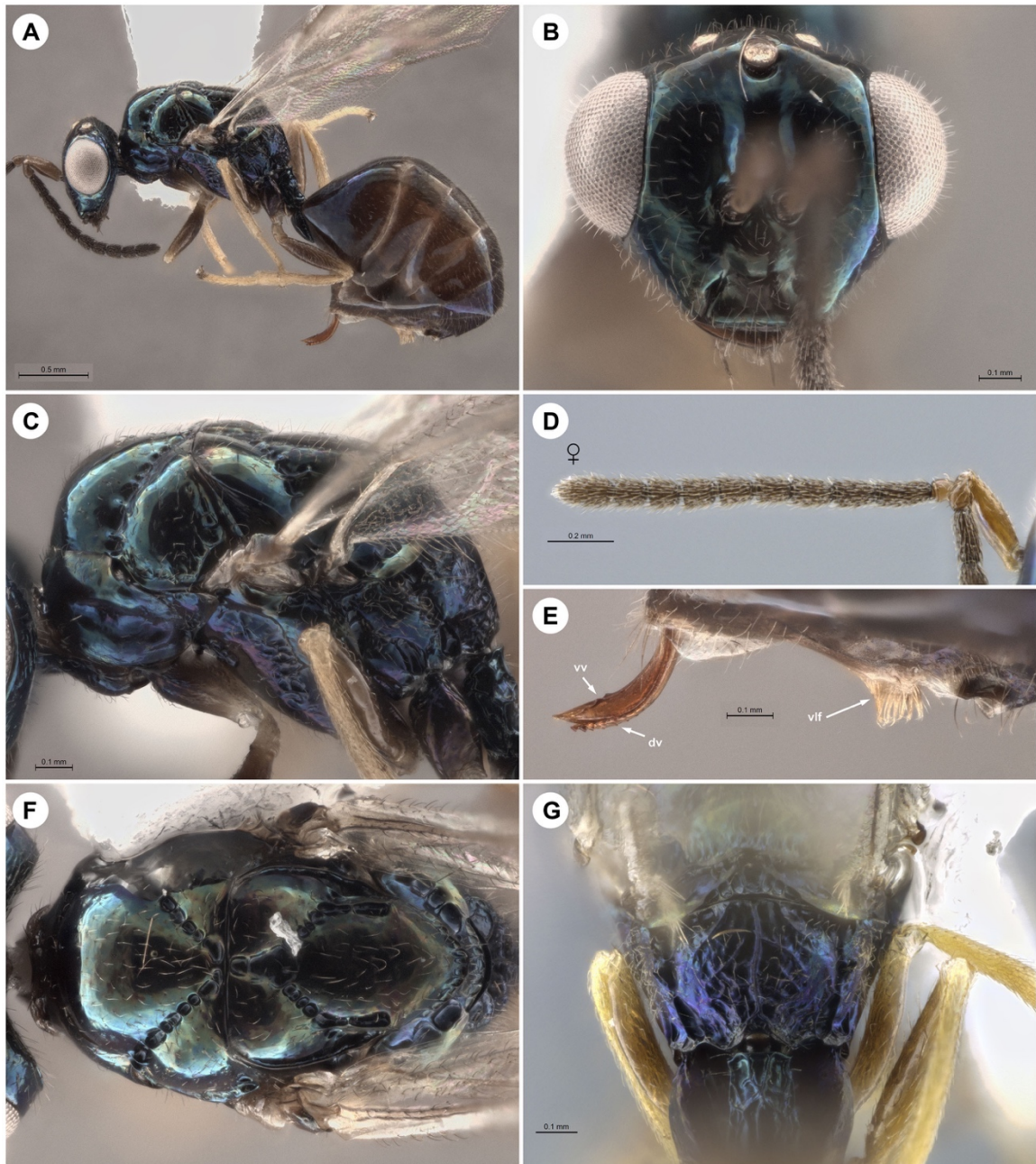


Figure 2.34: *Orasema spyrogaster*. Holotype female (UCRCENT00540573): **A**, habitus, lateral; **B**, head, anterior; **C**, mesosoma, lateral; **D**, antenna; **E**, ovipositor and valvifer, lateral; **F**, mesosoma, dorsal; **G**, propodeum, posterior.



Figure 2.35: Distribution map of species in the *Orasema heacoxi* species group.

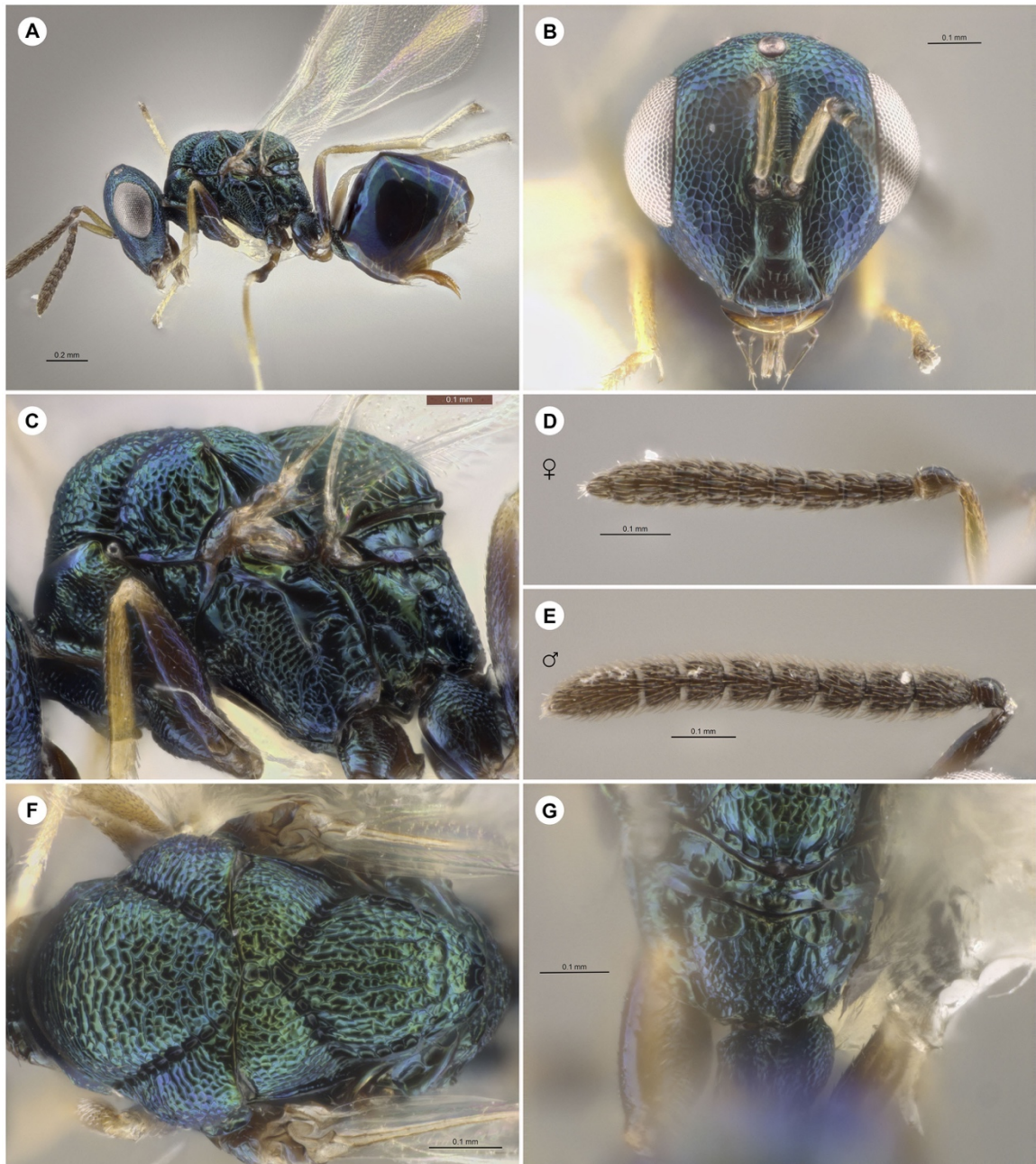


Figure 2.36: *Orasema heacoxi*. Holotype female (UCRCENT00414529): **A**, habitus, lateral; **B**, head, anterior; **C**, mesosoma, lateral; **D**, antenna; **F**, mesosoma, dorsal; **G**, propodeum, posterior. Paratype male (UCRCENT00436485): **E**, antenna.

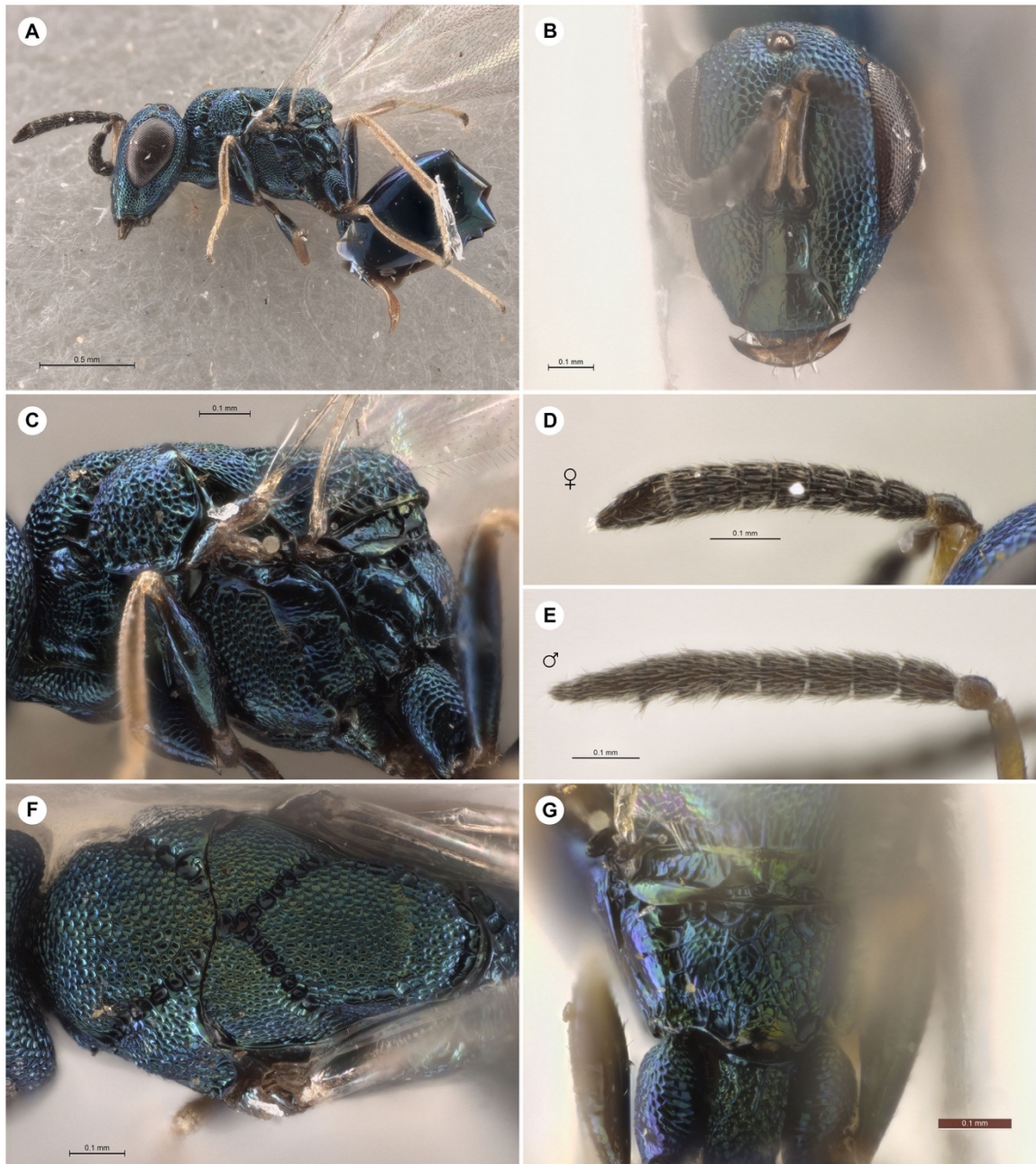


Figure 2.37: *Orasema masonicki*. Holotype female (INBIOCRI002242095): **A**, habitus, lateral; **B**, head, anterior; **C**, mesosoma, lateral; **D**, antenna; **F**, mesosoma, dorsal; **G**, propodeum, posterior. Paratype male (INBIOCRI002133102): **E**, antenna.



Figure 2.38: Distribution map of unplaced *Orasema* species.

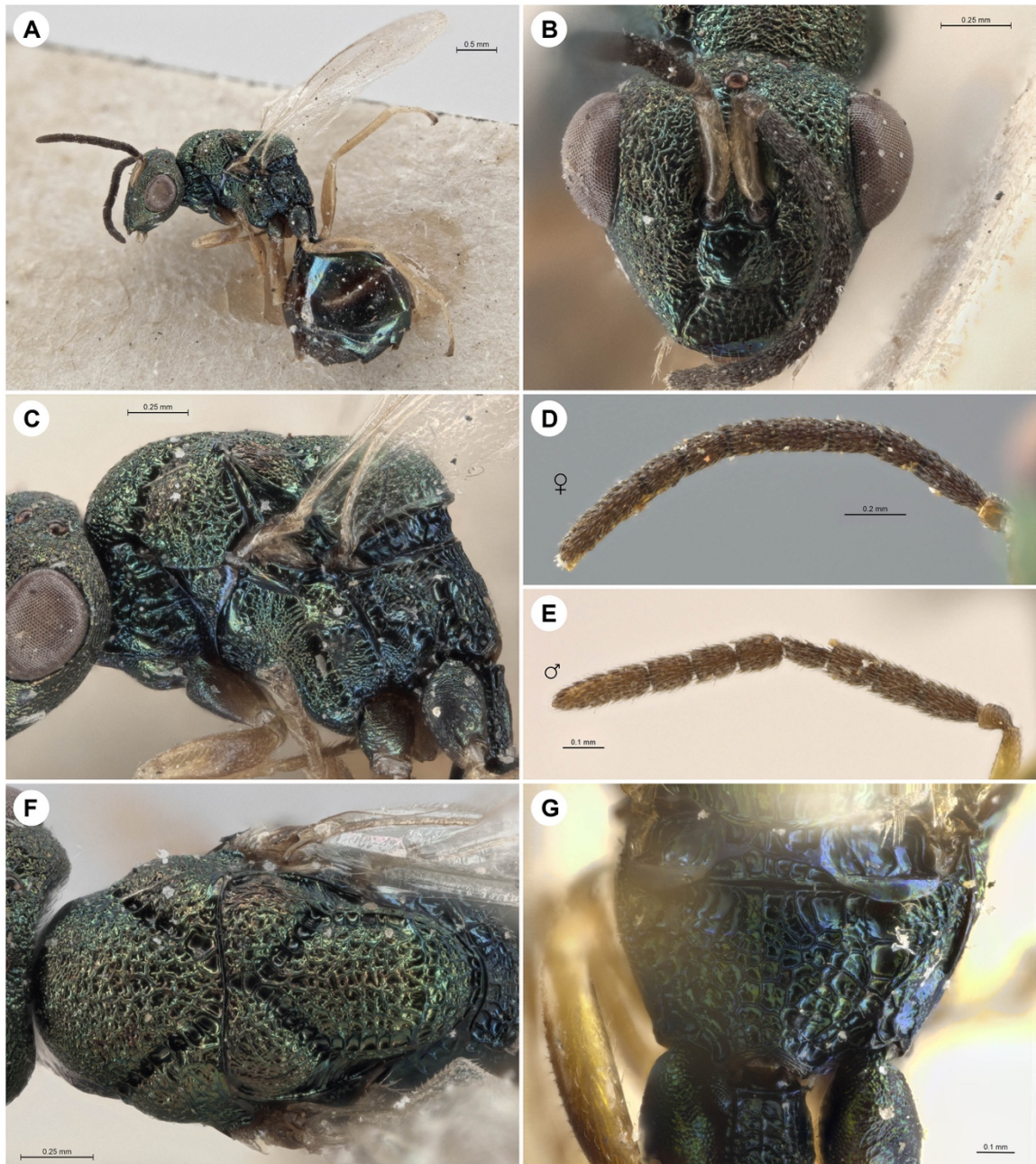


Figure 2.39: *Orasema brasiliensis*. Syntype female (UCRCENT00439039): **A**, habitus, lateral; **B**, head, anterior; **C**, mesosoma, lateral; **D**, antenna; **F**, mesosoma, dorsal; **G**, propodeum, posterior. Male (UCRCENT00238118): **E**, antenna.



Figure 2.40: *Orasema cirrhocnemis*. Holotype female (UCRCENT00417413): **A**, habitus, lateral (inset: stigmatal vein, wing apex to the right); **B**, head, anterior; **C**, mesosoma, lateral; **D**, antenna; **E**, metatibia and tarsus; **F**, mesosoma, dorsal; **G**, propodeum, posterior.

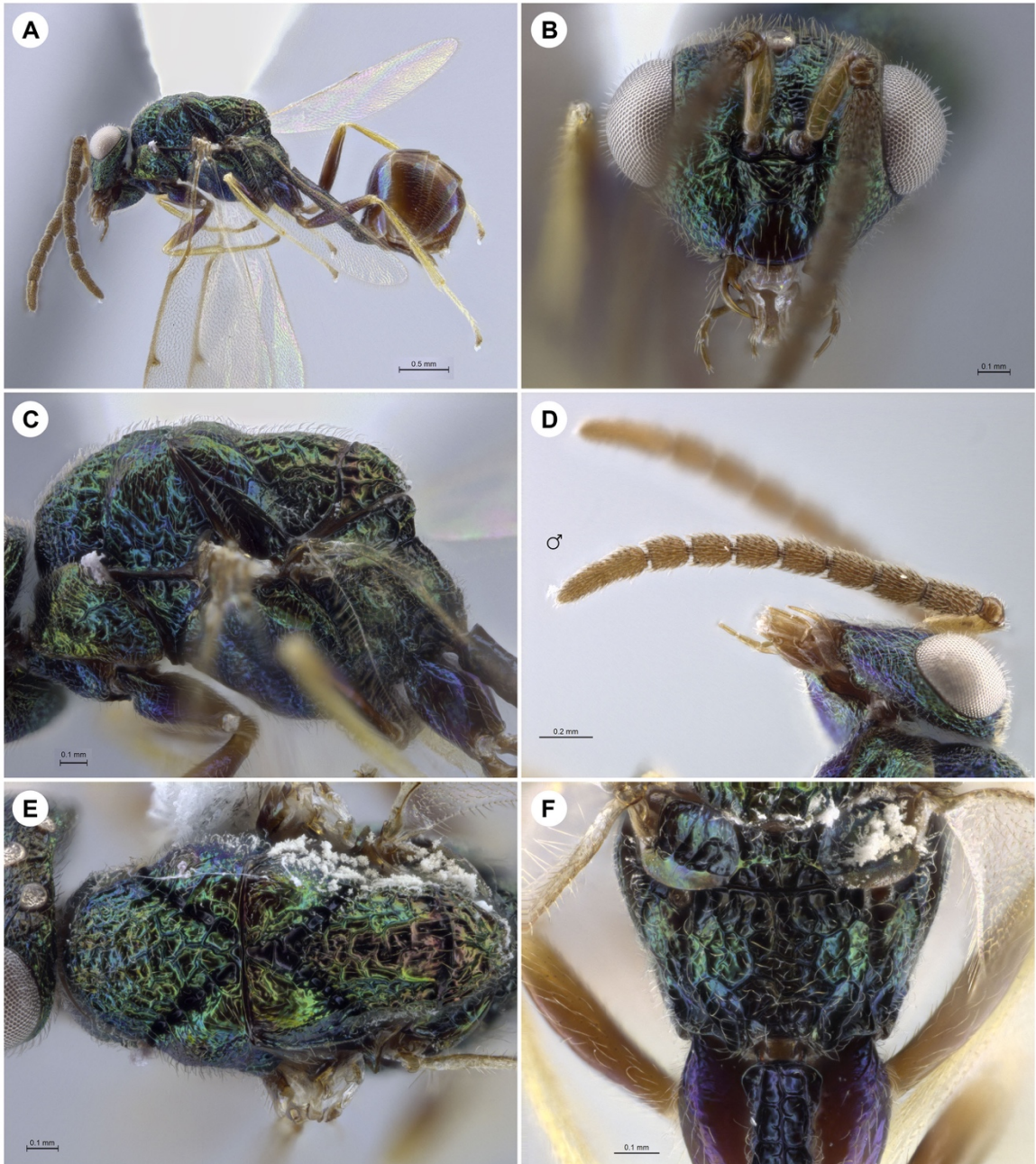


Figure 2.41: *Orasema monstrosa*. Holotype male (UCRCENT00434585): **A**, habitus, lateral; **B**, head, anterior; **C**, mesosoma, lateral; **D**, antenna; **E**, mesosoma, dorsal; **F**, propodeum, posterior.

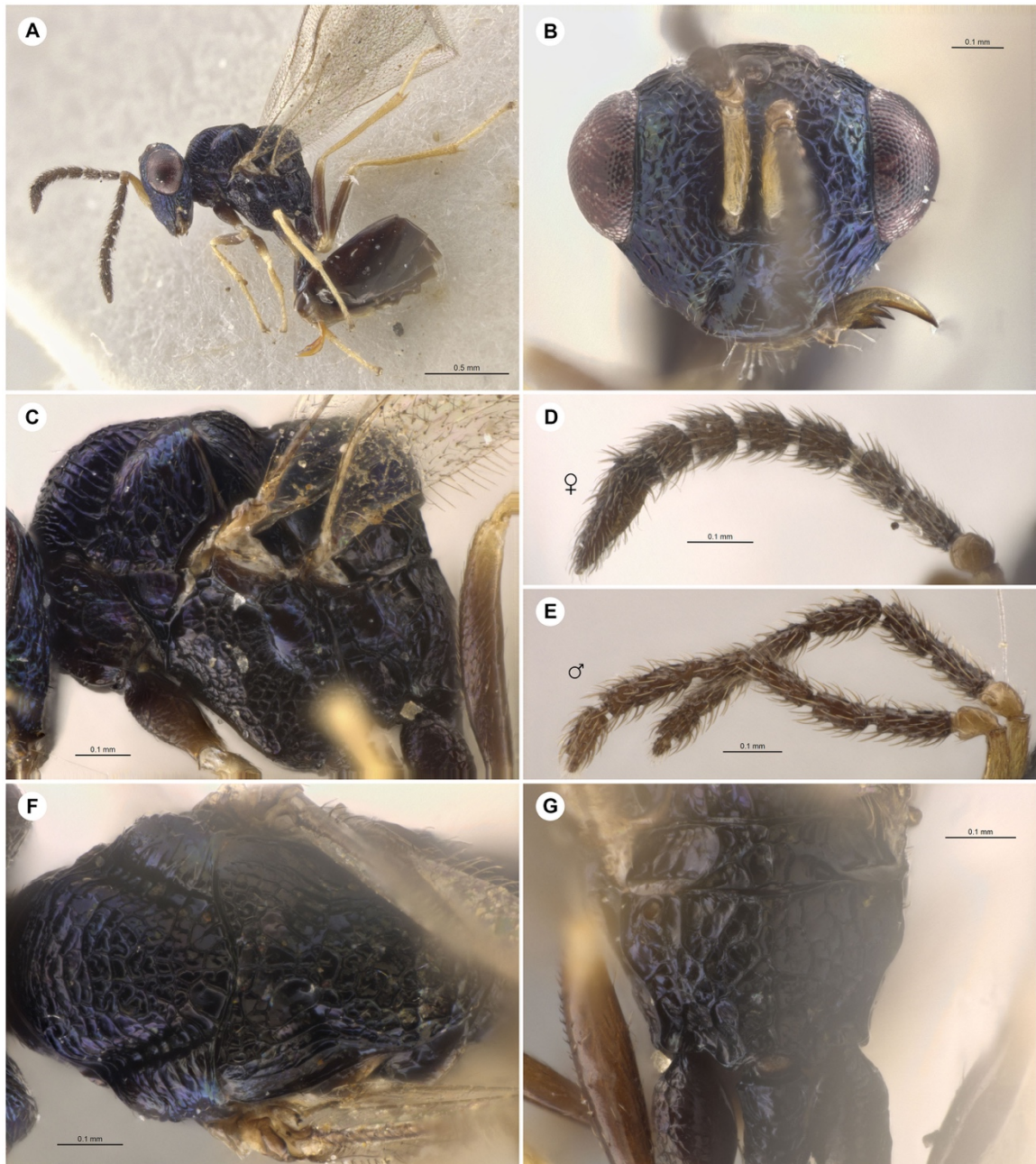


Figure 2.42: *Orasema mutata*. Holotype female (INBIOCRI00426110): **A**, habitus, lateral; **B**, head, anterior; **C**, mesosoma, lateral; **D**, antenna; **F**, mesosoma, dorsal; **G**, propodeum, posterior. Paratype male (INB03983200): **E**, antenna.

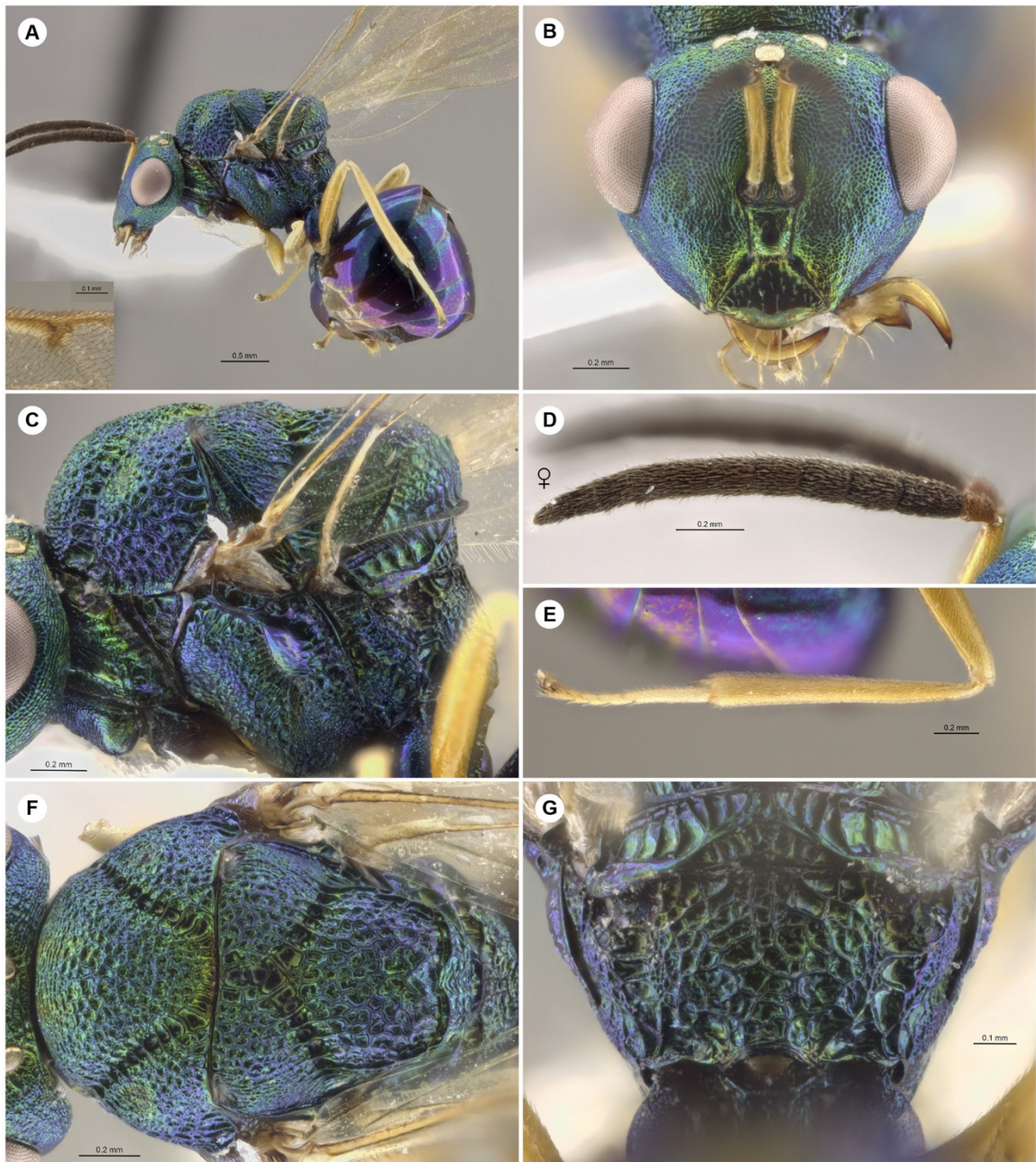


Figure 2.43: *Orasema psarops*. Holotype female (UCRCENT00434755): **A**, habitus, lateral (inset: stigmal vein, wing apex to the right); **B**, head, anterior; **C**, mesosoma, lateral; **D**, antenna; **E**, metatibia and tarsus; **F**, mesosoma, dorsal; **G**, propodeum, posterior.

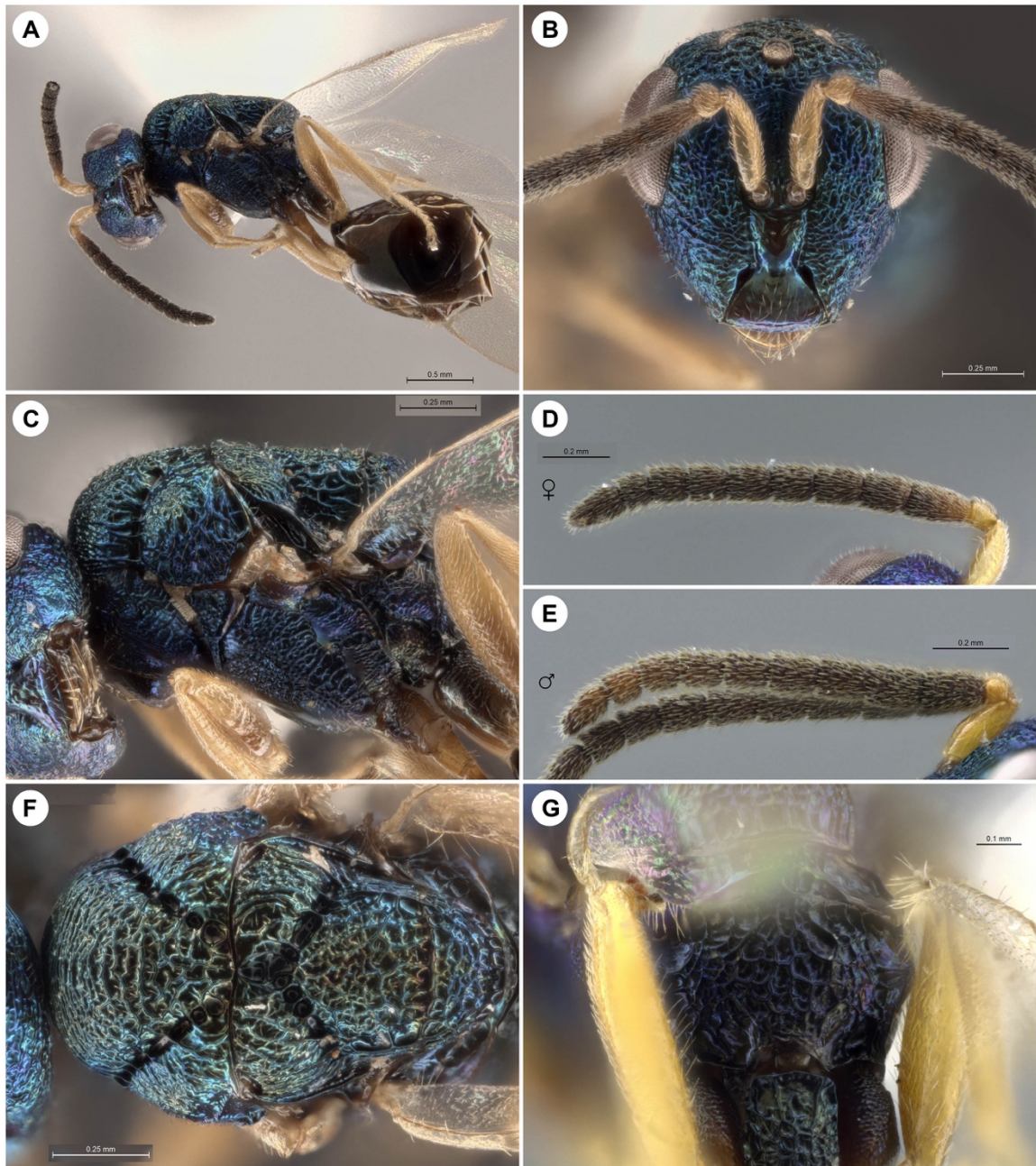


Figure 2.44: *Orasema roppai*. Holotype female (UCRCENT00415610): **A**, habitus, lateral; **B**, head, anterior; **C**, mesosoma, lateral; **D**, antenna; **F**, mesosoma, dorsal; **G**, propodeum, posterior. Paratype male (UCRCENT00436518): **E**, antenna.

Chapter 3: Larval morphology and life history of *Eutrichosoma mirabile* Ashmead and description of a new species of *Eutrichosoma* (Hymenoptera, Chalcidoidea)

Abstract

The larval morphology and life history of the weevil parasitoid *Eutrichosoma mirabile* Ashmead (Hymenoptera, Chalcidoidea, Pteromalidae) are described, and the phylogenetic placement of the subfamily Eutrichosomatinae within Chalcidoidea is determined using larval morphological characters. A description of *Eutrichosoma burksi* sp. nov. and key to the species of *Eutrichosoma* are provided.

Introduction

Eutrichosoma is a widespread, but infrequently collected, genus of weevil parasitoids in the subfamily Eutrichosomatinae (Hymenoptera, Chalcidoidea, Pteromalidae). Three species are known: *Eutrichosoma mirabile* Ashmead found throughout North America and Brazil, *E. flabellatum* Bouček from Brazil, and *E. burksi* sp. nov. from California, USA. The natural history is only known for *E. mirabile*, which parasitizes seed-feeding weevil larvae in the genera *Auleutes* and *Smicronyx* (Curculionidae) found on *Parthenium* and *Helianthus* (Asteraceae) (Crawford 1908; Bouček 1974; Charlet and Seiler 1994). *Auleutes* (Ceutorhynchinae) is typically associated with plants in the family Onagraceae and *Smicronyx* (Curculioninae) is typically associated with plants in the

families Asteraceae and Convolvulaceae, however, the plant hosts for the weevils and the weevil hosts for the wasps are likely broader than what is currently known.

Eutrichosomatinae includes two other monotypic genera: *Peckianus laevis* Provancher, a parasitoid of *Apion* (Brentidae) (Bouček and Heydon 1997), ranging from Canada to Brazil; and *Collessina pachyneura* Bouček from Australia, whose natural history is unknown. The taxonomic placement of this group was originally in Cleonyminae (Cleonymidae) by Ashmead (1899), who later placed it within Tanaostigmini (Encyrtidae) when he first provided the species name *Eutrichosoma mirabile* without a description (Ashmead 1904). It was first published as its own family, Eutrichosomatidae, by Peck (1951) and then reclassified as the subfamily Eutrichosomatinae within Pteromalidae by Bouček (1974). The digitate labral morphology of adult *E. mirabile* was regarded as similar to that of Eucharitidae and Perilampidae but independently derived (Darling 1988); however, the phylogenetic placement of this group based on a combination of morphological and molecular data suggests that Eutrichosomatinae belong within the Perilampidae+Eucharitidae clade (Heraty et al. 2013), which we here term the ‘Planidial Larva Clade’ (PLC) for their highly derived first-instar larvae.

Planidia, which means “diminutive wanderers,” are hypermetamorphic, active first-instar larvae (Clausen 1940a). The eggs are often laid away from the host, which requires the planidia to be adapted for free-living, being more mobile and more sclerotized than typical parasitoid larvae and showing host-seeking behavior. Planidia undergo metamorphosis between the first and second instar, with the latter typically

resembling sessile, non-planidial larvae that, within Hymenoptera, are termed hymenopteriform (Clausen 1940a; Pinto 2009). Within the PLC, planidia first attach externally to the host larva and begin further development through later instars on the host pupa (Clausen 1940b; Darling and Miller 1991; Darling 1992; Darling 1999). Until the host pupates, the planidia need to be mobile and able to find/recognize their hosts so that they can detach and reattach when their hosts molt. There are several groups of Diptera that have planidial first-instar larvae (Acroceridae, Nemestrinidae, Bombyliidae, Tachinidae, Asilidae) as well as Hymenoptera (Eucharitidae, Perilampidae, *Euceros* in Ichneumonidae), with multiple origins of planidial larvae present in both orders. We predict a single origin for planidial larvae in Chalcidoidea, and thus, if part of the PLC, the first-instar larvae of *Eutrichosoma mirabile* should have planidial morphology or otherwise some transitional form. We were able to collect and study the larvae of *E. mirabile* in Arizona to better understand their life history, and we provide support for the phylogenetic placement within the PLC based on larval morphology. In the process of examining museum material, we discovered a distinctive new species from California.

Methods and Materials

Eutrichosoma mirabile was collected at a field site close to Portal, Arizona, along Foothills Rd (31.952°N, 109.139°W) in August 2016, 2018, and September 2018. Adult *Eutrichosoma mirabile* were swept off of whitethorn acacia (*Vachellia constricta* (Benth.) Seigler & Ebinger; Fabaceae). Seedpods of whitethorn acacia were collected and

individually dissected in lab. Larvae of hosts and parasitoids were collected into 95% ethanol. Voucher specimens were assigned individual plasticized barcodes and deposited in the Entomology Research Museum at the University of California Riverside (**UCRC**). For slide mounting, larvae were cleared with 10% KOH, and then slide mounted in Hoyer's medium; after drying, slides were sealed with clear nail polish. Some larval specimens were retained in 95% ethanol. For scanning electron microscopy (SEM), larvae were dried using hexamethyldisilazane (Heraty and Hawks 1998), mounted on double sided sellotape, and sputter coated with palladium. SEM images were taken at the University of California Riverside using a Tescan Mira3 GMU. Stacked digital images were taken using a Leica Imaging System with a Z16 APO A microscope.

Morphological Terms. Terms used for adult morphology follow Heraty et al. (2018). Terms used for larval morphology follow Heraty and Darling (1984), Darling and Miller (1991), and Darling (1992).

Molecular Sequencing. Specimens were extracted using the DNeasy[®] blood and tissue kit manufactured by Qiagen (Valencia, CA, USA) with 1 μ L RNase A added after incubation. Two gene regions were sequenced. The ribosomal gene 28S D2 used the following primers and thermocycler protocol: D2F (CGG GTT GCT TGA GAG TGC AGC) and D2Ra (CTC CTT GGT CCG TGT TTC); initial denaturization: 94°C 3min; (denaturization: 94°C 1 min; annealing: 55°C 1 min; extension: 72°C 1 min) \times 34; final extension: 75°C 7 min. The mitochondrial gene COI-barcoding (COI-BC) used the

following primers and thermocycler protocol: LCO1490 (GGT CAA CAA ATC ATA AAG ATA TTG G) and HCO2198 (TAA ACT TCA GGG TGA CCA AAA AAT CA); initial denaturization: 93°C 3 min; (denaturization: 93°C 15 sec; annealing: 46°C 45 sec; extension: 68°C 45 sec) ×34; final extension: 68°C 7 min. PCR products were purified with DNA Clean & Concentrator™ -5 kits by Zymo Research (Irvine, CA, USA). PCR product concentrations were measured using Nanodrop 2000c (Thermo Scientific™). Each gene was PCR amplified individually and Sanger sequenced using both primers. Samples for Sanger sequencing were sent to Retrogen Inc. (San Diego, CA, USA) for sequencing on an Applied Biosystems 3730xl DNA Analyzer. Chromatograms were inspected for base calling errors and edited in Mesquite v.3.31 (Maddison and Maddison 2017b) using Chromaseq v.1.2 (Maddison and Maddison 2017a).

Molecular identification. We attempted to identify (or verify) specimens of parasitoid and host by comparing sequences with the online databases NCBI BLAST (Johnson et al. 2008) and BOLD (Ratnasingham and Hebert 2007) (Tables S3.1–S3.2).

Morphological phylogenetics. We tested the placement of Eutrichosomatinae within the PLC by first using the planidial morphology data matrix developed by Heraty and Darling (1984) and later modified by Darling (1992). Within the PLC, the subfamilies of Perilampidae are paraphyletic in recent molecular studies (Munro et al. 2011; Heraty et al. 2013), and we treat Chrysolampinae, Perilampinae, and Philomidinae as separate terminal taxa and equivalent to Eucharitidae. We refined these previous character sets to

include only informative and unambiguous characters at the family or subfamily level. Parsimony analyses were performed in PAUP* v4.0a (Swofford 2002) with default settings. We provide a detailed list of the characters, including character states, polarity inferences, and modifications from earlier studies (Heraty and Darling 1984; Darling 1992), with justifications for inclusion or exclusion of those characters.

Character 1. *Egg shape*: 0 = ovoid; 1 = stalked. Stalked eggs were regarded by Heraty and Darling (1984) as a synapomorphy for Eucharitidae, however at least three genera within Eucharitidae (*Indosema*, *Orasemorpha*, and *Timioderus*) lack egg stalks (Heraty 1994), and Chrysolampinae (Darling and Miller 1991), Philomidinae (Heraty et al. 2019), and Eutrichosomatinae all have egg stalks. The polarity cannot be inferred because the presence of egg stalks seems to be widespread throughout Chalcidoidea (e.g. *Aphelinus*, *Leucospis*, *Tetrastichus*, *Torymus*, and many more (Parker 1924)). We excluded this character from the analysis.

Character 2. *Egg sculpture*: 0 = smooth; 1 = ridged. Smooth eggs were inferred to be plesiomorphic by Heraty and Darling (1984), with ridged eggs only appearing in Perilampinae. This character is an autapomorphy for Perilampinae, thus excluded.

Character 3. *Sclerotization of terga (=tergites)*: 0 = absent; 1 = present. Heraty and Darling (1984) treated this character as a combination of sclerotization and distinctiveness of terga, which was present in all of our ingroup taxa. Darling (1992)

made this into two distinct characters: character 3 was sclerotization and character 3' was the shape of the terga (0 = completely encircling body; 1 = incomplete ventrad). All ingroup taxa were coded as sclerotized, and all ingroup taxa except Chrysolampinae and Eutrichosomatinae were coded as incomplete ventrad. The interpretation that Chrysolampinae and Eutrichosomatinae are more sclerotized than outgroup taxa with the terga completely encircling the body seems to be questionable, so we did not include the sclerotization character (3) but to only use the shape character (3'), which is treated here as character 20.

Character 4. *Setal pattern of tergum III (TIII)*: 0 = ventral setae absent; 1 = present.

Heraty and Darling (1984) treated this character as a loss of the ventral setae in Chrysolampinae and Oraseminae (Eucharitidae). The ventral pair of setae are difficult to define by position and are more accurately coded as the third pair of setae on TIII that are located ventrolaterally. Having the seta located on the ventrolateral margin is an autapomorphy of Eucharitidae, although it is not found in all taxa (Heraty and Barber 1990). However, these ventrolateral setae do appear to be present in both Chrysolampinae (Darling and Miller 1991) and Eutrichosomatinae, rendering this character uninformative for this analysis, thus it was excluded.

Character 5. *Distribution of dorsal setae*: 0 = absent; 1 = setae present on TI–III, V, VII, IX, XI; 2 = setae present on TI–III, V, VII, IX; 3 = setae present on TI–III, V. Heraty and Darling (1984) and Darling (1992) treated the absence of setae as the plesiomorphic

condition, which is not easily justified given the widespread presence of setae in chalcidoid first-instar larvae (e.g. *Leucospis*, *Torymus*, *Eupelmus*, *Eurytoma* (Parker 1924)). For this analysis, the only informative dorsal seta is on TX. We excluded character 5, but added the presence of a seta on TX as character 21.

Character 6. *Dorsal fusion of terga I and II (TI and TII)*: 0 = absent; 1 = present. Heraty and Darling (1984) treated this as a synapomorphy of Eucharitidae, however Oraseminae lack this fusion, and *Monacon* and *Krombeinius* (Perilampinae) have the terga fused (Darling 1995; Darling and Roberts 1999). This character is uninformative for this analysis and therefore excluded.

Character 7. *Ventral spines*: 0 = absent; 1 = present. Heraty and Darling (1984) noted that ventral spines are present in many ectoparasitic chalcidoid larvae. Spines of any kind are absent in Eucharitidae, and because Perilampidae are polymorphic, they interpreted the absence of spines as a synapomorphy of these two families. Darling (1992) combined character 7 (spines) with character 8 (tubercles) using the states: 0 = absent; 1 = tubercles present; 2 = spicules (spines) present. This is problematic because multiple terms have been applied to these spines (e.g. the ventral spines in *Chrysolampus* have been referred to as tubercles, pustules, and spicules without any clear distinction (Darling and Miller 1991)). Additionally, Chrysolampinae and Philomidinae were coded as having spicules (but not tubercles), and Perilampinae are coded as having tubercles (but not spicules) despite contradicting descriptions (cf. Darling and Miller 1991). We treat spines as a

separate character from tubercles. Spines, represented as hook-like structures on the ventral region of the body segments and located between the tergal margins (cf. figs 17, 34, 37 in Heraty and Darling 1984), are a feature found only in some Perilampinae. They are uninformative for this analysis and excluded.

Character 8. *Lateral tubercles*: 0 = absent; 1 = present. Eutrichosomatinae have a series of tubercles across the ventral region of body segments II–XII (Fig. 3.1B, D, F; *tbs*). Heraty and Darling (1984) treated this as an autapomorphy of Chrysolampinae based on the description by Askew (1980). This character was further explored and illustrated on two species of *Chrysolampus* by Darling and Miller (1991), occurring on body segments II–XII. A similar patch of tubercles was found on the ventral region of body segment I in Philomidinae (Darling 1992). We excluded this character because of the difficulty assessing the homology of the various types of ventral and lateral protuberances.

Character 9. *Spiracles*: 0 = spiracles on TII, IV, V, VI; 1 = spiracles on TII; 2 = absent. Heraty and Darling (1984) noted that the plesiomorphic condition in Chalcidoidea is having pairs of spiracles on TII, IV, V, and VI, which is the state found in Eutrichosomatinae and several outgroup taxa (Parker 1924). Perilampinae and Philomidinae have lost all spiracles except on TII, and Eucharitidae and Chrysolampinae lack spiracles entirely.

Character 10. *Tergopleural line*: 0 = absent; 1 = present. This longitudinal line of thin, unpigmented cuticle going through the lateral sides of TII–IX is found in most Eucharitidae. It is absent in most Oraseminae, although present in *Orasemorpha* (Heraty 2000). In Eucharitinae, it is absent only in *Pseudochalcura* (Heraty and Barber 1990). It is present in Gollumiellinae, which is sister to Oraseminae + Eucharitinae (Heraty 2004), hence it is interpreted as a synapomorphy of Eucharitidae. It is uninformative for this analysis and was excluded.

Character 11. *Caudal cerci*: 0 = present as undifferentiated setae; 1 = absent; 2 = present as differentiated (longer and/or stouter) setae. These structures are defined as setae arising on the dorsum of TXII (Heraty and Darling 1984), which are larger than the setae on other body segments and often prolonged as stout spines or long hairs. If this character is treated as a synapomorphy of Eucharitidae and Perilampidae, the definition is not adequate because several groups have short setae (e.g. *Gollumiella longipetiolata* Hedqvist (Heraty 2004), *Hydrorhoa stevensoni* (Risbec) (Heraty 2002), *Australosema valgius* (Walker) and *Orasemorpha didentata* (Girault) (Heraty 2000)) and some have other setae on the body as long as the setae on TXII (e.g. *Perilampus chrysopae* Crawford (Clancy 1946), *Steffanolampus salicetum* (Steffan) (Darling 1999)). Eutrichosomatinae and Philomidinae both have short socketed setae on TXII and TXIII that are located more laterally (Eutrichosomatinae; Fig. 3.1H) or ventrally (Philomidinae). These setae appear to be homologous with cerci but without the enlargement and proposed specialized locomotion functions associated with Perilampinae

and Eucharitidae (e.g. providing support to hold the body in an upright posture); therefore, we created another character state (state 0) for these taxa. Only Chrysolampinae has entirely lost setae on TXII. The position of the cerci on Eucharitidae appears to be between TXII and XIII, which is a synapomorphy for the family but uninformative for this analysis.

Character 12. *Caudal pad*: 0 = absent; 1 = present. The last segment (TXIII) is membranous and expanded in Eucharitidae and Perilampinae to adhere to surfaces (Heraty and Darling 1984). However, the morphology does not appear to be different from other taxa in the PLC. We also think that polarity (absent ancestrally) cannot be assumed for this character because multiple other chalcidoid taxa have differentiated posterior segments with “suckers” or other ornamentations (e.g. *Leucospis* (Parker 1924)). This was excluded from the analysis.

Character 13. *Antenna*: 0 = present; 1 = reduced; 2 = absent. The short, conical, papilliform antenna (state 0) is considered plesiomorphic (Heraty and Darling 1984). These are present in Eutrichosomatinae and Chrysolampinae and are widespread across Chalcidoidea (e.g. *Leucospis*, *Torymus*, *Eupelmus*, *Eurytoma*, and more (Parker 1924)). Philomidinae have low, broad swellings that may indicate reduced antennae (Darling 1992).

Character 14. *Cranial setae*: 0 = present; 1 = absent. It is noted by Darling (1992) that the distinction and homology between cranial setae and cranial spines is not clear, which resulted in a combination of characters 14 and 15 with the states: 0 = 3–4 pairs; 1 = reduced number. Philomidinae was the only taxon coded as having complete cranial setae, however, all Perilampinae have 3 pairs of setae on the cranium. Because of the difficulty assessing polarity and homology for this character, it has been excluded.

Character 15. *Cranial spines*: 0 = present; 1 = absent. Some species of *Perilampus* have stout, recurved spines (Heraty and Darling 1984), which may be derived setae. This character is uninformative and excluded from this analysis.

Character 16. *Prelabium*: 0 = membranous; 1 = with sclerotized marginal rim. The prelabium is a depressed area with a sclerotized marginal rim and labial palpi on the margins (Heraty and Darling 1984). Presence of the labial sclerite was considered a synapomorphy for Eucharitidae and Perilampidae and is most easily identified when the palpi appear within or on the marginal rim. In Philomidinae, the labial palpi are not associated with a sclerite, which is thought to be the plesiomorphic condition (Darling 1992). This structure is extremely minute and difficult to score for most slide-mounted larvae. It is excluded from this analysis because the structure could not be verified in many of the taxa, although it is clearly present in *Eutrichosoma* (Fig. 3.1B, D, E, G; *prl*).

Character 17. *Postlabium*: 0 = non-eversible; 1 = enlarged and eversible. In Eucharitidae and Perilampinae, the postlabium is an eversible membranous sac surrounding the prelabium (Heraty and Darling 1984). This may be the same in Philomidinae (Darling 1992). Observations of specimens with everted postlabia are the only accurate way to code this character, and we could not observe this in Eutrichosomatinae, therefore it was excluded.

Character 18. *Labial plates*: 0 = absent; 1 = present. These are two sclerites found posterior to the prelabium in Eucharitidae (absent in Oraseminae). This character is uninformative for this analysis and excluded.

Character 19. *Pleurostomal setae*: 0 = present; 1 = spine-like; 2 = fused spines. These are setae lateral to the mouth, and they are present in most chalcidoid taxa (Heraty and Darling 1984). These setae do not appear to be modified in Eutrichosomatinae, Chrysolampinae, Philomidinae, or most Perilampinae, despite being previously coded as spine-like (Darling 1992). In Eucharitidae this has been coded as fused spines, but what was observed was not a socketed seta but instead a pointed projection of the cranial cuticle. This character was excluded from the analysis.

Character 20. *Shape of terga*: 0 = completely encircling body; 1 = incomplete ventrad. This is character 3' from Darling (1992). Terga encircling the body is seen in all other known chalcidoid first-instar larvae (Parker 1924) and is considered plesiomorphic for

the PLC. Philomidinae, Perilampinae, and Eucharitidae all have incomplete terga. One exception is in the genus *Monacon* (Perilampinae), where the posterior terga (VII–XI) are ventrally fused, while the anterior terga are not (Darling and Roberts 1999). This could be treated as a third character state for a polymorphic coding of Perilampinae, but it would not have an impact on the relationships in this analysis.

Character 21 (new). *Seta on tergum X*: 0 = present; 1 = absent. Setae present on all terga is treated here as the plesiomorphic state for the PLC based on the presence in many other chalcidoid taxa. Most taxa in the PLC have lost setae on TX, with the exception of Eutrichosomatinae, which maintains the ground plan configuration. We chose to focus on TX because the presence of setae on other terga are either present in all taxa (TI–III, V), only lost in Eucharitidae (TVII, IX), or require interpretation of the dorsal/lateral/ventral homology of the multiple setae present (TIV, VI, VIII).

Character 22 (new). *Seta on tergum XI*: 0 = present; 1 = absent. Loss of setae on TXI is a synapomorphy of Eucharitidae and Perilampinae.

Character 23 (new). *Behavior*: 0 = not ectoparasitic koinobiont; 1 = ectoparasitic koinobiont. All members of the PLC are ectoparasitic koinobionts. There are several examples of planidia residing internally (e.g. *Perilampus* spp.) or transdermally (e.g. *Orasema* spp.) within a host, but they always emerge to an external position to continue development through later instars; therefore, we do not consider these taxa endoparasitic

sensu Heraty and Murray (2013). No other chalcidoids (where behavior is known) are ectoparasitic koinobionts because of the unique challenge of reattaching to the host after each molt, which requires increased mobility and host-recognition.

Results

Morphological phylogenetics of planidia. Our dataset was reduced to seven characters (9, 11, 13, 20–23) for the parsimony analysis. We chose to discuss all of the characters previously used because they can be valuable for future phylogenetic analyses at different levels (e.g. the genera of Eucharitidae). The major limitation for this analysis was finding informative characters with minimal ambiguity in the interpretation of their homology, which can be difficult for groups with simple morphology and large evolutionary gaps between sampled taxa. The most parsimonious tree was 11 steps and included only one homoplastic character (Fig. 3.2). We recovered the same topology as Heraty and Darling (1984) and Darling (1992) with the addition of Eutrichosomatinae, which was placed as the most plesiomorphic member of the PLC.

***Eutrichosoma* adult generic diagnosis.** The inclusion of the new species of *Eutrichosoma* has modified the generic diagnosis (Bouček 1974). Margin of clypeus without incision; advanced occipital ridge directly posterior to the ocelli present or absent; the anterior transverse carina on the pronotal collar present or absent; mesoscutal midlobe completely separating the axillae medially, posteriorly reaching the

mesoscutellum; fore wing without marginal fringe; postmarginal vein on the fore wing present, rudimentary (difficult to distinguish), or absent. It differs from *Peckianus* by the iridescent blue or green coloration of the body, posterior end of the mesoscutal midlobe broadly separating the axillae (by 0.18–0.23× the length of the mesoscutal midlobe; 0.08–0.09× in *Peckianus*), marginal vein on fore wing short (0.1–0.13× the length of the fore wing; 0.2–0.21× in *Peckianus*). It differs from *Collessina* by having a moderately setose body (setae sometimes spatulate), head and mesosoma more coarsely reticulate, antenna with two anelli, scape not reaching median ocellus, notauli and scutoscutellar sulcus distinct, marginal vein on fore wing with a continuous width (not increasing distally).

Key to the species of *Eutrichosoma*

- 1) Body covered with distinctly wide, spatulate setae; stigmal vein angulate medially
 *Eutrichosoma mirabile* Ashmead
- Body covered with thin, simple setae; stigmal vein nearly straight, without
 obvious angle 2
- 2) Occipital carina present; mesoscutellar disc finely granulate; male antenna
 flabellate (females unknown); body length 2.9–3.1 mm
 *Eutrichosoma flabellatum* Bouček
- Occipital carina absent; mesoscutellar disc transversely imbricate; female antenna
 simple (males unknown); body length 1.9 mm *Eutrichosoma burksi* **sp. n.**

***Eutrichosoma mirabile* Ashmead**

urn:lsid:zoobank.org:act:AB2C77FF-2020-4273-AC42-1AAEEA4F53C4

(Fig. 3.1)

Eutrichosoma mirabile Ashmead 1904: 375. Lectotype designated by Gahan and Peck (1946: 315): USA: Montana: Helena (female). Deposited in USNM.

Eutrichosoma albipes Crawford 1908: 158–159. Synonymy by Bouček, 1975. Holotype: USA: Texas: Dallas (female). Deposited in USNM.

E. mirabile; Bouček 1975: 132–133. Redescription and identification key.

Biology and life history. Eggs and first-instar larvae were found inside the early (green) seedpods of *Vachellia constricta* and associated with the presence of weevil eggs and larvae (Curculionidae). *Eutrichosoma mirabile* eggs are laid among the host eggs inside the seedpods between the ovule and the inner wall of the pod. Hatching of the parasitoid seems to coincide with or precede hatching of the host because parasitoid eggs were never observed without host eggs. The majority of planidia found were parasitizing first- or second-instar weevils (~85%). Typically, only one planidium was found per host, positioned anterodorsally on the body just behind the head attached by the mandibles; always on the external surface and never penetrating the cuticle. The remaining unattached planidia were observed crawling around near clusters of host eggs. Eggs and planidia were the only life stages of the wasps observed in the seedpods. While there may be several eggs and early instars of weevil (up to ~10) per ovule within a seedpod, by the time the weevils are in their fourth instar, there is only one individual per ovule

remaining. Considering the wasps are ectoparasitic koinobionts, they are likely detaching then reattaching and repositioning themselves on their hosts between host molts or transferring between individual host larvae. Given the similarities between *E. mirabile* and chrysolampines (discussed below), it is assumed that the *E. mirabile* planidia remain attached externally to the weevil when it leaves the seedpod to pupate in the soil, where the parasitoid likely finishes development. We were not able to keep the weevil larvae alive outside of the pods to allow the parasitoid to develop further. Parasitism rates shown in Table S3.3.

Egg (Fig. 3.1A). Egg body length approximately 0.2 mm, maximum width approximately 0.07 mm; ovoid; caudal stalk about half as long as the body of the egg. Eggs separate, not forming tight clusters.

Planidium (Fig. 3.1B–H). Length approximately 0.13 mm, maximum width approximately 0.05 mm; fusiform in shape. Body and cranium white, darkened around mouth (Fig. 3.1C). Cranium with one pair of short, papilliform antennae (*ant*), one pair of longer, thinner pleurostomal setae (*plst*), and one pair of minute, lateral cranial spines (*cs*); postlabium (*psl*) large, flat, circular, and surrounding prelabium (*prl*); labial palp (*lp*) present; pleurostomal bridge (*psb*) present and connected by thin integument (Fig. 3.1E). Thirteen body segments beyond head; terga lightly sclerotized and ring-like, encircling the body; band of 1–2 irregular rows of tubercles (*tbs*) on anteroventral side of terga II–XII; prominent dorsolateral spines (*spn*) on terga I and III–XI; setae (*set*) present on terga I–VIII and XII, with three pairs on tergum II and two pairs on tergum III; short cerci present on XIII (*cer*); spiracles on terga II, IV–VI (*spi*) (Fig. 3.1B, D, F–G).

Determining if a first-instar larva is a type I planidium (i.e. undergoes hypermetamorphosis sensu Pinto (2009)) requires examination of subsequent instars, which we did not find for *Eutrichosoma*. However, the mobility of the larvae observed in the seedpods and inferred from their koinobiont ectoparasitic behavior suggests that *Eutrichosoma* behavior is congruent with other PLC larvae, even if their morphology is not as derived as Eucharitidae, Perilampinae, or Philomidinae, which are all more heavily sclerotized and generally lack ventral fusion of the terga. Larvae of Eutrichosomatinae and Chrysolampinae appear to be somewhat intermediate between typically hymenopteriform first instars of other chalcidoid taxa and the highly derived planidial larvae in the PLC.

Material examined. USA: Arizona: Cochise Co.: Canadian Lane, Portal, 1426m, 31°55'1"N 109°07'37"W, 28.viii.2016, A. Baker & S. Heacox, **AB16.024** [2 larvae slide mounted, UCRCENT00513221–2]; 4.viii.2018, A. Baker, S. Heacox, L. Kresslein, **AB18.007** [larvae in alcohol, UCRCENT00513223] **deposition UCRC.**

***Eutrichosoma burksi* sp. n.**

urn:lsid:zoobank.org:act:A3F880D1-467D-4201-A113-E39BE80A644F

(Fig. 3.3)

Diagnosis. Recognized from other *Eutrichosoma* by the following combination of characters: body with metallic green coloration; stigma enlarged, stigmal vein short and

not elbowed; setae relatively thin and sparse; transversely imbricate sculpture on mesosoma dorsally; lacking vertexal carina.

Description. Female. Length 1.9 mm. **Color.** Head, mesosoma, scape, pedicel, and coxae dark green; anellus and flagellum brown; mandible reddish brown; maxilla and labium brown. Femora and tibiae dark brown with green reflections medially, pale at tips. Fore wing hyaline, venation pale brown. Gaster dark brown with green iridescence. **Head** (Fig. 3.3B). Head in frontal view subcircular; head width:height 1.24; face reticulate; scrobal depression shallow, laterally rounded; eyes with minute setae; malar sulcus present; clypeus smooth with rounded margin; epistomal sulcus distinct and sharply defined; anterior tentorial pit shallow; anteclypeus distinct, broadly rounded; palpal formula 4:3; mandibular formula not observed; occiput strigate, emarginate in dorsal view, dorsal margin evenly rounded; temples present, rounded. Antennal scape not reaching median ocellus; pedicel elongate, more than 1.5× as long as broad; antenna with 12 flagellomeres, including small terminal button (F12) at end of clava (clava 4-segmented); flagellum length:head height 0.81; anellus disc-shaped; second flagellomere (F2) 0.78× as long as broad, 0.75× as long as F3; following flagellomeres subequal in length, gradually broader; clava subconical. **Mesosoma** (Fig. 3.3C–F). Mesosoma length:height 1.28; mesoscutal midlobe, lateral lobe, axilla, and mesoscutellum transversely imbricate to coriaceous, sparsely setose (Fig. 3.3E); notauli deeply impressed along entire length; axilla dorsally rounded, on roughly same plane as mesoscutellar disc; scutoscutellar sulcus broad, irregularly foveate, fused with transscutal articulation medially; propodeal disc broadly rounded, reticulate, with median carina (Fig. 3.3F);

callus bulbous, projecting posteriorly beyond the lateral margins of the propodeum, reticulate, with several long hairs; mesepisternum reticulate; upper mesepimeron smooth; lower mesepimeron reticulate; transepimeral sulcus distinct; propleuron nearly flat, transversely imbricate. Hind femur 3.39× as long as broad, with long stout setae; hind tibia with long stout setae. Fore wing 2.13× as long as broad, basal cell and speculum bare, costal cell sparsely setose, wing disc moderately setose; marginal fringe absent; submarginal vein with nine long setae dorsally; marginal vein with eight long setae along the margin; parastigmal vein slightly thicker than submarginal, constricted at connection with marginal vein; stigmal vein straight, narrow, short; stigma large, slightly angled; uncus absent; postmarginal vein short but obvious; hind wing costal cell with a broad bare area medially. **Metasoma.** Gaster appears sessile, petiole short and indistinct; first gastral tergum longer than subsequent terga; sparsely setose dorsally, with more setae laterally. Ovipositor sheaths protruding a short distance past the last gastral tergum.

Male. Unknown.

Biology. Unknown

Material examined. Holotype: USA: California: San Bernardino Co.: Kelso Dunes Rd, 775m, 34°53'23"N, 115°43'05"W, 19.v.2001, D. Yanega [1 ♀, UCRCENT00221857], **deposition UCRC.**

Etymology. Named in honor of Roger A. Burks, whose expertise led to the recognition of this specimen as a new species.

Discussion

The larval morphology and life history of *Eutrichosoma mirabile* is quite similar to species of *Chrysolampus* (Chrysolampinae). Both taxa lay their eggs in seedpods infested with seed-feeding weevil larvae (Darling and Miller 1991). The larvae of these wasps are strikingly similar, with the position of the spines and setae being the most obvious means to differentiate the two. These observations along with the digitate labral morphology for adults (Darling 1988) and the molecular phylogenetic support from both traditional Sanger sequencing datasets (Heraty et al. 2013) and next-generation sequencing datasets (Heraty et al. unpublished; Rasplus et al. unpublished), make placement of Eutrichosomatinae in the PLC highly supported. The position of this subfamily within the PLC, however, is far less certain. While the planidia of *E. mirabile* may morphologically appear plesiomorphic to the rest of the PLC (Darling 1988), it is not consistently placed as sister to the remaining PLC with molecular data (Heraty et al. unpublished). Our analysis of a limited number of morphological characters of the first-instar larvae supports the sister-group relationship between Eutrichosomatinae and the remaining PLC, but interpretations of larval character homologies at the family level are very difficult to make.

Pinto (2009) defines planidium as a legless type I hypermetamorphic first-instar larva; type I is characterized by the larva having to locate its own food source, survive for considerable time without desiccating or feeding, and being active, slender, and well-sclerotized. This definition accurately describes the larvae of Eucharitidae, Perilampinae, and Philomidinae, but it cannot be unambiguously applied to Chrysolampinae or

Eutrichosomatinae. Females of these two taxa oviposit into seedpods, their larvae are not directly exposed to an external environment, and heavy sclerotization of the body segments is less necessary. As well, the enclosed environment does not necessitate the need for the various ornamentation of setal modifications of the other taxa that may be associated with extreme mobility. Highly mobile ectoparasitic first-instar larvae are known in other Chalcidoidea, but these are usually idiobionts where eggs are laid onto and develop on a single developmental stage of the host, with the larvae searching for an appropriate place to initiate feeding (i.e. *Spalangia* (Richardson 1913; Clausen 1940a)) or even using the first instar to cruise the host and kill competing sibling larvae before initiating feeding (i.e. *Leucospis* (Graenicher 1906; Clausen 1940a)). *Eutrichosoma mirabile* and *Chrysolampus* are unique in Chalcidoidea in that they are both ectoparasitic koinobionts, with the first instars not only highly mobile but able to pass through different life stages of the host, in this case from the host first instar to pupa. This combination is rare in Hymenoptera, being found in some Ichneumonidae, Braconidae, and Dryinidae (Gauld and Bolton 1988; Gauld and Hansen 1995; Quicke 1997). Some Eulophidae have been designated ectoparasitic koinobionts: *Eulophus larvarum* (L) (Shaw 1981) and *Euplectrus* sp. (Neser 1973); however, these taxa are fundamentally different than all of the other ectoparasitic koinobionts because they develop on a single instar of their host caterpillar, which will continue to feed for a time but does not continue developing and renders the parasitoids' status as koinobionts ambiguous. The first-instar larvae of Chrysolampinae and Eutrichosomatinae appear to represent the transition between idiobiont hymenopteriform larvae (limited mobility, weakly

sclerotized) and koinobiont planidia (highly mobile, heavily sclerotized). We feel that the application of a combination of behavioral characters (koinobiont, ectoparasitoid, with eggs not directly placed on the host) allows inclusion of these transitional forms into what we term planidial larvae.

While the 28S-D2 gene region confirmed the identity of the parasitoid, which had an exact match between larva and adult (Table S3.1), the identification of the larval host weevils remains a mystery. There were no exact matches between the sequenced larval weevils and any adult weevils that we collected from the acacia. Furthermore, the BLAST and BOLD results for the host larva were inconclusive past the family level (Curculionidae) for both gene regions, with the top hits being distant matches to multiple subfamilies, including Curculioninae, Ceutorhynchinae, and Tychiinae (Table S3.2).

References

- Ashmead, W.H. (1899) On the genera of the Cleonymidae. *Proceedings of the Entomological Society of Washington*, **4**, 200–206.
- Ashmead, W.H. (1904) Classification of the chalcid flies or the superfamily Chalcidoidea, with descriptions of new species in the Carnegie Museum, collected in South America by Herbert H. Smith. *Memoirs of the Carnegie Museum*, **1**, 225-533.
- Askew, R.R. (1980) The biology and larval morphology of *Chrysolampus thenae* (Walker) (Hym., Pteromalidae). *Entomologist's Monthly Magazine*, **115**, 155-159.
- Bouček, Z. (1974) The pteromalid subfamily Eutrichosomatinae (Hymenoptera: Chalcidoidea). *Journal of Entomology*, **43**, 129-138.
- Bouček, Z. & Heydon, S.L. (1997) Pteromalidae. *Annotated keys to the genera of Nearctic Chalcidoidea (Hymenoptera)* (ed. by G.A.P. Gibson, J.T. Huber & J.B. Woolley), pp. 541–692. Monograph Publishing Program, Canada.
- Charlet, L.D. & Seiler, G.J. (1994) Sunflower seed weevils (Coleoptera: Curculionidae) and their parasitoids from native sunflowers (*Helianthus*) in the Northern Great Plains. *Annals of the Entomological Society of America*, **87**, 831-835.
- Clancy, D.W. (1946) *The insect parasites of the Chrysopidae (Neuroptera)*. University of California Press, Berkeley and Los Angeles.
- Clausen, C.P. (1940a) *Entomophagous Insects*. McGraw-Hill Book Company, Inc., New York and London.
- Clausen, C.P. (1940b) The immature stages of the Eucharidae. *Proceedings of the Entomological Society of Washington*, **42**, 161–170.
- Crawford, J.C. (1908) Some new Chalcidoidea. *Proceedings of the Entomological Society of Washington*, **9**, 157-160.
- Darling, D.C. (1988) Comparative morphology of the labrum in Hymenoptera: The digitate labrum of Perilampidae and Eucharitidae (Chalcidoidea). *Canadian Journal of Zoology*, **66**, 2811-2835.
- Darling, D.C. (1992) The life history and larval morphology of *Aperilampus* (Hymenoptera: Chalcidoidea: Philomidinae), with a discussion of the phylogenetic affinities of the Philomidinae. *Systematic Entomology*, **17**, 331-339.

- Darling, D.C. (1995) New species of *Krombeinius* (Hymenoptera: Chalcidoidea: Perilampidae) from Indonesia, and the first description of first-instar larva for the genus. *Zoologische Mededelingen (Leiden)*, **69**, 209–229.
- Darling, D.C. (1999) Life history and immature stages of *Steffanolampus salicetum* (Hymenoptera: Chalcidoidea: Perilampidae). *Proceedings of the Entomological Society of Ontario*, **130**, 3-14.
- Darling, D.C. & Miller, T.D. (1991) Life history and larval morphology of *Chrysolampus* (Hymenoptera: Chalcidoidea: Chrysolampinae) in western North America. *Canadian Journal of Zoology*, **69**, 2168-2177.
- Darling, D.C. & Roberts, H. (1999) Life history and larval morphology of *Monacon* (Hymenoptera: Perilampidae), parasitoids of ambrosia beetles (Coleoptera: Platypodidae). *Canadian Journal of Zoology*, **77**, 1768–1782.
- Gahan, A.B. & Peck, O. (1946) Notes on some Ashmeadian genotypes in the hymenopterous superfamily Chalcidoidea. *Journal of the Washington Academy of Sciences*, **36**.
- Gauld, I. & Bolton, B. (1988) *The Hymenoptera*. Oxford University Press, New York.
- Gauld, I.D. & Hansen, P. (1995) Carnivory in the larval Hymenoptera. *The Hymenoptera of Costa Rica* (ed. by P. Hansen & I.D. Gauld), pp. 893. Oxford University Press, Oxford.
- Graenicher, S. (1906) On the habits and life-history of *Leucospis affinis* (Say). A parasite of bees. *Bulletin of Wisconsin Natural History Society*, **4**, 153–160.
- Heraty, J.M. (1994) Classification and evolution of the Oraseminae in the Old World, including revisions of two closely related genera of Eucharitinae (Hymenoptera: Eucharitidae). *Life Sciences Contributions*, **157**, 1–174.
- Heraty, J.M. (2000) Phylogenetic relationships of Oraseminae (Hymenoptera: Eucharitidae). *Annals of the Entomological Society of America*, **93**, 374–390.
- Heraty, J.M. (2002) A revision of the genera of Eucharitidae (Hymenoptera: Chalcidoidea) of the world. *Memoirs of the American Entomological Institute*, **68**, 1–359.
- Heraty, J.M. (2004) Three new species of *Gollumiella* Hedqvist (Hymenoptera : Eucharitidae). *Zootaxa*, 1-10.

- Heraty, J.M. & Barber, K.N. (1990) Biology of *Obeza floridana* (Ashmead) and *Pseudochalcura gibbosa* (Provancher) (Hymenoptera: Eucharitidae). *Proceedings of the Entomological Society of Washington*, **92**, 248-258.
- Heraty, J.M., Burks, R.A., Cruaud, A., *et al.* (2013) A phylogenetic analysis of the megadiverse Chalcidoidea (Hymenoptera). *Cladistics*, **29**, 466-542.
- Heraty, J.M., Burks, R.A., Mbanyana, N. & Van Noort, S. (2018) Morphology and life history of an ant parasitoid, *Psilocharis afra* (Hymenoptera: Eucharitidae). *Zootaxa*, **4482**, 491–510.
- Heraty, J.M. & Darling, D.C. (1984) Comparative morphology of the planidial larvae of Eucharitidae and Perilampidae (Hymenoptera: Chalcidoidea). *Systematic Entomology*, **9**, 309-328.
- Heraty, J.M., Derafshan, H.A. & Moghaddam, M.G. (2019) Review of the Philomidinae Ruschka (Hymenoptera: Chalcidoidea: Perilampidae), with description of three new species. *Arthropod Systematics and Phylogeny*, **77**, 39–56.
- Heraty, J.M. & Hawks, D. (1998) Hexamethyldisilazane - A chemical alternative for drying insects. *Entomological News*, **109**, 369-374.
- Heraty, J.M. & Murray, E. (2013) The life history of *Pseudometagea schwarzii*, with a discussion of the evolution of endoparasitism and koinobiosis in Eucharitidae and Perilampidae (Chalcidoidea). *Journal of Hymenoptera Research*, **35**, 1–15.
- Johnson, M., Zaretskaya, I., Raytselis, Y., Merezhuk, Y., McGinnis, S. & Madden, T.L. (2008) NCBI BLAST: a better web interface. *Nucleic Acids Research*, **36**, W5-9.
- Maddison, D.R. & Maddison, W.P. (2017) *Chromaseq: a Mesquite package for analyzing sequence chromatograms. Version 1.3.*
<http://mesquiteproject.org/packages/chromaseq>.
- Maddison, W.P. & Maddison, D.R. (2015) *Mesquite: a modular system for evolutionary analysis*.
- Munro, J.B., Heraty, J.M., Burks, R.A., *et al.* (2011) A molecular phylogeny of the Chalcidoidea (Hymenoptera). *PLoS One*, **6**, e27023.
- Neser, S. (1973) Biology and behaviour of *Euplectrus* species near *Laphygmae* Ferrière (Hymenoptera: Eulophidae). *Entomology Memoir, Department of Agriculture Technical Services, Republic of South Africa, No. 32*, 1–31.
- Parker, H.L. (1924) Recherches sur les formes post-embryonnaires des chalcidiens.

- Peck, O. (1951) Superfamily Chalcidoidea. *Hymenoptera of America north of Mexico - Synoptic catalog* (ed. by C.F.W. Muesebeck, K.V. Krombein & H.K. Townes), pp. 410-594. Agriculture Monographs U.S. Department of Agriculture, Washington D.C.
- Pinto, J.D. (2009) Hypermetamorphosis. *Encyclopedia of Insects* (ed. by V.H. Resh & R.T. Carde), pp. 484-486. Academic Press.
- Quicke, D.L.J. (1997) *Parasitic Wasps*. Chapman & Hall, London.
- Ratnasingham, S. & Hebert, P.D.N. (2007) BOLD: The barcode of life data system (www.barcodinglife.org). *Molecular Ecology Notes*.
- Richardson, C.H. (1913) Studies on the habits and development of a hymenopterous parasite, *Spalangia muscidarum* Richardson. *Journal of Morphology*, **24**, 513–557.
- Shaw, M.R. (1981) Delayed inhibition of host development by the nonparalyzing venoms of parasitic wasps. *Journal of Invertebrate Pathology*, **37**, 215–221.
- Swofford, D.L. (2002) *PAUP* v.4.0: phylogenetic analysis using parsimony (* and other methods)*. Sinauer, Sunderland, Massachusetts, USA.

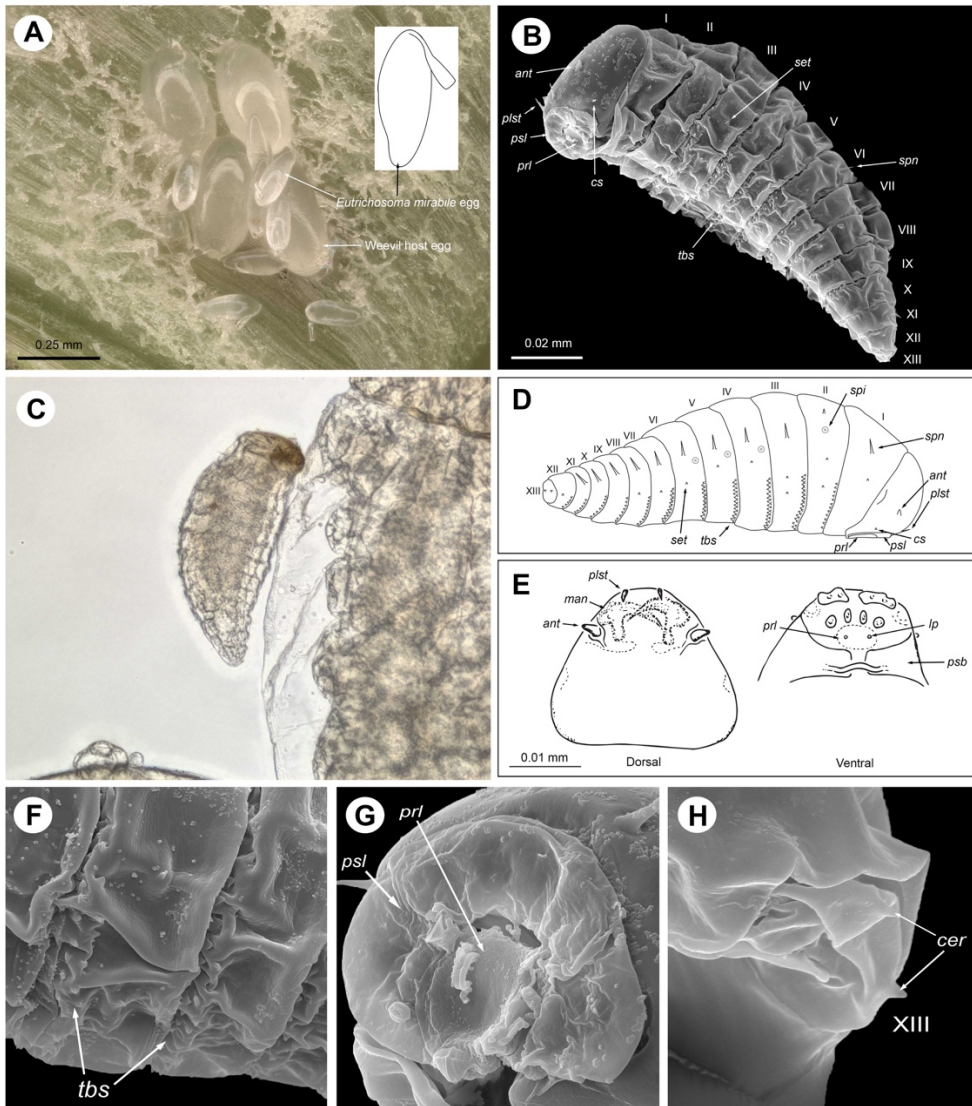


Figure 3.1: *Eutrichosoma mirabile* immature stages. **A**, eggs of *Eutrichosoma mirabile* (small, stalked) laid on top of the eggs of their weevil host (large, unstaked) within a seed pod of *Vechellia constricta*; inset: *Eutrichosoma mirabile* egg; **B**, SEM ventrolateral habitus image of a planidium of *Eutrichosoma mirabile*; **C**, planidium attached to host weevil larva; **D**, setal map of a *Eutrichosoma mirabile* planidium, modified from an illustration by Darling & Miller (1991); **E**, head capsule of planidium, dorsal and ventral views; **F**, planidium TIII–IV, ventral tubercles; **G**, head, anterolateral view, showing the labial structure; **H**, TXIII with cerci, dorsolateral view. Abbreviations: *ant* = antenna, *cer* = cerci, *cs* = cranial spine, *lp* = labial palp, *man* = mandible, *plst* = pleurostomal seta, *prl* = prelabium, *psb* = pleurostomal bridge, *psl* = postlabium, *set* = seta, *spi* = spiracle, *spn* = spine, *tbs* = tubercles, I–XIII = terga numbered from anterior to posterior.

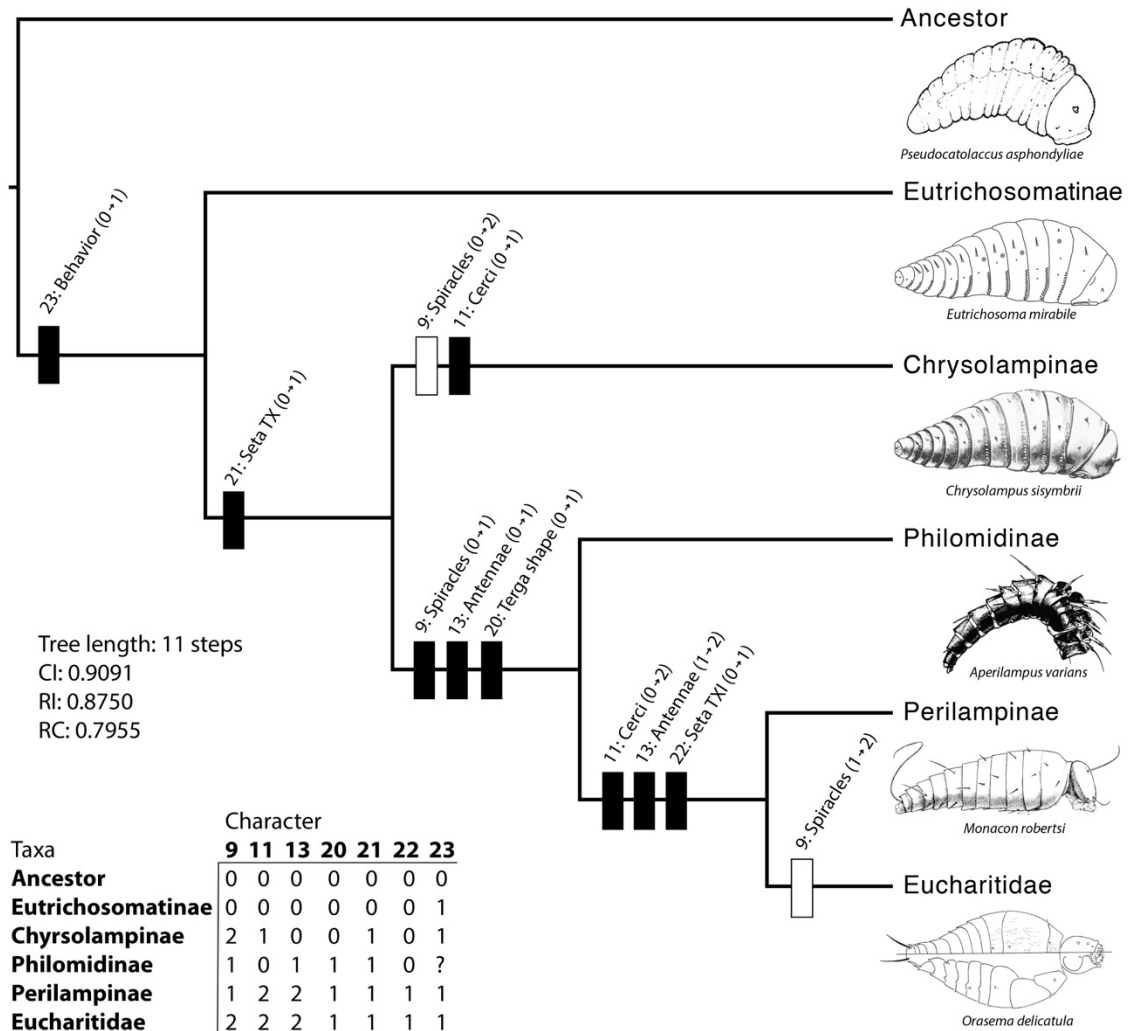


Figure 3.2: Most parsimonious tree from larval morphology, PAUP* analysis. Character state changes on branches are indicated by black bars (synapomorphies) and white bars (homoplasies). Character state matrix and tree statistics included. *Pseudocatolaccus asphondyliae* is shown as an example of a generic hymenopteriform larva with morphology that fits a hypothetical ancestor to the PLC. Illustrations of *Pseudocatolaccus asphondyliae* modified from Parker (1924); *Chrysolampus sisymbrii* modified from Darling & Miller (1991); *Aperilampus varians* modified from Darling (1992); *Monacaon robertsi* modified from Darling & Roberts (1999); *Orasema delicatula* modified from Burks et al. (2015).

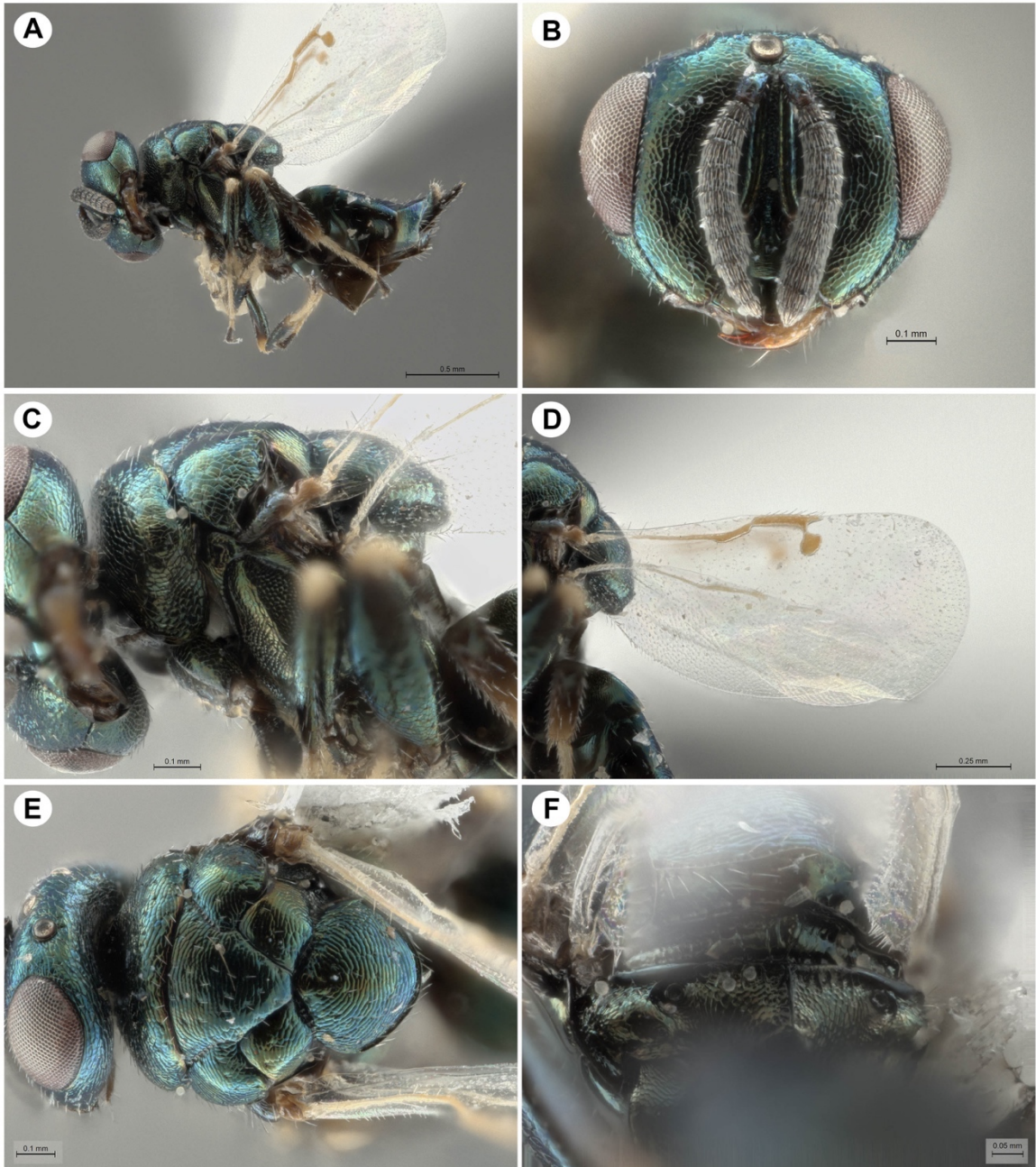


Figure 3.3: *Eutrichosoma burksi* holotype, adult female. **A**, lateral habitus; **B**, anterior head; **C**, lateral mesosoma; **D**, lateral wing; **E**, dorsal mesosoma; **F**, posterior propodeum.

Conclusions

Analyses using a Sanger sequencing dataset and an Anchored Hybrid Enrichment (AHE) dataset both independently and combined and using multiple phylogenetic frameworks, including parsimony, maximum likelihood, Bayesian, and coalescent methods has resulted in largely congruent phylogenetic hypotheses of Oraseminae. The significant results include a well-supported paraphyletic grade of Old World genera leading to a single New World clade, which is further supported by the quartet mapping method of estimating support. Using Sanger data alone did not result in Old World paraphyly but when combined with AHE data or when analyzing AHE data alone, the support for this hypothesis was overwhelming. Previously defined species groups of *Orasema* and the Old World genera were also largely supported across most analyses with the main exception being a polyphyletic *Hayatosema* Heraty & Burks.

The direction of dispersal for Oraseminae was concluded to go from the Old World to the New World, which is in the opposite direction of their ancestral host ant genus (supported by ancestral state mapping), *Pheidole*. The estimated timing of *Pheidole* and Oraseminae dispersing into new landmasses largely overlaps, and based on the results of biogeographic analyses, Oraseminae dispersed first into the Nearctic. This Nearctic-first pattern around 24–30 Ma supports the hypothesis that both ants and parasitoids used the Bering Land Bridge during a relatively tropical period of time to disperse. With the changing northern climate during the Oligocene, this may have created a narrow window of time for these groups to disperse, limiting their ability to disperse

back into their respective areas of endemism, a pattern that is not seen on the phylogenies.

The New World genus *Orasema* is far more diverse than the Old World genera, which is supported by a diversification rate shift as they entered the New World. With the inclusion of this research, *Orasema* now contains 94 described species organized into 16 species groups (with 10 of those species unplaced to species group). The keys and figure plates provided herein will greatly improve the ability to identify species and species groups of *Orasema*, and the included larval descriptions, ant and plant host information, and distributional information should make future research on this group far more convenient.

Phylogenetic analysis based on planidial morphology and behavior support Eutrichosomatinae as sister to Perilampidae+Eucharitidae. The larvae of *Eutrichosoma*, similar to *Chrysolampus*, have a more hymenopteriform appearance while maintaining behaviors similar to the other planidial larvae. Koinobiont ectoparasitism is unique to this planidial clade within Chalcidoidea and appears to be an important evolutionary step for transitioning into the more derived planidia as seen in Eucharitidae, Perilampinae, and Philomidinae. By providing new natural history information about *Eutrichosoma mirabile*, we have set the stage for further exploration into the evolution of larval morphology across Chalcidoidea.

Appendix A: List of Supplemental Files

Table S1.2: Voucher specimens and GenBank accession numbers

Table S1.3: Primers and protocols for Sanger sequencing

Table S1.4: AHE phylogenetic informativeness profiles

Table S1.5: Dispersal rates for biogeographic analyses in DEC and DEC+J

Table S1.6: Genomic resources for probe design (Hym_Cha)

Table S1.7: AHE assembly data

Table S3.1: Top hits from NCBI and BOLD databases for parasitoid larvae

Table S3.2: Top hits from NCBI and BOLD databases for host larvae

Table S3.3: Parasitism rates

Additional Materials Examined